

Pyridine / Pyrazine as Supramolecular Building Blocks for Molecular Capsule and Heterometallic Complexes

BY

**GIRI TEJA ILLA
CHEM11201004006**

**National Institute of Science Education and Research Bhubaneswar
Jatni, Khurda, Odisha - 752050**

*A thesis submitted to the
Board of Studies in Chemical Sciences
In partial fulfilment of requirements
For the degree of*

**DOCTOR OF PHILOSOPHY
of
HOMI BHABHA NATIONAL INSTITUTE**

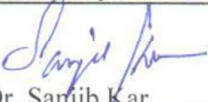
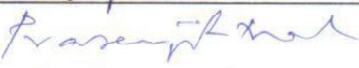
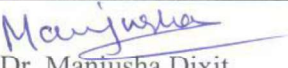


August, 2017

Homi Bhabha National Institute¹

Recommendations of the Viva Voce Committee

As members of the Viva Voce Committee, we certify that we have read the dissertation prepared by **Giri Teja Illa** entitled “**Pyridine / Pyrazine as Supramolecular Building Blocks for Molecular Capsule and Heterometallic Complexes**” and recommend that it may be accepted as fulfilling the thesis requirement for the award of Degree of Doctor of Philosophy.

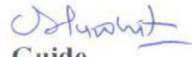
Chairman -		
	Prof. A. Srinivasan	Date: 02.04.18
Guide / Convener -		
	Dr. Chandra Shekhar Purohit	Date: 02/04/18
Examiner -		
	Prof. Dilip Kumar Chand, (IIT Madras)	Date: 02-04-18
Member 1-		
	Dr. Sanjib Kar	Date: 02-04-18
Member 2-		
	Dr. Prasenjit Mal	Date: 2.4.18
Member 3-		
	Dr. Manjusha Dixit	Date: 02/04/2018

Final approval and acceptance of this thesis is contingent upon the candidate's submission of the final copies of the thesis to HBNI.

I/We hereby certify that I/we have read this thesis prepared under my/our direction and recommend that it may be accepted as fulfilling the thesis requirement.

Date: 02/04/2018

Place: Jatni


Guide

¹ This page is to be included only for final submission after successful completion of viva voce.

STATEMENT BY AUTHOR

This dissertation has been submitted in partial fulfilment of requirements for an advanced degree at Homi Bhabha National Institute (HBNI) and is deposited in the Library to be made available to borrowers under rules of the HBNI.

Brief quotations from this dissertation are allowable without special permission, provided that accurate acknowledgement of source is made. Requests for permission for extended quotation from or reproduction of this manuscript in whole or in part may be granted by the Competent Authority of HBNI when in his or her judgment the proposed use of the material is in the interests of scholarship. In all other instances, however, permission must be obtained from the author.

GIRI TEJA ILLA

DECLARATION

I, hereby declare that the investigation presented in the thesis has been carried out by me. The work is original and has not been submitted earlier as a whole or in part for a degree / diploma at this or any other Institution / University.

GIRI TEJA ILLA

List of Publications

Published

- 1)[#] Hydrogen-bonded molecular capsules: probing the role of water molecules in capsule formation in modified cyclotricatechylene **Giri Teja Illa**, Sohan Hazra, Pardhasaradhi Satha and Chandra Shekhar Purohit. *CrystEngComm*, **2017**.DOI :10.1039/C7CE01075C
- 2)[#] Consecutive introduction of Ag(I) to an anionic homoleptic Co(III) complex: variable Ag(I) coordination mode. **Giri Teja Illa**, Pardhasaradhi Satha and Chandra Shekhar Purohit.*CrystEngComm*, **2016**, *18*, 5512-5518.
- 3) Propeller-Shaped Self-Assembled Molecular Capsules: Synthesis and Guest Entrapment. Pardhasaradhi Satha, **Giri Teja Illa**, and Chandra Shekhar Purohit. *Cryst. Growth Des.*,**2013**,*13*, 2636
- 4) Bio-inspired self-assembled molecular capsules. Pardhasaradhi Satha, **Giri Teja Illa**, and Chandra Shekhar Purohit.RSC Adv.,**2015**,*5*, 74457–74462
- 5) Guest-Induced, Self-Assembled Supramolecular Capsule: Effect of Guest and Counter Anions. Pardhasaradhi Satha, **Giri Teja Illa**, and Chandra Shekhar Purohit. *ChemistrySelect* **2016**, *1*, 1630

Communicated:

- 1)[#] Synthesis of Thiourea decorated cycloguaiacylene and its receptor properties. **Giri Teja Illa**, Pardhasaradhi Satha, SohanHazra, and Chandra Shekhar Purohit

Pertaining to thesis

Conferences Attended

- 1) Presented poster in “**JNOST-2015**” organized by **NISER, BHUBANESWAR** (14-17 DEC 2015). Title :**Synthesis of Pyrazine-2,6-diamide and its coordination behaviour with Ag⁺ ion.** Authors :**Giri Teja Illa**, Nayan kumar pradhan, Chandra Shekhar Purohit*
- 2) Presented poster in“**16th CRSI National Symposium**”in Chemistry & “**8th CRSI-RSC Symposium**”in Chemistry held at IIT Bombay (06-09 February 2014). Title :**Cyclotricatechylene based Self-Assembled Molecular Capsules:Synthesis and Guest Entrapment**; Authors : Pardhasaradhi Satha, **Giri Teja Illa**, Chandra Shekhar Purohit*
- 3) Participated in“**13th CRSI National Symposium**”in Chemistry & “**5th CRSI-RSC Symposium**”in Chemistry held at KIIT, Bhubaneswar (02-06 February 2011).
- 4) Participated in“**Indo-European Symposium**” on **Frontiers in Chemistry** held at NISER, Bhubaneswar (12-16 February 2012).
- 5) Participated in “**Indo-French Symposium**” held at NISER, Bhubaneswar (24-26 February 2014).

Dedicated to

My Family

ACKNOWLEDGEMENTS

*I take this opportunity to acknowledge my thesis supervisor **Dr. C. S Purohit** for his excellent guidance and consistent motivation provided to me throughout the course of this work. The encouragement, patience and the degree of freedom that he gave, made me to explore, adopt innovative learning and to develop a scientific temper.*

I wish to thank Prof. Sudhakar Panda (Director, NISER) Prof.V. Chandrasekhar (Former Director, NISER), Prof. T. K. Chandrashekar (Founder Director, NISER) for their help, support and valuable guidance. I would like to thank my Thesis Monitoring Committee members Prof. A.Srinivasan, Dr. S. Kar, Dr. P. Mal and Dr. M. Dikshit, for their valuable guidance. It is my privilege to thank Prof. A. Srinivasan, the Chairperson and Dr. Moloy Sarkar, the former Chairperson of School of Chemical Sciences, and Dr. N. K sharma (PGCS, School of Chemical Sciences), for their suggestions and help in the hours of need. I would like to thank Prof. T. K. Chandrashekar, Doctors S. Peruncheralathan, Moloy Sarkar, Arunachalam, P. Mal, J. N. Behera and Sudip Barman, for teaching me in my course work, which had uplifted my understanding of chemistry. I am also grateful to Dr. Arindam Ghosh for teaching me the NMR technique. I am sincerely thankful to all other faculty members of School of Chemical Sciences for their timely help in various aspects.

I sincerely thank Dr. Arun Kumar for helping me by providing lab chemicals whenever I need. I sincerely thank Sanjaya for recording the NMR spectra of my samples and Anuradha for recording GC of my samples. I would also like to acknowledge Amit and Raj for recording mass spectra of my samples. I would also like to thank Bhawani and Ashutosh for helping me by providing chemicals in need. I am thankful to Deepak for data collection of my single crystals. I thank all the non-academic staffs of School of Chemical Sciences and the Institute.

I am obliged to the infrastructural facilities and financial assistance of NISER, Bhubaneswar and express the sincere thanks for the same.

I also express my gratitude to my coworkers and lab-mates, Dr. Pardhasaradhi Satha, Dr. Pratap Deheri, Sidheshwary, Nayan, Manabnjan, Sanjay, Arun, Sohan, Krushna for their help and high degree of co-operation. My humble and sincere thanks to Dr. Subbareddy Marri (Subbu) for solving all the crystal structures.

I extend my heartily gratitude to Dr. Manoj, Dr. Subba reddy, Dr. Ajesh, Dr. Tapas, Dr. Adi, Dr. Ashim, Venkat, Peddarao, Thirupathi, Dhanu, Amar, Reddy, Balu, Mukund, Ramesh as friends for extending their helping hands whenever it was needed the most, with whom I spent lot of time during my stay at NISER, Bhubaneswar. I really enjoyed their company.

My deepest gratitude goes to the meticulous care and love of my parents (amma, Sowdamani and nanna, Nageswara rao) and my brother (Vijay). They inspired encouraged and supported me which helped me to complete my Ph. D work.

Above all, Thank You GOD for everything.....

Giri Teja Illa

Contents

	Page No.
Thesis Title	1
Statement by the author	3
Declaration	5
Publication list	7
Dedications	9
Acknowledgements	11
Contents	13
Synopsis	15
List of Schemes	27
List of Figures	29
List of Tables	49
List of Abbreviations	51
Chapter-1	53
Chapter-2	87
Chapter-3	129
Chapter-4	189
Chapter-5	231

Synopsis

Cyclotrimeratrylene (CTV) is a cyclic molecular host which is more stable in its crown conformation that gives it a bowl shape. CTV derivatives find applications in separations of fullerenes, dendrimers, gels, liquid crystals and metallocryptophanes architectures. There are relatively less reports of them being used in supramolecular capsules and ion sensor.¹ Our objective is to investigate the ability of CTV / CTC for molecular capsule by tailoring suitable chemical entity such as pyridine and also as a receptor by attaching thiourea moiety.

Pyridine moiety was extensively used as building block for variety of supramolecular architectures such as metallo-cages, coordination polymers, interlocked molecules such as rotaxane and catenanes.² We utilized pyridine derivative as ligand as hydrogen bond acceptor that finally transformed to handcuff catenane.

Heterometallic complexes received considerable attention during the past decade because of their structural diversities and unusual properties such as optical, magnetic, electrical, catalysis, luminescence, conduction and storage.³ Although many ligands along with heterocyclic ligands such as pyridine amide ligands were known, the analogous pyrazine amide ligands in this area is relatively less explored. Our objective is to study pyrazine-2,6-amide ligand and its ability to form heterometallic complexes.

Chapter 1: Introduction

This chapter contains two parts. One part includes a brief introduction about Cyclotrimeratrylene (CTV) and its derivative such as Cyclotriguaiacylene (CTG), Cyclotricatechylene (CTC). Derivatisation of CTG and CTC to get various CTV hosts which were utilized for the preparation of variety of supramolecular assemblies such as molecular capsules, metallocryptophanes, Solomon link, borromean rings etc.⁴ Along these, applications of CTV derivatives such as soft materials, sensing and separations, and in supramolecular chemistry were reviewed. Also, a brief introduction about pyridine moiety being used as

building block for Supramolecular architectures such as coordination polymers, hydrogen bonded assemblies, interlocked molecules such as rotaxanes and catenanes.²

Another part contains introduction about Pyrazine amide based ligands and its coordination complexes with various metals that were used to prepare molecular grids, Heterometallic architectures such as MOFs.⁵

Chapter 2: Self-assembled Molecular Capsule from Pyridine bridged cyclotricatechylene

Cyclotrimeratrylene (CTV) and its analogues have been used for complexation with different molecules. Cyclotricatechylene (CTC) has been used for few supramolecular complexes utilizing hydrogen bonded assemblies due to its easily functionalized phenolic –OH group. Although CTC is used as a scaffold for molecular capsule, the shallow cavity of CTC is a limitation. Thus, many groups have adopted methods to extend CTC that will help increase cavity size. Mostly, two approaches are implemented. One is to use CTG, a partially methylated version of CTC and attach functionalities (linkers) to phenolic groups. The other method is to attach bridging functionalities to the hydroxyl group of different catechol units. Utilizing this bridging method, Two new pyridine appended cavitands, CTC(Py)₂(OH)₂ and CTC(Py)₃ were synthesized and characterized. The solid state structure of both cavitands were studied by single crystal X-ray diffraction. CTC(Py)₂(OH)₂ resulted in a hydrogen bonded dimeric molecular capsule, entrapping two molecules of DMSO due to intervening water molecules those form hydrogen bonding to DMSO and CTC(Py)₂(OH)₂. When crystallized in absence of water, it forms a 2D polymer with hydrogen bonding of pyridine nitrogen and phenolic hydrogen atoms. CTC(Py)₃ gives no such capsule but contains a trapped water molecule in its cavity.

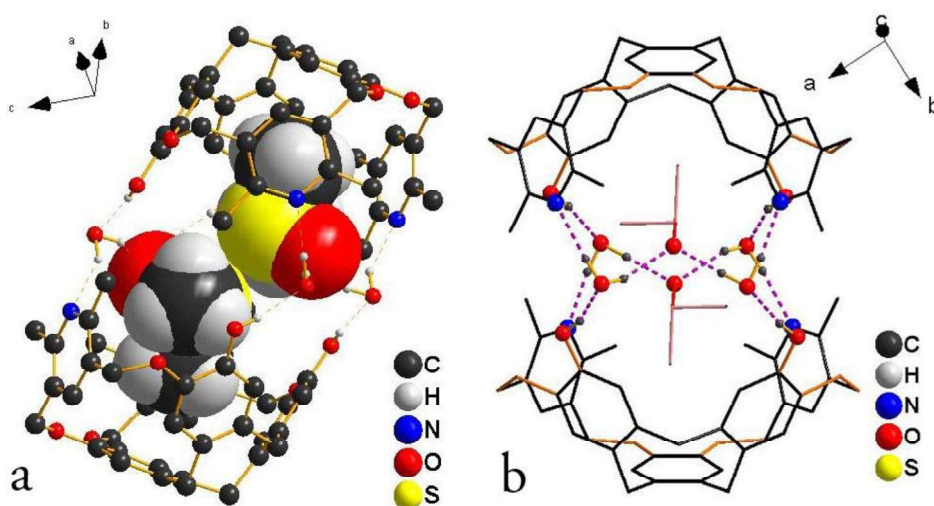
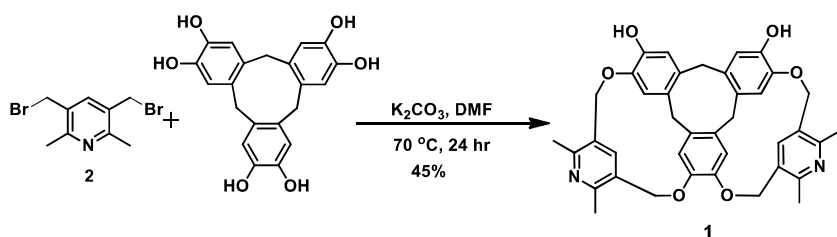


Figure 1. a) Crystal structure of **1** showing dimeric assembly. Non-hydrogen bonded hydrogen atoms are omitted for clarity. Encapsulated DMSO has been shown in spacefill model. b) Wireframe model of **1** forming a water mediated dimeric capsular assembly.

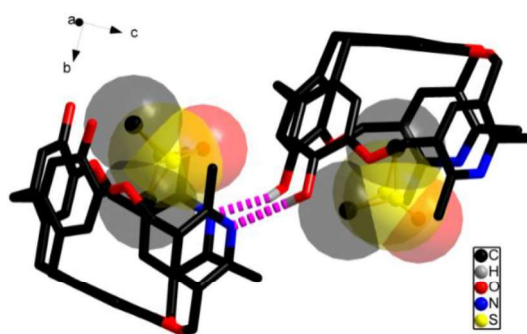
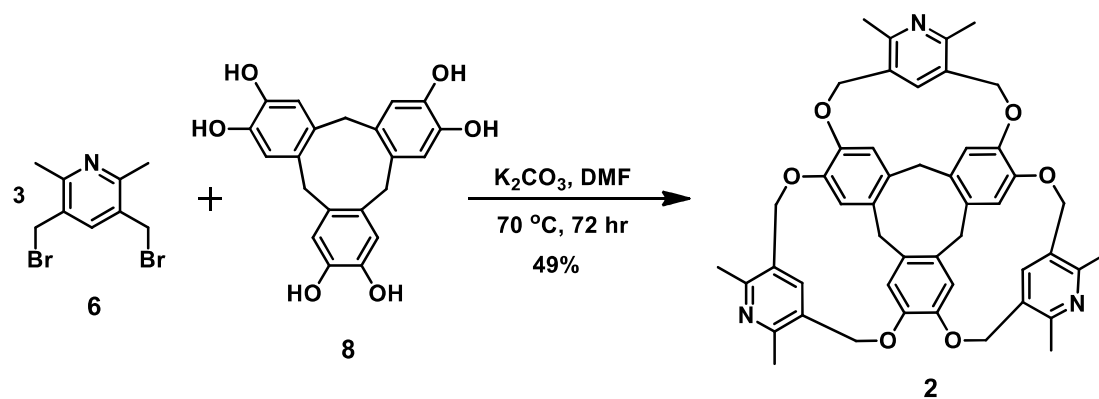


Figure 2. Crystal structure of **1** showing part of polymeric assembly in the absence of water. Hydrogen atoms (except those involved in hydrogen bonding) are removed for clarity.



Scheme 2. Synthesis of CTC(Py)₃ (2)

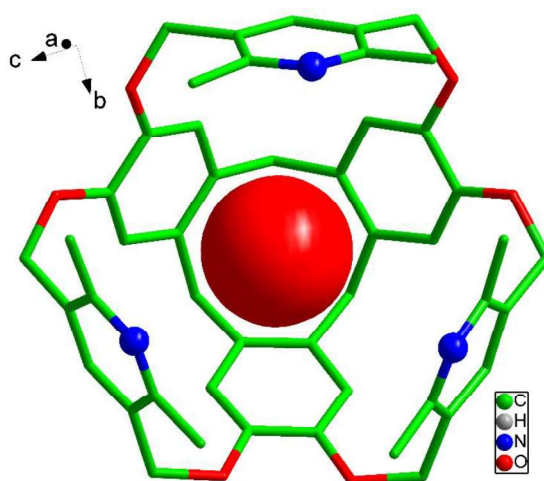


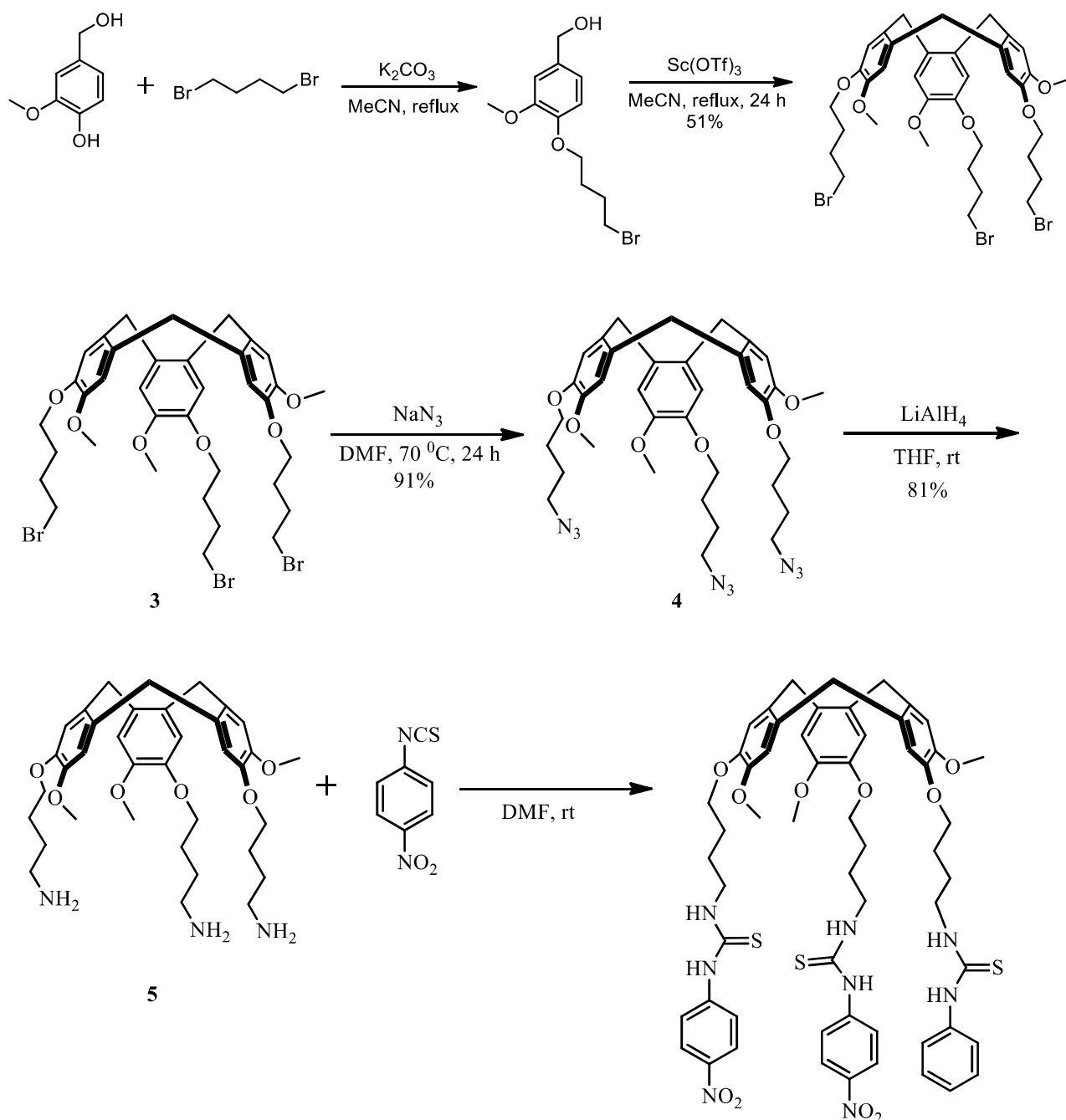
Figure 3. Crystal structure of 2, (top view), showing trapped water molecule (space fill). Hydrogen atoms have been removed for clarity.

Chapter 3: Tris-Thiourea appended Cyclotriguaiacylene : Synthesis and its receptor properties.

In 2009, Abraham and co-workers reported that under basic conditions, Cyclotri(2,4,6-trihydroxyphenyl)methane (CTC) in the presence of tetraethylammonium, Rb⁺ and Cs⁺ salts forms a dimeric capsular assemblies encapsulating cations via cation-π interaction in the solid state.^{6(a)} Recently our group reported that CTC forms dimeric capsule with tetraethylammonium salts encapsulating the cation in both solid and solution state under neutral conditions.^{6(b)} Based on these reports we envisaged that attaching the anion binding

groups such as thiourea to the CTV unit could act as both anion and cation receptor where anion binds at thiourea unit and cation binds to CTV cavity. The synthetic scheme of our designed receptor **A** is as follows.

Synthetic Scheme :



Scheme 3. Synthesis of receptor **A**

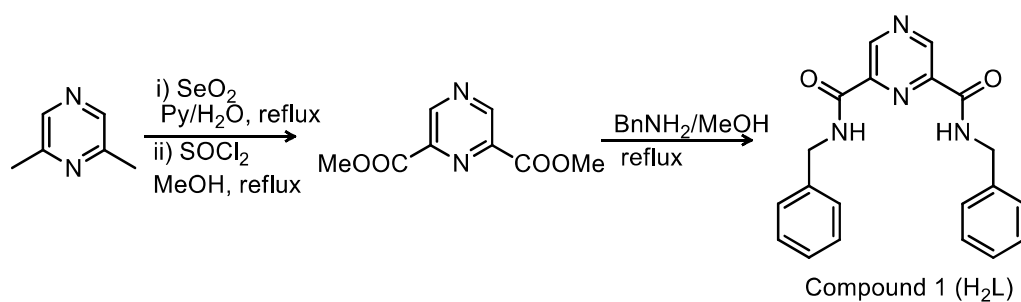
Initially, interaction of **A** with anions (as their respective tetrabutylammonium salts) were studied using UV-vis spectroscopy in DMSO at 1.42×10^{-5} M. The free receptor shows absorption peak at 358 nm. Among anions only F^- , CN^- ions addition shows a new absorption peak at 487 nm. Then we performed UV titration experiments for **A** by gradually increasing the concentration of anions (F^- , CN^-) until saturation point. By taking the titration data we measured binding constant using Benesi-Hildebrand equation to be $19.8 \times 10^7 \text{ M}^{-3}$ (for F^- ion) and $12.3 \times 10^8 \text{ M}^{-3}$ (for CN^- ion). $^1\text{HNMR}$ titration experiments in DMSO- d_6 shows that addition of anions causes deprotonation of thiourea amide protons.

The ion pair binding capability of **A** was studied using $^1\text{HNMR}$ by adding tetraalkylammonium chlorides in relatively less polar solvent 5% DMSO / CDCl_3 . Among these, tetraethylammonium chloride shows more shift (~ 0.2 ppm) in the presence **A**, suggesting relatively strong binding compared other chloride salts. In order to study the effect of anion on binding, $^1\text{HNMR}$ titration experiments were done by adding various tetraethylammonium salts ($X = F^-, \text{Cl}^-, \text{Br}^-, \text{I}^-, \text{ClO}_4^-$) to **A** in 5% DMSO- d_6 / CDCl_3 , which showed strong binding for F^- and Cl^- salts.

Next, we investigated amino acids, which are biologically relevant and zwitter ionic. Binding ability to **A** to amino acids are studied using $^1\text{HNMR}$ in 5% D_2O / DMSO- d_6 . NMR studies shows no proton shift for amino acids in the presence of **A**. But we observed colour change by addition of arginine. Hence, we investigated it further by UV titration experiment. Increasing concentration of arginine from 1.39×10^{-4} M to 4.3×10^{-3} M in 5% H_2O / DMSO gave a saturation point. $^1\text{HNMR}$ titration experiment shows deprotonation of amide protons occurs by the addition of arginine.

Chapter 4: Consecutive introduction of Ag(I) to an anionic homoleptic Co(III) complex: variable Ag(I) coordination mode.

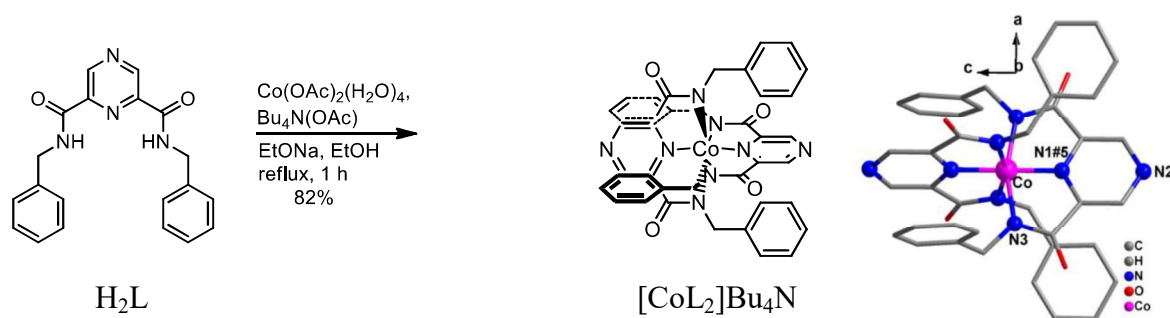
This chapter consists of synthesis of *N,N'*-Dibenzylpyrazine-2,6-dicarboxamide (H_2L) and its hetero-metallic complexes in a stepwise manner. The required ligand H_2L was synthesized in two steps from 2,6-dimethylpyrazine. It was first oxidized with SeO_2 and an esterification reaction was performed with methanol. The dimethyl ester of pyrazine-2,6-dicarboxylate was then reacted with benzyl amine in methanol to obtain the product H_2L .



Compound 1 (H_2L) **Scheme 4.** Synthesis

of H_2L (1)

The Ligand H_2L has two types of binding sites; one is a tridentate coordination site comprising one pyrazine nitrogen (N1) and two amide nitrogen atoms and the other one Pyrazine ring nitrogen atom (N4). Ligand H_2L was then metalated at tridentated site with $Co(OAc)_2$ in presence of base and the subsequent air oxidation obtained octahedral $[CoL_2]Bu_4N$. This complex was characterized by NMR, mass spectroscopy and single crystal X-ray diffraction.



Scheme 5. Synthesis of $[CoL_2]Bu_4N$

The cobalt complex has two pyrazine nitrogen atoms free. These two free pyrazine nitrogen atoms were studied for their coordination with $Ag(I)$, resulting in three heterometallic

complexes, $C_{40}H_{34}AgCoN_8O_5$, $C_{42}H_{38}Ag_3CoN_{10}O_{11}$ and $C_{42}H_{53}AgCoN_9O_{13}$. The mode of coordination could be controlled by varying the metal to ligand ratio and varying the counter anion. Moreover, we found conditions that make the ligand to either coordinate or not coordinate to Ag^+ . Some of these complexes also display the rare organometallic (C–Ag) bond.

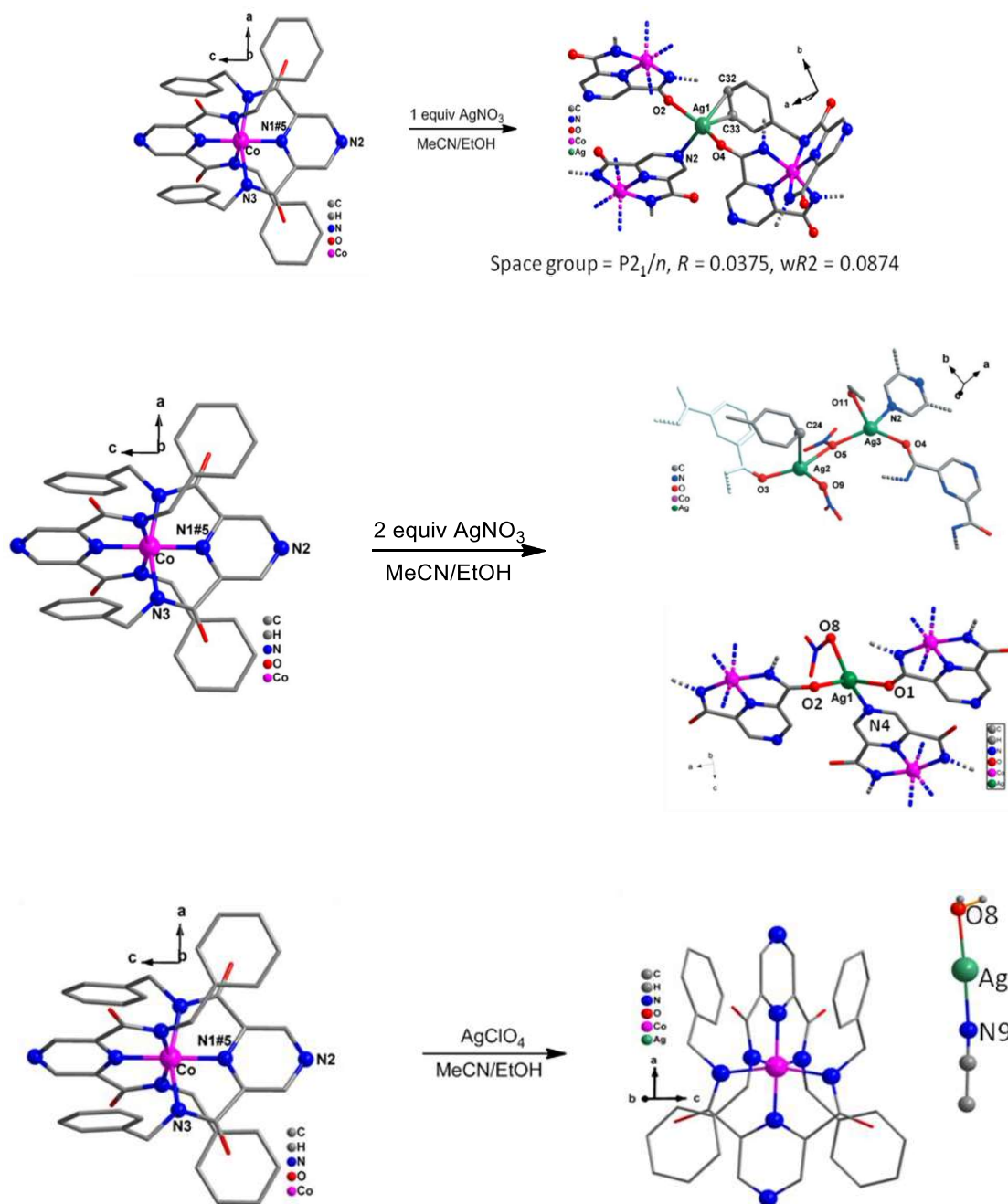


Figure 4. Synthesis of heterometallic complexes from $[CoL_2]Bu_4N$

Chapter 5: Attempted synthesis of [3]catenane

Catenanes are two or more mechanically interlocked macrocycles. These are particularly interesting for polymer chemistry because the macromolecule constitutes of several rings connected mechanically which have a independent motion- rotation and translation that may shows unique novel properties.^{7(a)} There are several classes of polycatenanes. Among them linear polycatenanes i.e.,[n]catenanes possess a synthetic challenge.^{7(b)} Therefore, much attention has been paid on synthesis on [2]catenane and only a few reports are available in literature for [3]catenane synthesis. We attempted to prepare [3]catenane using a new approach as shown in following scheme.

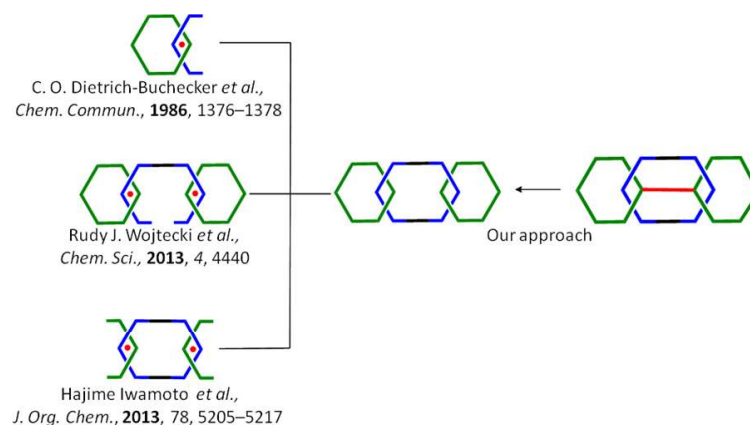
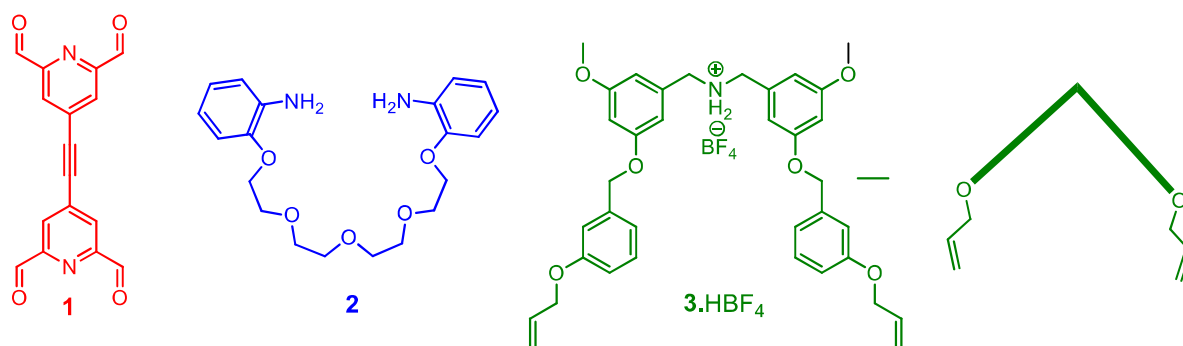


Figure 5. Previous reports and our approach to [3]catenane

[3]catenanes synthesised so far are dimerization of [2]pseudorotaxane, double ring closing of [3]rotaxane and single ring closure of [3]rotaxane. Our approach is based on cleavage of Handcuff catenane. Handcuff catenane comprises of macrocycle threaded into two

Synthetic precursors :



rings that are connected via a covalent bond. According to literature handcuff catenane was synthesized by donor acceptor approach, metal templation, anion templation. We have synthesized using crown ether – ammonium ion recognition motif to get handcuff catenane appended with a cleavable triple bond as shown above.

Using the above precursors and following a literature report⁸ we have prepared following alkyne appended handcuff catenane (Figure 6). Attempts to cleave the alkyne bond using known literature methods to get [3]catenane was so far unsuccessful.

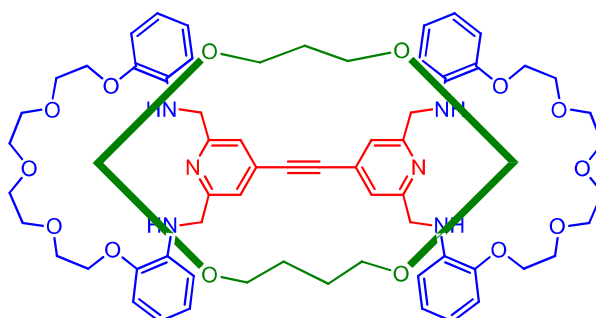


Figure 6. Structure of handcuff catenane

Summary of the work:

Two new pyridine appended CTV based cavitands $\text{CTC(Py)}_2(\text{OH})_2$ and CTC(Py)_3 were synthesized and characterized.

Solid state studies shows that $\text{CTC(Py)}_2(\text{OH})_2$ forms a capsular assembly in presence of water but a polymeric assembly in its absence.

Tris-thiourea appended cyclotriguaiacylene (CTGTU) was synthesised and characterised.

CTGTU acts as a colourimetric sensor for fluoride, cyanide ions and arginine.

We have for the first time studied a pyrazine -2,6-diamide ligand for making heterometallic complexes by a stepwise synthesis method.

Three heterometallic complexes, $\text{C}_{40}\text{H}_{34}\text{AgCoN}_8\text{O}_5$, $\text{C}_{42}\text{H}_{38}\text{Ag}_3\text{CoN}_{10}\text{O}_{11}$ and $\text{C}_{42}\text{H}_{53}\text{AgCoN}_9\text{O}_{13}$ were synthesised and characterised by single crystal XRD

We have successfully synthesised a alkyne appended Handcuff catenane.

Attempts to cleave alkyne bond of Handcuff catenane to get [3]catenane was so far unsuccessful.

Selected References :

1. Recent advances in the chemistry of Cyclotrimeratrylene. M. J. Hardie, *Chem. Soc. Rev.*, **2010**, *39*, 516.
2. (a) Controlling assembly of Cyclotrimeratrylene-derived coordination cages. James J. Henkelis and Michael J. Hardie. *Chem. Comm*, **2015**, *51*, 11929. (b) Recent developments in the preparation and chemistry of Metallacycles and Metallacages via coordination. Timothy R. Cook and Peter J. Stang. *Chem. Rev.* **2015**, *115*, 7001–7045.
3. Molecularly designed architectures – the Metalloligand way. Girijesh Kumar and Rajeev Gupta. *Chem. Soc. Rev.*, **2013**, *42*, 9403.
4. Self-assembled Cages and Capsules Using Cyclotrimeratrylene-type Scaffolds. M. J. Hardie, *Chem. Lett.*, **2016**, *45*, 1336.
5. (a) Control of molecular architecture by use of the appropriate ligand isomer: a mononuclear "corner-type" versus a tetranuclear [2 [times] 2] grid-type cobalt(iii) complex. Julia Hausmann and Sally Brooker *Chem. Commun.*, **2004**, 1530-1531; (b) Selective Gas Adsorption in a Pair of Robust Isostructural MOFs Differing in Framework Charge and Anion Loading. Matthew G. Cowan *et al.*, *Inorg. Chem.* **2014**, *53*, 12076–12083.
6. (a) Closed and Open Clamlike Structures Formed by Hydrogen-Bonded Pairs of Cyclotricatechylene Anions that Contain Cationic "Meat". B. F. Abrahams, N. J. FitzGerald, T. A. Hudson, R. Robson and T. Waters, *Angew. Chem. Int. Ed.*, **2009**, *48*, 3129. (b) Guest-Induced, Self-Assembled Supramolecular Capsule: Effect of Guest and Counter Anions. P. Satha, G. Illa, A. Ghosh and C. S. Purohit, *ChemistrySelect*, **2016**, *1*, 1630.

7. (a) Non-Rusty [2]Catenanes with Huge Rings and Their Polymers. Adelheid godt *Eur. J. Org. Chem.* **2004**, 1639-1654 (b) Polycatenanes. Zhenbin Niu and Harry W. Gibson, *Chem. Rev.* **2009**, *109*, 6024–6046.
8. Template-Directed Synthesis of a [2]Rotaxane by the Clipping under Thermodynamic Control of a Crown Ether Like Macrocycle Around a Dialkylammonium Ion. Peter T. Glink, *et al.*, *Angew. Chem. Int. Ed.* **2001**, *40*, 1870.

List of Schemes

	Page No.
Scheme 1.1 Synthesis of mononuclear metalloligand $[\text{Be}(\text{L}^1)_2]$	73
Scheme 2.1 General synthesis of extended CTVs from CTC	96
Scheme 2.2 Synthesis of 3,5-bis(bromomethyl)-2,6-dimethylpyridine (6)	98
Scheme 2.3 Synthesis of $\text{CTC}(\text{Py})_2(\text{OH})_2$ (1)	99
Scheme 2.4 Synthesis of $\text{CTC}(\text{Py})_3$ (2)	106
Scheme 3.1 Synthesis of CTV	133
Scheme 3.2 Synthesis of CTG.	134
Scheme 3.3 Synthesis of CTC.	134
Scheme 3.4 Synthesis of metallated extended CTV.	136
Scheme 3.5 Abraham's closed clam CTC	138
Scheme 3.6 Synthesis of CTV receptor L .	141
Scheme 4.1 Beckmann rearrangement catalysed by Zn(II) heterobimetallic complex of L^2	196
Scheme 4.2 Strecker reaction catalysed by $\text{Cd}(\text{II})\text{-L}^2\text{-Cd}(\text{II})$ complex	196
Scheme 4.3 Epoxide ring opening reaction catalysed by 2D network of L^3 .	198
Scheme 4.4 Synthesis of ligand 1	201
Scheme 4.5 Synthesis cobalt complex $[\text{CoL}_2]\text{Bu}_4\text{N}$ from H_2L	202

Scheme 5.1	Synthesis of tetra aldehyde 1	247
Scheme 5.2	Synthesis of diamine 2	247
Scheme 5.3	Synthetic scheme for template 3 . HBF_4	249
Scheme 5.4	Synthesis of bis-rotaxane I	249
Scheme 5.5	Synthesis of handcuff catenane III .	250
Scheme 5.6	Attempted methods to cleave alkyne bond of handcuff catenane.	251

List of Figures

		Page No.
Figure 1.1	Cartoon representation of molecular capsule formation	56
Figure 1.2	First Carcerand reported by Cram	57
Figure 1.3	Guest induced formation of molecular capsule	58
Figure 1.4	Resorcinarene based hemicarcerand.	59
Figure 1.5	The anti and syn isomers of cyptophanes	59
Figure 1.6	pH sensitive hetero-dimeric molecular capsule	60
Figure 1.7	Resorcinarene based metallocapsule	61
Figure 1.8	Acid functionalized resorcinarene and its Metallocage	62
Figure 1.9	Pd ²⁺ metallocage of Pyridine functionalized homooxalix[3]arene	62
Figure 1.10	Structure of bipyridine appended resorcinarene based cavitand.	63
Figure 1.11	Two glycouril molecules connected by a durene molecule and cartoon representation of its self assembly	64
Figure 1.12	Carboxylic group functionalized calix[4]arene.	65
Figure 1.13	Structure of resorcinarene and its hexameric assembly.	65
Figure 1.14	Rebeck's soft ball catalyzing Diels-alder reaction	66
Figure 1.15	Fujita's cage directed [2+2] photodimerisation	66

Figure 1.16	Crystal structure of entrapped white phosphorous	67
Figure 1.17	Metallocenes appended calix[4]arene anion receptors	68
Figure 1.18	Calix[4]arene based sodium salts ion pair receptor	69
Figure 1.19	Jabin's heteroditopic receptor	70
Figure 1.20	Urea appended Pillar[5]arene ion pair receptor	70
Figure 1.21	Hemicryptophane based ion pair receptor	71
Figure 1.22	Heterometallic complexes of $[\text{Be}(\text{L}^1)_2]$	73
Figure 1.23	Mixed metal complexes of $[\text{Cu}(\text{L}^1)_2]$	74
Figure 1.24	Chemdraw structures of L^2 and L^3 .	74
Figure 1.25	Synthesis of polynuclear metalloligand L^4_{Ag} .	75
Figure 1.26	Synthesis of mixed metal complexes from L^4_{Ag}	75
Figure 1.27	Cartoon representation of (a) Rotaxane ; (b) Catenane.	76
Figure 1.28	Wasserman's statistical approach for [2]catenane	76
Figure 1.29	Hunter's hydrogen bond template [2]catenane.	77
Figure 1.30	Beer's anion template [2]catenane	78
Figure 1.31	Amidine-carboxylate salt bridge templated [2]catenane	79
Figure 2.1	(a) Cyclotrimeratrylene (CTV); (b) Cyclotriguaiacylene (CTG) ; (c) Cyclotricatechylene (CTC).	92
Figure 2.2	(a) CTV and C_{60} inclusion complex ¹⁶ ; (b) Dendric tris-	92

CTVs with varying size

Figure 2.3	(a) ureidopyrimidine's self-complimentary DDAA hydrogen bonding sequence ; (b) C70@CTV-UPy hydrogen-bonded capsule	93
Figure 2.4	Synthetic scheme of extended CTVs from CTG.	94
Figure 2.5	Metallocryptophane ; (b) tetrahedral metallocryptophane	94
Figure 2.6	(a) 3D triply interlocked [2]catenane ; (b) Solomon cube	95
Figure 2.7	Carboxylate functionalised triple bridged CTV forming 'bow-tie' cryptophane with Cu(II) ions.	96
Figure 2.8	Our design of extended-cavity CTVs	97
Figure 2.9	ESI-MS spectra of 1 showing along with dimer peak	100
Figure 2.10	Asymmetric unit of 1 . Hydrogen atoms of 1 have been deleted for clarity.	101
Figure 2.11	Crystal structure showing dimeric assembly 1	101
Figure 2.12	Water molecule mediated hydrogen bonded dimeric capsular self-assembly of 1	102
Figure 2.13	Packing diagram showing capsular assembly A arranged in 2:1 Herringbone pattern.	102
Figure 2.14	Arrangement of four monomers around a central molecule of 1 , mediated by π - π stacking	103

Figure 2.15	Crystal structure of 1 showing non-capsular assembly in the absence of water	104
Figure 2.16	Packing diagram of 1 showing zig-zag chain polymer	104
Figure 2.17	Hydrogen bonding between molecules of 1 which are part of two different chains.	105
Figure 2.18	Asymmetric unit of 2 . Hydrogen atoms are omitted for clarity	107
Figure 2.19	CH- π interaction between pyridine methyl group of one molecule of 2 , with pyridine ring of another	107
Figure 2.20	Steric hindrance between methyl groups of adjacent pyridine bridges in 2 .	108
Figure 2.21	^1H NMR and ^{13}C NMR of Diethyl 2,6-dimethylpyridine-3,5-dicarboxylate	116
Figure 2.22	^1H NMR and ^{13}C NMR of (2,6-Dimethylpyridine-3,5-diyl)dimethanol	117
Figure 2.23	^1H NMR and ^{13}C NMR of 3,5-bis(bromomethyl)-2,6-dimethylpyridine	118
Figure 2.24	^1H NMR and ^{13}C NMR of Cyclotrimeratrylene (CTV)	119
Figure 2.25	^1H NMR and ^{13}C NMR of Cyclotricatechylene (CTC)	120
Figure 2.26	^1H NMR and ^{13}C NMR of $(\text{CTC}(\text{Py})_2(\text{OH})_2)$	121
Figure 2.27	^1H NMR and ^{13}C NMR of $(\text{CTC}(\text{Py})_3)$	122

Figure 2.28	ESI-MS spectrum of CTC(Py) ₂ (OH) ₂	123
Figure 2.29	ESI-MS spectrum of CTC(Py) ₃	123
Figure 3.1	Cartoon representation of mechanism of anion sensing.	135
Figure 3.2	Metallated CTVs	135
Figure 3.3	Hollman's metallated cryptophane.	136
Figure 3.4	Tris-amide CTV anion receptors	137
Figure 3.5	Quinoline appended CTV capsule	137
Figure 3.6	CTV based actinide receptor	138
Figure 3.7	Guest induced CTC dimeric capsule	139
Figure 3.8	Our design of Heteroditopic CTV receptor.	140
Figure 3.9	UV-Vis plot of L with various anions	142
Figure 3.10	UV titration of L with F ⁻ ion in DMSO	143
Figure 3.11	UV titration of L with CN ⁻ ion in DMSO	143
Figure 3.12	BH plot of L with F ⁻ ion	144
Figure 3.13	BH plot of L with CN ⁻ ion.	144
Figure 3.14	¹ HNMR titration of L with F ⁻ ion.	145
Figure 3.15	¹ HNMR titration of L with CN ⁻ ion.	145
Figure 3.16	Receptor L with various anions in DMSO	145

Figure 3.17	Mechanism of internal charge transfer (ICT).	146
Figure 3.18	Chemical structure of L and Tetraalkyl ammonium salts	146
Figure 3.19	Chemical shift differences of α -protons of ammonium salts in the presence of L .	147
Figure 3.20	Partial ^1H NMR spectra of TEACl salt with (blue) and without (red) L	148
Figure 3.21	Plausible binding of TEAX to L	148
Figure 3.22	Plot showing chemical shift differences of methylene protons of TEAX in presence of L versus number of equivalents of TEAX.	151
Figure 3.23	Predicted binding of amino acid to L .	152
Figure 3.24	UV-Vis titration of L with various amino acids.	153
Figure 3.25	UV-Vis titration plot of L with arginine in 5% $\text{H}_2\text{O}/\text{DMSO}$.	153
Figure 3.26	5% $\text{H}_2\text{O}/\text{DMSO}$ solution of L in presence of various amino acids	154
Figure 3.27	^1H NMR spectrum of compound 2	159
Figure 3.28	^{13}C NMR spectrum of compound 2	159
Figure 3.29	^1H NMR spectrum of compound 3	160
Figure 3.30	^{13}C NMR spectrum of compound 3	160

Figure 3.31	^1H NMR spectrum of compound 4	161
Figure 3.32	^{13}C NMR spectrum of compound 4	161
Figure 3.33	^1H and ^{13}C NMR spectrum of compound L	162
Figure 3.34	^1H NMR spectra showing shift of peak corresponding to methyl groups of TMACl in the presence of L	163
Figure 3.35	^1H NMR spectra showing shift of peak corresponding to ethyl groups of TEACl in the presence of L	163
Figure 3.36	^1H NMR spectra showing shift of peak corresponding to methylene groups of TPACl in the presence of L	164
Figure 3.37	^1H NMR spectra showing minor shift of peak corresponding to N-methylene group of TBACl in the presence of L	164
Figure 3.38	(a) 0.5 mL of L (0.00313 M) in 5% DMSO- d_6 /CDCl $_3$ + 3 μL DMSO- d_6 . (b) 0.5 mL of L (0.00313 M) in 5% DMSO- d_6 /CDCl $_3$ + 0.2 equiv. 0.1 M TEAF in DMSO- d_6 . (3 μL) (c) 0.5 mL 5% DMSO- d_6 /CDCl $_3$ + 3 μL 0.1 M TEAF in DMSO- d_6 .	165
Figure 3.39	(a) 0.5 mL of L (0.00313 M) in 5% DMSO- d_6 /CDCl $_3$ + 6 μL DMSO- d_6 . (b) 0.5 mL of L (0.00313 M) in 5% DMSO- d_6 /CDCl $_3$ + 0.4 equiv. 0.1 M TEAF in DMSO- d_6 . (6 μL) (c) 0.5 mL 5% DMSO- d_6 /CDCl $_3$ + 6 μL 0.1 M TEAF in	165

DMSO-d₆.

- Figure 3.40** (a) 0.5 mL of **L** (0.00313 M) in 5% DMSO-d₆/CDCl₃ + 9 μL DMSO-d₆. (b) 0.5 mL of **L** (0.00313 M) in 5% DMSO-d₆/CDCl₃ + 0.6 equiv. 0.1 M TEAF in DMSO-d₆. (9 μL) (c) 0.5 mL 5% DMSO-d₆/CDCl₃ + 9 μL 0.1 M TEAF in DMSO-d₆. 166
- Figure 3.41** (a) 0.5 mL of **L** (0.00313 M) in 5% DMSO-d₆/CDCl₃ + 11 μL DMSO-d₆. (b) 0.5 mL of **L** (0.00313 M) in 5% DMSO-d₆/CDCl₃ + 0.8 equiv. 0.1 M TEAF in DMSO-d₆. (11 μL) (c) 0.5 mL 5% DMSO-d₆/CDCl₃ + 11 μL 0.1 M TEAF in DMSO-d₆. 166
- Figure 3.42** (a) 0.5 mL of **L** (0.00313 M) in 5% DMSO-d₆/CDCl₃ + 14 μL DMSO-d₆. (b) 0.5 mL of **L** (0.00313 M) in 5% DMSO-d₆/CDCl₃ + 1 equiv. 0.1 M TEAF in DMSO-d₆. (14 μL) (c) 0.5 mL 5% DMSO-d₆/CDCl₃ + 14 μL 0.1 M TEAF in DMSO-d₆. 167
- Figure 3.43** (a) 0.5 mL of **L** (0.00313 M) in 5% DMSO-d₆/CDCl₃ + 17 μL DMSO-d₆. (b) 0.5 mL of **L** (0.00313 M) in 5% DMSO-d₆/CDCl₃ + 1.2 equiv. 0.1 M TEAF in DMSO-d₆. (17 μL) (c) 0.5 mL 5% DMSO-d₆/CDCl₃ + 17 μL 0.1 M TEAF in DMSO-d₆. 167
- Figure 3.44** (a) 0.5 mL of **L** (0.00313 M) in 5% DMSO-d₆/CDCl₃ + 20 μL DMSO-d₆. (b) 0.5 mL of **L** (0.00313 M) in 5% DMSO-d₆/CDCl₃ + 1.5 equiv. 0.1 M TEAF in DMSO-d₆. (20 μL) (c) 0.5 mL 5% DMSO-d₆/CDCl₃ + 20 μL 0.1 M TEAF in DMSO-d₆. 168

μL DMSO- d_6 . (b) 0.5 mL of **L** (0.00313 M) in 5% DMSO- d_6 / CDCl_3 + 2 equiv. 0.1 M TEAF in DMSO- d_6 . (20 μL) (c) 0.5 mL 5% DMSO- d_6 / CDCl_3 + 20 μL 0.1 M TEAF in DMSO- d_6 .

Figure 3.45 (a) 0.5 mL of **L** (0.00313 M) in 5% DMSO- d_6 / CDCl_3 + 23 μL DMSO- d_6 . (b) 0.5 mL of **L** (0.00313 M) in 5% DMSO- d_6 / CDCl_3 + 5 equiv. 0.1 M TEAF in DMSO- d_6 . (23 μL) (c) 0.5 mL 5% DMSO- d_6 / CDCl_3 + 23 μL 0.1 M TEAF in DMSO- d_6 . 168

Figure 3.46 (a) 0.5 mL of **L** (0.00313 M) in 5% DMSO- d_6 / CDCl_3 + 3 μL DMSO- d_6 . (b) 0.5 mL of **L** (0.00313 M) in 5% DMSO- d_6 / CDCl_3 + 0.2 equiv. 0.1 M TEACl in DMSO- d_6 . (3 μL) (c) 0.5 mL 5% DMSO- d_6 / CDCl_3 + 3 μL 0.1 M TEACl in DMSO- d_6 . 169

Figure 3.47 (a) 0.5 mL of **L** (0.00313 M) in 5% DMSO- d_6 / CDCl_3 + 6 μL DMSO- d_6 . (b) 0.5 mL of **L** (0.00313 M) in 5% DMSO- d_6 / CDCl_3 + 0.4 equiv. 0.1 M TEACl in DMSO- d_6 . (6 μL) (c) 0.5 mL 5% DMSO- d_6 / CDCl_3 + 6 μL 0.1 M TEACl in DMSO- d_6 . 169

Figure 3.48 (a) 0.5 mL of **L** (0.00313 M) in 5% DMSO- d_6 / CDCl_3 + 9 μL DMSO- d_6 . (b) 0.5 mL of **L** (0.00313 M) in 5% DMSO- d_6 / CDCl_3 + 0.6 equiv. 0.1 M TEACl in DMSO- d_6 . (9 μL) 170

(c) 0.5 mL 5% DMSO-d₆/CDCl₃ + 9 μL 0.1 M TEACl in DMSO-d₆.

- Figure 3.49** (a) 0.5 mL of **L** (0.00313 M) in 5% DMSO-d₆/CDCl₃ + 11 μL DMSO-d₆. (b) 0.5 mL of **L** (0.00313 M) in 5% DMSO-d₆/CDCl₃ + 0.8 equiv. 0.1 M TEACl in DMSO-d₆. (11 μL)(c) 0.5 mL 5% DMSO-d₆/CDCl₃ + 11 μL 0.1 M TEACl in DMSO-d₆ 170
- Figure 3.50** (a) 0.5 mL of **L** (0.00313 M) in 5% DMSO-d₆/CDCl₃ + 14 μL DMSO-d₆. (b) 0.5 mL of **L** (0.00313 M) in 5% DMSO-d₆/CDCl₃ + 1 equiv. 0.1 M TEACl in DMSO-d₆. (14 μL)(c) 0.5 mL 5% DMSO-d₆/CDCl₃ + 14 μL 0.1 M TEACl in DMSO-d₆. 171
- Figure 3.51** (a) 0.5 mL of **L** (0.00313 M) in 5% DMSO-d₆/CDCl₃ + 17 μL DMSO-d₆. (b) 0.5 mL of **L** (0.00313 M) in 5% DMSO-d₆/CDCl₃ + 1.2 equiv. 0.1 M TEACl in DMSO-d₆. (17 μL)(c) 0.5 mL 5% DMSO-d₆/CDCl₃ + 17 μL 0.1 M TEACl in DMSO-d₆ 171
- Figure 3.52** (a) 0.5 mL of **L** (0.00313 M) in 5% DMSO-d₆/CDCl₃ + 20 μL DMSO-d₆. (b) 0.5 mL of **L** (0.00313 M) in 5% DMSO-d₆/CDCl₃ + 2 equiv. 0.1 M TEACl in DMSO-d₆. (20 μL)(c) 0.5 mL 5% DMSO-d₆/CDCl₃ + 20 μL 0.1 M TEACl in DMSO-d₆. 172

- Figure 3.53** (a) 0.5 mL of **L** (0.00313 M) in 5% DMSO- d_6 /CDCl $_3$ + 23 μ L DMSO- d_6 . (b) 0.5 mL of **L** (0.00313 M) in 5% DMSO- d_6 /CDCl $_3$ + 5 equiv. 0.1 M TEACl in DMSO- d_6 . (23 μ L)(c) 0.5 mL 5% DMSO- d_6 /CDCl $_3$ + 23 μ L 0.1 M TEACl in DMSO- d_6 . 172
- Figure 3.54** a) 0.5 mL of **L** (0.00313 M) in 5% DMSO- d_6 /CDCl $_3$ + 3 μ L DMSO- d_6 . (b) 0.5 mL of **L** (0.00313 M) in 5% DMSO- d_6 /CDCl $_3$ + 0.2 equiv. 0.1 M TEABr in DMSO- d_6 . (3 μ L) (c) 0.5 mL 5% DMSO- d_6 /CDCl $_3$ + 3 μ L 0.1 M TEABr in DMSO- d_6 . 173
- Figure 3.55** (a) 0.5 mL of **L** (0.00313 M) in 5% DMSO- d_6 /CDCl $_3$ + 6 μ L DMSO- d_6 . (b) 0.5 mL of **L** (0.00313 M) in 5% DMSO- d_6 /CDCl $_3$ + 0.4 equiv. 0.1 M TEABr in DMSO- d_6 . (6 μ L) (c) 0.5 mL 5% DMSO- d_6 /CDCl $_3$ + 6 μ L 0.1 M TEABr in DMSO- d_6 . 173
- Figure 3.56** (a) 0.5 mL of **L** (0.00313 M) in 5% DMSO- d_6 /CDCl $_3$ + 9 μ L DMSO- d_6 . (b) 0.5 mL of **L** (0.00313 M) in 5% DMSO- d_6 /CDCl $_3$ + 0.6 equiv. 0.1 M TEABr in DMSO- d_6 . (9 μ L) (c) 0.5 mL 5% DMSO- d_6 /CDCl $_3$ + 9 μ L 0.1 M TEABr in DMSO- d_6 . 174
- Figure 3.57** (a) 0.5 mL of **L** (0.00313 M) in 5% DMSO- d_6 /CDCl $_3$ + 11 μ L DMSO- d_6 . (b) 0.5 mL of **L** (0.00313 M) in 5% DMSO-

$d_6/CDCl_3$ + 0.8 equiv. 0.1 M TEABr in DMSO- d_6 . (11 μ L)(c) 0.5 mL 5% DMSO- $d_6/CDCl_3$ + 11 μ L 0.1 M TEABr in DMSO- d_6

Figure 3.58 (a) 0.5 mL of **L** (0.00313 M) in 5% DMSO- $d_6/CDCl_3$ + 14 μ L DMSO- d_6 . (b) 0.5 mL of **L** (0.00313 M) in 5% DMSO- $d_6/CDCl_3$ + 1 equiv. 0.1 M TEABr in DMSO- d_6 . (14 μ L)(c) 0.5 mL 5% DMSO- $d_6/CDCl_3$ + 14 μ L 0.1 M TEABr in DMSO- d_6 175

Figure 3.59 (a) 0.5 mL of **L** (0.00313 M) in 5% DMSO- $d_6/CDCl_3$ + 17 μ L DMSO- d_6 . (b) 0.5 mL of **L** (0.00313 M) in 5% DMSO- $d_6/CDCl_3$ + 1.2 equiv. 0.1 M TEABr in DMSO- d_6 . (17 μ L)(c) 0.5 mL 5% DMSO- $d_6/CDCl_3$ + 17 μ L 0.1 M TEABr in DMSO- d_6 175

Figure 3.60 (a) 0.5 mL of **L** (0.00313 M) in 5% DMSO- $d_6/CDCl_3$ + 20 μ L DMSO- d_6 . (b) 0.5 mL of **L** (0.00313 M) in 5% DMSO- $d_6/CDCl_3$ + 2 equiv. 0.1 M TEABr in DMSO- d_6 . (20 μ L)(c) 0.5 mL 5% DMSO- $d_6/CDCl_3$ + 20 μ L 0.1 M TEABr in DMSO- d_6 . 176

Figure 3.61 (a) 0.5 mL of **L** (0.00313 M) in 5% DMSO- $d_6/CDCl_3$ + 23 μ L DMSO- d_6 . (b) 0.5 mL of **L** (0.00313 M) in 5% DMSO- $d_6/CDCl_3$ + 5 equiv. 0.1 M TEABr in DMSO- d_6 . (23 μ L)(c) 0.5 mL 5% DMSO- $d_6/CDCl_3$ + 23 μ L 0.1 M TEABr in DMSO- d_6 . 176

TEABr in DMSO-d₆.

- Figure 3.62** (a) 0.5 mL of **L** (0.00313 M) in 5% DMSO-d₆/CDCl₃ + 3 μL DMSO-d₆. (b) 0.5 mL of **L** (0.00313 M) in 5% DMSO-d₆/CDCl₃ + 0.2 equiv. 0.1 M TEAI in DMSO-d₆. (3 μL)(c) 0.5 mL 5% DMSO-d₆/CDCl₃ + 3 μL 0.1 M TEAI in DMSO-d₆. 177
- Figure 3.63** (a) 0.5 mL of **L** (0.00313 M) in 5% DMSO-d₆/CDCl₃ + 6 μL DMSO-d₆. (b) 0.5 mL of **L** (0.00313 M) in 5% DMSO-d₆/CDCl₃ + 0.4 equiv. 0.1 M TEAI in DMSO-d₆. (6 μL) (c) 0.5 mL 5% DMSO-d₆/CDCl₃ + 6 μL 0.1 M TEAI in DMSO-d₆. 177
- Figure 3.64** (a) 0.5 mL of **L** (0.00313 M) in 5% DMSO-d₆/CDCl₃ + 9 μL DMSO-d₆. (b) 0.5 mL of **L** (0.00313 M) in 5% DMSO-d₆/CDCl₃ + 0.6 equiv. 0.1 M TEAI in DMSO-d₆. (9 μL) (c) 0.5 mL 5% DMSO-d₆/CDCl₃ + 9 μL 0.1 M TEAI in DMSO-d₆. 178
- Figure 3.65** (a) 0.5 mL of **L** (0.00313 M) in 5% DMSO-d₆/CDCl₃ + 11 μL DMSO-d₆. (b) 0.5 mL of **L** (0.00313 M) in 5% DMSO-d₆/CDCl₃ + 0.8 equiv. 0.1 M TEAI in DMSO-d₆. (11 μL)(c) 0.5 mL 5% DMSO-d₆/CDCl₃ + 11 μL 0.1 M TEAI in DMSO-d₆. 178
- Figure 3.66** (a) 0.5 mL of **L** (0.00313 M) in 5% DMSO-d₆/CDCl₃ + 14 μL DMSO-d₆. (b) 0.5 mL of **L** (0.00313 M) in 5% DMSO-d₆/CDCl₃ + 1.0 equiv. 0.1 M TEAI in DMSO-d₆. (14 μL)(c) 0.5 mL 5% DMSO-d₆/CDCl₃ + 14 μL 0.1 M TEAI in DMSO-d₆. 179

μL DMSO- d_6 . (b) 0.5 mL of **L** (0.00313 M) in 5% DMSO- d_6 / CDCl_3 + 1 equiv. 0.1 M TEAI in DMSO- d_6 . (14 μL)(c) 0.5 mL 5% DMSO- d_6 / CDCl_3 + 14 μL 0.1 M TEAI in DMSO- d_6 .

Figure 3.67 (a) 0.5 mL of **L** (0.00313 M) in 5% DMSO- d_6 / CDCl_3 + 17 μL DMSO- d_6 . (b) 0.5 mL of **L** (0.00313 M) in 5% DMSO- d_6 / CDCl_3 + 1.2 equiv. 0.1 M TEAI in DMSO- d_6 . (17 μL)(c) 0.5 mL 5% DMSO- d_6 / CDCl_3 + 17 μL 0.1 M TEAI in DMSO- d_6 179

μL DMSO- d_6 . (b) 0.5 mL of **L** (0.00313 M) in 5% DMSO- d_6 / CDCl_3 + 1.2 equiv. 0.1 M TEAI in DMSO- d_6 . (17 μL)(c) 0.5 mL 5% DMSO- d_6 / CDCl_3 + 17 μL 0.1 M TEAI in DMSO- d_6

Figure 3.68 (a) 0.5 mL of **L** (0.00313 M) in 5% DMSO- d_6 / CDCl_3 + 23 μL DMSO- d_6 . (b) 0.5 mL of **L** (0.00313 M) in 5% DMSO- d_6 / CDCl_3 + 5 equiv. 0.1 M TEAI in DMSO- d_6 . (23 μL)(c) 0.5 mL 5% DMSO- d_6 / CDCl_3 + 23 μL 0.1 M TEAI in DMSO- d_6 . 180

μL DMSO- d_6 . (b) 0.5 mL of **L** (0.00313 M) in 5% DMSO- d_6 / CDCl_3 + 5 equiv. 0.1 M TEAI in DMSO- d_6 . (23 μL)(c) 0.5 mL 5% DMSO- d_6 / CDCl_3 + 23 μL 0.1 M TEAI in DMSO- d_6 .

Figure 3.69 (a) 0.5 mL of **L** (0.00313 M) in 5% DMSO- d_6 / CDCl_3 + 3 μL DMSO- d_6 . (b) 0.5 mL of **L** (0.00313 M) in 5% DMSO- d_6 / CDCl_3 + 0.2 equiv. 0.1 M TEA ClO_4 in DMSO- d_6 . (3 μL)(c) 0.5 mL 5% DMSO- d_6 / CDCl_3 + 3 μL 0.1 M TEA ClO_4 in DMSO- d_6 . 181

μL DMSO- d_6 . (b) 0.5 mL of **L** (0.00313 M) in 5% DMSO- d_6 / CDCl_3 + 0.2 equiv. 0.1 M TEA ClO_4 in DMSO- d_6 . (3 μL)(c) 0.5 mL 5% DMSO- d_6 / CDCl_3 + 3 μL 0.1 M TEA ClO_4 in DMSO- d_6 .

Figure 3.70 (a) 0.5 mL of **L** (0.00313 M) in 5% DMSO- d_6 / CDCl_3 + 6 μL DMSO- d_6 . (b) 0.5 mL of **L** (0.00313 M) in 5% DMSO- d_6 / CDCl_3 + 0.4 equiv. 0.1 M TEA ClO_4 in DMSO- d_6 . (6 μL)(c) 0.5 mL 5% DMSO- d_6 / CDCl_3 + 6 μL 0.1 M TEA ClO_4 in DMSO- d_6 . 181

μL DMSO- d_6 . (b) 0.5 mL of **L** (0.00313 M) in 5% DMSO- d_6 / CDCl_3 + 0.4 equiv. 0.1 M TEA ClO_4 in DMSO- d_6 . (6 μL)(c) 0.5 mL 5% DMSO- d_6 / CDCl_3 + 6 μL 0.1 M TEA ClO_4 in DMSO- d_6 .

μL (c) 0.5 mL 5% DMSO- d_6 /CDCl₃ + 6 μL 0.1 M TEAClO₄ in DMSO- d_6 .

Figure 3.71 (a) 0.5 mL of **L** (0.00313 M) in 5% DMSO- d_6 /CDCl₃ + 9 μL DMSO- d_6 . (b) 0.5 mL of **L** (0.00313 M) in 5% DMSO- d_6 /CDCl₃ + 0.6 equiv. 0.1 M TEAClO₄ in DMSO- d_6 . (9 μL) (c) 0.5 mL 5% DMSO- d_6 /CDCl₃ + 9 μL 0.1 M TEAClO₄ in DMSO- d_6 . 182

Figure 3.72 (a) 0.5 mL of **L** (0.00313 M) in 5% DMSO- d_6 /CDCl₃ + 11 μL DMSO- d_6 . (b) 0.5 mL of **L** (0.00313 M) in 5% DMSO- d_6 /CDCl₃ + 0.8 equiv. 0.1 M TEAClO₄ in DMSO- d_6 . (11 μL) (c) 0.5 mL 5% DMSO- d_6 /CDCl₃ + 11 μL 0.1 M TEAClO₄ in DMSO- d_6 . 182

Figure 3.73 (a) 0.5 mL of **L** (0.00313 M) in 5% DMSO- d_6 /CDCl₃ + 14 μL DMSO- d_6 . (b) 0.5 mL of **L** (0.00313 M) in 5% DMSO- d_6 /CDCl₃ + 1 equiv. 0.1 M TEAClO₄ in DMSO- d_6 . (14 μL) (c) 0.5 mL 5% DMSO- d_6 /CDCl₃ + 14 μL 0.1 M TEAClO₄ in DMSO- d_6 . 183

Figure 3.74 (a) 0.5 mL of **L** (0.00313 M) in 5% DMSO- d_6 /CDCl₃ + 17 μL DMSO- d_6 . (b) 0.5 mL of **L** (0.00313 M) in 5% DMSO- d_6 /CDCl₃ + 1.2 equiv. 0.1 M TEAClO₄ in DMSO- d_6 . (17 μL) (c) 0.5 mL 5% DMSO- d_6 /CDCl₃ + 17 μL 0.1 M TEAClO₄ in DMSO- d_6 . 183

Figure 3.75	(a) 0.5 mL of L (0.00313 M) in 5% DMSO- d_6 /CDCl $_3$ + 20 μ L DMSO- d_6 . (b) 0.5 mL of L (0.00313 M) in 5% DMSO- d_6 /CDCl $_3$ + 2 equiv. 0.1 M TEAClO $_4$ in DMSO- d_6 . (20 μ L)(c) 0.5 mL 5% DMSO- d_6 /CDCl $_3$ + 20 μ L 0.1 M TEAClO $_4$ in DMSO- d_6 .	184
Figure 3.76	(a) 0.5 mL of L (0.00313 M) in 5% DMSO- d_6 /CDCl $_3$ + 23 μ L DMSO- d_6 . (b) 0.5 mL of L (0.00313 M) in 5% DMSO- d_6 /CDCl $_3$ + 5 equiv. 0.1 M TEAClO $_4$ in DMSO- d_6 . (23 μ L)(c) 0.5 mL 5% DMSO- d_6 /CDCl $_3$ + 23 μ L 0.1 M TEAClO $_4$ in DMSO- d_6 .	184
Figure 3.77	(a) L (0.00313 M) in 5% H $_2$ O/DMSO- d_6 (0.5 mL); (b) L (0.00313 M) in 5% H $_2$ O/DMSO- d_6 (0.5 mL) + 0.2 equiv. of 0.2 M arginine in H $_2$ O	185
Figure 3.78	ESI-Mass Spectrum of 3	186
Figure 3.79	ESI-Mass Spectrum of 4	186
Figure 3.80	ESI-Mass Spectrum of L	187
Figure 4.1	Schematic representation of Heterometallic complex by stepwise manner	193
Figure 4.2	Pyridine amide based metalloligands	194
Figure 4.3	Synthesis of discrete heteromonometallic complex from Metalloligand L ¹	195

Figure 4.4	Synthesis of discrete heterobimetallic complex from Metalloligand L^2	195
Figure 4.5	Coordination of metalloligand L^2 with Cd(II) ions resulting 2D network	197
Figure 4.6	Coordination of L^3 with Zn(II) ions resulting hexagonal network	197
Figure 4.7	Ni(II) or Cu(II) coordination with $[L^5]^{-2}$ resulting [2 x 2] molecular grid	198
Figure 4.8	Coordination of Co(III) with $[L^6]^{-2}$ resulting [2 x 2] molecular grid.	199
Figure 4.9	Synthesis of $Ag_2(HL^7)_2$ and $Co(L^7)_2$ from HL^7	199
Figure 4.10	Coordination of Ag^+ ion with $Co(L^7)_2$ resulting a discrete heterometallic complex.	200
Figure 4.11	Structure of pyrazine-2,6-diamide showing different type of binding sites	200
Figure 4.12	Anionic part of 2 , showing the coordination around of Co(III) atom.	203
Figure 4.13	Unit cell of complex 2 . Tetrabutylammonium cations are shown in black.	203
Figure 4.14	ESI MS spectra of cobalt complex 2 after adding 2 equivalents of $AgNO_3$.	204
Figure 4.15	Crystal structure of complex 3 showing coordination around Ag^+ . Hydrogen atoms and groups which are not coordinated to Ag^+ are omitted for clarity.	205

Figure 4.16	Packing diagram of complex 3 . Hydrogen atoms and benzyl groups, which are not coordinated are omitted for clarity.	206
Figure 4.17	Coordination around Ag ⁺ (Ag1) in complex 4 . Hydrogen atoms and groups	207
Figure 4.18	Coordination around Ag ⁺ (Ag2 and Ag3) in complex 4 . Hydrogen atoms and groups	207
Figure 4.19	Packing diagram of complex 4 . Hydrogen atoms are omitted for clarity.	208
Figure 4.20	Crystal structure of complex 5 . The non-coordinated water molecules	209
Figure 4.21	Packing diagram of complex 5 . Water, acetonitrile and hydrogen atoms	210
Figure 4.22	¹ H NMR of Dimethyl pyrazine-2,6-dicarboxylate	217
Figure 4.23	¹³ C NMR of Dimethyl pyrazine-2,6-dicarboxylate	217
Figure 4.24	¹ H NMR of Compound 1	218
Figure 4.25	¹³ C NMR of Compound 1	218
Figure 4.26	¹ H NMR of [CoL ₂]Bu ₄ N	219
Figure 4.27	¹³ C NMR of [CoL ₂]Bu ₄ N	219
Figure 4.28	ESI-MS spectrum of Dimethyl pyrazine-2,6-dicarboxylate	220
Figure 4.29	ESI-MS spectrum of compound 1	220

Figure 4.30	ESI-MS spectrum of $[\text{CoL}_2]\text{Bu}_4\text{N}$	221
Figure 5.1	Cartoon representation of [2]catenane	234
Figure 5.2	Schill's covalent directed [2]catenane	236
Figure 5.3	Sauvage's first metal template synthesis of [2]catenane.	237
Figure 5.4	Sauvage's molecular switch controlled by oxidation state	238
Figure 5.5	Sauvage's pH controlled molecular switch	239
Figure 5.6	Beer's anion receptor	239
Figure 5.7	Sauvage's metal template synthesis of [3]catenane.	240
Figure 5.8	Stoddart's donor/acceptor [3]catenane.	241
Figure 5.9	Host-guest interactions template [3]catenane.	242
Figure 5.10	Fujita's Pd(II) [3]catenane	242
Figure 5.11	Meyer's double ring closing strategy for [3]catenane	243
Figure 5.12	Cartoon representation of previous reports and our approach of [3]catenane synthesis.	244
Figure 5.13	Sauvage's Handcuff catenane.	244
Figure 5.14	Stoddart's [2]rotaxane by clipping.	245
Figure 5.15	Precursors for the synthesis of handcuff catenane.	246
Figure 5.16	ESI-Mass spectrum of macrocycle IV .	252
Figure 5.17	^1H and ^{13}C of Compound 4	266

Figure 5.18	^1H and ^{13}C of Compound 5	267
Figure 5.19	^1H and ^{13}C of Compound 6	268
Figure 5.20	^1H and ^{13}C of Compound 7	269
Figure 5.21	^1H and ^{13}C of Compound 9	270
Figure 5.22	^1H and ^{13}C of Compound 1	271
Figure 5.23	^1H and ^{13}C of Compound 10	272
Figure 5.24	^1H and ^{13}C of Compound 11	273
Figure 5.25	^1H and ^{13}C of Compound 2	274
Figure 5.26	^1H and ^{13}C of Compound 13	275
Figure 5.27	^1H and ^{13}C of Compound 14	276
Figure 5.28	^1H and ^{13}C of Compound 15	277
Figure 5.29	^1H and ^{13}C of Compound 16	278
Figure 5.30	^1H and ^{13}C of Compound 17	279
Figure 5.31	^1H and ^{13}C of Compound 18	280
Figure 5.32	^1H and ^{13}C of Compound 19	281
Figure 5.33	^1H and ^{13}C of Compound 20	282
Figure 5.34	^1H and ^{13}C of Compound 22	283
Figure 5.35	^1H and ^{13}C of Compound 3	284

List of Tables

		Page No.
Table 2.1	Optimisation table for synthesis of 1	99
Table 2.2	Crystal data and structure refinement for CTC(Py) ₂ (OH) ₂ (1) forming capsular assembly.	124
Table 2.3	Hydrogen bonds for CTC(Py) ₂ (OH) ₂ (1) [Å and °].(Capsular assembly)	125
Table 2.4	Crystal data and structure refinement for CTC(Py) ₂ (OH) ₂ (1) forming non-capsular assembly	125
Table 2.5	Hydrogen bonds for CTC-Py ₂ [Å and °].(non-capsular assembly)	126
Table 2.6	Crystal data and structure refinement for CTC(Py) ₃ (2).	127
Table 3.1	¹ HNMR chemical shifts of tetraalkyl ammonium protons in presence of L .	147
Table 3.2	¹ HNMR Chemical shift differences of TEAClO ₄ protons and N1 proton of L with equivalents	149
Table 3.3	¹ HNMR Chemical shift differences of TEAI protons and N1 proton of L with equivalents	149
Table 3.4	¹ HNMR Chemical shift differences of TEABr protons and N1 proton of L with equivalents	150

Table 3.5	¹ HNMR Chemical shift differences of TEACl protons and N1 proton of L with equivalents	150
Table 3.6	¹ HNMR Chemical shift differences of TEAF protons and N1 proton of L with equivalents	151
Table 4.1	Summary of crystal data	222
Table 4.2	Bond lengths and Bond angles of [CoL ₂]Bu ₄ N, 3	223
Table 4.3	Bond lengths and Bond angles of 4	223
Table 4.4	Bond lengths and Bond angles of 5	225
Table 4.5	Bond lengths and Bond angles of 6	226

List of Abbreviations

CH ₃ CN	Acetonitrile
BF ₃ .OEt ₂	Borontrifluoridediethyletherate
BBr ₃	Borontribromide
Br ⁻	Bromide ion
BF ₄ ⁻	Tetrafluoroborate ion
Cl ⁻	Chloride ion
CCDC	Cambridge crystallographic data centre
CHCl ₃	Chloroform
CD ₃ OCD ₃	Deuteriated acetone
CD ₃ OD	Deuteriated methanol
CDCl ₃	Deuteriated chloroform
CD ₃ CN	Deuteriated acetonitrile
CTV	Cyclotrimeratrylene
CTC	Cyclotricatechylene
CTG	Cyclotriguaiacylene
DCM	Dichloromethane
DMF	Dimethylformamide
DMA	Dimethyl acetamide
DFT	Density functional theory
DMSO	Dimethylsulphoxide
FT-IR	Fourier transformation infra red
EtOAc	Ethyl acetate
ESI	Electron spray ionization
equiv.	Equivalents

RT	Room temperature
K_2CO_3	Potassium Carbonate
h	hours
min	minutes
NMR	Nuclear magnetic resonance
H_2SO_4	Sulfuric acid
TFA	Trifluoroacetic acid
THF	Tetrahydrofuran
UV	Ultraviolet
TLC	Thin layer chromatography
TMS	Tetramethylsilane
p-TSA	para-toluene sulphonic acid
PF_6	Hexafluorophosphate ion
Phe	1,10-Phenanthroline
Na_2SO_4	Sodium Sulphate
TEA	Tetraethyl ammonium cation
TMA	Tetramethyl ammonium cation
TPA	Tetrapropyl ammonium
TBA	Tetrabutyl ammonium
TEAX	Tetraethyl ammonium salts
TEAF	Tetraethyl ammonium fluoride
TEACl	Tetraethyl ammonium chloride
TEABr	Tetraethyl ammonium bromide
TEAI	Tetraethyl ammonium iodide
TEAClO ₄	Tetraethyl ammonium perchlorate

Chapter-1

INDEX

Introduction	55
Part-I	
1.1. Molecular Capsules.	56
1.2. Cavitand based receptors for anions and ion pairs	68
Part-II	
1.3. Metal Organic architectures	72
Part-III	
1.4. Interlocked Molecules	76
1.5. References.	80

Introduction

Heterocyclic compounds are the cyclic compounds containing at least one heteroatom in one or more rings. These compounds are ubiquitous in nature and are vital for many biological functions. Heterocyclic containing DNA and RNA carry genetic information. Some amino acids contains heterocyclic residue which are essential for human body. Most of the drugs, pesticides, herbicides and dyes contain heterocyclic moiety.

Apart from biological and medicinal applications, Heterocyclic compounds play a major role in coordination and supramolecular chemistry which are the chemistry of non-covalent interactions. Utilizing the hydrogen bonding and metal coordinating ability of heteroatom of heterocyclic rings many supramolecular architectures were synthesized. Among heterocyclics pyridine moiety was well studied for the construction of variety of supramolecular assemblies such as metallo capsules, metal-organic architectures, interlocked molecules etc.

Our aim is to investigate the ability of pyridine moiety (a) For the formation of hydrogen bonded and metallated molecular capsule. (b) For the construction of higher order interlocked molecule [3]catenane. (c) Its analogue Pyrazine moiety for the construction of metal-organic architectures.

Part-I

1.1. Molecular Capsules

Molecules having a space inside and large enough to act as a host for other atoms or molecules are known as molecular capsules or molecular containers (Figure 1.1). Initially these molecules were synthesized by covalent linkage. Later, inspired by natural self-assembly of DNA and proteins governed by non-covalent interactions chemists successfully adapted these interactions to make self-assembled molecular capsules or otherwise termed as supramolecular capsules. These non-covalent interactions include hydrogen bonding, cation- π interaction, hydrophobic interaction and metal coordination.

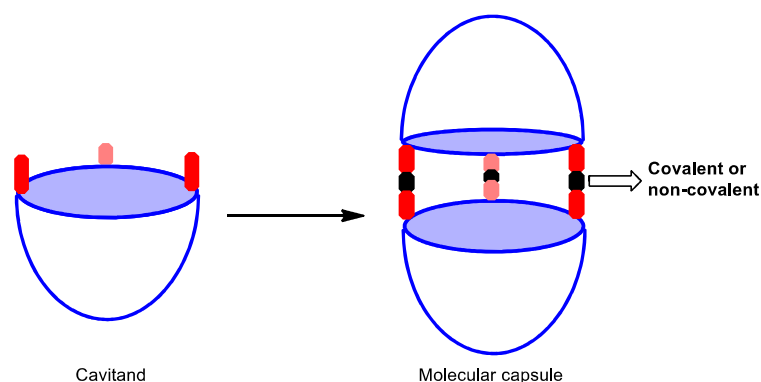


Figure 1.1. Cartoon representation of molecular capsule formation.

The idea of molecular capsule has been emerged from the work of Cram's molecular cavidands and Lehn's cryptand.¹⁻³ Both of these molecules were utilized to trap small cations and solvent molecules from bulk solvent. Later chemists realized the disadvantage of these molecules to be useful as they have limited space, unable to release guest and poor yields. Over the past decades, research in this area is well exploited and numerous molecules have been reported in the literature.

Applications of the molecular capsules include drug delivery, using them as reaction vessels, stabilising unstable molecules, sensing etc.

1.1.1. Covalent Molecular Capsules

1.1.1.1. Carcerands and Hemicarcerands

In 1985, D. J. Cram first described the synthesis of carcerands by joining two cavitands with a covalent bond (Figure 1.2).³ Its solvation properties were studied and used it as reaction vessel.⁴⁻⁵ Carcerands entraps guest molecules forming complexes called carceplexes. These guest cannot escape without breaking covalent bond of the carcerand.⁶ By attaching pyrazine and quinoxaline moieties, a novel cavitands with different conformations were obtained.⁷ The synthesis of first carceplex was reported by Cram in 1988 where it entraps solvent molecules and Cs^+ ion used during the reaction.⁸

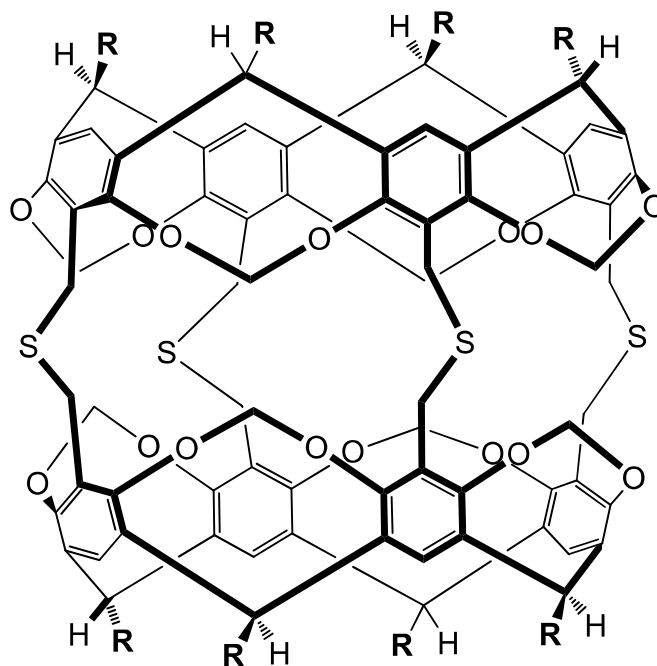


Figure 1.2. First Carcerand reported by Cram.

Hemicarceplexes are similar to carceplexes but contains small gateways through which guest molecules can enter and exit the cavity at high temperatures without breaking covalent bond.⁶ First of this kind was reported by cram where it entraps solvents molecules and they escape the cavity upon heating.⁹ Under suitable conditions this cavity serves as a host for Xe atom. Another report demonstrates that shell closure reaction of hemicarceplexes depends on the solvent used in the reaction which in turn acts as a guest.¹⁰ A hemicarceplex having a large internal cavity was synthesized to entrap large molecules such as fullerenes.¹¹

Guest templated cage formation was reported by cram where NMP acts as a poor template for cyclisation via covalent approach and Pyrazine acts a perfect template for molecular capsule formation via non-covalent approach (Figure 1.3).¹²

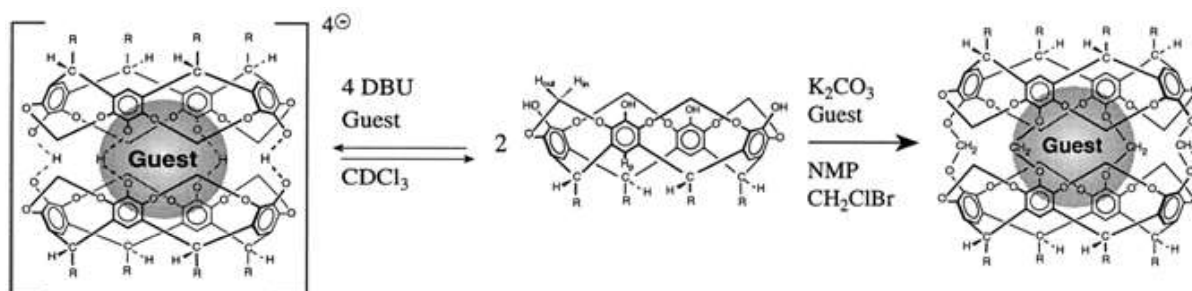


Figure 1.3. Guest induced formation of molecular capsule

Water soluble hemicarceplex was also synthesized by installing carboxylic groups.¹³ Its evolution, guest binding properties are thoroughly described.¹⁴ An imine based hemicarceplex was reported in 1991 by the condensation of aldehyde appended resorcinarene and 1,3-diaminobenzene. This was utilized in binding guest molecules such as ferrocene and 9,10-anthraquinone (Figure 1.4).¹⁵

Covalent capsule using calix[n]arene scaffold was first reported by bolhmer and co-workers.¹⁶ Following this many different type of capsules based on calix[n]arene were reported in the literature.¹⁷⁻²⁰

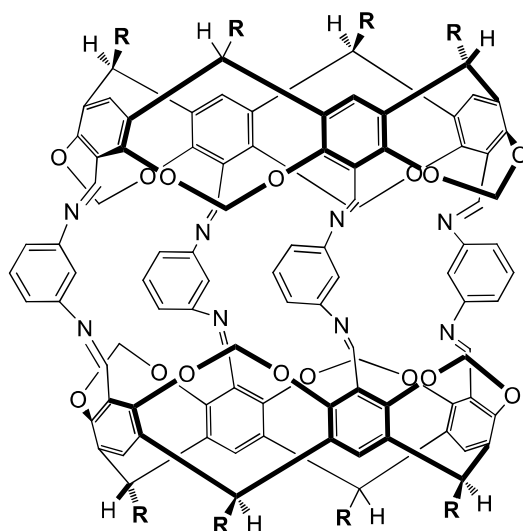


Figure 1.4. Resorcinarene based hemicarcerand.

1.1.1.2. Cryptophanes

Cryptophanes are the molecules made of two Cyclotrimerteratrylene (CTV) units pointing face to face manner connecting with the three bridges. CTV is cyclic trimer of veratrole that is having a threefold symmetry. Collet and co-workers synthesized first cryptophane by joining Cyclotriguaiacylene with veratryl alcohol and then intramolecular cyclisation leads to bis(cyclotrimerteratrylenyl) macrocage.²¹ In general synthesis of cryptophanes lead to syn and anti diastereomers (Figure 1.5).

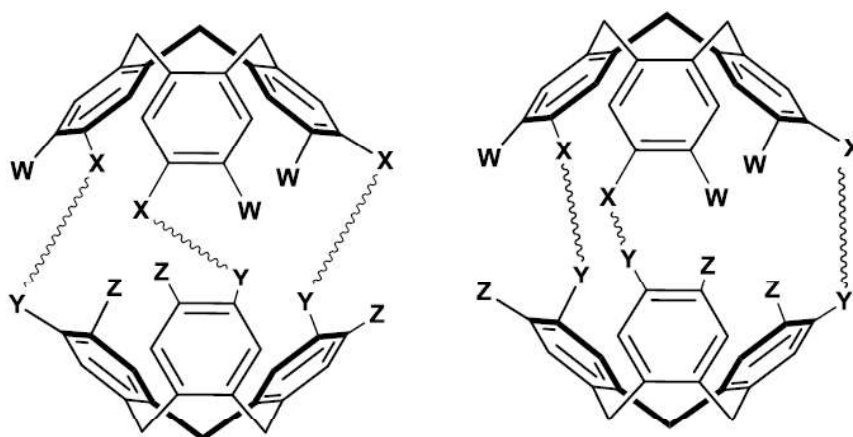


Figure 1.5. The anti and syn isomers of cyptophanes

Cram and co-workers reported a rigid cryptophane by coupling of acetylene functionalised CTV units. This can encapsulate solvent organic molecules.²² Brotin and co-workers synthesized a deuterium labelled cryptophane and studied the Xe binding using NMR chemical shift with ^{129}Xe .²³ Apart from these, many examples of cryptophanes and their properties were well discussed in an excellent review.²⁴

Covalently linked hetero-dimeric capsule based on CTV has also been reported. It was synthesised by the condensation of Cyclotricatechylene and boronic acid-appended hexahomotrioxacalix[3]arene via boranate esterification. It was demonstrated as pH sensitive capsule (Figure 1.6).²⁵

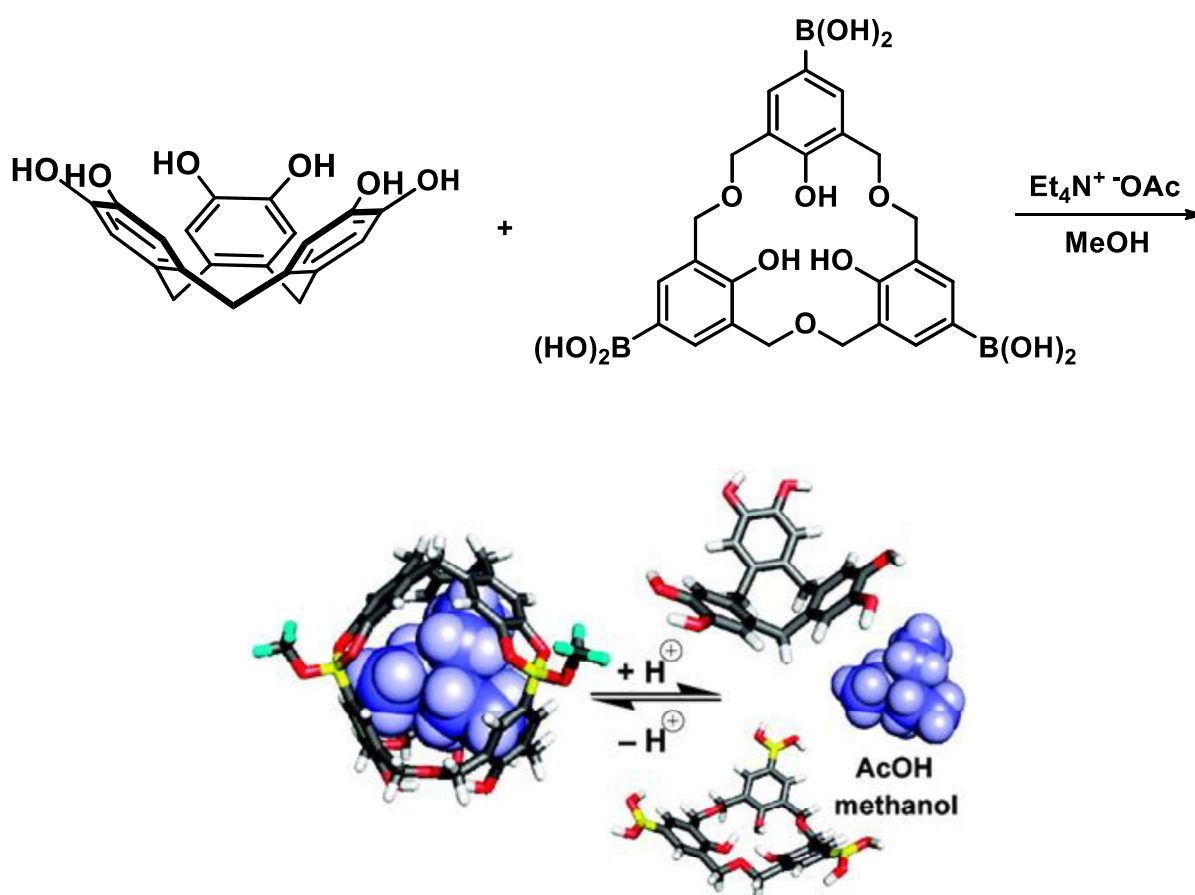


Figure 1.6. pH sensitive hetero-dimeric molecular capsule.

1.1.2. Metallocapsules

Capsular assemblies driven by metal coordination are known as metallocapsules. These are dynamic in nature compared to rigid covalent capsules. A metal ion can organize a flexible ligand into different architectures such as helicates, squares, rings, cages etc.

The first metallocage was reported by Enrico Dalcanale in 1997 by joining tetra cyano resorcinarene based cavitanad with square planar metals Pd, Pt (Figure 1.7). The cage was characterised by mass and NMR analysis.²⁶ Trifluoroacetate ion entrapment was confirmed by ¹⁹F NMR studies. The same group extended this work to obtain different type of cages and studied their anion binding ability. They also demonstrated the reversible nature of these capsule by adding competitive ligand like triethylamine that destroys capsular formation and was restored by triflic acid addition.²⁷

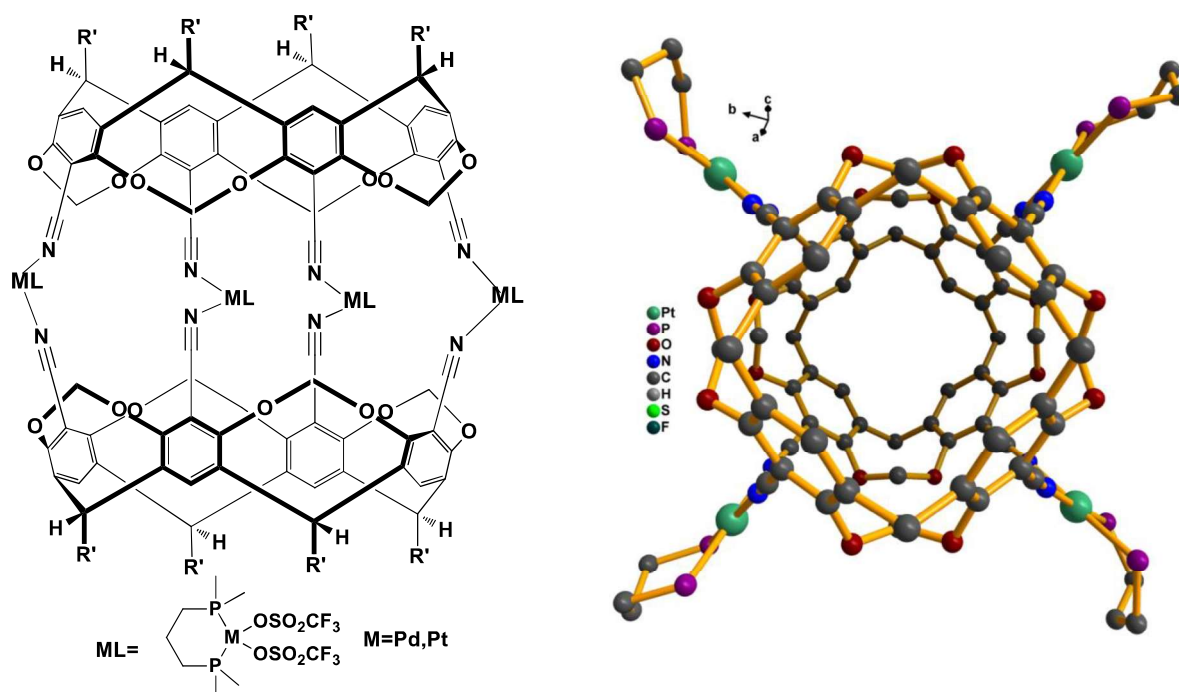


Figure 1.7. Resorcinarene based metallocapsule.

Harrison reported a pH dependent coordination cage by metalation of acid functionalized resorcinarene with CoCl_2 in the presence of base (Figure 1.8).²⁷

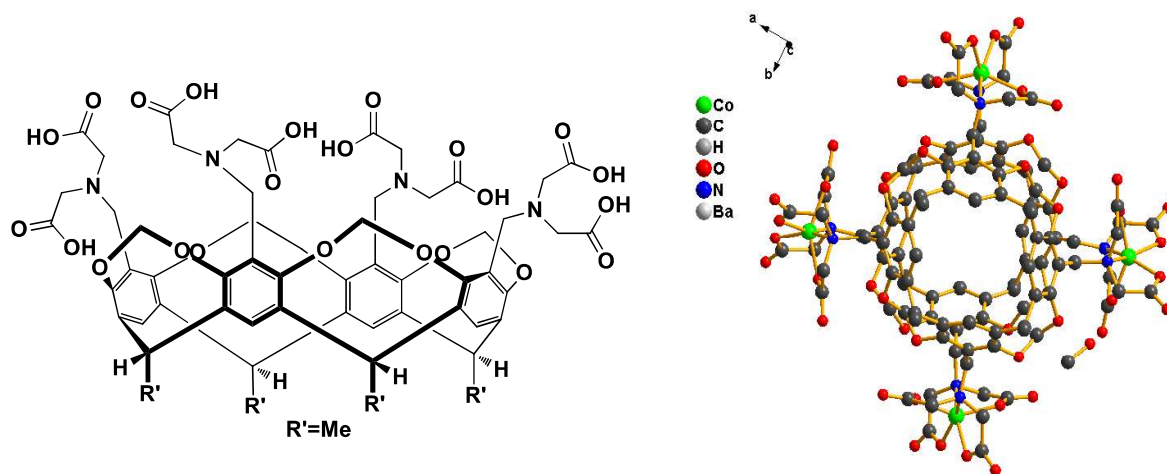


Figure 1.8. Acid functionalized resorcinarene and its Metallo cage.

A report by Shinkai and co-workers shows that Pyridine appended homooxalix[3]arene upon complexation with Pd^{2+} forms a coordination cage and it could entrap fullerene molecule (Figure 1.9).²⁸

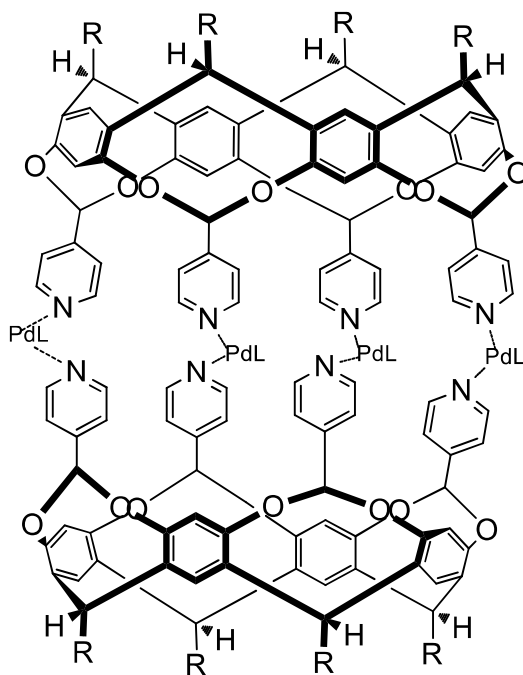


Figure 1.9. Pd^{2+} metallo cage of Pyridine functionalized homooxalix[3]arene

2,2'-bipyridine containing resorcinarene forms an extended cavity metallocage with Ag^+ . It was confirmed by NMR and mass analysis. The void space was found to trap large aromatic guest molecules (Figure 1.10).²⁹

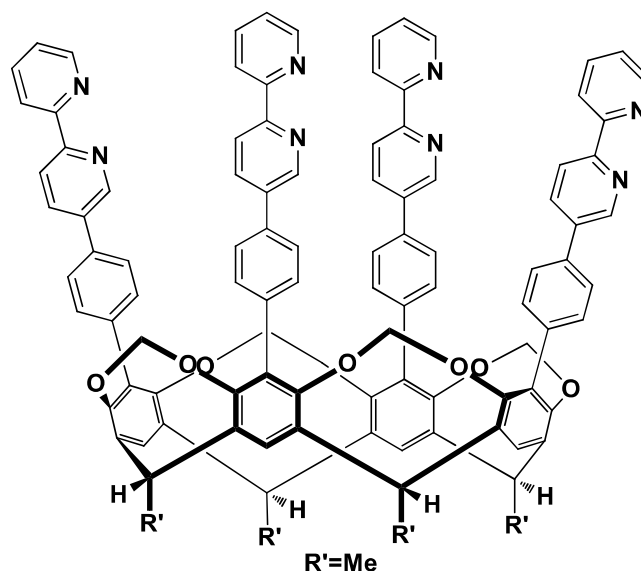


Figure 1.10. Structure of bipyridine appended resorcinarene based cavitand.

Cyclotrimeratrylene (CTV), apart from forming covalent capsule cryptophanes can also form metallo capsules known as metallocryptophanes. Abraham's group first reported this kind in 2010 with Cyclotricatechylene (CTC), a complete demethylated product of CTV. By deprotonating CTC with $\text{Ca}(\text{OH})_2$ as a base and the resultant anionic CTC binds to vanadium forming a tetrahedral cage.³⁰ Yamaguchi group published cycloguaiacylene (CTG) based metallocage. They attached pyridine to the upper rim of CTG and metallated with Pd^{2+} to get metallocryptophane.³¹

Michaele J. Hardie did a pioneering work on metallosupramolecular chemistry of CTV by attaching different heterocyclic rings with various metals to form metalloassemblies such as cage, catenane, borromean ring, Solomon cube which are illustrated in a nice review.³²

1.1.3. Hydrogen bonded molecular capsules

Capsular formations driven and held by hydrogen bonding are known as hydrogen bonded molecular capsules. Among numerous examples, here only few are presented. The first of this kind was reported by Rebek using a acyclic glycouril derivative which forms a dimeric spherical assembly (Figure 1.11). They named it as a tennis ball. It was characterized by NMR and mass spectroscopy.³³

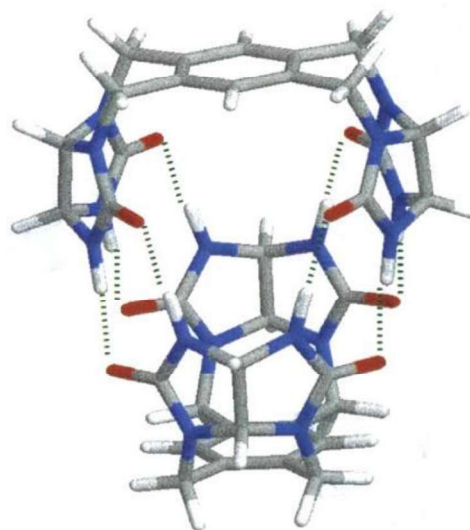
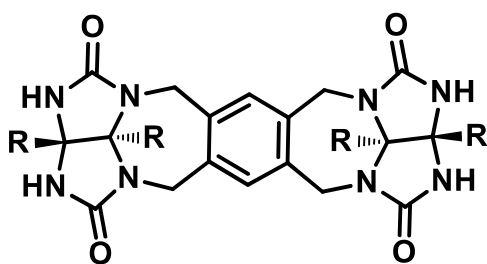


Figure 1.11. Two glycouril molecules connected by a durene molecule and cartoon representation of its self assembly to form a capsule.

Another examples is functionalized calix[4]arene with carboxylic acid group dimerizes to form capsular assembly which is confirmed by crystal structure (Figure 1.12).³⁴ Extending the size to calix[6]arene with three carboxylic groups at the upper rim undergoes self-assembly to form a capsule with extended interior volume.³⁵ amidinium functionalised Calix[4]arenes on one side and the complementarily negatively charged sulfonyl groups appended calix[4]arene on the other side resulted in formation of capsular assembly with ionic interactions in polar solvents.³⁶

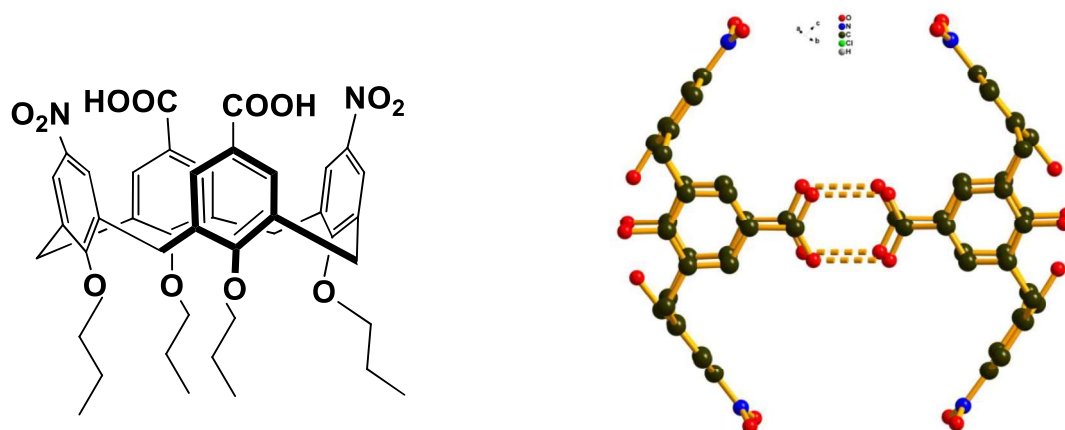


Figure 1.12. Carboxylic group functionalized calix[4]arene and its hydrogen bonded capsular assembly.

Resorcinarene is a rigid bowl shaped molecule with a suitably placed hydroxyl groups that can form hydrogen bond with the suitable acceptors. Atwood and co-workers reported hexameric assembly of resorcinarene with 60 hydrogen bonds and 8 water molecules between them (Figure 1.13).³⁷

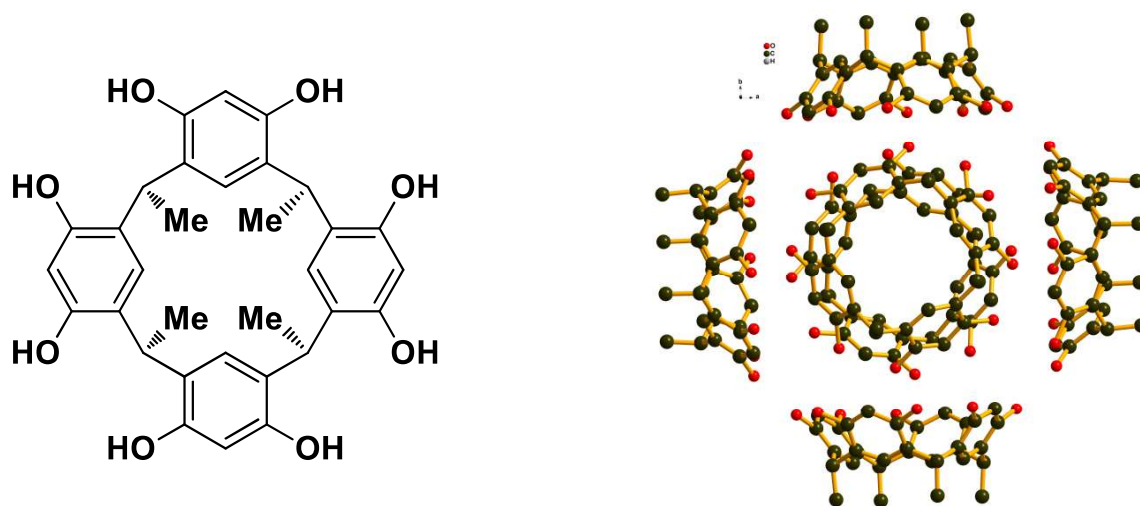


Figure 1.13. Structure of resorcinarene and its hexameric assembly.

1.1.4. Functional Properties

One of the many applications of molecular capsules is using it as a reaction vessel. Rebek and co-workers demonstrated that self-assembled soft ball accelerated diels-alder reaction by two fold magnitude at room temperature. The true catalytic activity was not studied because of the product having strong binding affinity towards capsule (Figure 1.14).³⁸

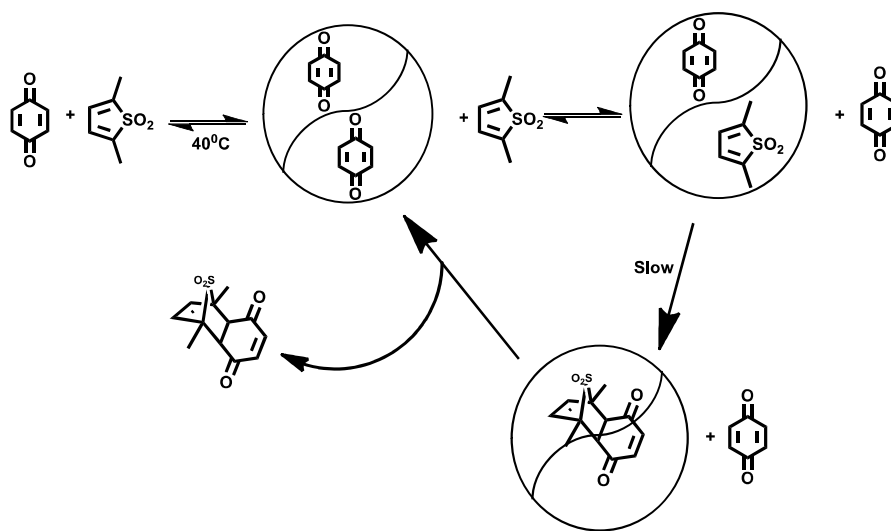


Figure 1.14. Rebeck's soft ball catalysing Diels-alder reaction.

Fujita and co-workers have utilized metalcages as reactors. They performed [2+2] photodimerisation of acenaphthylenes, naphthaquinones in aqueous medium in the presence of cage that give rise to only syn and head-to-tail isomers (Figure 1.15).³⁹

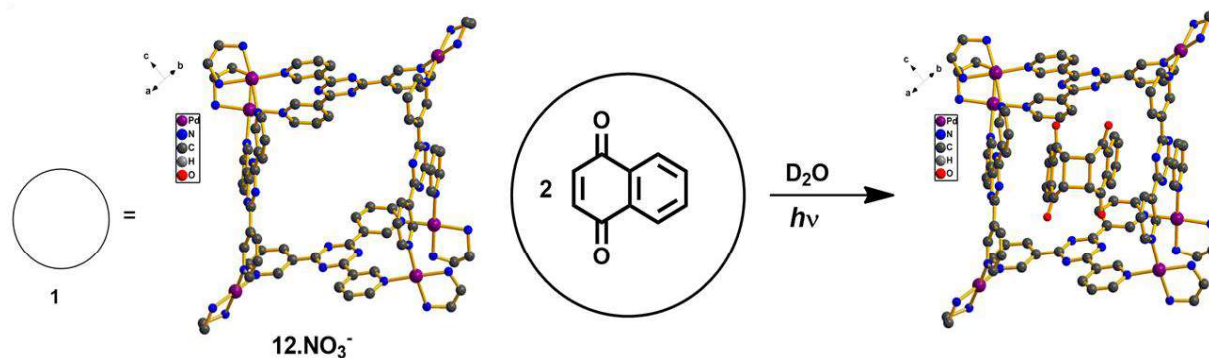


Figure 1.15. Fujita's cage directed stereoselective [2+2] photodimerisation.

Molecular capsules can also be used to store reactive and unstable species. Cram's group synthesized unstable cyclobutadiene and conducted reactions with cyclobutadiene inside the cage.⁴⁰ In 2009, Jonathan R. Nitschke and co-workers encapsulated white phosphorous inside a tetrahedral capsule and thus made it air stable (Figure 1.16).⁴¹

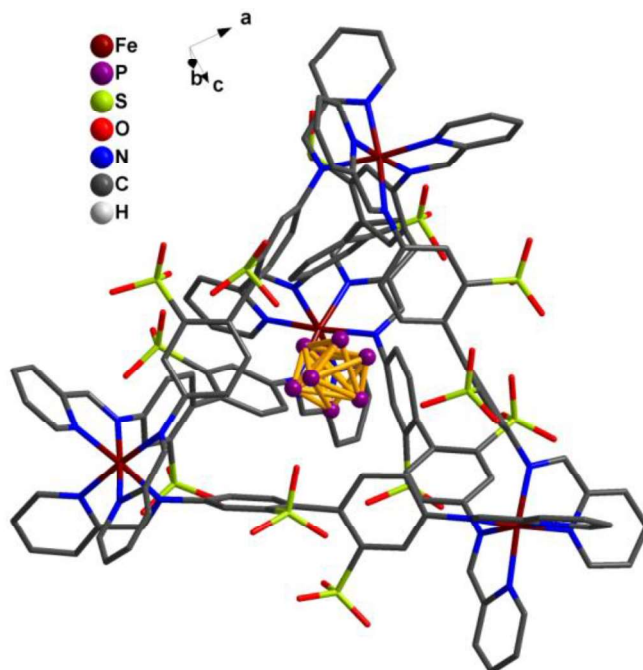


Figure 1.16. Crystal structure of white phosphorous entrapped in a tetrahedral capsule ⁴¹

1.2. Cavitiand based receptors for anions and ion-pairs

The design of artificial receptors for molecular recognition and sensing is a topic of great interest in Supramolecular chemistry.⁴²⁻⁴³ Such receptors play a crucial role in biological, environmental and chemical sciences. Among many receptors cavitiand based receptors are particularly fascinating because they offer shape, rigidity, symmetry, preorganisation and hosting properties.⁴⁴ So far considerable effort has been made towards the recognition and sensing of either anion or cation but less attention has been paid to ion-pair receptors that simultaneously bind cation and anion. In recent years, chemists focussed on designing of these receptors⁴⁵⁻⁴⁶ owing to their potential applications that include salt extraction, solubilisation and as membrane transfer agents (Figure 1.17).⁴⁷⁻⁴⁸

Calix[n]arenes are the macrocyclic molecules that possess a concave shape have been widely used for both anion and ion pair recognition.⁴⁹⁻⁵¹ For example, Early reports include attaching metallocene units via amide bond to the calix[4]arene that offers a combination of hydrogen bonding and electrostatic interaction which in turn acts as a anion sensor through electrochemical and spectrochemical methods.⁵²

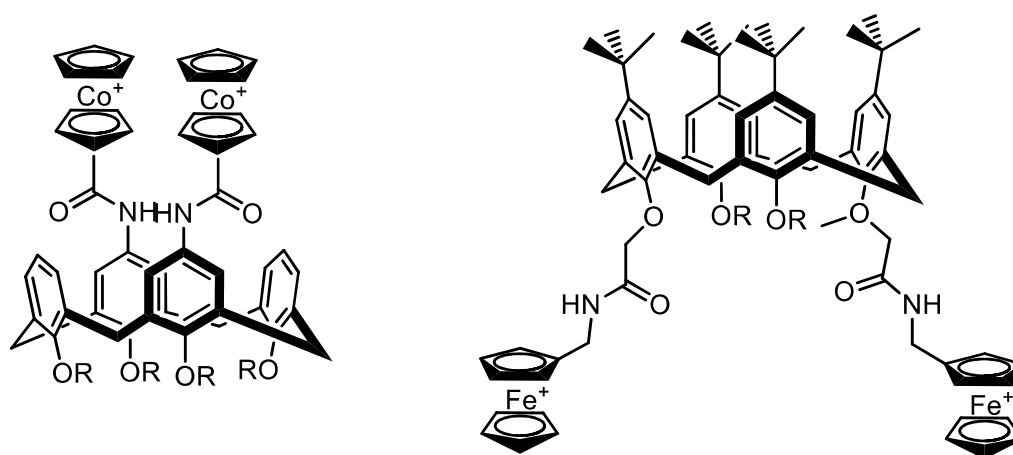


Figure 1.17. Metallocenes appended calix[4]arene anion receptors.

Later numerous anion receptors based calix[4]arene were developed by attaching variety of functional groups such as urea, Thiourea, quaternary ammonium and phosphonium salts etc.⁴⁹ Further calix[4]arene hosts were explored as ion-pair receptors.^{51, 53} Reinhoudt and co-workers reported this kind by attaching anion binding urea units at upper rim and ester functionality at the lower rim of the calix[4]arene that results ionophores selective for sodium ion. Thus the combination of these binding units makes this as sodium salts receptor and also it even solubilises sodium salts in chloroform (Figure 1.18).⁵⁴

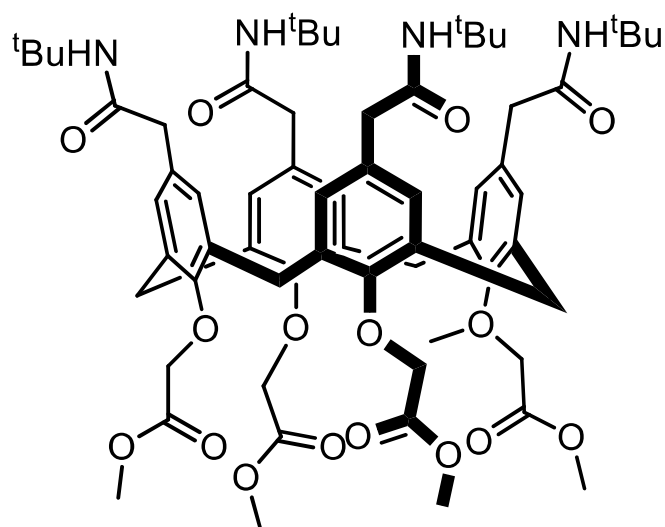


Figure 1.18. Calix[4]arene based sodium salts ion pair receptor.

Based on this report many receptors were designed by attaching different combination of anion (urea, thiourea, calixpyrrole etc.) and cation (crown ethers) binding groups.⁵¹ Jabin and co-workers extended this idea to make calix[6]arene receptors where unlike calix[4]arene receptors, cation here was stabilized by the cavity of the calix[6]arene moiety (Figure 1.19).⁵⁵⁻⁵⁸ They studied binding properties of these receptors towards anions and cations particularly ammonium salts using NMR, UV-Vis spectroscopy, fluorescence spectroscopy.

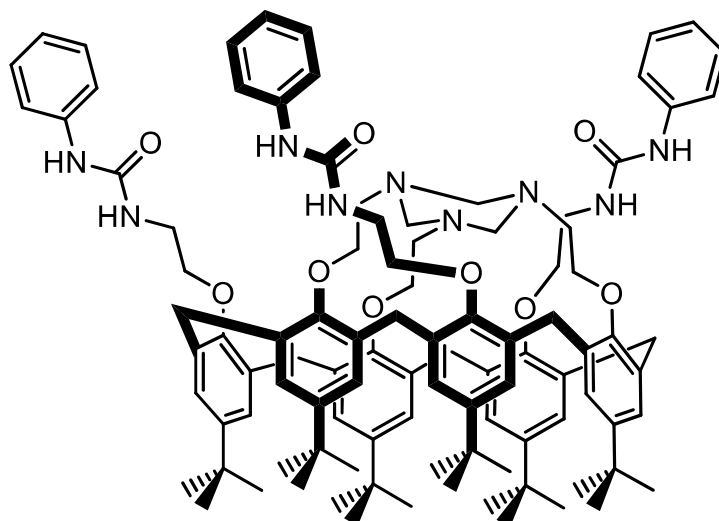


Figure 1.19. Jabin's heteroditopic receptor.

Pillar[n]arenes are a class macrocyclic compounds that comprises of hydroquinone units joined by methylene bridges at para position. Due to this, aromatic rings aligned in a cyclic pillar architecture making the cavity electron rich. As a result these molecules were able to bind electron deficient species.⁵⁹ By making use of this electron rich cavity, recently an ion pair receptor was reported by attaching urea unit to the pillar[5]arene (Figure 1.20).⁶⁰⁻

61

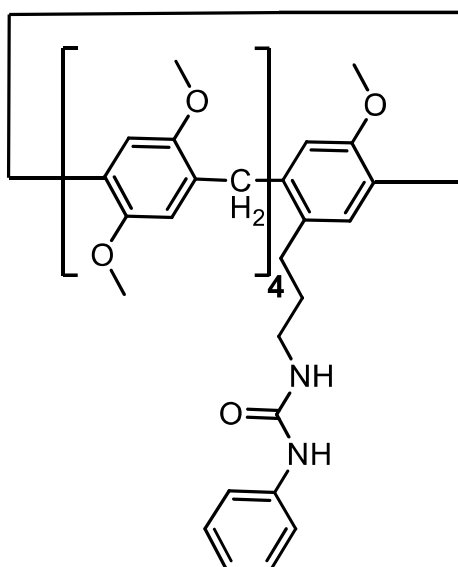


Figure 1.20. Urea appended Pillar[5]arene ion pair receptor

Hemicryptophanes are the molecular containers that consists of Cyclotrimeratrylene (CTV) unit joined by C_3 -symmetric organic group. ⁶²⁻⁶³ CTV is a rigid cyclic trimer of veratrole. Its pyramidal structure gives it a hydrophobic cavity that acts as molecular host for cationic species. Datusta and co-workers first time reported the heteroditopic receptor based on hemicryptophane by attaching tripodal anion binding site. This receptor forms inclusion complexes with tetramethylammonium salts (Figure 1.21).⁶⁴

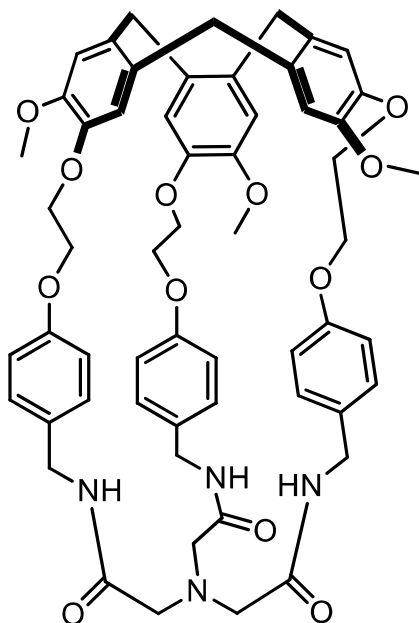


Figure 1.21. Hemicryptophane based ion pair receptor.

Apart from these examples, calix[4]pyrrole⁶⁵, resorcinarene⁶⁶ based anion and ion pair receptors are also known in the literature.

Part-II

1.3. Metal Organic Architectures

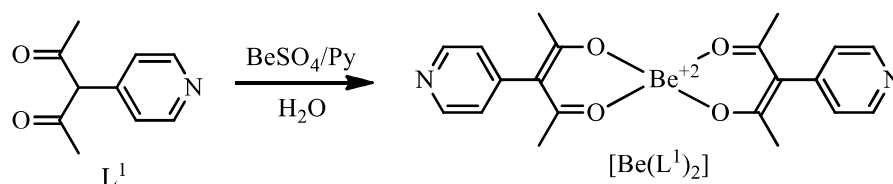
The organisation of single functional molecule to designed materials with predictable and controllable architectures has received enormous attention recent years⁶⁷⁻⁶⁸ owing to their fascinating properties which include separation,⁶⁹ sensing,⁷⁰ ion exchange and transport,⁷¹ luminescent materials and devices,⁷² optics,⁷⁰ magnetism⁷³ and catalysis.⁷⁴ These architectures are often three dimensional and are known as metal organic frameworks (MOFs), coordination networks (CNs) and coordination polymers (CPs).

These can be synthesized by mixing organic ligand with the metal salt. This is the simple method by which many MOFs, CNs, CPs were prepared.⁷⁵⁻⁷⁶ But the resultant architecture was not always predictable and mostly serendipitous. The major disadvantage is the formation of mixture of different architectures if different metal salts were used. Therefore a step wise method was implemented where organic ligand is first converted to metalloligand by metalltion and then addition of second metal lead to formation of heterometallic architecture. A metalloligand is a discrete coordinate complex and also consists of vacant coordinating sites for secondary metal ions. These can be mono, di, polynuclear depends on the choice of ligand.

1.3.1. Mononuclear metalloligands

These are the complexes where single metal atom or ion was surrounded by organic ligands with vacant coordinating sites. Wide range molecules were exploited in the literature as a mononuclear metalloligands that were effectively utilized for variety of heterometallic complexes.⁶⁷⁻⁶⁸ Examples include derivatives of acetylacetonate, β -diketonate, dipyrromethane, phophyrin, salen, 2,5-pyridine dicarboxylate etc.

Acetylacetonate ligand is a O,O-donor that forms neutral complexes of type $[M^{2+}L_2]$ and $[M^{+3}L_3]$ in the presence of base. Domasevitch *et al* reported a Be^{2+} centered metalloligand with 3-pyridylacetylacetonate (L^1) and its mixed metal complexes.⁷⁷ The metalloligand $[Be(L^1)_2]$ was prepared by the treatment of L^1 with $BeSO_4$ and pyridine in the aqueous solution. (Scheme 1.1)



Scheme 1.1. Synthesis of mononuclear metalloligand $[Be(L^1)_2]$

This metalloligand with cobalt(II) sulphate forms a 2D polymer where sulphate anion connects between two cobalt atoms. $[Be(L^1)_2]$ also forms coordination polymers with Cu_2X_2 (X - Cl, Br) where Cu(I) and mixed valent Cu(I,II) exists with copper-halogenide linkage. A square grid network was observed with Cu_2Br_2 . (Figure 1.22)

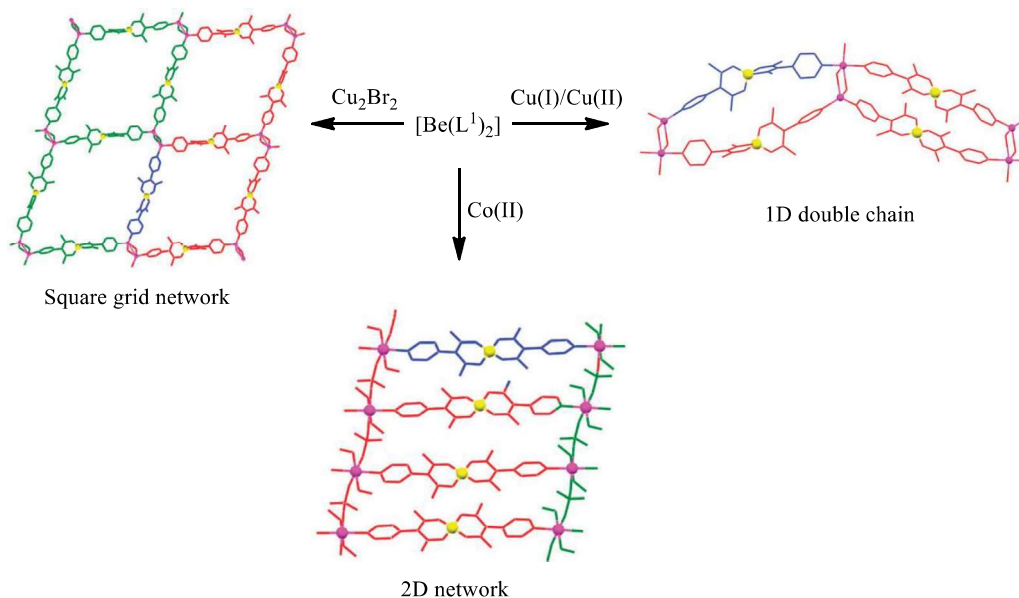


Figure 1.22. Heterometallic complexes of $[Be(L^1)_2]$

Later maverick and co-workers utilized the same ligand L^1 to prepare metalloligand $[Cu(L^1)_2]$ for the construction of heterometallic complexes.⁷⁸ The metalloligand with $Cd(NO_3)_2$ forms 1D non-interpenetrated ladder network and with square planar $CdCl_2$ forms 2D square grid network (Figure 1.23). Both these networks have a high porosity that could be useful for host-guest interactions at Cu^{2+} sites, but these were not stable under guest/solvent exchange condition.

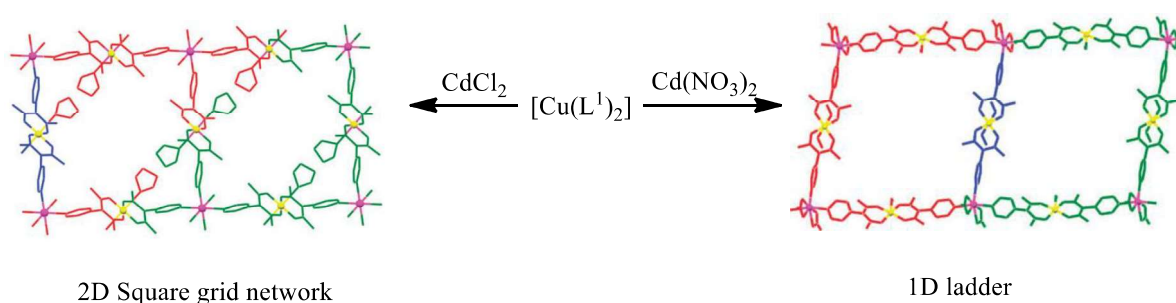


Figure 1.23. Mixed metal complexes of $[Cu(L^1)_2]$

1.3.2. Dinuclear metalloligands

Coordination complexes having two metal ions assisted by organic ligands with vacant sites are known as dinuclear metalloligands. Few ligands in this class are known such as ortho-Phenylene-bis(oxamate) (L^2)⁷⁹, pyrazolyl pyridine (L^3)⁸⁰ derivatives etc. (Figure 1.24.)

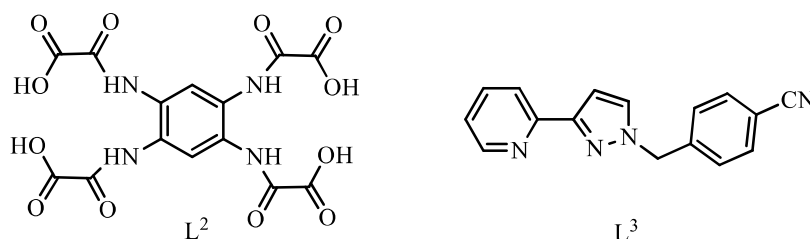


Figure 1.24. Chemdraw structures of L^2 and L^3 .

1.3.3. Polynuclear metalloligands

Owing to the synthetic difficulty, polynuclear metalloligands were rarely documented in the literature. For example 2-mercaptopyridine-3-carboxylic acid (L^4) was utilized for the construction of polynuclear Metalloligand and its heterometallic complexes.⁸¹ Reaction of L^4 with $AgNO_3$ in water gives precipitate which was treated with aq. NH_3 to obtain silver hexanuclear anionic Metalloligand (L^4_{Ag}) (Figure 1.25).

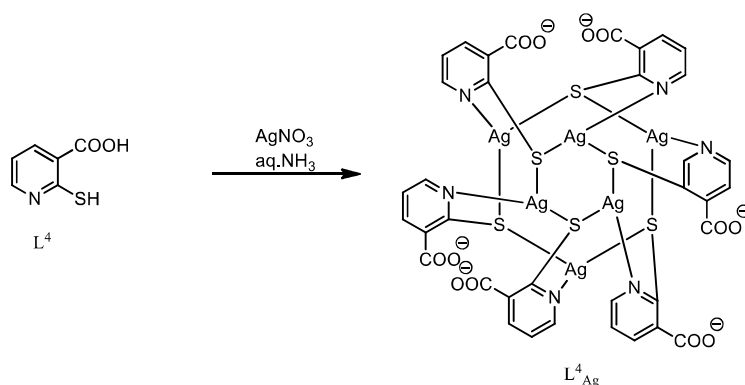


Figure 1.25. Synthesis of polynuclear metalloligand L^4_{Ag} .

Treating L^4_{Ag} with $Cu(II)OAc$ and bipyridine resulting a 1D chain heterometallic complex where as with $Zn(II)OAc$ and ethylene diamine gives a 2D sheet structure (Figure 1.26).

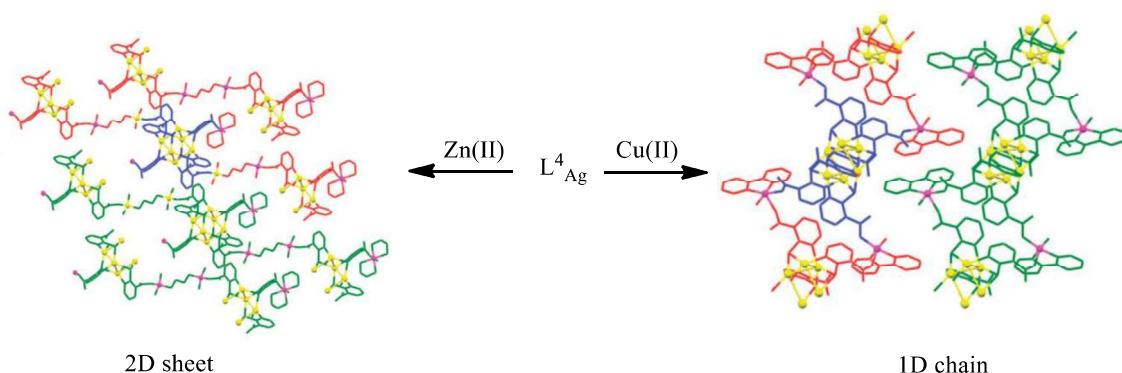


Figure 1.26. Synthesis of mixed metal complexes from L^4_{Ag} .

Part-III

1.4. Interlocked Molecules

Interlocked molecules are the molecules where the components were held each other mechanically i.e., by mechanical bond such that the components cannot be detached without breaking at least one chemical bond.⁸² The two main examples include rotaxane and catenane. A rotaxane derived from the Latin words *rota* and *axis*, meaning wheel and axle, respectively, is composed of a linear chain, referred to as an axle, which threads through a ring. A catenane is a interlocked rings (Figure 1.27). The nomenclature for rotaxane is [n]rotaxane and for catenane is [n]catenane where n is the number of components connected by mechanical bond. These molecules have found potential applications that include molecular machines, molecular rotor, chemical sensing and catalysis etc.⁸³⁻⁸⁴

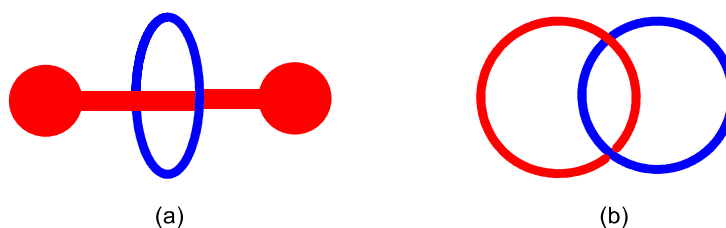


Figure 1.27. Cartoon representation of (a) Rotaxane ; (b) Catenane.

Wasserman prepared the first interlocked molecule, [2]catenane using a statistical approach which relies on the chance formation of one macrocycle while threaded through

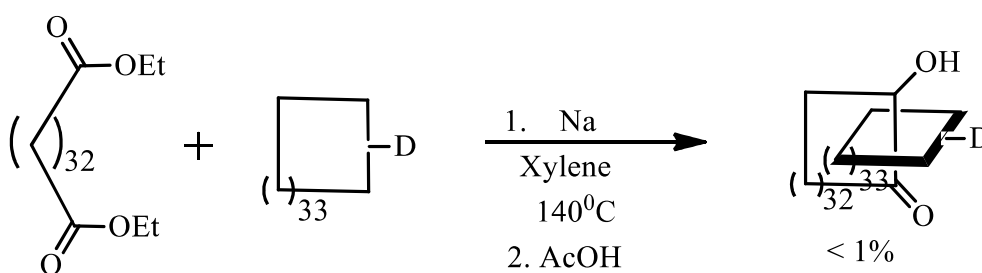


Figure 1.28. Wasserman's statistical approach for [2]catenane.

another. An acycloin condensation which is a macrocyclisation reaction was performed in the presence of a macrocycle lead to [2]catenane in < 1% yield (Figure 1.28).⁸⁵

Later template directed methods were developed for the synthesis of catenanes. First of this kind was reported by Sauvage and co-workers using metal as a template.⁸⁵ (Detailed explanation was given the chapter-5). Following this many templated methods were reported in the literature.

1.4.1. Hydrogen bond templated [2]catenane

In 1992 Vogtle and Hunter independently reported amide based assembly of [2]catenane driven by hydrogen bonding of an amide N-H to a carbonyl oxygen. (Figure 1.29).⁸⁶⁻⁸⁷

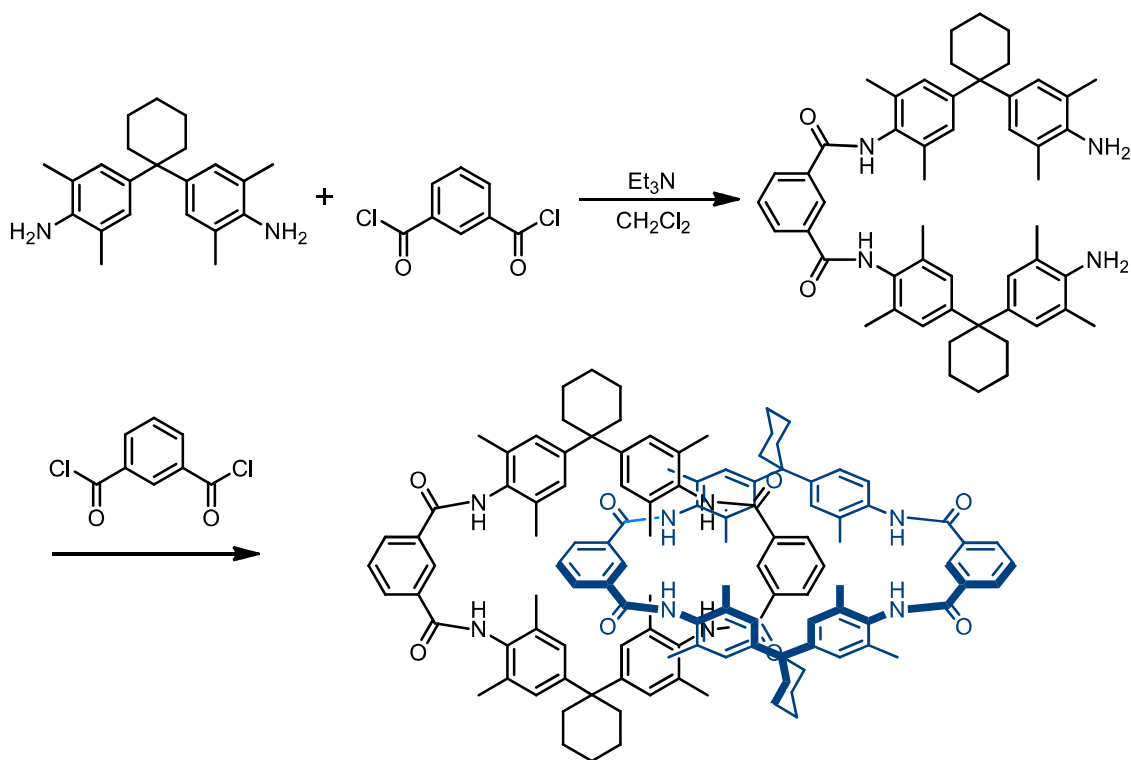


Figure 1.29. Hunter's hydrogen bond template [2]catenane.

Later Leigh and co-workers reported synthesis of [2]catenane templated by hydrogen bonding. Reacting equimolar ratio of isophthaloyl dichloride and para-xylenediamine yields [2]catenane in 20% yield.⁸⁸

1.4.2. Aromatic donor-acceptor templated [2]catenane

Stoddart and co-workers first reported this kind by reacting a bis-pyridine-bis-pyridinium molecule with 1,4-bis(bromomethyl)benzene, in the presence of bis-para-phenylene-34-crown-10 undergoes threading during cyclisation due to donor-acceptor interactions between electron rich hydroquinone and the electron-poor bipyridinium units resulting [2]catenane in 70% yield.⁸⁹ (exemplified in chapter-5)

1.4.3. Anion templated [2]catenane

Beer and co-workers first time synthesised [2]catenane by chloride ion templation by RCM of pyridinium chloride thread in the presence of isophthalamide macrocycle in 45% yield where as if bromide was used in the place of chloride yield was reduced to 6% and with iodide, hexafluorophosphate no catenane was observed confirming the role of chloride anion as a template (Figure 1.30).⁹⁰

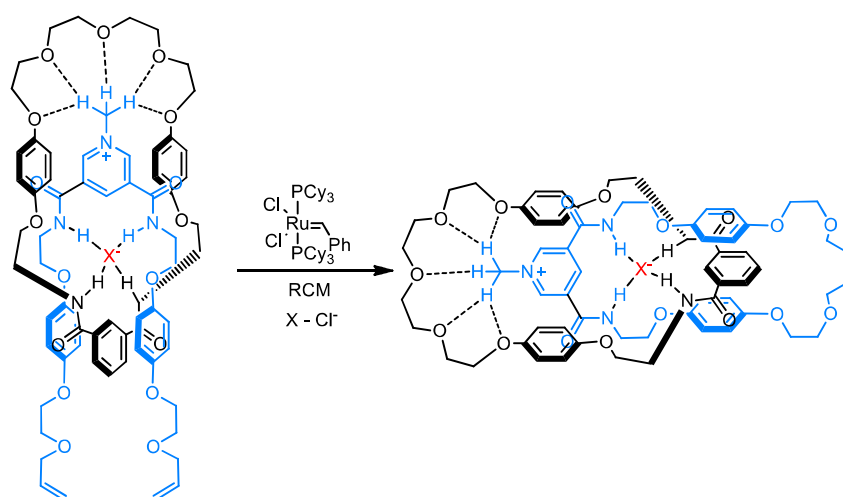


Figure 1.30. Beer's anion template [2]catenane.

1.4.4. Salt bridge templated [2]catenane

Yoshima and co-workers reported this kind by utilising amidine-carboxylate salt bridge followed by RCM (Figure 1.31).

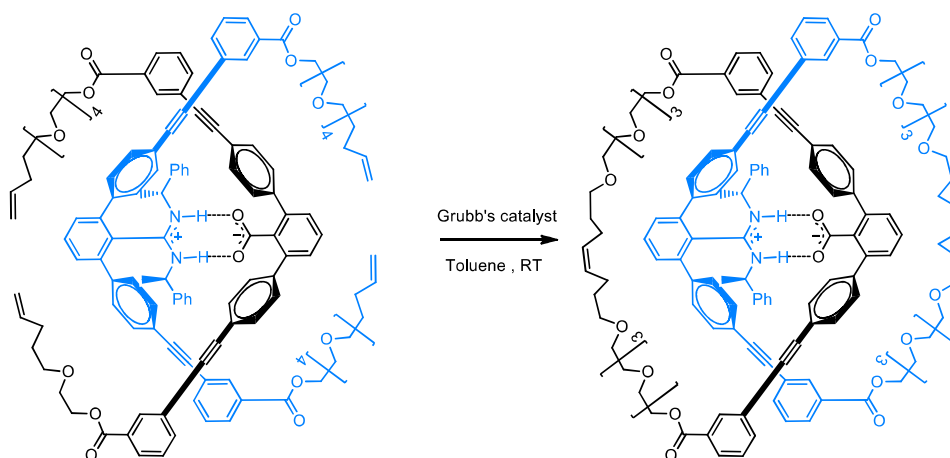


Figure 1.31. Amidine-carboxylate salt bridge templated [2]catenane.

Apart from these Fujita's thermodynamically controlled [2]catenane,⁹¹ crown ether-dibenzylammonium catenane,⁹² sodium templated approach,⁹³ radical templated method⁹⁴, Halogen bonding template method⁹⁵ etc were also known in the literature.

Objective of the Thesis

The main objective of the thesis is (a) Capsules and cages are well studied for calix[n]arene systems but less explored for CTC and its derivatives. In chapter-2 synthesis and characterisation of a molecular capsule based on CTC is described. It is established that the molecule forms a capsular structure in solid state. (b) A CTC based receptor is designed and studied for its binding properties. This is elaborated in chapter-3. (c) Heterometallic complexes based on pyridine are well documented but its analogue pyrazine was less studied. A heterometallic Pyrazine complexes are described in chapter-4. The complexes were studied by single crystal X-ray spectroscopy. (d) A bis-pyridine system for making [3]catenane is

described in chapter-5. The [3]catenane would be obtained by cleaving bis-pyridine derivative.

1.5. References

1. Lehn, J. M., *Acc. Chem. Res.* **1978**,*11*, 49.
2. Cram, D. J., *Science* **1983**,*219*, 1177.
3. Cram, D. J.; Karbach, S.; Kim, Y. H.; Baczynskyj, L.; Kallemeyn, G. W., *J. Am. Chem. Soc.* **1985**,*107*, 2575.
4. Cram, D. J., *Angew. Chem. Int. Ed.* **1986**,*25*, 1039.
5. Cram, D. J., *Nature* **1992**,*356*, 29.
6. Jasat, A.; Sherman, J. C., *Chemical Reviews* **1999**,*99*, 931.
7. Moran, J. R.; Ericson, J. L.; Dalcanale, E.; Bryant, J. A.; Knobler, C. B.; Cram, D. J., *J. Am. Chem. Soc.* **1991**,*113*, 5707.
8. Cram, D. J.; Karbach, S.; Kim, Y. H.; Baczynskyj, L.; Marti, K.; Sampson, R. M.; Kallemeyn, G. W., *J. Am. Chem. Soc.* **1988**,*110*, 2554.
9. Cram, D. J.; Tanner, M. E.; Knobler, C. B., *J. Am. Chem. Soc.* **1991**,*113*, 7717.
10. Robbins, T. A.; Knobler, C. B.; Bellew, D. R.; Cram, D. J., *J. Am. Chem. Soc.* **1994**,*116*, 111.
11. von dem Bussche-Hunnefeld, C.; Buhring, D.; Knobler, C. B.; Cram, D. J., *J. Chem. Soc., Chem. Commun.* **1995**, 1085.
12. Chapman, R. G.; Olovsson, G.; Trotter, J.; Sherman, J. C., *J. Am. Chem. Soc.* **1998**,*120*, 6252.
13. Yoon, J.; Cram, D., *Chem. Commun.* **1997**, 497.
14. Warmuth, R.; Yoon, J., *Acc. Chem. Res.* **2001**,*34*, 95.
15. Quan, M. L. C.; Cram, D. J., *J. Am. Chem. Soc.* **1991**,*113*, 2754.

16. Böhmer, V.; Goldmann, H.; Vogt, W.; Vicens, J.; Asfari, Z., *Tetrahedron Lett.* **1989**,*30*, 1391.
17. Timmerman, P.; Verboom, W.; van Veggel, F. C. J. M.; van Hoorn, W. P.; Reinhoudt, D. N., *Angew. Chem. Int. Ed.* **1994**,*33*, 1292.
18. Böhmer, V., *Angew. Chem. Int. Ed.* **1995**,*34*, 713.
19. Neri, P.; Bottino, A.; Cunsolo, F.; Piattelli, M.; Gavuzzo, E., *Angew. Chem. Int. Ed.* **1998**,*37*, 166.
20. Lücking, U.; Tucci, F. C.; Rudkevich, D. M.; Rebek, J., *J. Am. Chem. Soc.* **2000**,*122*, 8880.
21. Gabard, J.; Collet, A., *J. Chem. Soc., Chem. Commun.* **1981**, 1137.
22. Cram, D. J.; Tanner, M. E.; Keipert, S. J.; Knobler, C. B., *J. Am. Chem. Soc.* **1991**,*113*, 8909.
23. Brotin, T.; Devic, T.; Lesage, A.; Emsley, L.; Collet, A., *Chem. Eur. J.* **2001**,*7*, 1561.
24. Brotin, T.; Dutasta, J.-P., *Chemical Reviews* **2009**,*109*, 88.
25. Kataoka, K.; James, T. D.; Kubo, Y., *J. Am. Chem. Soc.* **2007**,*129*, 15126.
26. Jacopozzi, P.; Dalcanale, E., *Angew. Chem. Int. Ed.* **1997**,*36*, 613.
27. Fochi, F.; Jacopozzi, P.; Wegelius, E.; Rissanen, K.; Cozzini, P.; Marastoni, E.; Fisicaro, E.; Manini, P.; Fokkens, R.; Dalcanale, E., *J. Am. Chem. Soc.* **2001**,*123*, 7539.
28. Ikeda, A.; Udzu, H.; Yoshimura, M.; Shinkai, S., *Tetrahedron* **2000**,*56*, 1825.
29. Haino, T.; Kobayashi, M.; Chikaraishi, M.; Fukazawa, Y., *Chem. Commun.* **2005**, 2321.
30. Abrahams, B. F.; FitzGerald, N. J.; Robson, R., *Angew. Chem. Int. Ed.* **2010**,*49*, 2896.
31. Zhong, Z.; Ikeda, A.; Shinkai, S.; Sakamoto, S.; Yamaguchi, K., *Organic Letters* **2001**,*3*, 1085.
32. Henkelis, J. J.; Hardie, M. J., *Chem. Commun.* **2015**,*51*, 11929.

33. Wyler, R.; de Mendoza, J.; Rebek, J., *Angew. Chem. Int. Ed.* **1993**,32, 1699.
34. Struck, O.; Verboom, W.; J. J. Smeets, W.; L. Spek, A.; N. Reinhoudt, D., *J. Chem. Soc., Perkin Trans. 2* **1997**, 223.
35. Arduini, A.; Domiano, L.; Ogliosi, L.; Pochini, A.; Secchi, A.; Ungaro, R., *J. Org. Chem.* **1997**,62, 7866.
36. Corbellini, F.; Fiammengo, R.; Timmerman, P.; Crego-Calama, M.; Versluis, K.; Heck, A. J. R.; Luyten, I.; Reinhoudt, D. N., *J. Am. Chem. Soc.* **2002**,124, 6569.
37. MacGillivray, L. R.; Atwood, J. L., *Nature* **1997**,389, 469.
38. Kang, J.; Rebek, J., *Nature* **1997**,385, 50.
39. Yoshizawa, M.; Takeyama, Y.; Kusakawa, T.; Fujita, M., *Angew. Chem. Int. Ed.* **2002**,41, 1347.
40. Cram, D. J.; Tanner, M. E.; Thomas, R., *Angew. Chem. Int. Ed.* **1991**,30, 1024.
41. Mal, P.; Breiner, B.; Rissanen, K.; Nitschke, J. R., *Science* **2009**,324, 1697.
42. Lehn, J.-M., *Supramolecular Chemistry: Concepts and Perspectives*; Wiley-VCH: Weinheim, Germany, **1995**.
43. Steed, J. W.; Turner, D. R. W., K. J., *Core Concepts in Supramolecular Chemistry and Nanochemistry*; Wiley, Chichester, U.K **2007**.
44. Coquiere, D.; Le Gac, S.; Darbost, U.; Seneque, O.; Jabin, I.; Reinaud, O., *Org. Biomol. Chem.* **2009**,7, 2485.
45. Gale, P. A., *Coord. Chem. Rev.* **2003**,240, 191.
46. "Ion Pair Recognition by Ditopic Receptors" : B. D. Smith in *Macrocyclic Chemistry: Current Trends and Future Perspectives* (Ed.: K. Gloe), Springer, Dordrecht. **2005**, 137

47. Rudkevich, D. M.; Mercer-Chalmers, J. D.; Verboom, W.; Ungaro, R.; de Jong, F.; Reinhoudt, D. N., *J. Am. Chem. Soc.* **1995**,*117*, 6124.
48. J. White, D.; Laing, N.; Miller, H.; Parsons, S.; A. Tasker, P.; Coles, S., *Chem. Commun.* **1999**, 2077.
49. Matthews, S. E.; Beer, P. D., *Supramolecular Chemistry* **2005**,*17*, 411.
50. Lo, P. K. W., M.S. , *Sensors* **2008**,*8*, 5313.
51. Kim, S. K.; Sessler, J. L., *Chem. Soc. Rev.* **2010**,*39*, 3784.
52. Beer, P. D., *Chem. Commun.* **1996**, 689.
53. McConnell, A. J.; Beer, P. D., *Angew. Chem. Int. Ed.* **2012**,*51*, 5052.
54. Scheerder, J.; van Duynhoven, J. P. M.; Engbersen, J. F. J.; Reinhoudt, D. N., *Angew. Chem. Int. Ed.* **1996**,*35*, 1090.
55. Hamon, M.; Ménand, M.; Le Gac, S.; Luhmer, M.; Dalla, V.; Jabin, I., *J. Org. Chem.* **2008**,*73*, 7067.
56. Le Gac, S.; Ménand, M.; Jabin, I., *Org. Lett.* **2008**,*10*, 5195.
57. Ménand, M.; Jabin, I., *Org. Lett.* **2009**,*11*, 673.
58. Brunetti, E.; Picron, J.-F.; Flidrova, K.; Bruylants, G.; Bartik, K.; Jabin, I., *J. Org. Chem.* **2014**,*79*, 6179.
59. Xue, M.; Yang, Y.; Chi, X.; Zhang, Z.; Huang, F., *Acc. Chem. Res.* **2012**,*45*, 1294.
60. Ni, M.; Guan, Y.; Wu, L.; Deng, C.; Hu, X.; Jiang, J.; Lin, C.; Wang, L., *Tetrahedron Lett.* **2012**,*53*, 6409.
61. Gao, L.; Dong, S.; Zheng, B.; Huang, F., *Eur. J. Org. Chem.* **2013**,*2013*, 1209.
62. Canceill, J.; Collet, A.; Gabard, J.; Kotzyba-Hibert, F.; Lehn, J.-M., *Helv. Chim. Acta* **1982**,*65*, 1894.
63. Rapenne, G.; Diederich, F.; Crassous, J.; Collet, A.; Echegoyen, L., *Chem. Commun.* **1999**, 1121.

64. Perraud, O.; Robert, V.; Martinez, A.; Dutasta, J.-P., *Chem. Eur. J.* **2011**,*17*, 4177.
65. Kim, S. K.; Sessler, J. L., *Acc. Chem. Res.* **2014**,*47*, 2525.
66. Beyeh, N. K.; Weimann, D. P.; Kaufmann, L.; Schalley, C. A.; Rissanen, K., *Chem. Eur. J.* **2012**,*18*, 5552.
67. Kumar, G.; Gupta, R., *Chem. Soc. Rev.* **2013**,*42*, 9403.
68. Srivastava, S.; Gupta, R., *CrystEngComm* **2016**,*18*, 9185.
69. O’Keeffe, M.; Yaghi, O. M., *Chem. Rev.* **2012**,*112*, 675.
70. Hu, Z.; Deibert, B. J.; Li, J., *Chem. Soc. Rev.* **2014**,*43*, 5815.
71. Brozek, C. K.; Dinca, M., *Chem. Soc. Rev.* **2014**,*43*, 5456.
72. Wang, C.; Zhang, T.; Lin, W., *Chem. Rev.* **2012**,*112*, 1084.
73. Wang, X.-Y.; Wang, Z.-M.; Gao, S., *Chem. Commun.* **2008**, 281.
74. Ma, L.; Abney, C.; Lin, W., *Chem. Soc. Rev.* **2009**,*38*, 1248.
75. Kurmoo, M., *Chem. Soc. Rev.* **2009**,*38*, 1353.
76. Cook, T. R.; Stang, P. J., *Chem. Rev.* **2015**,*115*, 7001.
77. Vreshch, V. D.; Chernega, A. N.; Howard, J. A. K.; Sieler, J.; Domasevitch, K. V., *Dalton Trans.* **2003**, 1707.
78. Chen, B.; Fronczek, F. R.; Maverick, A. W., *Inorg. Chem.* **2004**,*43*, 8209.
79. Ruiz, R.; Faus, J.; Lloret, F.; Julve, M.; Journaux, Y., *Coord. Chem. Rev.* **1999**,*193–195*, 1069.
80. Fenton, H.; Tidmarsh, I. S.; Ward, M. D., *Dalton Transactions* **2010**,*39*, 3805.
81. Sun, D.; Wang, D.-F.; Han, X.-G.; Zhang, N.; Huang, R.-B.; Zheng, L.-S., *Chemical Communications* **2011**,*47*, 746.
82. Amabilino, D. B.; Stoddart, J. F., *Chem. Rev.* **1995**,*95*, 2725.
83. Gibson, H. W.; Bheda, M. C.; Engen, P. T., *Prog. Polym. Sci.* **1994**,*19*, 843.
84. Gil-Ramírez, G.; Leigh, D. A.; Stephens, A. J., *Angew. Chem. Int. Ed.* **2015**,*54*, 6110.

85. Wasserman, E., *J. Am. Chem. Soc.* **1960**,*82*, 4433.
86. Dietrich-Buchecker, C. O.; Sauvage, J. P.; Kintzinger, J. P., *Tetrahedron Lett.* **1983**,*24*, 5095.
87. Hunter, C. A., *J. Am. Chem. Soc.* **1992**,*114*, 5303.
88. Vögtle, F.; Meier, S.; Hoss, R., *Angew. Chem. Int. Ed* **1992**,*31*, 1619.
89. Johnston, A. G.; Leigh, D. A.; Pritchard, R. J.; Deegan, M. D., *Angew. Chem. Int. Ed* **1995**,*34*, 1209.
90. Ashton, P. R.; Goodnow, T. T.; Kaifer, A. E.; Reddington, M. V.; Slawin, A. M. Z.; Spencer, N.; Stoddart, J. F.; Vicent, C.; Williams, D. J., *Angew. Chem. Int. Ed* **1989**,*28*, 1396.
91. Sambrook, M. R.; Beer, P. D.; Wisner, J. A.; Paul, R. L.; Cowley, A. R., *J. Am. Chem. Soc.* **2004**,*126*, 15364.
92. Fujita, M.; Ibukuro, F.; Hagihara, H.; Ogura, K., *Nature* **1994**,*367*, 720.
93. Guidry, E. N.; Cantrill, S. J.; Stoddart, J. F.; Grubbs, R. H., *Org. Lett.* **2005**,*7*, 2129.
94. Tung, S.-T.; Lai, C.-C.; Liu, Y.-H.; Peng, S.-M.; Chiu, S.-H., *Angew. Chem. Int. Ed.* **2013**,*52*, 13269.
95. Barnes, J. C.; Fahrenbach, A. C.; Cao, D.; Dyar, S. M.; Frasconi, M.; Giesener, M. A.; Benítez, D.; Tkatchouk, E.; Chernyashevskyy, O.; Shin, W. H.; Li, H.; Sampath, S.; Stern, C. L.; Sarjeant, A. A.; Hartlieb, K. J.; Liu, Z.; Carmieli, R.; Botros, Y. Y.; Choi, J. W.; Slawin, A. M. Z.; Ketterson, J. B.; Wasielewski, M. R.; Goddard, W. A.; Stoddart, J. F., *Science* **2013**,*339*, 429.
96. Caballero, A.; Zapata, F.; White, N. G.; Costa, P. J.; Félix, V.; Beer, P. D., *Angew. Chem. Int. Ed.* **2012**,*51*, 1876.

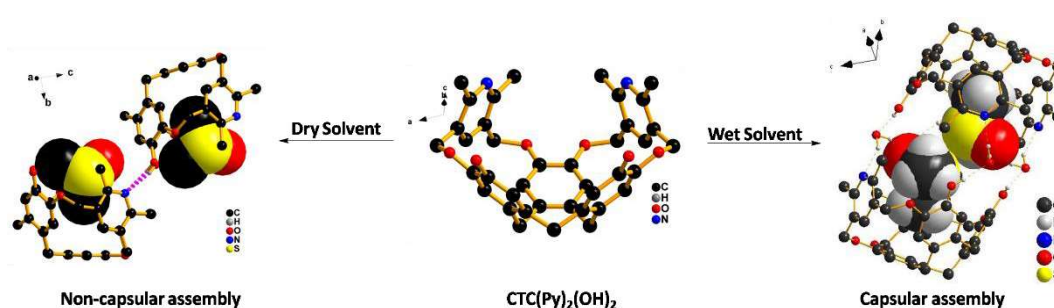
Chapter-2

Hydrogen Bonded Molecular Capsule: Probing Role of Water Molecules for Capsule Formation in a Modified Cyclotriphosphazene

2.1. Abstract.	89
2.2. Introduction.	91
2.3. Results and Discussion.	98
2.4. Experimental Section.	108
2.5. References.	112
2.6. Spectral Data.	116
2.7. Crystal Data.	124

2.1. Abstract

Two new pyridine moiety-appended cavitands, CTC(Py)₂(OH)₂ and CTC(Py)₃, were synthesized and characterized. The solid state structures of both cavitands were studied by single crystal X-ray diffraction. CTC(Py)₂(OH)₂ resulted in a hydrogen-bonded dimeric molecular capsule, entrapping two molecules of DMSO and intervening water molecules that formed hydrogen bonding to DMSO and CTC(Py)₂(OH)₂. When crystallized in the absence of water, it forms a 2D polymer by hydrogen bonding of pyridine nitrogen and phenolic hydrogen atoms. CTC(Py)₃ forms no such capsule



2.2. Introduction

Molecular capsules have attracted much attention of synthetic chemists and chemical biologists in the past few decades.¹⁻³ These are macro-molecules or supra-molecules, which have space inside to conceal other molecules as guests. First synthesis of these type of molecules were reported by Cram *et al.*⁴⁻⁵ These were formed by networks of covalent bonds that sealed-in their guests using mechanical forces rather than chemical ones. Apart from using covalent bonds for incarceration of guests (i.e., cryptands), non-covalent interactions like ionic interactions⁶, metal coordination⁷⁻¹⁰, hydrogen bonding¹¹⁻¹³, hydrophobic interactions¹⁴, or a combination of them^{15, 2} are used for entrapping guests. Recently halogen bonding has also been utilized for formation of capsular assembly.¹⁶ Guest molecules can also induce capsule formation.¹⁷⁻¹⁸ Formation of capsule by non-covalent interactions has the advantage of reversibly binding and releasing guest molecules, controlled by chemical and physical stimuli. One of the widely used non-covalent interaction for encapsulation is hydrogen-bonding.¹⁵ Some of the motifs like glycolurils^{1, 11, 19-22, 23-25} and resorcinarenes^{6, 14, 26-28} have been used information of hydrogen bonded molecular capsules. The rate of encapsulation can be varied, depending on the size and shape of guest(s)²⁹, as well as the feasibility of breaking salvation cage and allowing guest molecule to approach the host.³⁰

Cyclotrimeratrylene (CTV) is a C_3 -symmetric cyclic trimer of veratrole. It has a crown conformation which adopts a bowl shape with a molecular cavity³¹. CTV derivatives find potential applications in soft materials, sensing, separations, dendrimers, host-guest chemistry, metallo-supramolecular assemblies etc. CTV can be synthesized by acid catalysed condensation of veratrole alcohol. The members of CTV family include Cyclotriguaiacylene (CTG), a C_3 -symmetric trihydroxy derivative of CTV and Cyclotricatechylene (CTC), a complete demethylated product of CTV (Figure 2.1). Although CTV is capable of binding

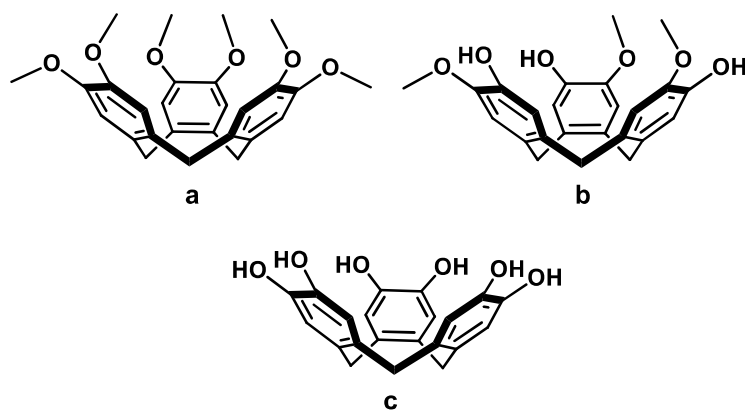


Figure 2.1.(a) *Cyclotrimeratrylene (CTV)*; (b) *Cyclotriguaiacylene (CTG)*; (c) *Cyclotricatechylene (CTC)*.

guest molecules, its host-guest chemistry is limited because of its shallow cavity. This problem was addressed by using extended-cavity CTVs. CTV can be extended by mostly two approaches. One is to use CTG that can undergo substitution reactions with suitable alkyl halides to give ether-tethered side arms or acid chlorides to give ester-tethered side arms in the presence of base. Synthesis of novel CTV hosts by this method was well documented in the literature³¹⁻³². For instance CTV forms 1:1 inclusion complex with fullerene (C_{60}) via π - π interaction.³³ The binding ability of C_{60} is improved by using dendric tris-CTV. The binding constant increases with increase in the number of dendric substituents on the CTV core ($G_3 > G_2 > G_1$) (Figure 2.2).³⁴

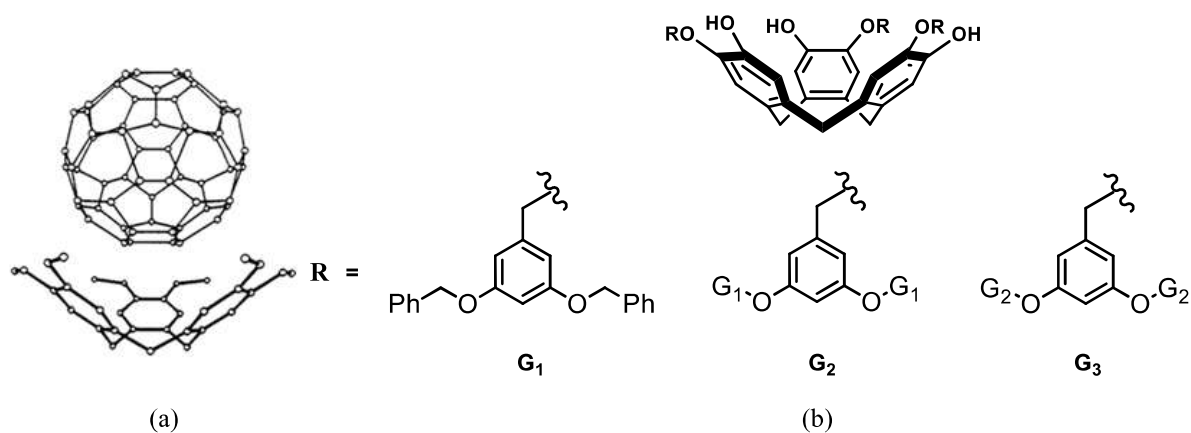


Figure 2.2.(a) *CTV and C_{60} inclusion complex*³³; (b) *Dendric tris-CTVs with varying size*

Extended-cavity CTVs can also be used to effect the fullerene separations. Mendoza and co-workers synthesized tris-(4-ureidopyrimidone) CTV (CTV-UPy) which has capability to form self-assembled dimeric capsule utilizing the self-complimentary DDAA (D – donor, A - acceptor) hydrogen bonding sequence of 4-ureidopyrimidine unit (Figure 2.3).³⁵⁻³⁶ This host is particularly selective for higher order fullerenes and the binding constant follows the order $C_{84} > C_{70} > C_{60}$. Separation and recovery of fullerene is based on the polarity of the solvent used. The CTV host forms a dimeric capsule encapsulating particular order of fullerene from the fullerite in non-polar solvent which is separated and recovered by adding polar solvent where the capsular assembly was unstable.

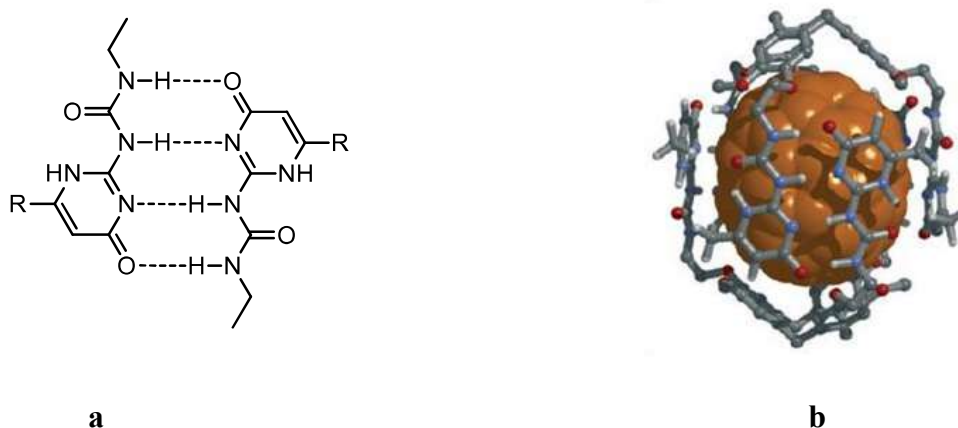


Figure 2.3. (a) ureidopyrimidine's self-complimentary DDAA hydrogen bonding sequence ; (b) $C_{70}@CTV-UPy$ hydrogen-bonded capsule.³⁶

CTV scaffold was extensively studied in metallo-supramolecular chemistry by attaching various heterocyclic rings³¹. First of this kind was reported by Shinkai and co-workers where pyridyl appended CTV hosts were connected to form trigonal bipyramidal capsule using *cis*-protected Pd(II).³⁷ Following this, numerous reports of metallo-supramolecular assemblies of CTV analogues with novel topologies appeared in the literature.^{32, 38} For instance, Hardie's group reported³⁹ the synthesis of $[Ag_2(\text{tris}(3\text{-pyridylmethylamino})\text{cyclotriguiacylene})_2(\text{CH}_3\text{CN})_2] \cdot 2\text{PF}_6$ dimeric capsule (Figure 2.5 (a)) where the ligand tris(3-pyridylmethylamino)cyclotriguiacylene was prepared by treating

assembles to form a triply interlocked [2]catenane, $[\text{Ag}_6(\text{L}_\text{B})_4]^{6+}$ (Figure 2.6 (a)). This is unusual because L_B forms mechanically interlocked complex without a template which is often required for the mechanical bond formation. Similarly tris-(3-(3-pyridyl)-benzoyl)cyclotriguaiacylene) (L_F) in presence of Pd(II) self-assembles to form interesting and synthetically challenging structure solomon cube, $[\text{Pd}_4(\text{L}_\text{F})_4(\text{NO}_3)_2(\text{H}_2\text{O})_2]^{6+}$ (Figure 2.6 (b)). Solomon cube is a mechanically interlocked molecule having four topological cross points i.e., it is simply a doubly interlocked [2]catenane. Here in this case also mechanical bond forms in the absence of a template, although the interlocking mechanism in the both cases are still unknown.

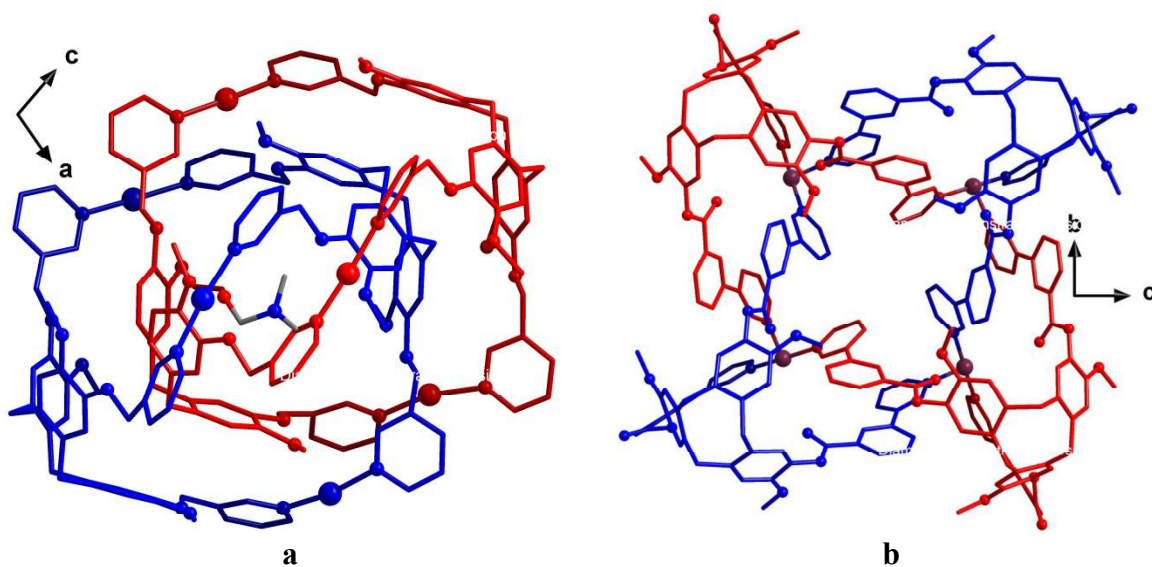
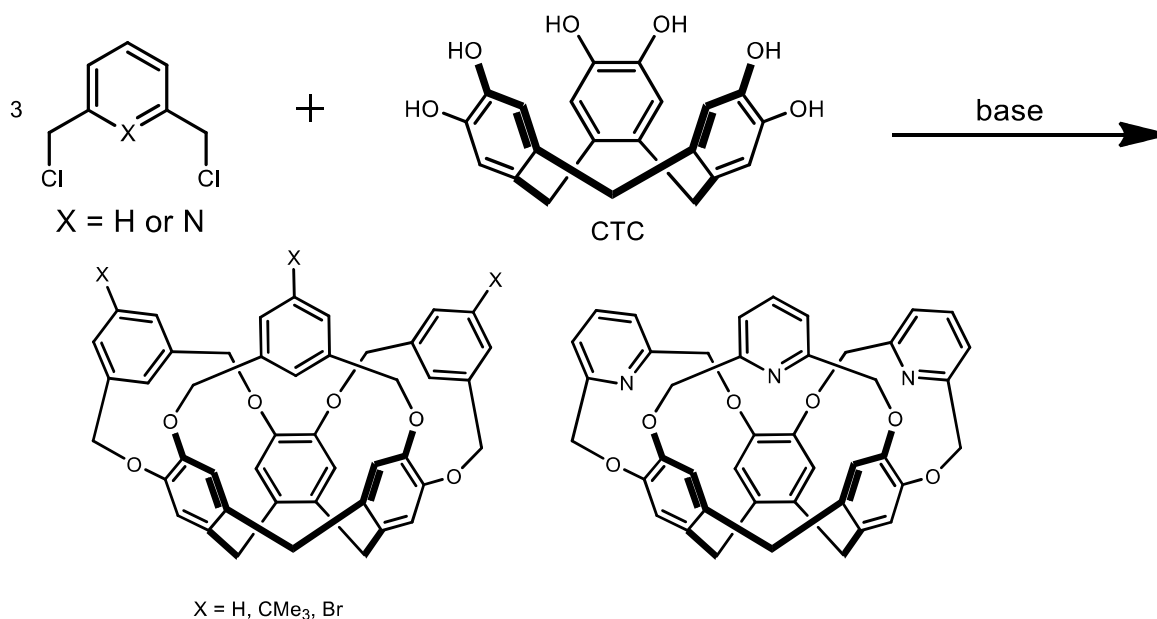


Figure 2.6. (a) 3D triply interlocked [2]catenane ; (b) Solomon cube

The above mentioned supramolecular assemblies of extended-cavity CTVs are derived from CTG. Another method of extending the CTV cavity is the functionalization of CTC with *m*-dihalomethyl arenes or activated haloarenes in the presence of base that yields triple bridged CTC. In 1988, Cram and co-workers demonstrated this method⁴⁰ by synthesizing the family of extended CTV cavitands (Scheme 2.1). Following this, Hardie's team designed and



Scheme 2.1. General synthesis of extended CTVs from CTC

synthesized carboxylic group functionalized cavitand and its corresponding metallo-cryptophane (Figure 2.7).⁴¹ The required triple bridged ligand tris[3,5-bis(methyl)benzoic acid]cyclotricatechylene was prepared by reacting CTC with ethyl-3,5-bis(bromomethyl)benzoate in the presence of base under inert conditions to get ester appended cavitand which was subsequently hydrolysed with K₂CO₃ followed by neutralisation with HCl.

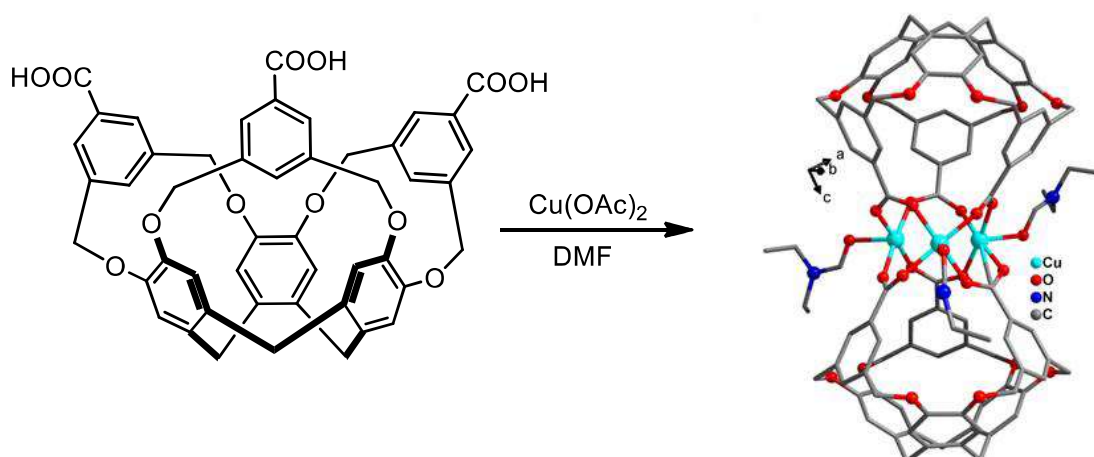


Figure 2.7. Carboxylate functionalised triple bridged CTV forming 'bow-tie' cryptophane with Cu(II) ions.

Under solvothermal conditions this tris-carboxylate ligand forms a dimeric metallocryptophane with Cu(II) salt resembling a ‘bow-tie’ structure. Unlike the above mentioned metallocryptophanes, this has a pinched appearance that features a limited accessible void space.

In the Cram’s report⁴⁰, during the synthesis of triple bridged CTVs there were able to isolate the double bridged CTV as a side product (15% yield). In this case the absence of the third bridge would allow small molecules to enter. By this, we assumed that if two pyridine moieties can be appended to CTC (Figure 2.8.(1)), it will form a donor-acceptor system. In this molecule, unbridged phenolic hydrogen could act as H-bond donor while nitrogen atoms in pyridine rings could be H-bond acceptor.⁴²⁻⁴⁶ This kind of molecule would have the potential to form homo-dimeric capsular complexes.

The metallo-cryptophanes corresponding to triple bridged CTCs have a pinched-in rim. This shows, even though the cavity volume can be increased, the opening of the cavity narrows down, preventing the guest molecule from entering the cavity. For that reason, we were interested to investigate the effect of introduction three pyridine bridge (Figure 2.8.(2)) with methyl groups at 2,6 positions to increase the steric crowding between bridging groups assuming this may help the cavity to open and also the pyridine nitrogen can be utilized for

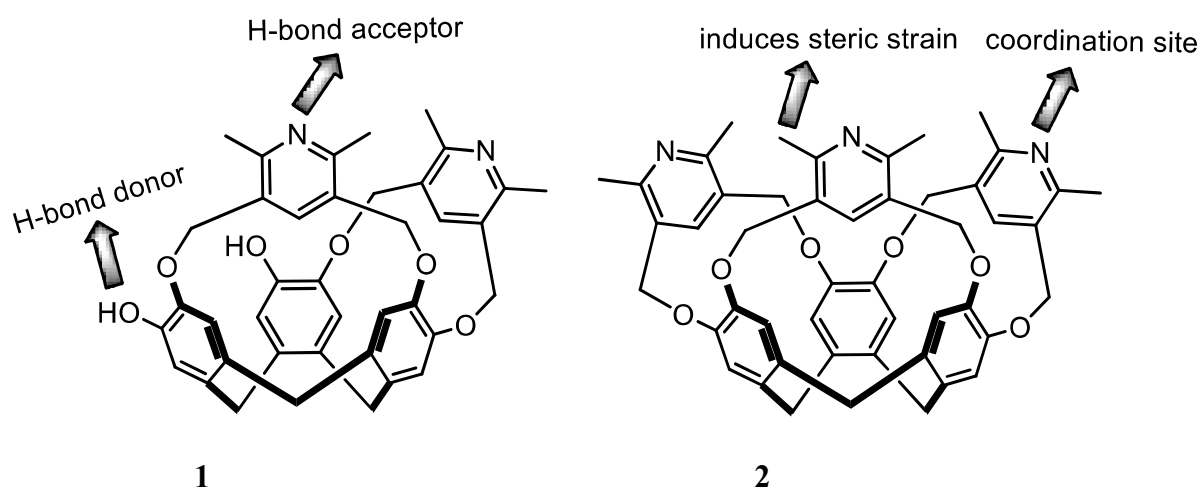
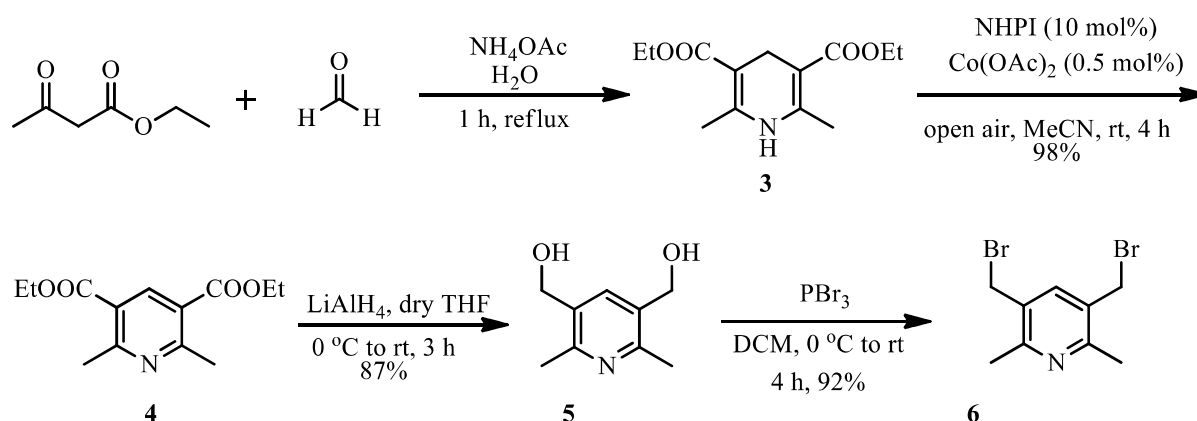


Figure 2.8. Our design of extended-cavity CTVs

. either metal coordination or hydrogen bonding

2.3. Results and Discussion

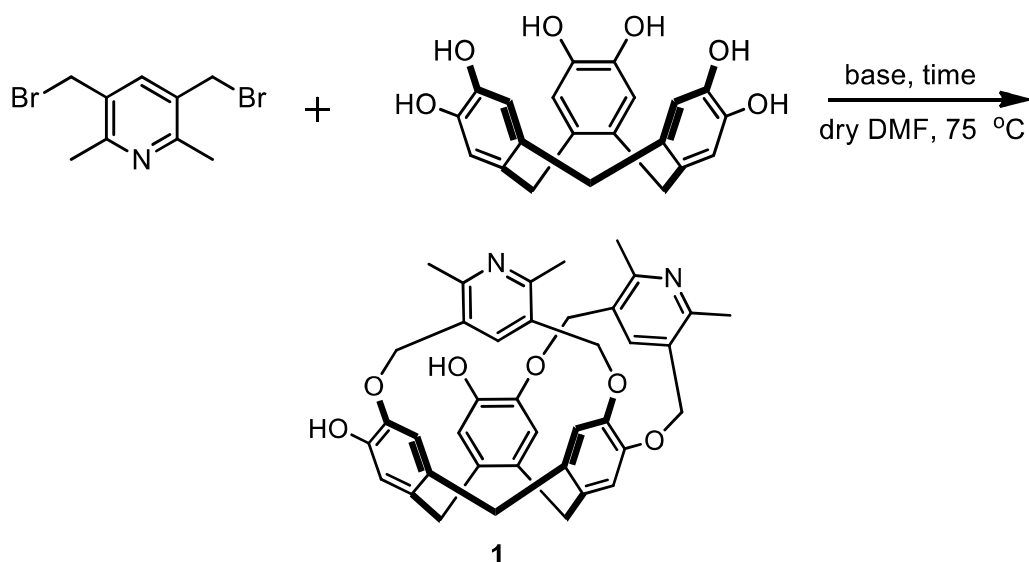
We synthesised Hantzsch pyridine diester, from which required 3,5-dibromomethyl pyridine moiety can be obtained. The Hantzsch dihydropyridine diester was prepared according to literature procedure.⁴⁷ Oxidation of Hantzsch dihydro pyridine was done with cobalt diacetate and N-hydroxyphthalimide, both used in catalytic amounts.⁴⁸ Reduction went smoothly as per literature reports⁴⁹ to yield **4**. Bromination of **4** was done using PBr₃ in 1,4-dioxane which gave satisfactory yields of **5** (Scheme 2.2). Cyclotricatechylene was synthesised in two steps, following literature reports.⁵⁰⁻⁵¹



Scheme 2.2. Synthesis of 3,5-bis(bromomethyl)-2,6-dimethylpyridine (**6**)

To synthesise the double bridged CTC, we adapted slightly modified reported procedure.⁴¹ Using cesium carbonate for bridging, gave multiple products, as detected by TLC. So, we used a milder base, potassium carbonate, for the cyclisation. We were able to isolate the desired product in 29% yield. To improve the yield, we performed the reaction by varying reaction time. While 24 h reaction gave the highest yield of 45%, 12 h, 36 h and 48 h reactions gave 35%, 32% and 29% respectively.

The double bridged product, $\text{CTC}(\text{Py})_2(\text{OH})_2$ (**1**) was initially characterised by ESI-MS, m/z at 629.2644 $[\text{M} + \text{H}]^+$ (calc. 629.2646). In ^1H NMR spectra of **1**, characteristic



Scheme 2.3. *Synthesis of CTC(Py)₂(OH)₂(1)*

Table 1: Optimisation table for synthesis of **1**

S.No.	Base	Time	% Yield of 3
1	Cs ₂ CO ₃	48 h	Traces
2	K ₂ CO ₃	48 h	29%
3	K ₂ CO ₃	36 h	32%
4	K ₂ CO ₃	24 h	45%
5	K ₂ CO ₃	12 h	35%

singletaryl-CTC peak is split into three peaks, indicating absence of three fold symmetry, as compared to CTC. Similarly, the two characteristic doublets are split into four doublets, in 2:1 ratio within each pair. Comparing the integration values of bridge methylene protons and pyridine aromatic protons, at 5.11-5.14 ppm and 8.5 ppm respectively, with those of CTC scaffold confirms the formation of doubly bridged CTC cavitand, **1**.

In the mass spectrum along with monomer peak ($m/z = 629.2644$), one more peak appears at $m/z = 1257.5093$ which corresponds to a dimer (Figure 2.9), possibly indicating

formation of capsular assemble under mass spectroscopic conditions.

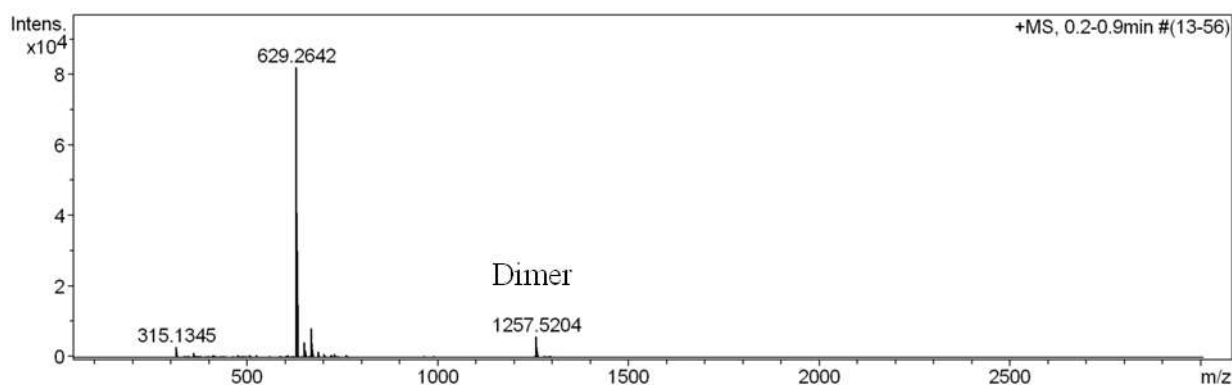


Figure 2.9. ESI-MS spectra of **1** showing along with dimer peak

This encouraged us to investigate the assembly in solid state by single crystal X-ray diffraction. Owing to the limited solubility of the compound in low polar solvents, crystallisation was done in high polar solvents. Crystallisation of **1** was tried in various solvents systems and crystals suitable for X-ray diffraction were obtained in DMSO / chloroform. Slow evaporation of a very dilute solution of **1** gave reddish-brown rectangular crystals in about two weeks. Compound **1** crystallised in monoclinic crystal system with $P2_{1/n}$ space group (No. 14). The asymmetric unit shows a molecule of **1** containing a DMSO molecule near its cavity and one molecule of DMSO along with three molecules of water outside the cavity (Figure 2.10). It became evident during further analysis, that **1** is forming a water molecule mediated dimeric self-assembly, encapsulating two molecules of DMSO.

Phenolic -OH and pyridine nitrogen are taking part in hydrogen bonding, they do not interact with each other directly, as we expected. Instead, four water molecules conveniently mediate between two molecules resulting in a molecular capsule (Figure 2.11). Each water molecule form two hydrogen bonding one with a phenolic OH and another with pyridine nitrogen atom in two different molecules. The lattices extended by π - π interaction and non-classical hydrogen bonding of CH...O. Apart from holding the dimeric form, each water molecule also forms hydrogen bond with oxygen of DMSO trapped inside the cavity.

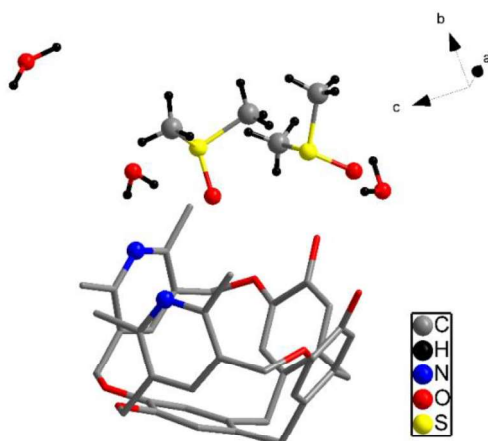


Figure 2.10. *Asymmetric unit of 1. Hydrogen atoms of 1 have been deleted for clarity.*

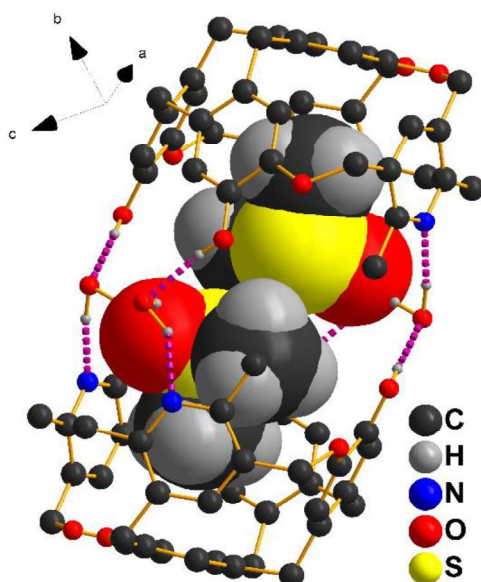


Figure 2.11. *Crystal structure showing dimeric assembly 1. Non-hydrogen bonded hydrogen atoms are omitted for clarity. Encapsulated DMSO has been shown in space fill model*

In all, four water molecules are involved in twelve hydrogen bonds in the capsular assembly, out of which eight bonds are used in forming the dimer (Figure 2.12). Three kinds of hydrogen bonding are present in the capsular assembly: water with phenolic O-H (~ 2.7 Å), pyridine nitrogen with water hydrogen (~ 2.8 Å) and DMSO oxygen with water hydrogen (~ 2.75 Å). The two DMSO molecules are oppositely faced, with the sulphur atoms in proximity to each other.. The sulphur-sulphur distance is $3.698(9)$ Å, slightly above twice the

van der Waal's radius of sulphur (3.6 Å) indicating weak interactions between them. The solvent accessible volume is 1410 Å³, as calculated after removing solvent molecules

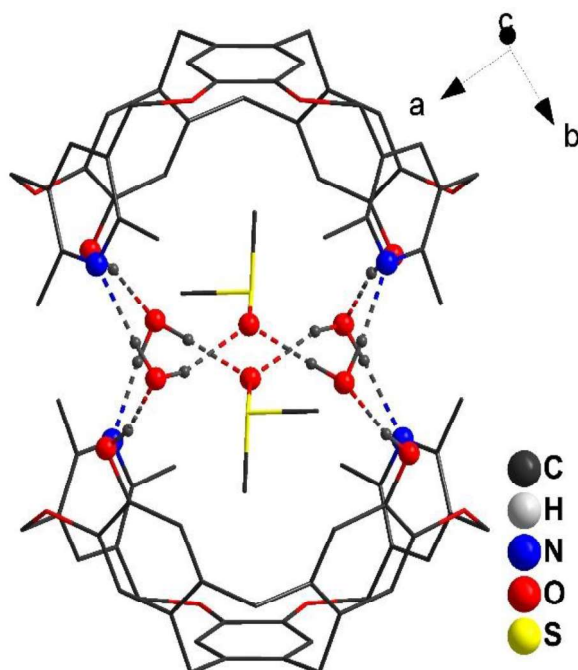


Figure 2.12. Water molecule mediated hydrogen bonded dimeric capsular self-assembly of **1**, encapsulating DMSO. Non-hydrogen bonded hydrogen atoms are deleted for clarity. Atoms participating in hydrogen-bonding are shown in ball-stick model.

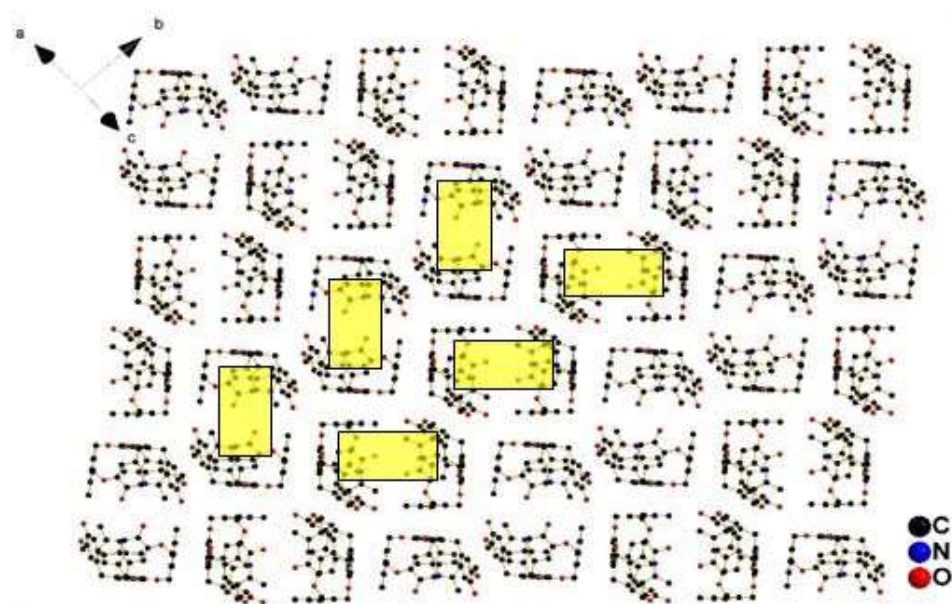


Figure 2.13. Packing diagram showing capsular assembly **A** arranged in 2:1 Herringbone pattern. Hydrogen atoms and DMSO have been omitted for clarity.

A simplified packing diagram of **1** is shown in Figure 2.13. The dimeric capsular assembly packs itself in a Herringbone pattern of 2:1 ratio in (-0.65, 0, -0.75) plane. This pattern is driven by weak π - π stacking between pyridine ring of the monomer of one capsule and CTC benzene ring at the base of the monomer of another capsule. Also, the parallel displaced arrangement of each dimeric capsule is facilitated by weak π - π stacking between each CTC benzene ring of opposite facing monomers in two different capsules (shown in red broken line). CTCbenzene rings has π - π stacking that helps in extending the lattice (Figure 2.14).

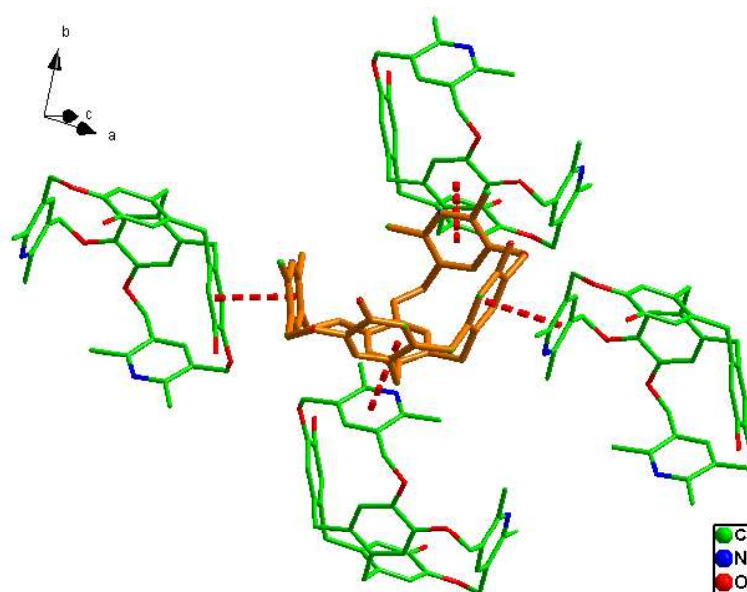


Figure 2.14. Arrangement of four monomers around a central molecule of **1**, mediated by π - π stacking (shown in red broken bonds). H atoms and solvent molecules have been omitted for clarity.

As **1** is forming water mediated dimeric capsule, we were curious to know whether **1** would forms a dimeric capsule via phenol-pyridine hydrogen bonding in the absence water. Hence, we tried the crystallisation under anhydrous conditions, maintaining the same solvent system ($\text{CHCl}_3/\text{DMSO}$) as used previously.

Colourless crystals appeared after almost a month. In this condition, compound **1** crystallised in monoclinic system with $P2_1$ space group (No. 14). The asymmetric unit

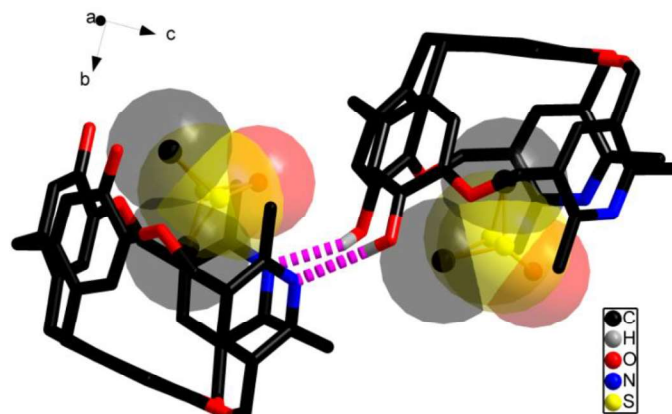


Figure 2.15. *Crystal structure of 1 showing non-capsular assembly in the absence of water.*

Non-hydrogen bonding hydrogen atoms are removed for clarity.

consists of two molecules of **1** along with three molecules of DMSO, two of which are in the cavity of **1**. Further analysis revealed, although there exists direct phenol-pyridine hydrogen bonding interaction between two molecules of **1**, it does not form dimeric capsular assembly (Figure 2.15). In the absence of water, each molecule of **1** is involved in hydrogen bonding with two neighbouring molecules. Probably due to steric strain, they cannot occupy face to face position and therefore, no capsular assembly formed. As a result, **1** forms 1D zig-zag chain polymer driven by hydrogen bonding interactions between phenol-pyridine (Figure 2.16).

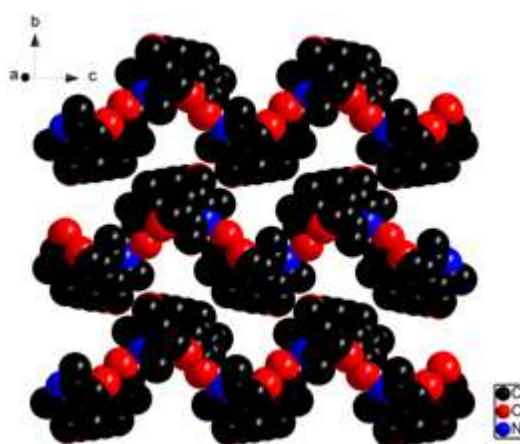


Figure 2.16. *Packing diagram of 1 showing zig-zag chain polymer in the absence of water*

Two consecutive linear chains are held to each other by weak hydrogen bonding interactions. Each molecule of **1** forms three hydrogen bonds with another molecule of the

same in the subsequent chain (Figure 2.17). Two of these are between the methylene protons of bridge moiety of one molecule of **1** with bridged oxygen in CTC scaffold of another ($d_{C29-O11} = 3.444(5) \text{ \AA}$, $d_{C11-O5} = 3.428(3) \text{ \AA}$). The third hydrogen bond is between the methyl proton of pyridine of one molecule with bridged oxygen atom of another ($d_{C31-O10} = 3.475(1) \text{ \AA}$).

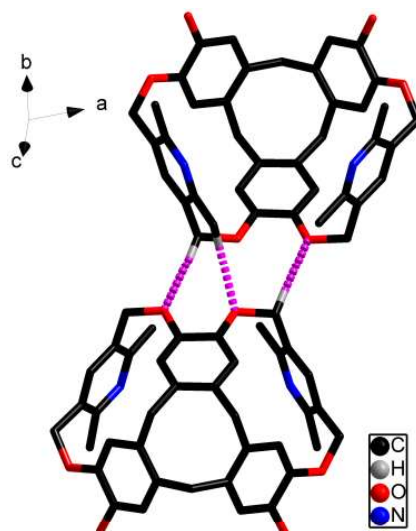
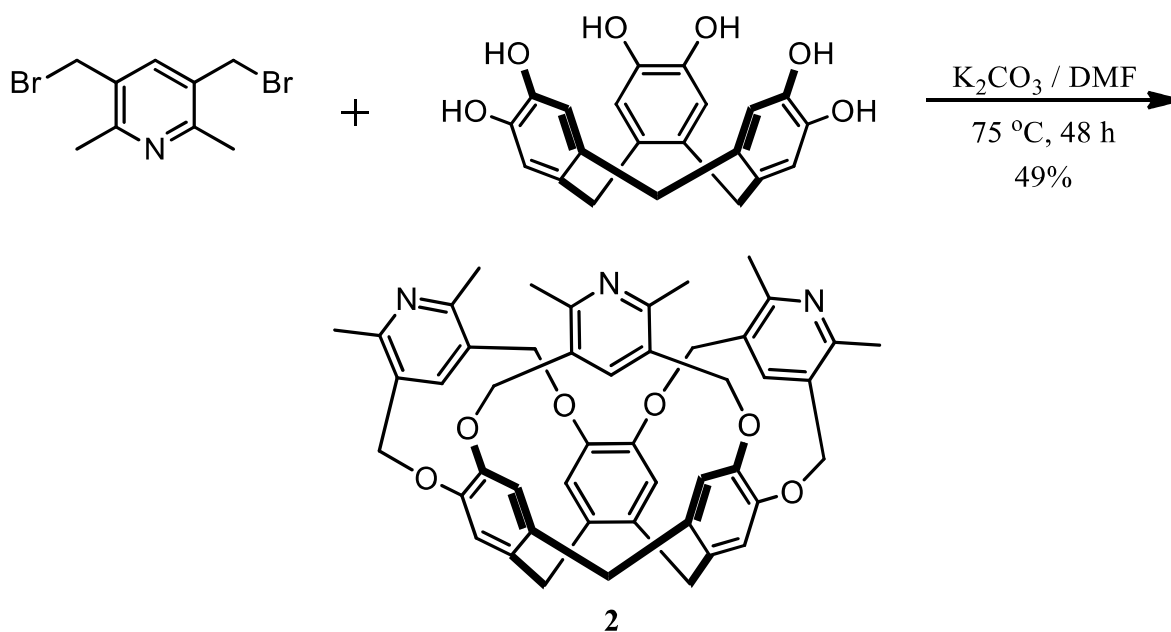


Figure 2.17. Hydrogen bonding between molecules of **1** which are part of two different chains. Non-hydrogen bonding hydrogen atoms are removed for clarity.

After successfully probing **1**, in solid state, we thought it would be interesting to probe the triple bridged pyridine molecule, CTC(Py)₃. This would have three nitrogen for hydrogen bonding, if water molecule would lend assistance like in **1**, it might also results in a molecular capsule.

Cram *et al* have reported⁴⁰ CTC triple-bridging with 2,6-lutidylene group, where the position of pyridine nitrogen is such that it makes itself unavailable for H-bonding with another molecule. In our system, we wanted the nitrogen atom of pyridine ring to face outwards and available for hydrogen bonding or metal coordination. Therefore, we attached 3,5-disubstituted pyridine molecule to synthesize the desired molecules. During the synthesis of **1**, we isolated this molecule, CTC(Py)₃ (**2**) in small amount while synthesizing **1**. This was

characterised by NMR and ESI-MS, m/z 760.3378 $[M + H]^+$ (calc. 760.3381). The major peak in the mass spectra appears at m/z 380.6733 corresponds to $[M + 2H]^{2+}$. While the peak



Scheme 2.4. Synthesis of CTC(Py)₃ (**2**)

at m/z 628.2552, corresponds to $[M - Py]^+$. The NMR spectra of **2** shows the characteristic singlet aryl-CTC peak at 6.43 ppm, indicating retention of threefold symmetry similar to CTC. Comparing the integration values of bridge methylene and pyridine aromatic protons at 5 and 7.68 ppm respectively, with those of CTC scaffold, confirms the formation of triply bridged CTC cavitand **2**. We optimised the synthesis of this molecule by modifying reported procedure,⁴¹ using potassium carbonate instead of caesium carbonate. After 48 hrs, CTC(Py)₃ (**2**) was obtained in 49% yield as white solid (Scheme 2.4).

To study the solid-state structure of **2**, we crystallised it using DMSO-THF as solvent. Colourless, needle-like crystals were obtained within a week, which were degrading rapidly on exposure to air. Diffraction data was collected by placing these crystals inside a capillary, in presence of the mother liquor. **2** was crystallized in orthorhombic crystal system with $Pna2_1$ space group (No. 33). The asymmetric unit shows a molecule of **2** as in Figure 2.18. The solvent accessible volume, as calculated after removing solvent molecules, is 1667 Å³.

Packing is driven by weak C-H/ π stacking between methyl C-H on pyridine ring with pyridine ring of adjacent molecule of **2** (Figure 2.19). The values for d between C and aromatic ring

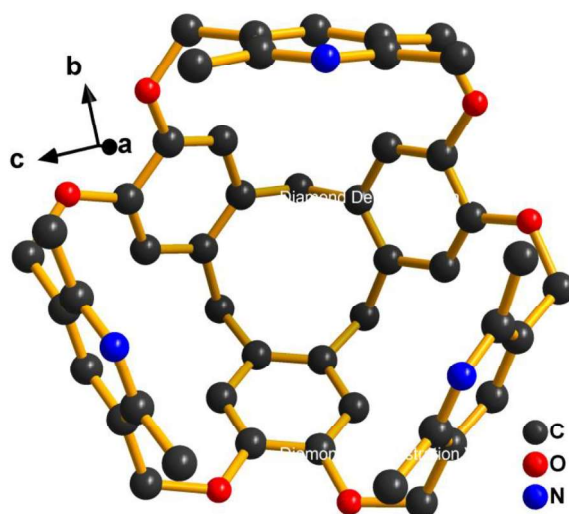


Figure 2.18. Asymmetric unit of **2**. Hydrogen atoms are omitted for clarity

centroid, θ and ϕ angles are 3.755(6) Å, 16.5° and 143° respectively. In Cram's report, the triple *m*-xylene bridged CTC had one out of three rings facing outwards.⁴⁰ Also, in case of Hardie's bow-tie metallo-cryptophane, the bridged aryl groups of cavitand have metal coordination and are thus forced into facing upwards.⁴¹ But it is interesting to note that in the case of CTC(Py)₃ (**2**), all the bridge groups are facing upwards without any coordination. The steric hindrance between methyl groups of pyridine was shown in Figure 2.20.

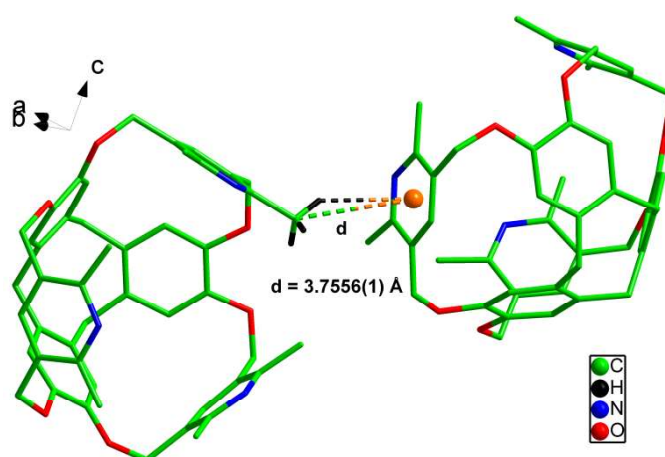


Figure 2.19. CH- π interaction between pyridine methyl group of one molecule of **2**, with pyridine ring of another. C and H interactions with centroid (orange in colour) of aromatic

ring are shown in broken bonds. Rest hydrogen atoms and solvent molecules have been omitted for clarity

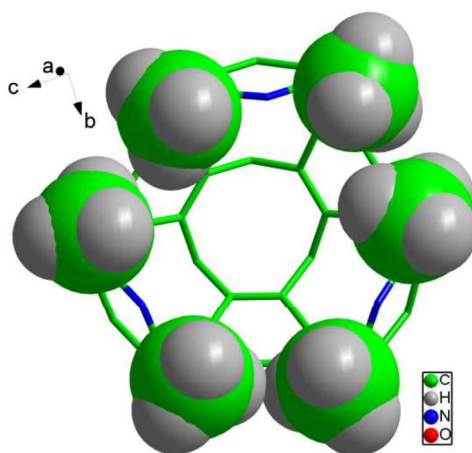


Figure 2.20. Steric hindrance between methyl groups (shown in space fill model) of adjacent pyridine bridges in **2**. Non-methyl H atoms and water molecules have been removed for clarity.

In summary, we have synthesized two new pyridine bridged cavitands, with two (CTC(Py)₂(OH)₂) and three (CTC(Py)₃) pyridine moieties bridge between CTC aryl rings. CTC(Py)₂(OH)₂ was designed to exhibit a hydrogen bond donor-acceptor property, aiming to form a dimeric capsule. This doubly bridged cavitand shows dimeric capsular self-assembly via water molecule mediated hydrogen bonding, entrapping two molecules of DMSO, while in the absence of water, forms 1D polymeric assembly. It is expected that the α , α' disubstitution might widen the opening in CTC(Py)₃. Our future task is to investigate the effect of different bridging moieties and the propensity of the resulting cavitands to form capsules in solution phase, in doubly and triply bridged CTC. Also, efforts to obtain metallo-cryptophanes for both **1** and **2** are underway.

2.4. Experimental Section

2.4.1. General

Reagent grade chemicals were acquired from Aldrich and used as received. All solvents were procured from Merck Limited, India. Solvents were purified prior to use following standard

procedures. NMR was recorded with a Bruker Avance-III 400MHz instrument. Single crystals X-ray diffraction studies were done on a Bruker 4-circle Kappa APEX-II diffractometer equipped with a CCD detector, the X-ray source being Mo K α (wavelength 0.71073 Å) at room temperature. Data collection was monitored with Apex II software, and pre-processing was done with SADBSS integrated with Apex II.30 Crystal Structure solution and refinement was done using WingX and PLATON software.³¹ In case of **1**- non capsular assembly, the sulphur atoms in DMSO molecules are disordered. They were splitted over two places and the methyl groups were not added hydrogen. In case of **2**, peaks were found in fourier maps that could be assigned to oxygen atoms for water. When assigned, found to have high thermal parameter. Therefore, they were squeezed using PLATON SQUEEZED command. HRMS was done in Bruker ESI-MS microTOFQ.

2.4.2. Synthesis of Diethyl 2,6-dimethyl-1,4-dihydropyridine-3,5-dicarboxylate (3**)⁴⁷**

Ethyl acetoacetate (6.5 g, 50 mmol), paraformaldehyde (0.75g, 250 mmol) and ammonium acetate (2.9 g, 37.6 mmol) were taken in a 100 mL beaker covered by a watch glass. Under slow stirring, the mixture was heated up to 70 °C. After the mixture turns yellowish paste, heating is stopped. A highly exothermic reaction results in the formation of a yellow solid. The mixture cooled to room temperature, water (100 mL) was added and the yellow suspension was stirred for 20 minutes at room temperature. The solid was filtered, washed thoroughly with water and taken in a round bottom flask (100 mL) along with Ethanol (50 mL). This was then refluxed for 15 minutes and cooled to room temperature with stirring. The solid was filtered and washed thoroughly with ethanol yielding **3** as a bright yellow solid, which was dried in vacuo and used without further purification.

2.4.3. Synthesis of Diethyl 2,6-dimethylpyridine-3,5-dicarboxylate (4**)⁴⁸**

A mixture of 1,4-dihydropyridine **3** (2.53 g, 10.00 mmol), NHPI(0.160 g, 1.00 mmol) and

Co(OAc)₂·4H₂O (0.012 g, 0.05 mmol) in dry acetonitrile (25 mL) was stirred under open air, at room temperature for 4 h. After removal of the solvent under reduced pressure, the residue was column chromatographed to afford the corresponding pyridine derivative **4** in quantitative yields. ¹H NMR (400 MHz, CDCl₃) δ: 8.66 (s, 1H), 4.37 (q, J = 7.1 Hz, 4H), 2.84 (s, 6H), 1.39 (t, J = 7.1 Hz, 6H). ¹³C NMR (100 MHz, CDCl₃) δ: 165.94, 162.25, 141.20, 123.30, 77.48, 77.16, 76.84, 61.56, 24.89, 14.38.

2.4.4. Synthesis of (2,6-Dimethylpyridine-3,5-diyl)dimethanol (**5**)⁴⁹

To an ice-cold mixture of lithium aluminium hydride (95%) (6.7g, 168 mmol) in anhydrous THF (500 mL) is added a solution of **4** (31.5 g, 125 mmol) in dry THF (250 mL) under nitrogen atmosphere. The ice bath was removed and stirred at room temperature and for 3 h. After completion, the reaction mixture was cooled to 0°C and a mixture of ethyl acetate:methanol: water (15:4:1) was added slowly. The resulting solids are filtered over CeliteR 545, washed with ethyl acetate (500 mL) and methanol (20 mL). The filtrate is concentrated and dried in vacuo and product obtained as a white solid (87% yield) which is used without further purification. ¹H NMR (400 MHz, DMSO-d₆) δ: 7.63 (s, 1H), 5.22 (s, 2H), 4.47 (s, 4H), 2.35 (s, 6H). ¹³C NMR (100 MHz, DMSO-d₆) δ: 152.36, 133.33, 132.23, 60.14, 39.84, 39.62, 39.31, 20.83.

2.4.5. Synthesis of 3,5-bis(bromomethyl)-2,6-dimethylpyridine (**6**)

To an ice-cold solution of **5** (2.93 g, 10 mmol) in 1,4-dioxane, PBr₃ (4.75 mL, 50 mmol) was added slowly under stirring. Solution was brought to room temperature and stirred for 4 h. After completion, reaction mixture was quenched with sodium bicarbonate solution and extracted with DCM. The aqueous layer was washed with DCM (2 x 50 mL) and the combined organic layers were dried over anhydrous sodium sulphate. Solvent was evaporated to obtain white crystalline solid **6**, with 92% yield. ¹H NMR (400 MHz, CDCl₃) δ: 7.54 (s, 1H),

4.44 (s, 4H), 2.61 (s, 6H). ^{13}C NMR (100 MHz, CDCl_3) δ : 156.96, 139.24, 129.68, 77.48, 77.16, 76.84, 30.04, 21.42.

2.4.6. Synthesis of Cyclotrimeratrylene (CTV) (7)⁵⁰

Veratryl alcohol (10 g, 0.06 mole) was taken in a 250 mL round bottom flask and heated in an oil bath up to 80 °C. 3-4 drops of H_3PO_4 was added and stirred for 2 h. Within that time, the reaction mixture became a white paste. Then the reaction mixture was cooled to room temperature and methanol (50 mL) was added to the off white solid while stirring. The crude solid was collected by filtration and recrystallized from DCM to obtain pure white crystals of CTV (7) in 40% yield. ^1H NMR (400 MHz, CDCl_3) δ : 6.83 (s, 2H), 4.72 (d, $J = 13.7$ Hz, 1H), 3.84 (s, 6H), 3.52 (d, $J = 13.8$ Hz, 1H). ^{13}C NMR (100 MHz, CDCl_3) δ : 147.73, 131.85, 113.15, 77.48, 77.16, 76.84, 56.07, 36.47.

2.4.7. Synthesis of Cyclotricatechylene (CTC) (8)⁵¹

In a two-necked 100 mL round bottom flask, solution of CTV (2.52 g, 5 mmol) in dry DCM was cooled to -40 °C under N_2 atmosphere. To this stirring solution, BBr_3 (3.3 mL, 35 mmol) was added. The cooling bath was removed and the purple coloured reaction mixture was brought to room temperature and stirred for further 15 min. Then it was refluxed for 12 h. After this time, the reaction mixture was slowly cooled to 0 °C. It was then quenched with slow addition of ice-cold water (50 mL). The resulting slurry was filtered and the residue was washed with water (200 mL) and acetonitrile (10 mL). The crude wet solid was recrystallized from ethanol to obtain brown crystals of CTC (8) in 87% yield. ^1H NMR (400 MHz, DMSO-d_6) δ : 8.55 (s, 2H), 6.65 (s, 2H), 4.48 (d, $J = 13.4$ Hz, 1H), 3.20 (d, $J = 13.6$ Hz, 1H). ^{13}C NMR (100 MHz, DMSO-d_6) δ : 143.49, 130.83, 116.74, 40.15, 39.94, 39.73, 39.52, 39.31, 39.10, 38.89, 35.07.

2.4.8. Synthesis of Bis-(3,5-bis(methyl)-2,6-dimethylpyridine)Cyclotricatechylene (CTC(Py)₂(OH)₂)

A solution of CTC (**8**) (100 mg, 0.271 mmol) and **6** (175 mg, 0.596 mmol) in dry degassed DMF (50 mL) was added under N₂ to a stirred solution of K₂CO₃ (3.5 g) in dry degassed DMF (100 mL). The suspension was stirred at 70 °C for 24 hours. K₂CO₃ was filtered off and DMF removed in vacuo. The residue was purified by column chromatography (silica, 0-5 % MeOH in CH₂Cl₂) to afford **1** as a white powder, with 45% yield. ¹H NMR (400 MHz, DMSO-d₆) δ 8.49 (s, 1H), 8.18 (s, 1H), 6.76 (s, 1H), 6.74 (s, 1H), 6.56 (s, 1H), 5.14 (s, 2H), 5.11 (s, 2H), 4.47 (d, J = 13.0 Hz, 1H), 4.35 (d, J = 13.1 Hz, 1H), 3.33 (d, J = 13.2 Hz, 1H), 3.14 (d, J = 13.5 Hz, 1H), 2.47 (s, 3H), 2.46 (s, 3H). ¹³C NMR (101 MHz, DMSO-d₆) δ: 157.54, 157.01, 145.43, 144.80, 144.43, 142.7, 131.39, 130.42, 125.68, 117.06, 116.30, 79.22, 68.15, -67.41, 67.23, 40.04, 39.80, 39.73, 39.52, 39.31, 39.10, 38.89, 34.59, 21.42. ESI-HRMS: *m/z* 629.2644 [M + H]⁺ (calc. 629.2646)

2.4.9. Synthesis of Tris(3,5-bis(methyl)-2,6-dimethylpyridine)Cyclotricatechylene

CTC(Py)₃

A solution of CTC (**8**) (100 mg, 0.271 mmol) and **6** (262 mg, 0.894 mmol) in dry degassed DMF (50 mL) was added under N₂ to a stirred solution of K₂CO₃ (4.5 g) in dry degassed DMF (100 mL). The suspension was stirred at 70 °C for 48 hours. K₂CO₃ was filtered off and DMF removed in vacuo. The residue was purified by column chromatography (silica, 0-5 % MeOH in CH₂Cl₂) to yield **2** as a white powder, with 49% yield. ¹H NMR (400 MHz, CDCl₃/CD₃OD (3:1)) δ 7.68 (s, 3H), 6.43 (s, 6H), 4.99 (m, 12H), 4.31 (d, J = 12 Hz, 3H), 3.16 (d, J = 12 Hz, 3H), 2.48 (s, 6H). ¹³C NMR (101 MHz, CDCl₃ / CD₃OD (3:1)) δ 156.85, 145.99, 144.75, 131.63, 126.91, 116.45, 67.36, 35.03, 29.25, 19.71. ESI-HRMS: *m/z* 760.3378 [M + H]⁺ (calc. 760.3381)

2.5. References

1. Grotzfeld, R. M.; Branda, N.; Rebek, J., *Science* **1996**, *271*, 487.
2. Hof, F.; Craig, S. L.; Nuckolls, C.; Rebek, J. J., *Angew. Chem. Int. Ed.* **2002**, *41*, 1488.

3. Ma, X.; Zhao, Y., *Chem. Rev.* **2015**,*115*, 7794.
4. Cram, D. J.; Karbach, S.; Kim, Y. H.; Baczynskyj, L.; Kallemeyn, G. W., *J. Am. Chem. Soc.* **1985**,*107*, 2575.
5. Sherman, J. C.; Knobler, C. B.; Cram, D. J., *J. Am. Chem. Soc.* **1991**,*113*, 2194.
6. Corbellini, F.; Di Costanzo, L.; Crego-Calama, M.; Geremia, S.; Reinhoudt, D. N., *J. Am. Chem. Soc.* **2003**,*125*, 9946.
7. Fujita, M.; Tominaga, M.; Hori, A.; Therrien, B., *Acc. Chem. Res.* **2005**,*38*, 369.
8. Jankolovits, J.; Andolina, C. M.; Kampf, J. W.; Raymond, K. N.; Pecoraro, V. L., *Angew. Chem. Int. Ed.* **2011**,*50*, 9660.
9. Kishi, N.; Li, Z.; Yoza, K.; Akita, M.; Yoshizawa, M., *J. Am. Chem. Soc.* **2011**,*133*, 11438.
10. Stang, P. J., *J. Am. Chem. Soc.* **2012**,*134*, 11829.
11. Kang, J.; Rebek, J., *Nature* **1996**,*382*, 239.
12. Atwood, J. L.; Barbour, L. J.; Jerga, A., *Proc. Natl. Acad. Sci. U.S.A* **2002**,*99*, 4837.
13. Ajami, D.; Rebek, J., *J. Org. Chem.* **2009**,*74*, 6584.
14. Gibb, C. L. D.; Gibb, B. C., *J. Am. Chem. Soc.* **2004**,*126*, 11408.
15. Conn, M. M.; Rebek, J., *Chem. Rev.* **1997**,*97*, 1647.
16. Dumele, O.; Trapp, N.; Diederich, F., *Angew. Chem. Int. Ed.* **2015**,*54*, 12339.
17. Shivanyuk, A.; Paulus, E. F.; Böhmer, V., *Angew. Chem. Int. Ed.* **1999**,*38*, 2906.
18. Yuan, D.; Wu, M.; Wu, B.; Xu, Y.; Jiang, F.; Hong, M., *Cryst. Growth Des.* **2006**,*6*, 514.
19. Wyler, R.; de Mendoza, J.; Rebek, J., *Angew. Chem. Int. Ed.* **1993**,*32*, 1699.
20. Branda, N.; Wyler, R.; Rebek, J., *Science* **1994**,*263*, 1267.
21. Branda, N.; Grotzfeld, R. M.; Valdes, C.; Rebek, J., Jr., *J. Am. Chem. Soc.* **1995**,*117*, 85.

22. Meissner, R. S.; Rebek, J.; de Mendoza, J., *Science* **1995**,*270*, 1485.
23. Rivera, J. M.; Martín, T.; Rebek, J., *J. Am. Chem. Soc.* **1998**,*120*, 819.
24. Szabo, T.; O'Leary, B. M.; Rebek, J. J., *Angew. Chem. Int. Ed.* **1998**,*37*, 3410.
25. Hof, F.; Nuckolls, C.; Craig, S. L.; Martín, T.; Rebek, J., *J. Am. Chem. Soc.* **2000**,*122*, 10991.
26. MacGillivray, L. R.; Atwood, J. L., *Nature* **1997**,*389*, 469.
27. Gerkensmeier, T.; Iwanek, W.; Agena, C.; Fröhlich, R.; Kotila, S.; Näther, C.; Mattay, J., *Eur. J. Org. Chem.* **1999**,*1999*, 2257.
28. Shivanyuk, A.; Rebek, J. J., *Chem. Commun.* **2001**, 2424.
29. Smulders, M. M. J.; Zarra, S.; Nitschke, J. R., *J. Am. Chem. Soc.* **2013**,*135*, 7039.
30. Hof, F.; Rebek, J., *Proc. Natl. Acad. Sci. U.S.A* **2002**,*99*, 4775.
31. Hardie, M. J., *Chem. Soc. Rev.* **2010**,*39*, 516.
32. Henkelis, J. J.; Hardie, M. J., *Chem. Commun.* **2015**,*51*, 11929.
33. Shivanyuk, A.; Rebek, J. J., *Chem. Commun.* **2001**, 2374.
34. Eckert, J.-F.; Byrne, D.; Nicoud, J.-F.; Oswald, L.; Nierengarten, J.-F.; Numata, M.; Ikeda, A.; Shinkai, S.; Armaroli, N., *New J. Chem.* **2000**,*24*, 749.
35. Huerta, E.; Cequier, E.; Mendoza, J. d., *Chem. Commun.* **2007**, 5016.
36. Huerta, E.; Metselaar, G. A.; Fragoso, A.; Santos, E.; Bo, C.; de Mendoza, J., *Angew. Chem. Int. Ed.* **2007**,*46*, 202.
37. Zhong, Z.; Ikeda, A.; Shinkai, S.; Sakamoto, S.; Yamaguchi, K., *Org. Lett.* **2001**,*3*, 1085.
38. Hardie, M. J., *Chem. Lett.* **2016**,*45*, 1336.
39. Murayama, K., *Chem. Commun.* **1998**, 607.
40. Cram, D. J.; Weiss, J.; Helgeson, R. C.; Knobler, C. B.; Dorigo, A. E.; Houk, K. N., *J. Chem. Soc., Chem. Commun.* **1988**, 407.

41. Ronson, T. K.; Nowell, H.; Westcott, A.; Hardie, M. J., *Chem. Commun.* **2011**,47, 176.
42. Biradha, K.; Zaworotko, M. J., *J. Am. Chem. Soc.* **1998**,120, 6431.
43. Vishweshwar, P.; Nangia, A.; Lynch, V. M., *CrystEngComm* **2003**,5, 164.
44. Satha, P.; Illa, G.; Purohit, C. S., *Cryst. Growth Des.* **2013**,13, 2636.
45. Chakraborty, S.; Rajput, L.; Desiraju, G. R., *Cryst. Growth Des.* **2014**,14, 2571.
46. Roy, S.; Titi, H. M.; Goldberg, I., *CrystEngComm* **2016**,18, 3372.
47. Barbe, G.; Charette, A. B., *J. Am. Chem. Soc.* **2008**,130, 18.
48. Han, B.; Liu, Z.; Liu, Q.; Yang, L.; Liu, Z.-L.; Yu, W., *Tetrahedron* **2006**,62, 2492.
49. Wang, J.-H.; Li, M.; Zheng, J.; Huang, X.-C.; Li, D., *Chem. Commun.* **2014**,50, 9115.
50. Shivanyuk, A.; Rissanen, K.; Kolehmainen, E., *Chem. Commun.* **2000**, 1107.
51. Mansikkamaki, H.; Nissinen, M.; Rissanen, K., *Chem. Commun.* **2002**, 1902.

2.6. Spectral Data

Figure 2.21. ^1H NMR and ^{13}C NMR of Diethyl 2,6-dimethylpyridine-3,5-dicarboxylate

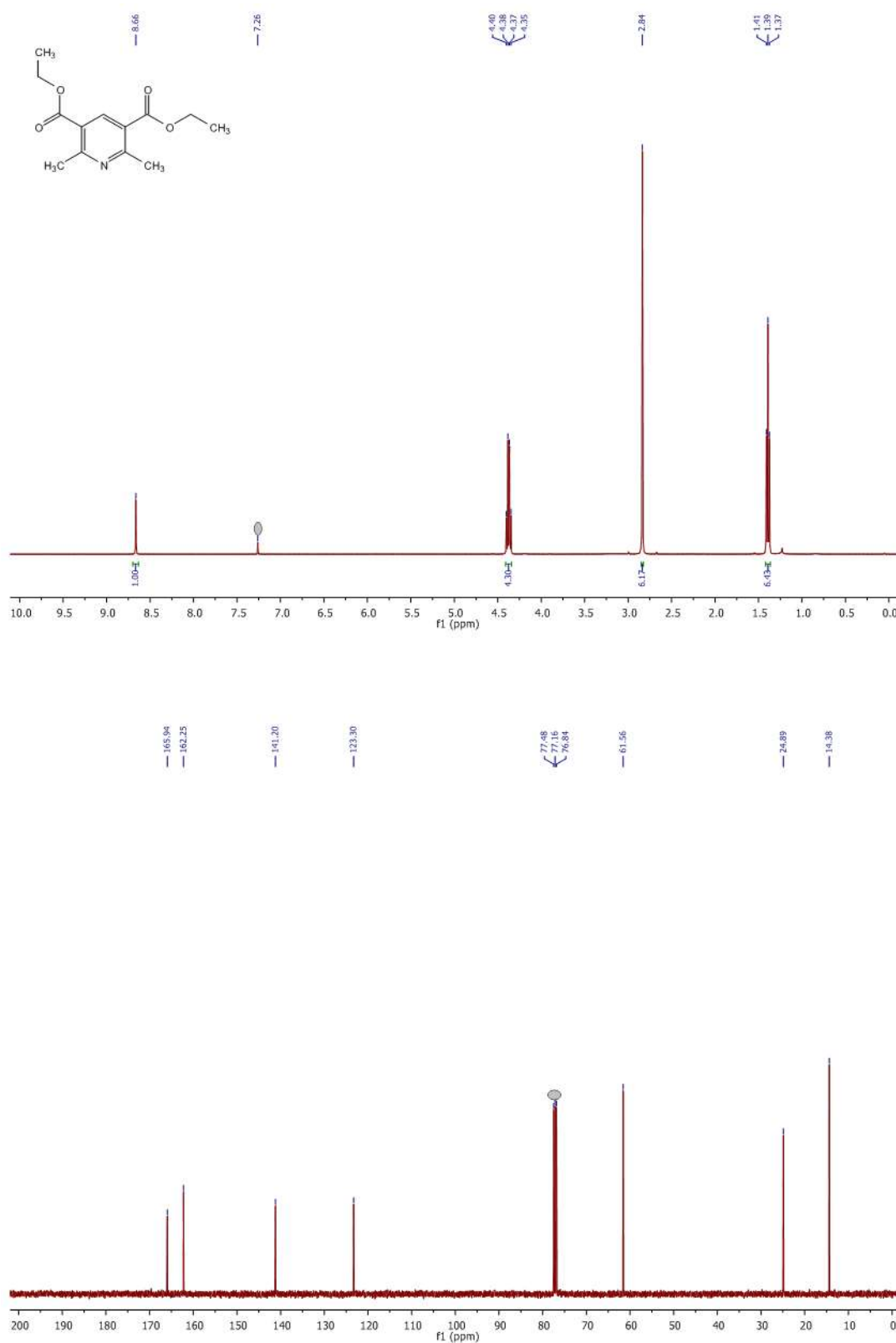


Figure 2.22. ^1H NMR and ^{13}C NMR of (2,6-Dimethylpyridine-3,5-diyl)dimethanol

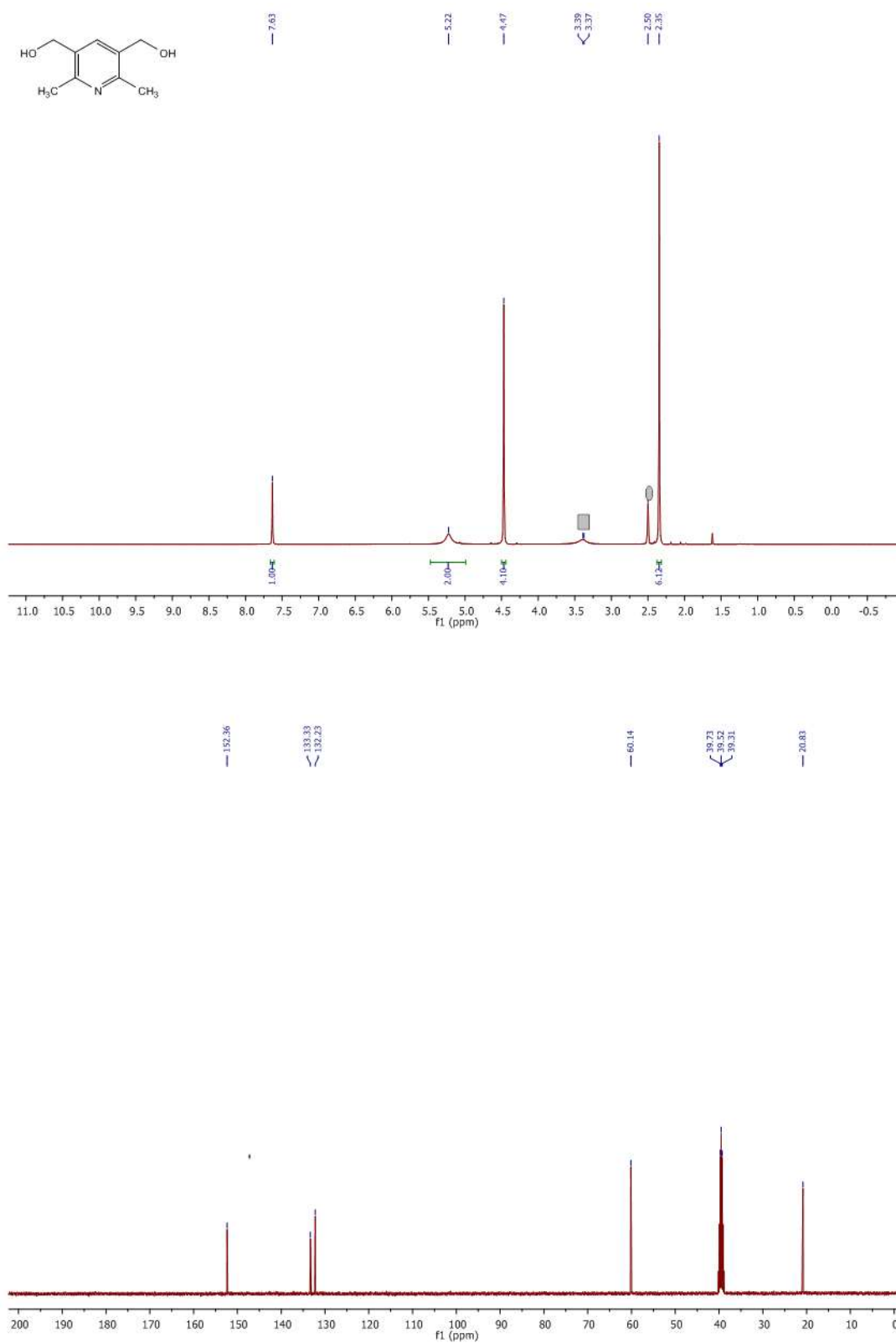


Figure 2.23. ^1H NMR and ^{13}C NMR of 3,5-bis(bromomethyl)-2,6-dimethylpyridine

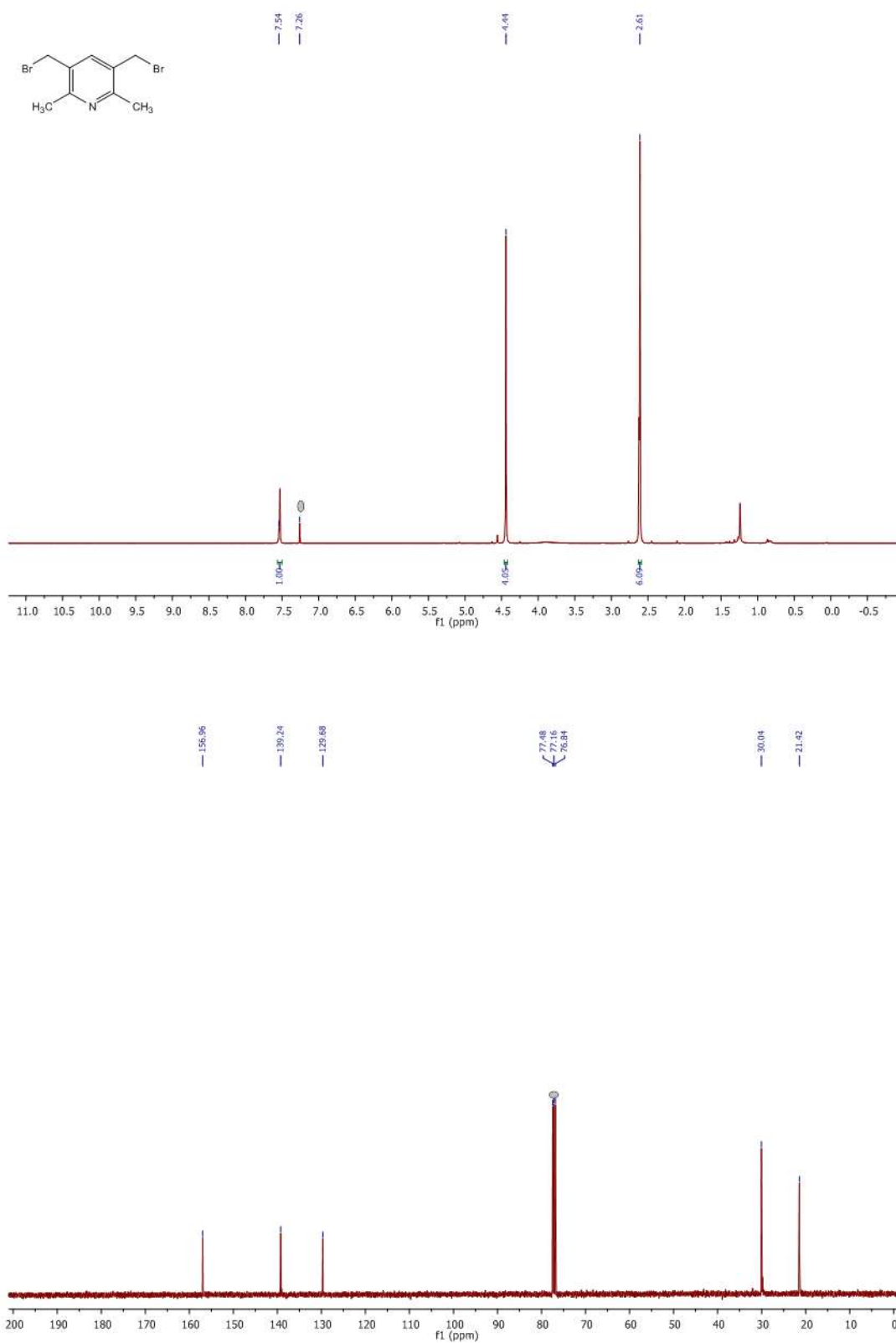


Figure 2.24. ^1H NMR and ^{13}C NMR of Cyclotrivenatrylene (CTV)

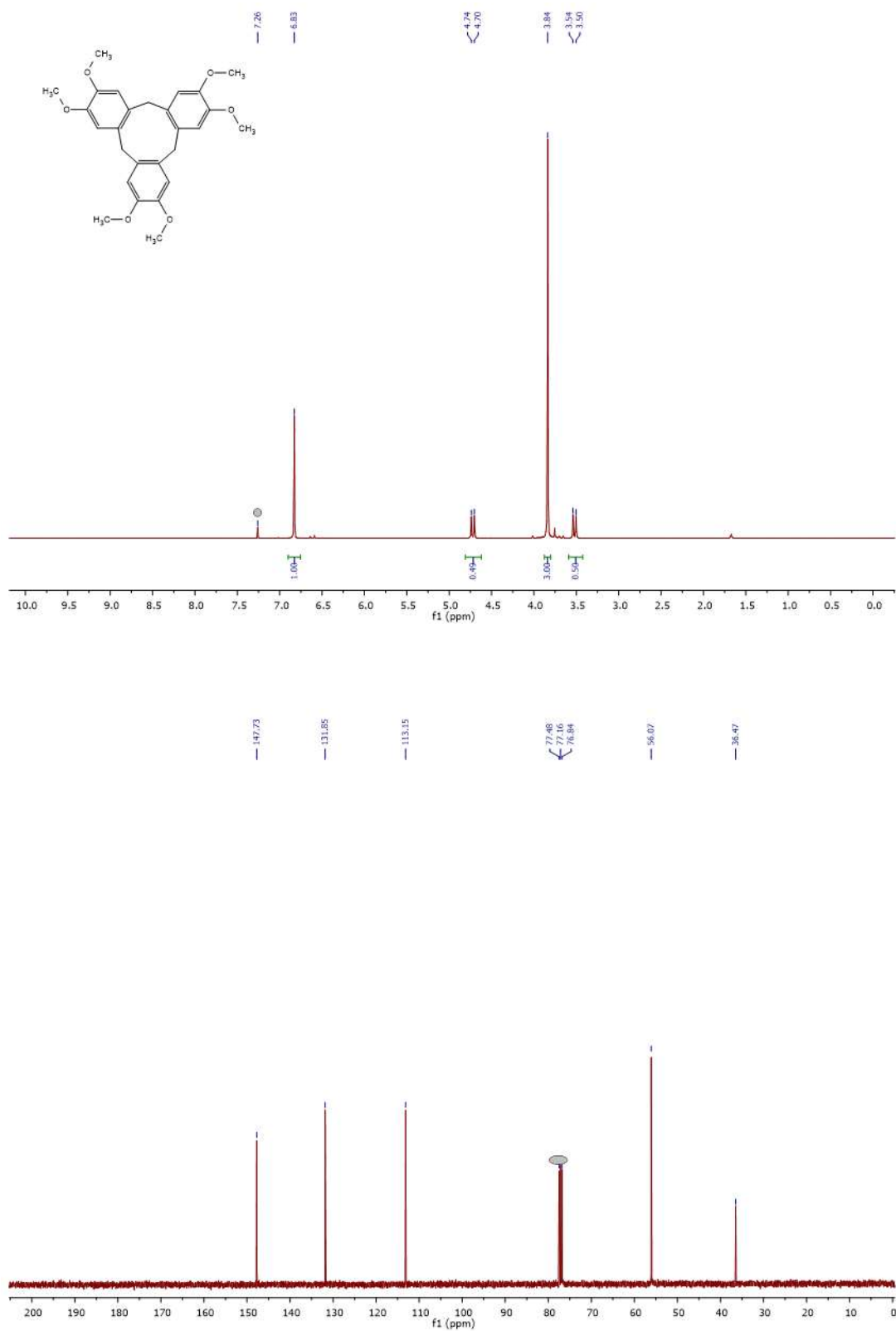


Figure 2.25. ^1H NMR and ^{13}C NMR of Cyclotricatechylene (CTC)

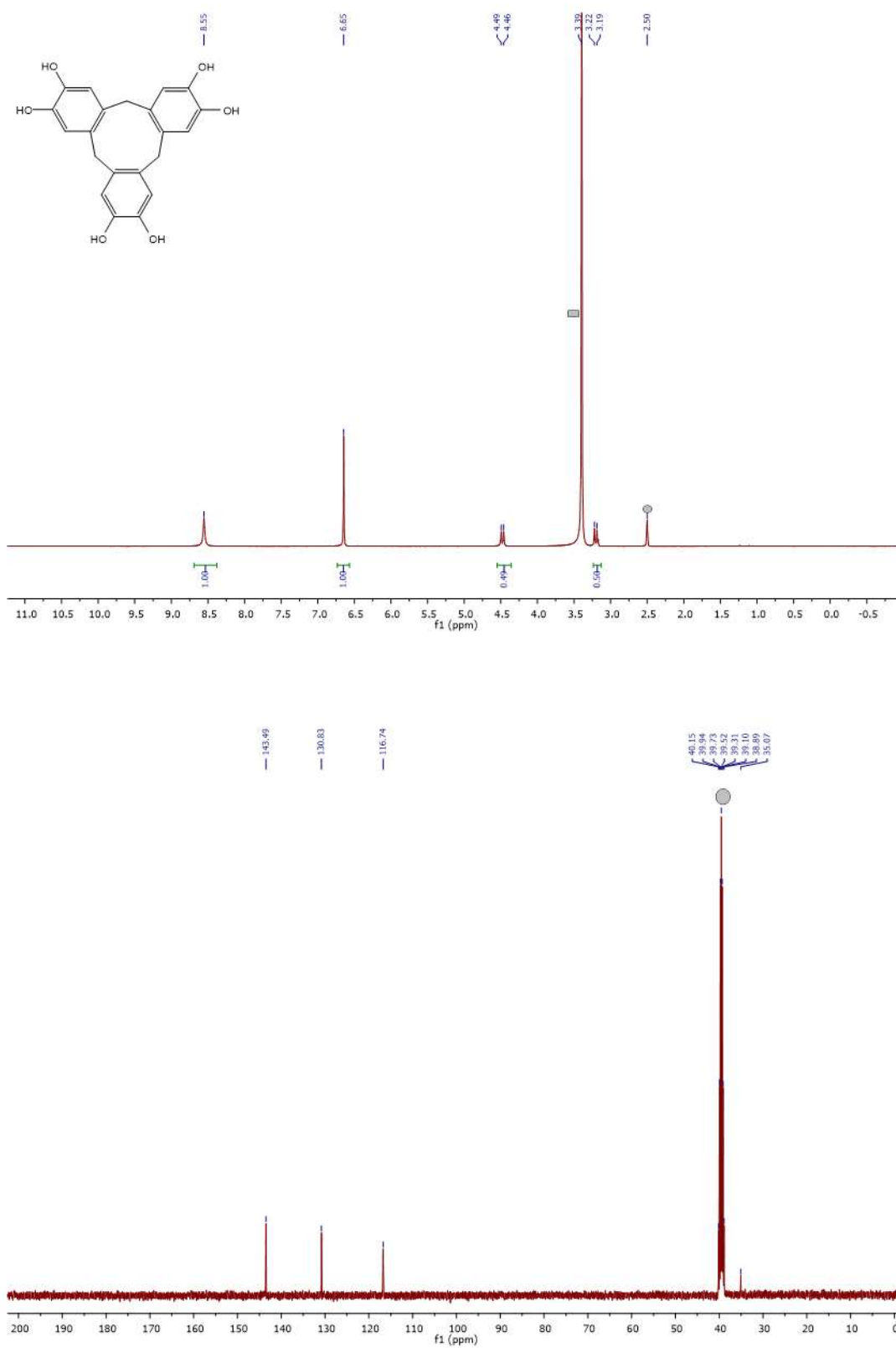


Figure 2.26. ^1H NMR and ^{13}C NMR of $(\text{CTC}(\text{Py})_2(\text{OH})_2)$

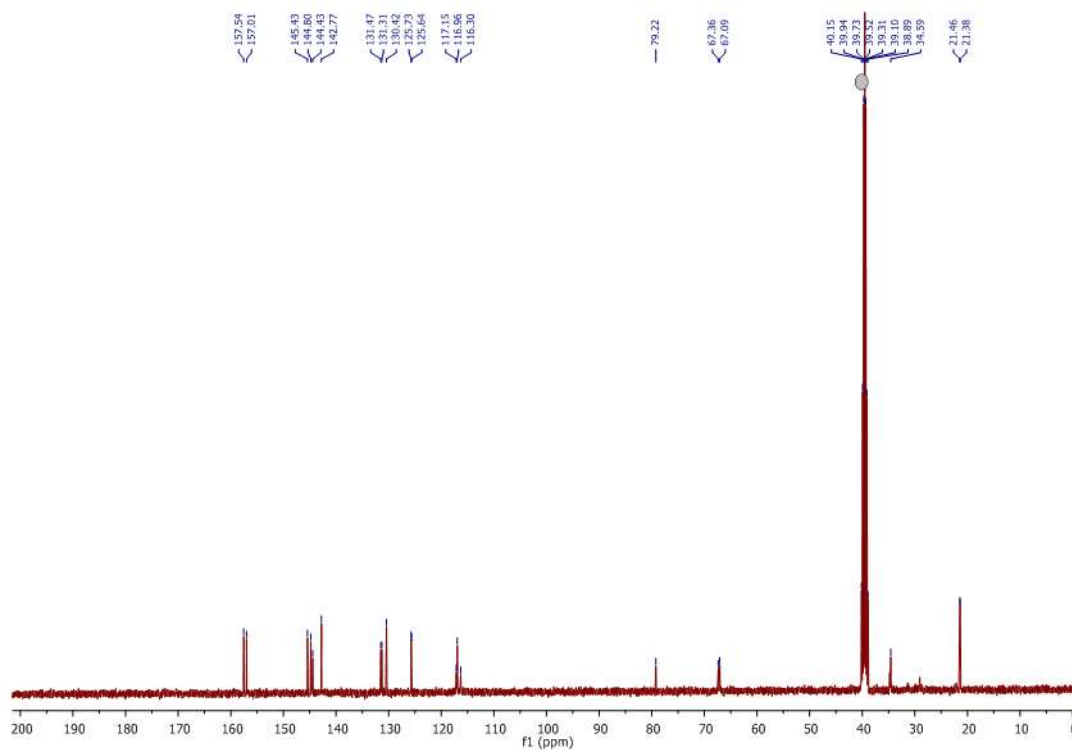
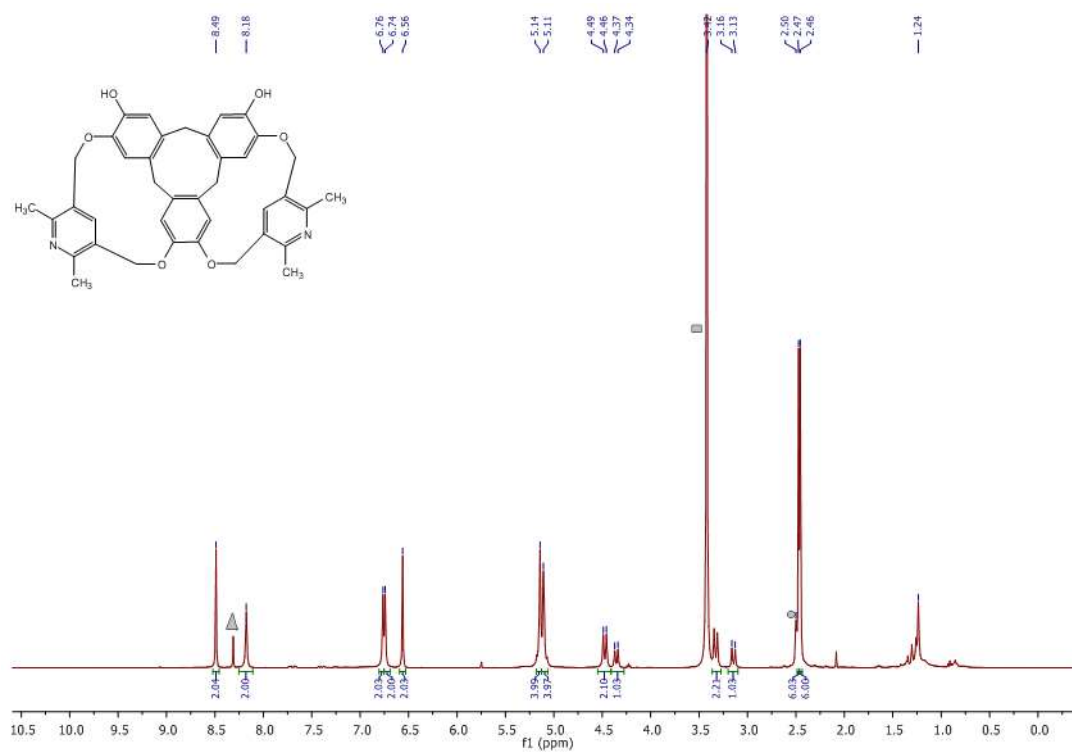


Figure 2.27. ^1H NMR and ^{13}C NMR of $(\text{CTC}(\text{Py})_3)$

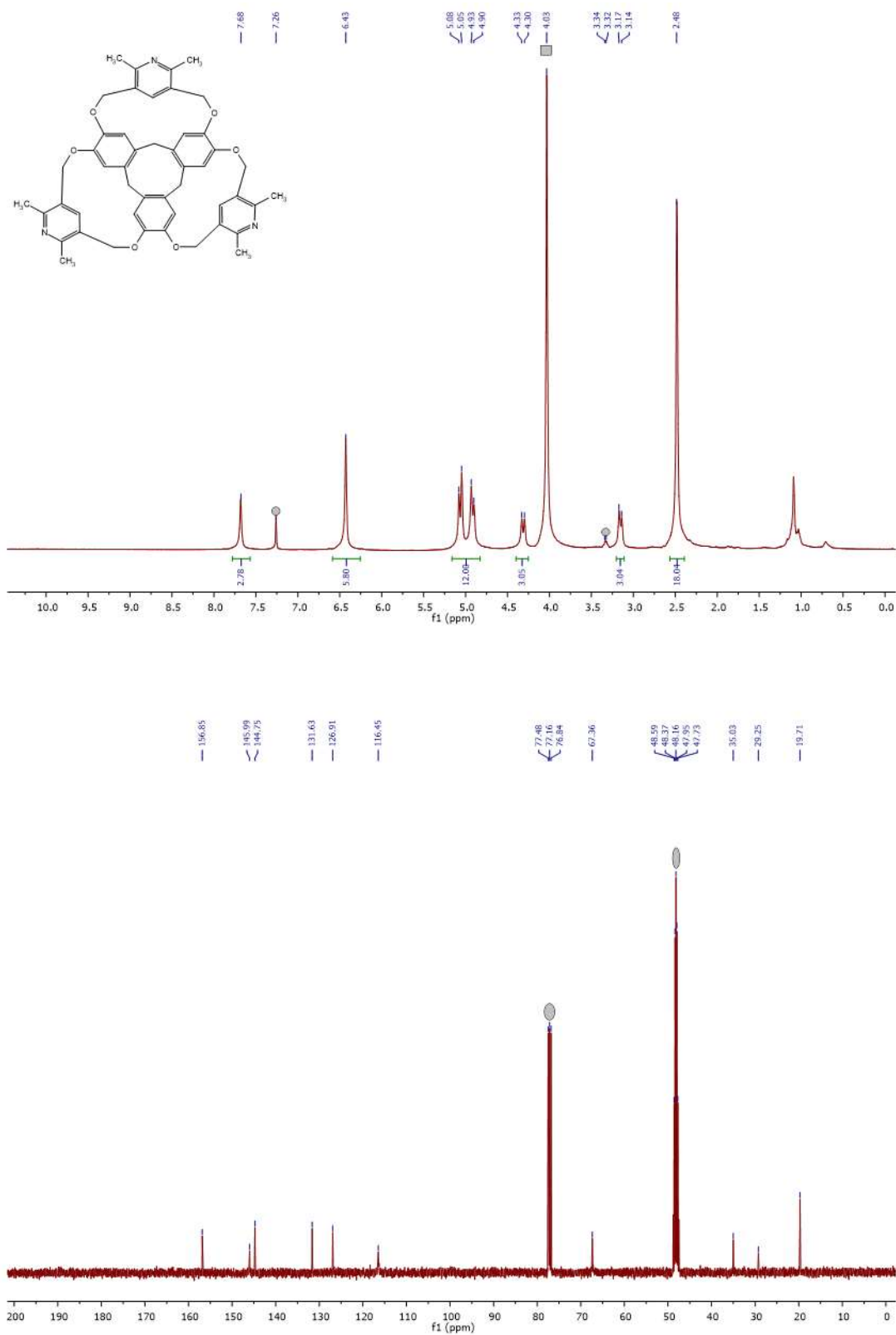


Figure 2.28. ESI-MS spectrum of CTC(Py)₂(OH)₂

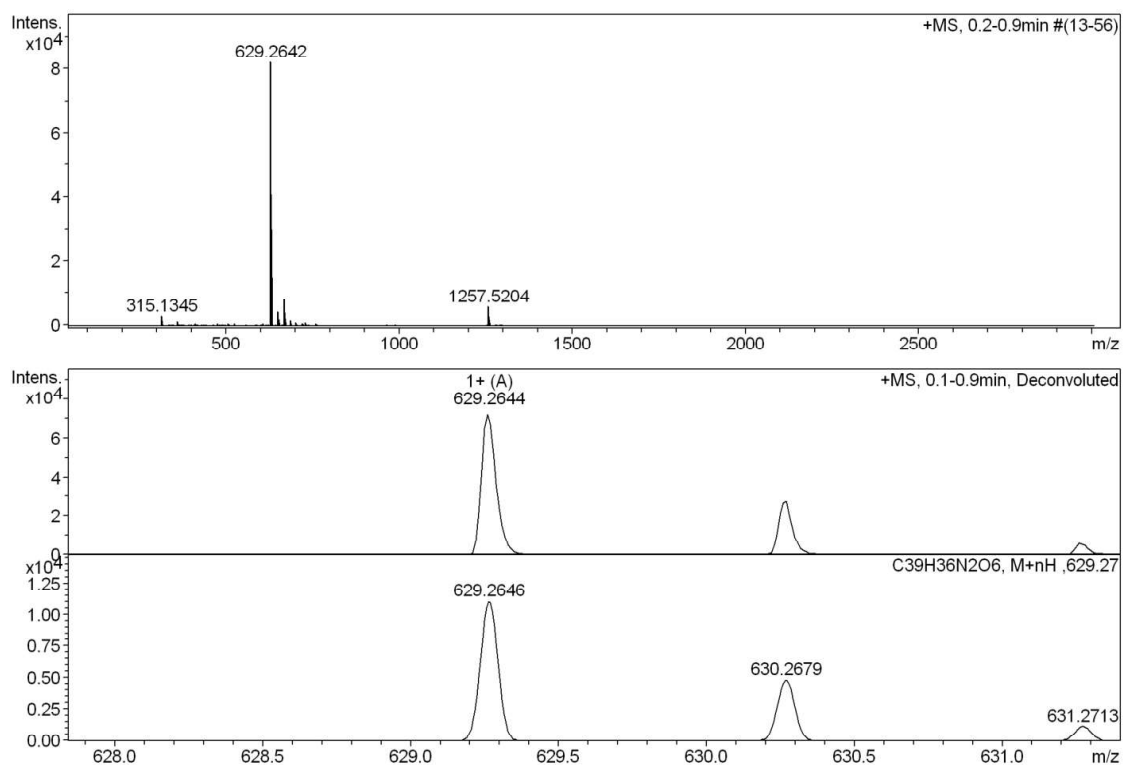
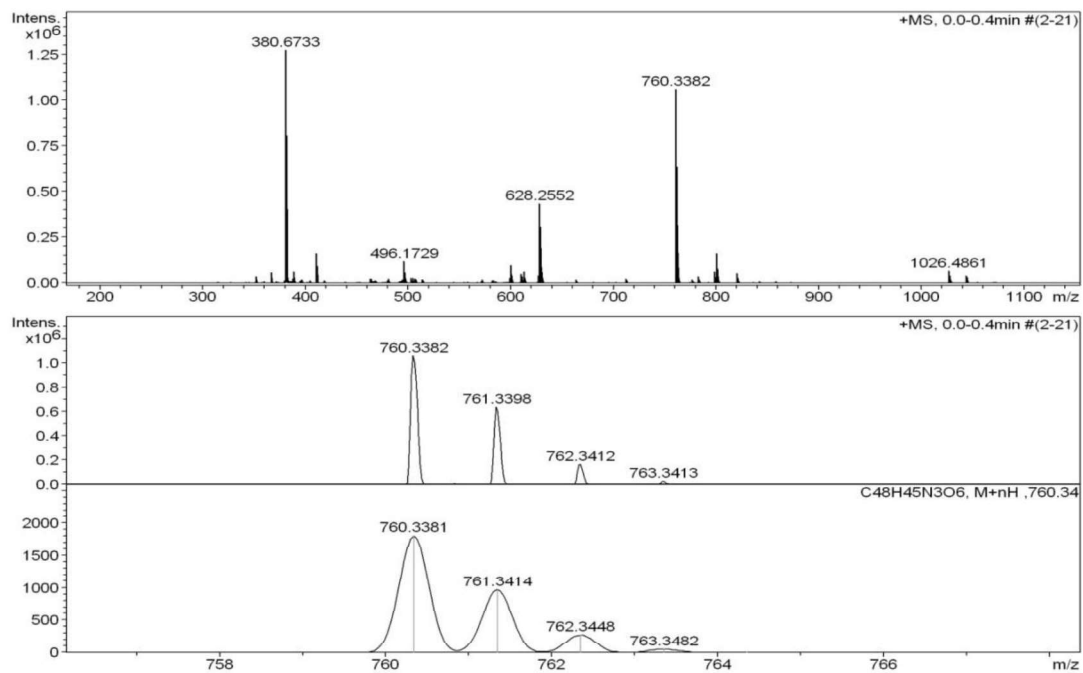


Figure 2.29. ESI-MS spectrum of CTC(Py)₃



2.7 Crystal Data

Table 2.2. Crystal data and structure refinement for CTC(Py)₂(OH)₂(1)forming capsular assembly.

Identification code	CTC-2Py	
Empirical formula	C42.60 H52.80 N2 O10.52 S1.80	
Formula weight	818.89	
Temperature	296(2) K	
Wavelength	0.71073 Å	
Crystal system	Monoclinic	
Space group	P 2 _{1/n}	
Unit cell dimensions	a = 16.8196(7) Å	α = 90°.
	b = 14.4225(5) Å	β = 99.568(3)°.
	c = 17.2295(8) Å	γ = 90°.
Volume	4121.4(3) Å ³	
Z	4	
Density (calculated)	1.320 Mg/m ³	
Absorption coefficient	0.181 mm ⁻¹	
F(000)	1741	
Crystal size	0.27 x 0.22 x 0.12 mm ³	
Theta range for data collection	2.825 to 26.019°.	
Index ranges	-20 ≤ h ≤ 16, -17 ≤ k ≤ 17, -21 ≤ l ≤ 20	
Reflections collected	22935	
Independent reflections	8104 [R(int) = 0.0368]	
Completeness to theta = 25.242°	99.8 %	
Refinement method	Full-matrix least-squares on F ²	
Data / restraints / parameters	8104 / 25 / 588	
Goodness-of-fit on F ²	1.045	
Final R indices [I > 2σ(I)]	R1 = 0.0736, wR2 = 0.2154	
R indices (all data)	R1 = 0.1042, wR2 = 0.2409	
Extinction coefficient	n/a	
Largest diff. peak and hole	1.088 and -0.638 e.Å ⁻³	
CCDC	1525712	

Table 2.3. Hydrogen bonds for CTC(Py)₂(OH)₂ (1) [Å and °]. (Capsular assembly)

D-H...A	d(D-H)	d(H...A)	d(D...A)	Angle(DHA)
O(5)-H(5)...O(10)	0.87	1.83	2.672(4)	161.5
O(10)-H(10A)...O(7)	1.01(2)	1.83(4)	2.750(4)	151(6)
O(6)-H(6)...O(11)#2	0.86(5)	1.86(5)	2.692(4)	164(4)
O(11)-H(11A)...N(2)	0.93(5)	1.91(5)	2.803(4)	159(4)
O(11)-H(11B)...O(7)#2	0.98(2)	1.83(3)	2.765(4)	159(5)
O(10)-H(10B)...N(1)#2	1.00(2)	1.89(4)	2.863(4)	162(8)

Symmetry transformations used to generate equivalent atoms:

#1 $x+1/2, -y+1/2, z+1/2$	#2 $-x+1, -y+1, -z+1$	#3 $x-1/2, -y+3/2, z-1/2$	#4 $x+1/2, -y+3/2, z+1/2$
---------------------------	-----------------------	---------------------------	---------------------------

Table 2. 4. Crystal data and structure refinement for CTC(Py)₂(OH)₂(1) forming non-capsular assembly.

Identification code	CTC-2Py-linear	
Empirical formula	C ₈₄ H ₉₀ N ₄ O ₁₅ S _{2.60}	
Formula weight	1478.95	
Temperature	296(2) K	
Wavelength	0.71073 Å	
Crystal system	Monoclinic	
Space group	P 2 ₁ /c	
Unit cell dimensions	$a = 12.3804(5)$ Å	$\alpha = 90^\circ$.
	$b = 25.0918(8)$ Å	$\beta = 110.287^\circ$.
	$c = 15.6377(5)$ Å	$\gamma = 90^\circ$.
Volume	$4556.5(3)$ Å ³	
Z	2	
Density (calculated)	1.2 mg/m ³	
Absorption coefficient	0.172 mm ⁻¹	

F(000)	1752
Crystal size	0.24 x 0.22 x 0.21 mm ³
Theta range for data collection	1.754 to 29.460°.
Index ranges	-17<=h<=16, -34<=k<=34, -21<=l<=21
Reflections collected	71938
Independent reflections	12641 [R _{int} = 0.0357, R _{sigma} = 0.0263]
Completeness to theta = 25.242°	99.9 %
Refinement method	Full-matrix least-squares on F ²
Data / restraints / parameters	12641 / 0 / 578
Goodness-of-fit on F ²	1.1
Final R indices [I>2sigma(I)]	R ₁ = 0.0719, wR ₂ = 0.2273
R indices (all data)	R ₁ = 0.1002, wR ₂ = 0.2478
Extinction coefficient	n/a
Largest diff. peak and hole	0.76 and -0.5 e.Å ⁻³
CCDC	1530352

Table 2.5. Hydrogen bonds for CTC-Py2 [Å and °]. (non-capsular assembly)

D-H...A	d(D-H)	d(H...A)	d(D...A)	<(DHA)
C(11)-H(11B)...O(5)#1	0.97	2.46	3.428(4)	178.7
C(18)-H(18)...O(14)#2	0.93	2.58	3.439(8)	153.3
C(21)-H(21)...O(14)#2	0.93	2.54	3.371(6)	148.7
C(29)-H(29A)...O(11)#3	0.97	2.48	3.446(5)	176.9
C(30)-H(30B)...O(12)	0.96	2.64	3.109(6)	110.8
C(31)-H(31A)...O(4)	0.96	2.58	3.194(6)	122.0
C(31)-H(31A)...O(10)#3	0.96	2.57	3.475(6)	156.7
C(41)-H(41A)...O(11)	0.96	2.54	3.164(6)	122.4
C(42)-H(42A)...O(3)	0.96	2.44	3.117(5)	127.5
C(46)-H(46A)...O(5)	0.96	2.52	3.149(6)	122.7
C(66)-H(66)...O(15)	1.04	2.58	3.484(8)	144.7
C(68)-H(68)...O(15)	0.93	2.48	3.296(6)	147.0
C(76)-H(76A)...O(9)	0.96	2.48	3.142(6)	125.9
C(76)-H(76B)...S(4)	0.96	2.99	3.704(6)	132.0
C(80)-H(80A)...O(6)	0.96	2.49	3.166(6)	127.3
C(80)-H(80C)...O(9)#4	0.96	2.62	3.385(6)	137.2
O(1)-H(1O)...N(3)	0.82	2.09	2.764(4)	139.1

O(2)-H(2O)...N(1)	0.82	2.04	2.707(4)	137.7
O(7)-H(7O)...N(4)#2	0.82	2.10	2.777(4)	140.4
O(8)-H(8O)...N(2)#2	0.82	2.04	2.741(4)	143.6

Table 2.6. Crystal data and structure refinement for CTC(Py)₃(2).

Identification code	CTC-3Py		
Empirical formula	C ₄₈ H ₄₅ N ₃ O ₁₁		
Formula weight	839.87		
Temperature	293(2) K		
Wavelength	0.71073 Å		
Crystal system	Orthorhombic		
Space group	P n a 21		
Unit cell dimensions	a = 20.6343(7) Å	α = 90°.	
	b = 20.0381(7) Å	β = 90°.	
	c = 12.2555(4) Å	γ = 90°.	
Volume	5067.3(3) Å ³		
Z	4		
Density (calculated)	0.996 mg/m ³		
Absorption coefficient	0.079 mm ⁻¹		
F(000)	1608.0		
Crystal size	0.28 x 0.21 x 0.15 mm ³		
Theta range for data collection	1.948 to 25.791°.		
Index ranges	-25 ≤ h ≤ 25, -24 ≤ k ≤ 24, -11 ≤ l ≤ 14		
Reflections collected	71022		
Independent reflections	9985 [R(int) = 0.0894]		
Completeness to theta = 25.242°	99.9 %		
Refinement method	Full-matrix least-squares on F ²		
Data / restraints / parameters	9985 / 1 / 520		
Goodness-of-fit on F ²	0.988		
Final R indices [I > 2σ(I)]	R ₁ = 0.0495, wR ₂ = 0.0862		
R indices (all data)	R ₁ = 0.1010, wR ₂ = 0.0945		
Largest diff. peak and hole	0.12 and -0.12 e.Å ⁻³		
CCDC	1525713		

Chapter-3

Thiourea Decorated Cyclotrimeratrylene : Synthesis and its Receptor

Properties

3.1. Abstract.	131
3.2. Introduction.	133
3.2.1. CTV analogues as anion and cation receptors.	134
3.3. Motivation.	139
3.4. Results and Discussion.	139
3.4.1. Anion binding studies of L:	140
3.4.2. Ion pair binding studies.	146
3.4.3. Amino acid binding studies.	152
3.5. Summary.	154
3.6. Experimental Section.	154
3.7. References.	157
3.8. Spectral data.	159

3.1. Abstract

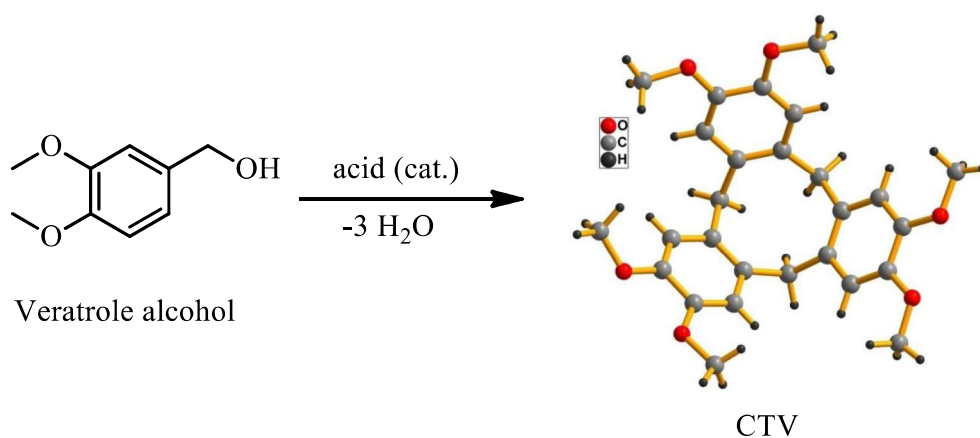
A new C_3 -symmetric CTV based host (**L**) was designed and synthesized by attaching thiourea groups. UV Binding studies showed that **L** acts as a colourimetric sensor for fluoride and cyanide anions in DMSO. Also CTV host **L** acts as ion pair receptor for tetraethyl ammonium salts in low polar solvent 5% $CDCl_3$ /DMSO and colourimetric sensor for zwitter ionic basic amino acid arginine in 5% H_2O /DMSO.

3.2. Introduction

Cations and anionic species plays a vital role in chemical, biological, environmental and medical processes. Over the decades there exists an immense interest of designing artificial receptors for cations and anions.¹ Recently, the research in designing the hosts for binding both cation and anion simultaneously is emerging as it is energetically favourable than binding discrete ion.²⁻³

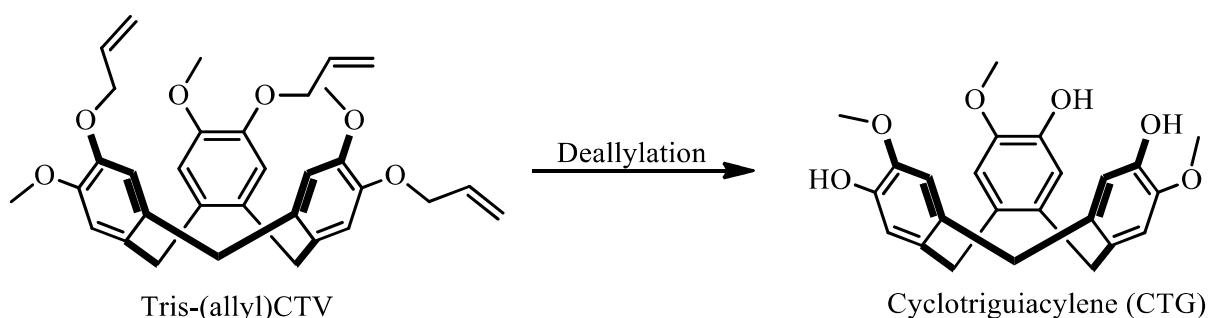
Cavitands are the molecules having the cavity which binds guest molecules via non-covalent interactions. These molecules offer preorganized geometry for guest binding.⁴ Examples include calix[n]arene, calix[n]pyrrole, resorcinarene, pillar[n]arene, Cyclotrimeratrylene (CTV) etc. Anion and ion pair recognition based on these molecules was well explored but relatively less effort has been made on CTV based receptors.

Cyclotrimeratrylene (CTV) is a cyclic molecular scaffold having a crown conformation. Thanks to its pyramidal geometry, as it offers an electron-rich and hydrophobic molecular cavity that displays fascinating host-guest properties.⁵⁻⁶ CTV is synthesized by acid catalysed condensation of veratrole alcohol and its derivatives can be synthesized via partially demethylated version, Cycloguaiacylene (CTG) and complete demethylated product, Cyclotricatechylene (CTC).

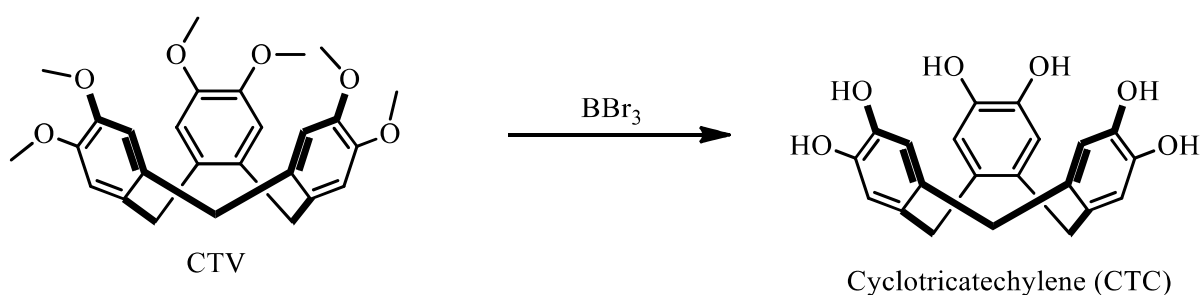


Scheme 3.1. *Synthesis of CTV*

CTG is synthesized by deallylation of tris-(allyl)CTV (Scheme 3.2) whereas CTC is formed by demethylation of CTV with BBr_3 (Scheme 3.3).



Scheme 3.2. *Synthesis of CTG.*



Scheme 3.3. *Synthesis of CTC.*

3.2.1. CTV analogues as anion and cation receptors

Anions are ubiquitous in nature. They play key role throughout biological systems. DNA is a polyanion and most of the enzyme substrates, co-factors are anionic. Chloride is found extensively in extracellular fluid, while its mis-regulation leads to diseases such as cystic fibrosis. Iodide is required for the biosynthesis of hormones by the thyroid gland. Bicarbonate is vital in the maintenance of pH levels in the body, whereas cyanide is highly toxic. Nitrate and sulphate are key components in the production of harmful acid rain.^{1,7}

Compared to cation, selective anion binding is tough because of its variable size, geometry, pH and solvation effects. If anion recognition by a receptor induces a response such as optical (colour or fluorescence), electrochemical etc., then it can be called as anion sensor (Figure 3.1).

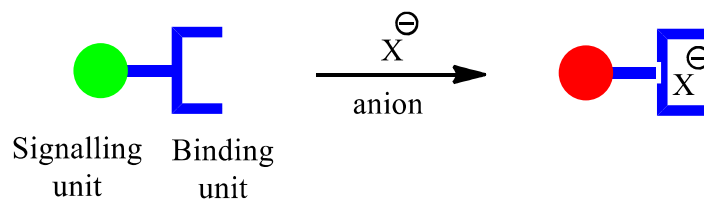


Figure 3.1. *Cartoon representation of mechanism of anion sensing.*

Anion receptors based on CTV are less explored compared to the analogues calixarene and resorcinarene. There are two types of strategies implemented for anion binding based on CTV hosts.⁵ One approach is the metallation of arene rings of the host that forms π -type ligands. As a result, the cavity of the host becomes electron deficient which makes it feasible to bind electron rich anions. First of this kind was reported by Steed and co-workers.⁸ They synthesized organometallic CTVs by reacting CTV with $[\text{Ru}(\eta^6\text{-arene})(\text{S})^3]^{2+}$ resulting a mono-, bi-, trimetallic CTV host molecules (Figure 3.2).

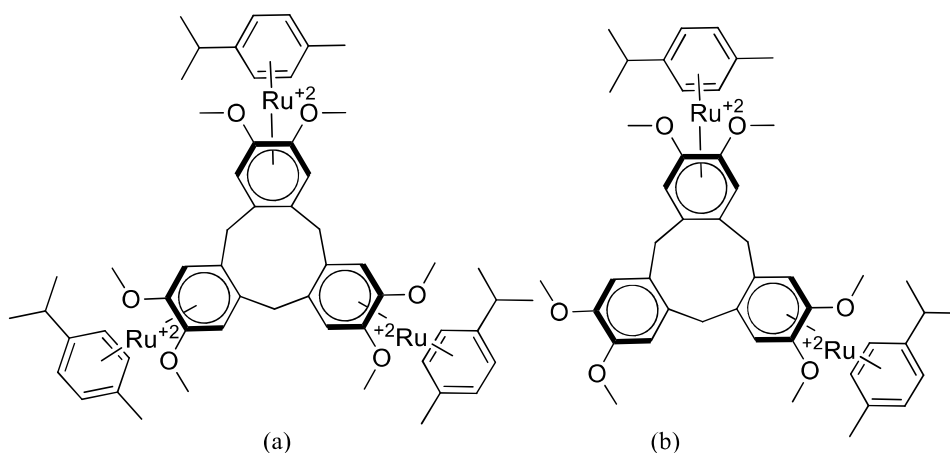
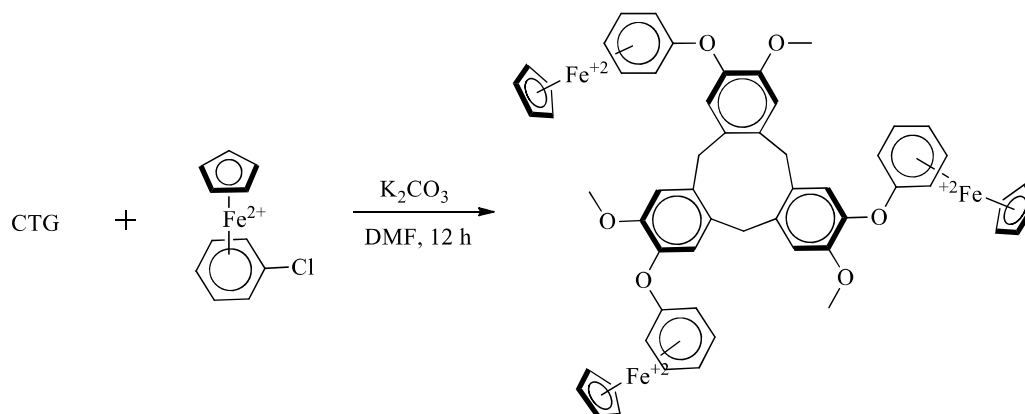


Figure 3.2. *Metallated CTVs*

The anion binding studies were performed by means of cyclic voltammetry. The CTV host (Figure 3.2(b)) displays interesting anion recognition properties. It shows more affinity for tetrahedral anions such as TcO_4^- which is a radioactive component of nuclear waste, ReO_4^- compared to halide ions and the order binding is $\text{TcO}_4^- > \text{ReO}_4^- > \text{ClO}_4^- > \text{NO}_3^- > (\text{SO}_4)_2^- > \text{Cl}^-$. Later Atwood's team demonstrated the improvement in the binding ability by utilizing metallated extended-CTV.⁹ This was prepared by nucleophilic aromatic substitution of

[CpFe(Chloroarene)][PF₆] with CTG in the presence of base (Scheme 3.4). Anion binding studies reveals that the metallated extended host shows remarkable selectivity towards TcO₄⁻, ReO₄⁻ and also it is able to extract >95% TcO₄⁻ from saline solution having different type of anions.



Scheme 3.4. Synthesis of metallated extended CTV.

Holman's group employed the same method for the preparation of metallated cryptophanes.¹⁰ They have synthesized [Cp*₂Ru]⁺ cryptophane by treating Ru²⁺ metal salt with collet's cryptophane (Figure 3.3). After metallation the volume of the cryptophane was enlarged. The size is fit for larger anions like CF₃SO₃⁻, PF₆⁻ in both solution and solid phase but it doesn't bind smaller anions

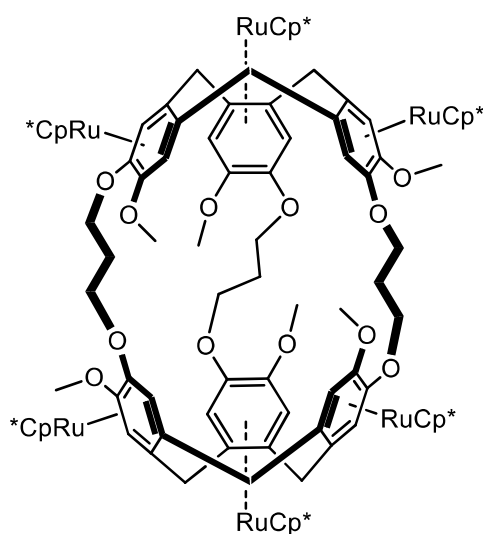


Figure 3.3. Hollman's metallated cryptophane.

The second approach is attaching the hydrogen bonding ability functional groups to the CTV host. For instance, Tris-amide CTV shows more selectivity for OAc^- and weakly binds H_2PO_4^- than halide, nitrate, and sulphate ions. Self-assembled monolayers (SAMs) of Tris-amide CTV were prepared by dipping the gold beads in the solution of CTV host and anion sensing ability was studied by cyclic voltammetry (CV). Studies reveals that the selectivity towards OAc^- was retained (Figure 3.4.).¹¹ Similar report demonstrated tris-amide CTV appended with ferrocene binds H_2PO_4^- , ATP^{2-} .¹²

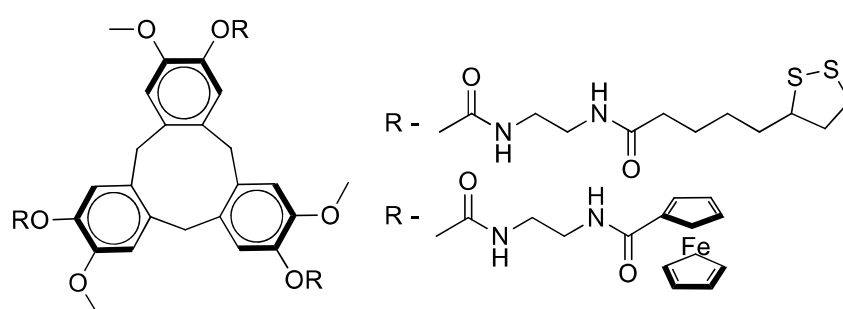


Figure 3.4. *Tris-amide CTV anion receptors*

CTV core was also utilized for cation binding. For example, C_3 -functionalised CTV(2-quinolinemethyl)₃ acts as a fluorometric sensor for Cu^{2+} (Figure 3.5.).¹³

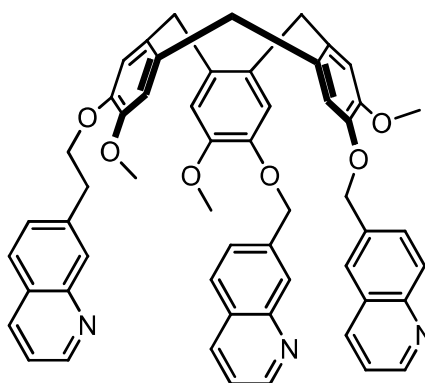


Figure 3.5. *Quinoline appended CTV capsule*

CTV analog was designed and synthesized for the radioactive actinides separation and extraction which is highly desirable.¹⁴ Although it gave a better extraction but unfortunately there is no selectivity for particular cation.(Figure 3.6)

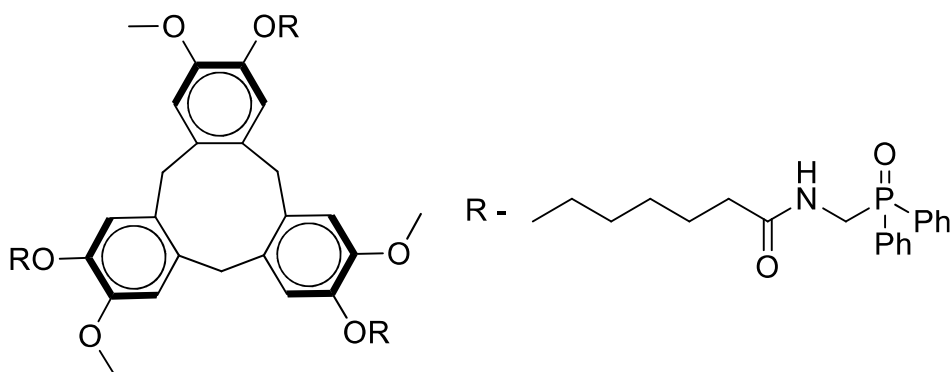
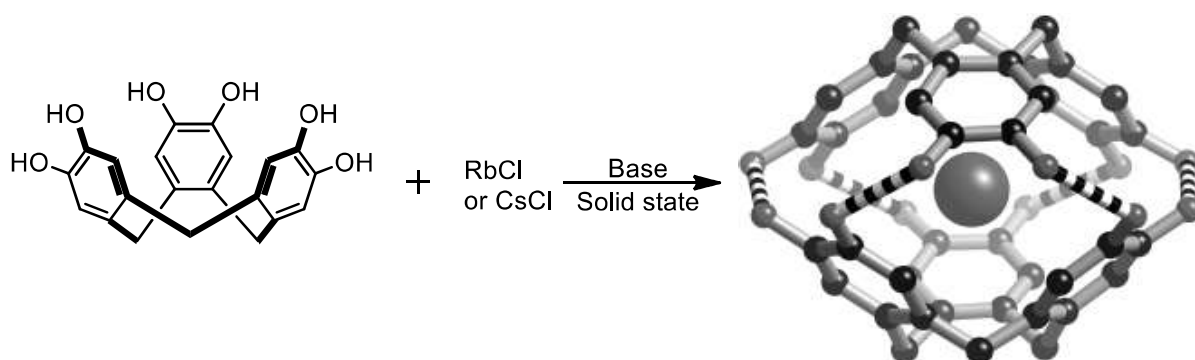


Figure 3.6. CTV based actinide receptor

The complete demethylated product of CTV, Cyclotricatechylene (CTC) also capable of forming capsules in the presence of cationic guest. In 2009, Abrahams *et al* demonstrated that CTC under basic conditions forms clam-like structure in the presence of Rb^{2+} and Cs^{2+} salts encapsulating the cation (Scheme 3.5).¹⁵ While with K^+ salt it doesn't form clam structure because the size of cation is too small to fit. They also investigated this with organic cations such as tetramethyl ammonium (Me_4N^+) and tetraethyl ammonium (Et_4N^+) cations.



Scheme 3.5. Abraham's closed clam CTC

Both the cations forms an open clam like structure encapsulation the tetraalkyl ammonium cations. CTV doesn't show this type of behaviour with both alkali and organic cations where the alkali cations coordinate to the dimethoxy groups of CTV.¹⁶

In 2016, we showed that under neutral conditions CTC forms dimeric capsule with tetraethyl ammonium salts encapsulating the cation in both solution and solid state (Figure

3.7). Also the dimeric capsule was not effected with the change in the anion of the ammonium salt.¹⁷

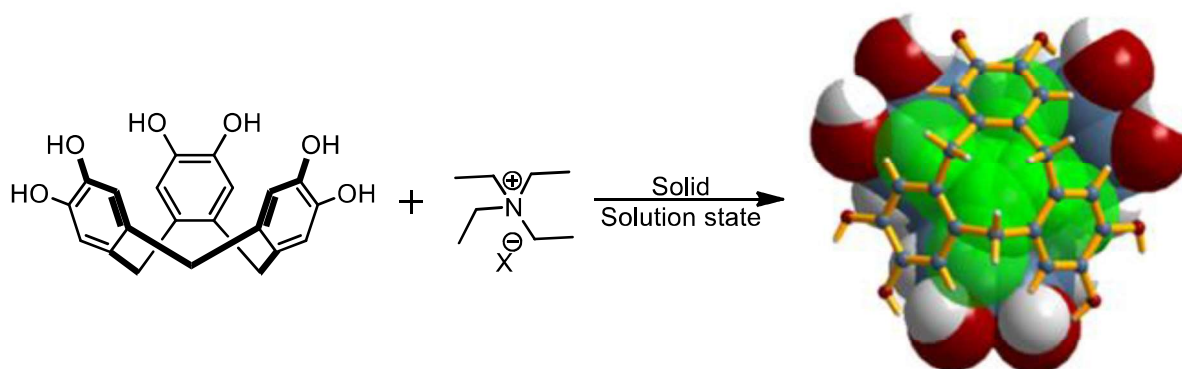


Figure 3.7. Guest induced CTC dimeric capsule

3.3. Motivation

Previous reports suggest that receptors based on CTV scaffold are less explored compared to the analogous calixarene and resorcinarene. Although there are few reports (above mentioned) in the literature utilized CTV core as anion receptor and electrochemical anion sensor, there are no optical sensors known so far. Thus, it would be highly desirable to develop a CTC based system that can be used as an optical sensor. While in the case of cation binding no systematic study has been done in the solution state with CTV host especially with organic cations noting that considerable effort with cryptophanes was well documented. Keeping this in mind, we have designed a CTV host (**L**) appended with well known anion binding 4-nitrophenylthiourea groups which acts as an optical signalling unit. As the CTV core has the ability to interact with cations we envisaged that our host could act as ion-pair receptor by stabilizing the cation in the cavity and the anion at the thiourea groups (Figure 3.8).

3.4. Results and Discussion

We started the synthesis with vanillyl alcohol by bromo butylating the phenolic hydroxyl group with excess of 1,4-dibromobutane in the presence of K_2CO_3 to get (4-(4-

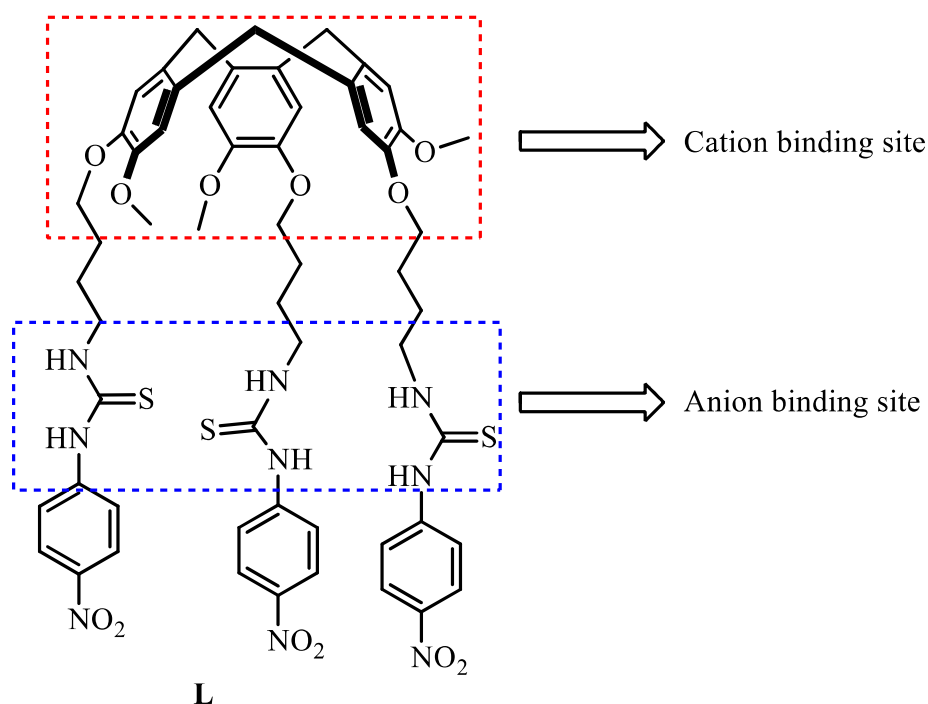
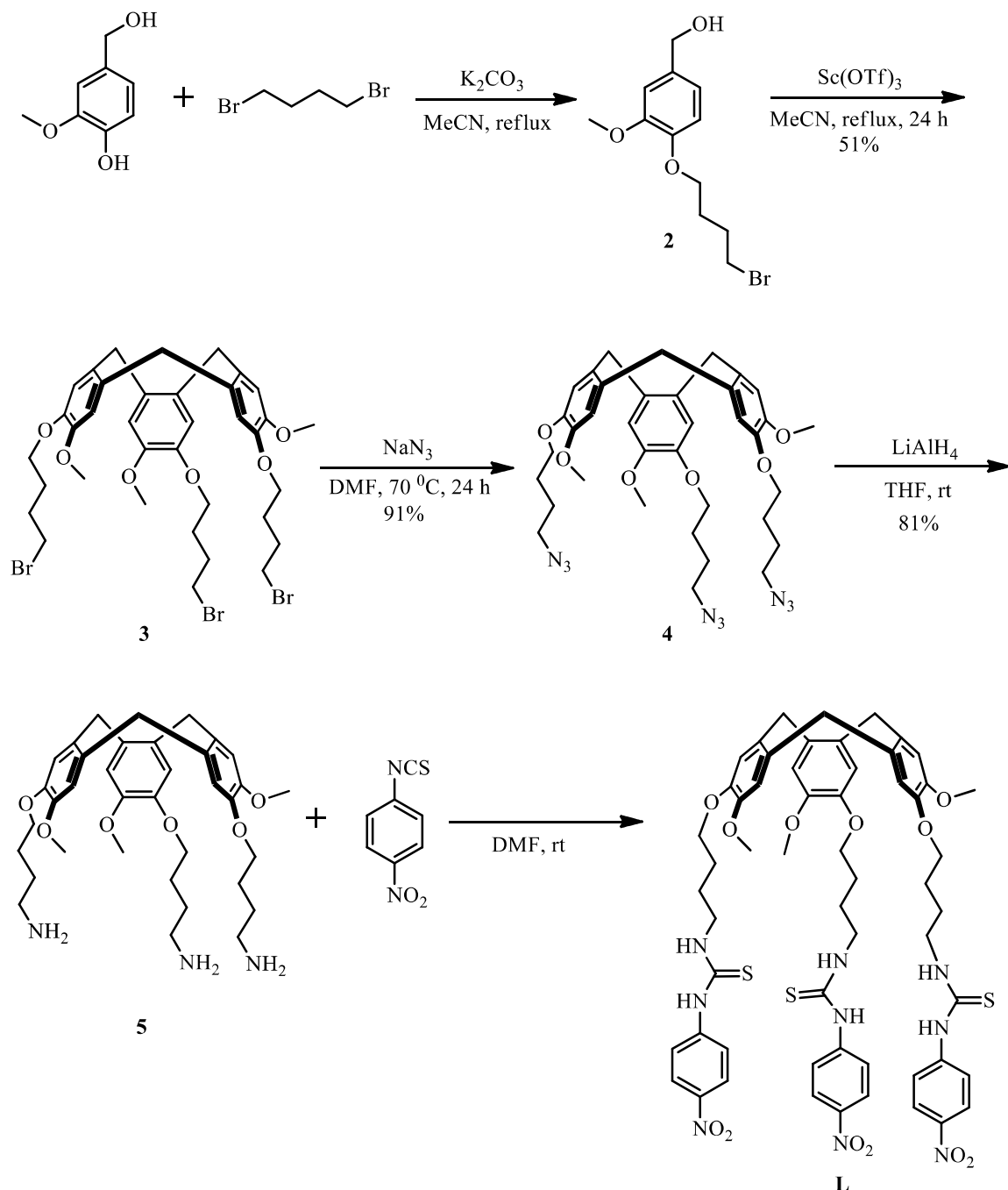


Figure 3.8. Our design of Heteroditopic CTV receptor.

bromobutoxy)-3-methoxyphenyl)methanol **2**. Then lewis acid catalysed condensation of **2** gives CTG-BuBr **3**. Reacting **3** with sodium azide in DMF yields corresponding azide CTG-BuN₃ **4**. Then the azide group was reduced with lithium aluminium hydride to get tris-amine derivative CTG-BuNH₂ **5**. This tris-amine was treated with 4-nitrophenyl isothiocyanate in DMF to obtain the desired tris-thiourea derivative (**L**) in 37 % yield from previous step (Scheme 3.6). This was characterised by NMR and mass spectroscopy. In ¹H NMR, the two merged singlet peaks at 7 ppm corresponding to aryl-CTG core and the two doublets of CTG methylene protons at 4.7 ppm and 3.5 ppm indicating the retention of three fold symmetry. Comparing the integration values of aryl-CTG and nitro phenyl protons which are in 1:2 ratio confirming our desired tris-thiourea appended CTV (**L**). The mass analysis showed peak at m/z 1184.369 $[M + Na]^+$ (calc 1184.365).

3.4.1. Anion binding studies of **L**:

Anion binding ability of **L** was studied by adding various anions (F^- , Cl^- , Br^- , I^- , CN^- , NO_3^- , PF_6^- , BF_4^- , OAc^- , HSO_4^- , SCN^-) as their tetrabutyl ammonium salts using UV-visible



Scheme 3.6. Synthesis of CTV receptor **L**.

spectroscopy in DMSO at 1.42×10^{-5} M. The characteristic absorption peak of **L** shows at 358 nm due to $\pi-\pi^*$ transition of chromophoric nitrophenyl group. With the addition of

fluoride and cyanide ion to **L** in DMSO the UV spectra shows new absorption at 487 nm where as no change in the absorption spectra of **L** was observed for the remaining anions (Figure 3.9). Therefore we performed UV titration experiments for **L** by gradually increasing the concentration of anions (F^- , CN^-) until the saturation point.

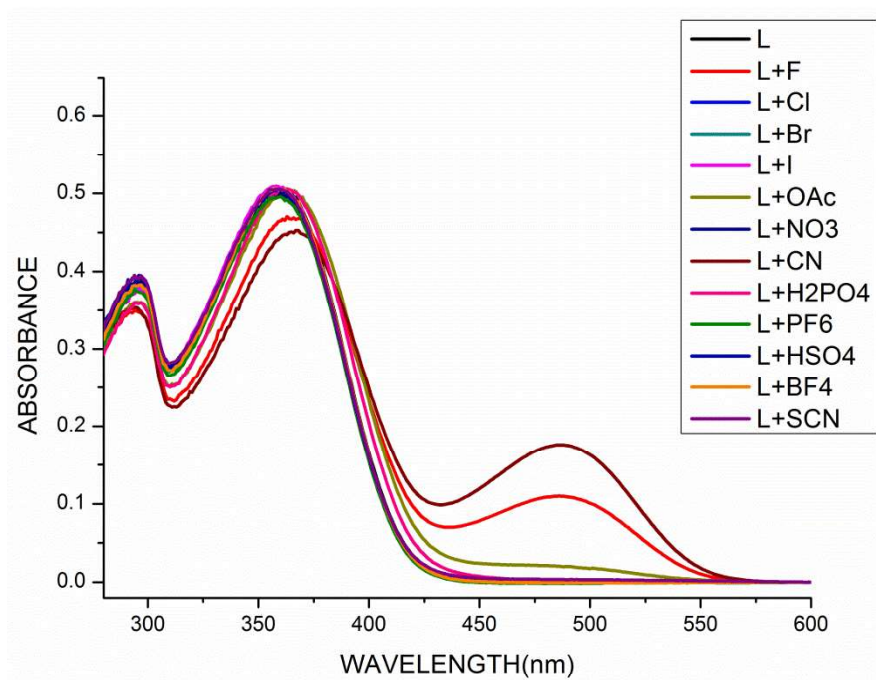


Figure 3.9. UV-Vis plot of **L** with various anions

Titration experiments were performed at $[L] = 1.42 \times 10^{-5}$ M in DMSO using 1 mL cuvette. For F^- ion, new absorption peak started to appear at 487 nm when $[F^-]$ is 1.42×10^{-4} M. With increase in the concentration of fluoride ion, the peak at 358 nm decreases where as the peak at 487 nm increases. The saturation point was reached at $[F^-] = 2.9 \times 10^{-3}$ M (Figure 3.10). The origin of new peak is due to internal charge transfer (ICT) between anion-thiourea and electron deficient $-NO_2$ moiety. As a result the colour of the solution changes from pale yellow to orange colour. Well defined isosbestic point at 409 nm suggests that there exists only one type of host-anion complex. Similar change was observed in the case of CN^- ion (Figure 3.11).

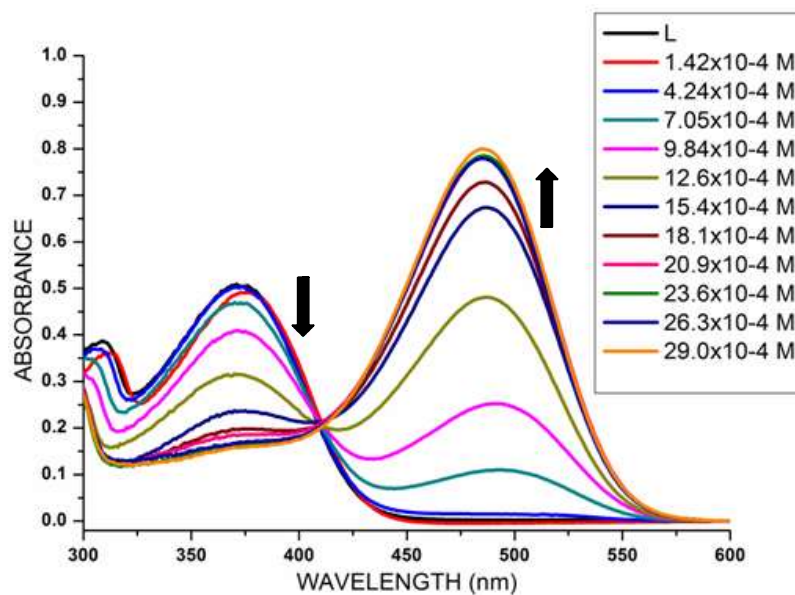


Figure 3.10. UV titration of **L** with F^- ion in DMSO

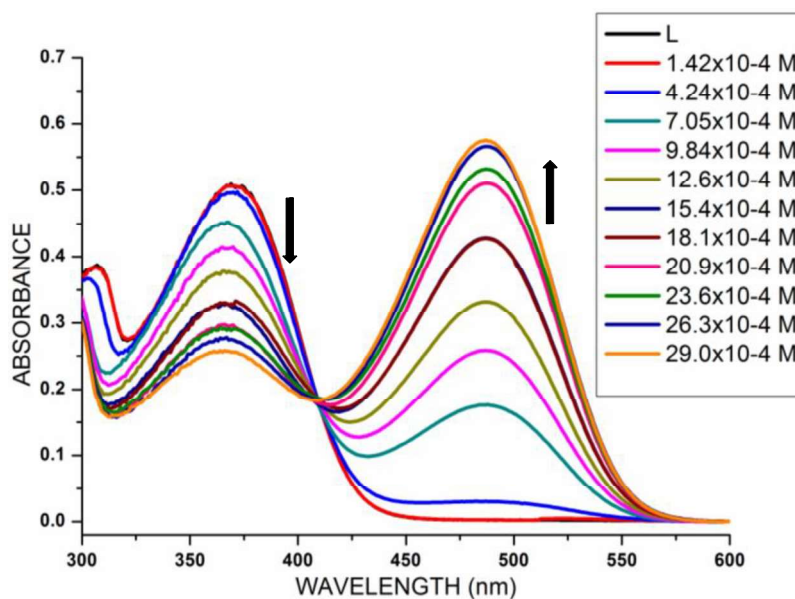


Figure 3.11. UV titration of **L** with CN^- ion in DMSO

Using this titration data, the binding constants of anions (F^- , CN^-) with **L** were measured by Benesi-Hildebrand(BH) plots. The Benesi-Hildebrand equation states that

$$\frac{1}{A_0 - A} = \frac{1}{(A_0 - A_{\max})K[G]^n} + \frac{1}{A_0 - A_{\max}}$$

Where A_0 – Absorbance in the absence of guest ; A – Absorbance in the presence of guest ; A_{\max} – Absorbance at saturation point ; K – Binding constant ; G – guest ; n – Stoichiometry

A graph of $1/A_0 - A$ vs $1/[G]^n$ was plotted. Linear plot obtained for both the anions when $n = 3$ suggests that host-anion complex exists in 1:3 stoichiometry.

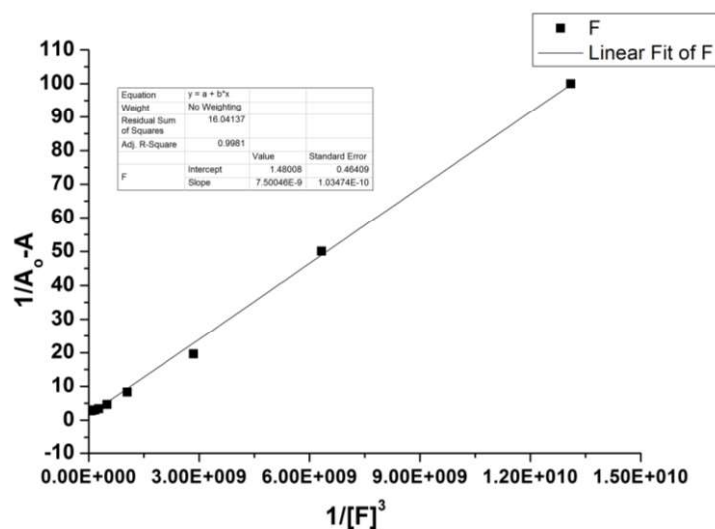


Figure 3.12. BH plot of *L* with F^- ion.

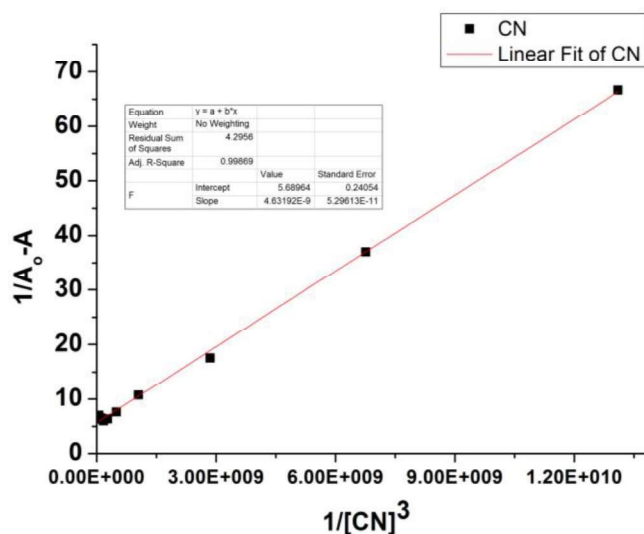


Figure 3.13. BH plot of *L* with CN^- ion.

Binding constants obtained by the ratio of intercept to the slope of the linear plot and are found to be $19.8 \times 10^7 \text{ M}^{-3}$ for F^- ion (Figure 3.12). where as for CN^- ion it is $12.3 \times 10^8 \text{ M}^{-3}$. (Figure 3.13)

For further insight, we performed a ^1H NMR titration experiment in DMSO-d_6 . Before addition of anions (F^- , CN^-), the NMR chemical shifts for Thiourea $-\text{NH}$ protons of **L** were appeared at 10.02δ and 8.28δ . With the addition of 0.1 equiv.of F^- ions to **L**, the

thiourea protons shows little broadness with decrease in intensity of the peak. Finally, both protons were disappeared by the addition of 0.45 equiv. of F^- ions (Figure 3.14). While in the case of CN^- ion both thiourea protons of **L** were disappeared by the addition of 0.2 equiv. (Figure 3.15)

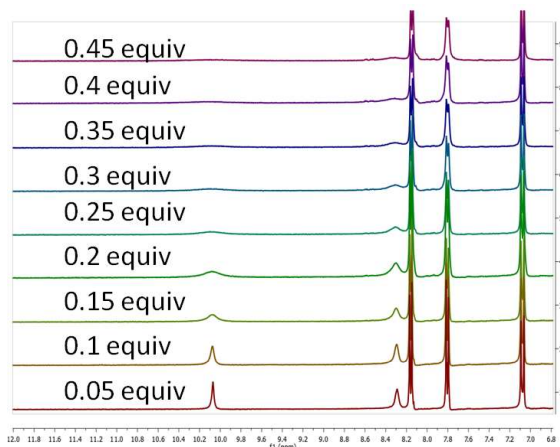


Figure 3.14. 1H NMR titration of **L** with F^- ion.

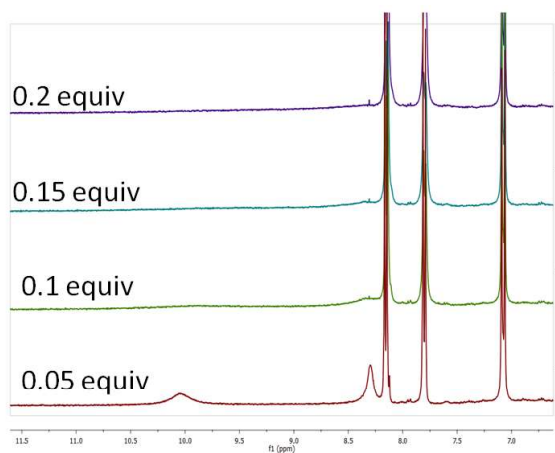


Figure 3.15. 1H NMR titration of **L** with CN^- ion.

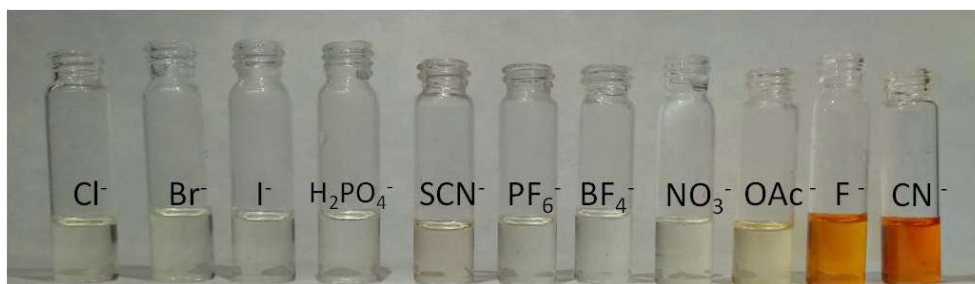


Figure 3.16. Receptor **L** ($1.42 \times 10^{-4} M$) with various anions in DMSO

The origin of the colour is due to internal charge transfer caused by the deprotonation of Thiourea –NH protons by the anions (F^- , CN^-). (Figure 3.17)

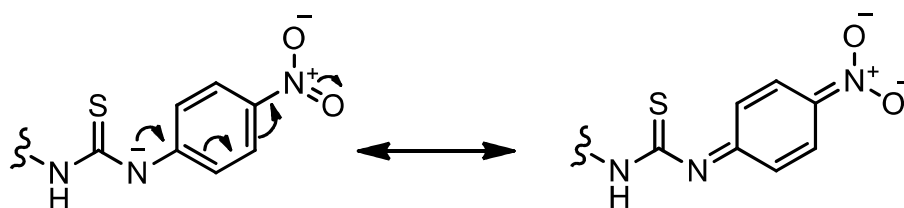


Figure 3.17. Mechanism of internal charge transfer (ICT).

3.4.2. Ion pair binding studies

The binding ability of the receptor **L** for the ion pairs was investigated using tetraalkyl ammonium salts by 1H NMR spectroscopy (Figure 3.18). Initially, we performed the 1H NMR experiment by adding 1 equiv. of 0.2 M DMSO- d_6 solution (8 μ L) of tetraalkyl ammonium chlorides to the 0.00313 M of receptor **L** in 5% DMSO/ $CDCl_3$ solution (0.5 mL). With the same concentration of DMSO- d_6 in $CDCl_3$ (5% DMSO/ $CDCl_3$ + 8 μ L DMSO- d_6) the 1H NMR spectra of **L** and tetraalkyl ammonium chlorides were recorded separately. Comparing these three corresponding spectra the chemical shift differences were obtained and those are the protons corresponding to tetraalkyl ammonium cation together with

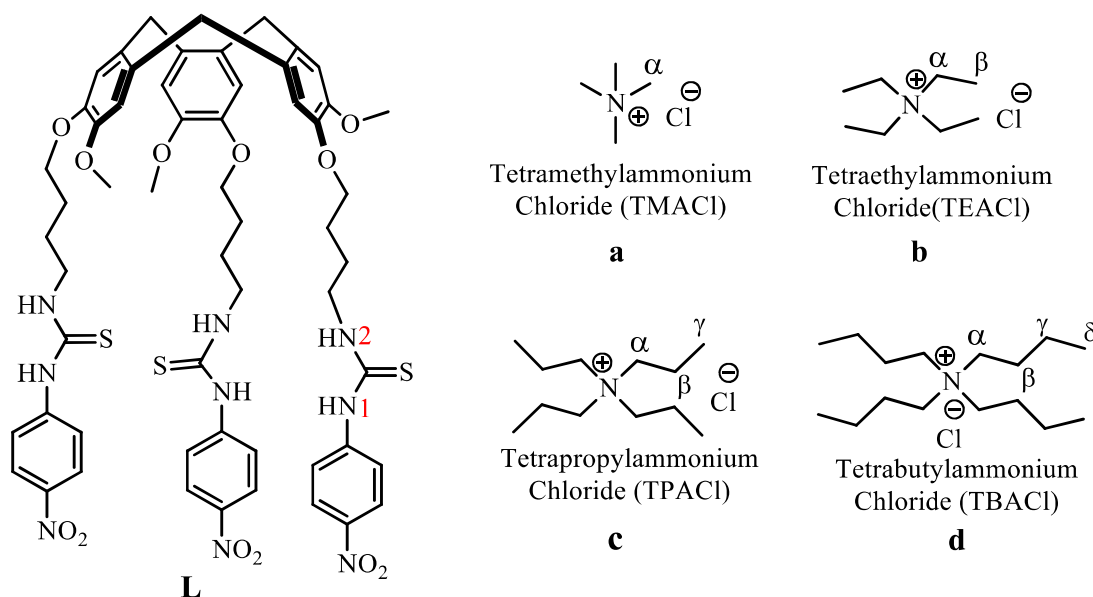


Figure 3.18. Chemical structures of **L** and tetraalkyl ammonium salts.

urea –NH protons of **L**. The chemical shift differences of various tetraalkyl ammonium chlorides in the presence of **L** were given in the following table.

Tetraalkylammonium chlorides	¹ H NMR Δδ (ppm)					
	α	β	γ	δ	N1 of L	N2 of L
a	0.19				0.37	0.30
b	0.33	0.15			0.61	0.40
c	0.16	0.05	0.04		0.60	0.40
d	0.15	0.04	0.04	0.0	0.60	0.40

Table 3.1. ¹H NMR chemical shifts of tetraalkyl ammonium protons in presence of **L**.

From the above table, it is clear that α-protons of tetraethyl ammonium chloride shows more shift compared to that of remaining salts in the presence of **L** (Figure 3.19). This suggest strong binding of tetraethyl ammonium cation with the receptor **L**.

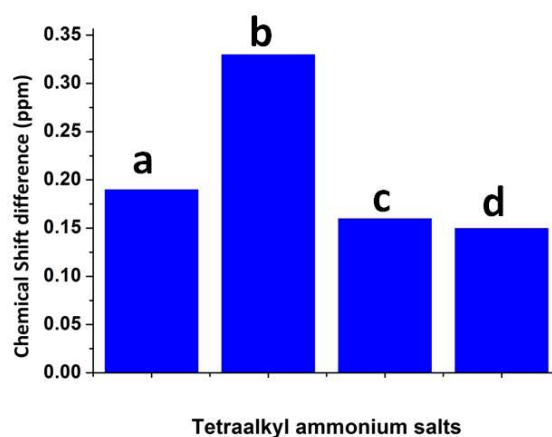


Figure 3.19. Chemical shift differences of α-protons of ammonium salts in the presence of **L**.

¹H NMR studies also reveal that mixing equimolar ratios of tetraalkyl ammonium salts with **L** results in upfield shifting of tetraalkyl ammonium protons suggesting that cation binds at

the CTV cavity (Figure 3.20(b)) where as Thiourea –NH protons of **L** experiences downfield shift (Figure 3.20(a)) indicating the anion interaction at this site.

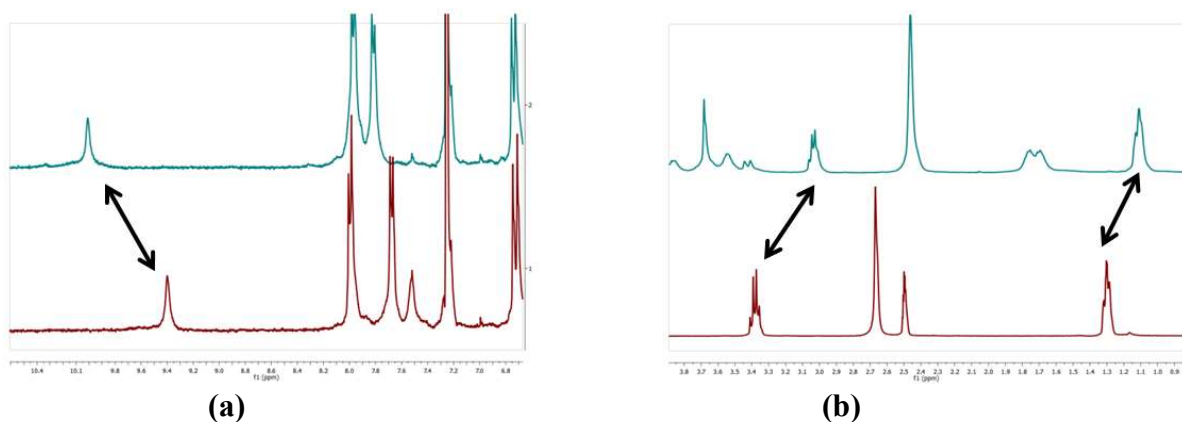


Figure 3.20. Partial ^1H NMR spectra of TEACl salt with (blue) and without (red) **L**

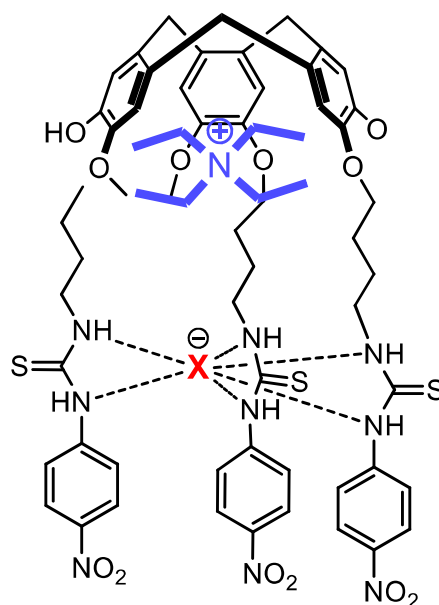


Figure 3.21. Plausible binding of TEAX to **L**

In order to investigate the effect of anion on the binding of tetraethyl ammonium cation, we performed ^1H NMR titration studies with various tetraethyl ammonium salts (TEA^+X^- ; X – F, Cl, Br, I, ClO_4). NMR was recorded for every 0.2 equiv. addition of 0.1 M DMSO- d_6 solution of TEA^+X^- up to 1.2 equiv. and then excess (2 and 5 equiv.) to 0.00313 M 5% DMSO/ CDCl_3 solution of **L** (0.5 mL) along with the corresponding spectra of **L** without

TEA⁺X⁻ and TEA⁺X⁻ without **L** maintaining the same NMR solvent ratio. The chemical shift differences of each salt were tabulated below.

Tetraethyl ammonium perchlorate (TEAClO₄)

No. of equiv.	¹ H NMR Δδ (ppm)		
	methylene	methyl	Thiourea N1 of L
0.2	0.09	0.06	0
0.4	0.09	0.06	0.02
0.6	0.05	0.03	0.04
0.8	0.04	0.02	0.04
1	0.03	0.03	0.04
1.2	0.03	0.02	0.03
2	0.03	0.01	0.02
5	0	0	0

Table 3.2. ¹H NMR Chemical shift differences of TEAClO₄ protons and N1 proton of **L** with equivalents

Tetraethyl ammonium iodide (TEAI)

No. of equiv.	¹ H NMR Δδ (ppm)		
	methylene	methyl	Thiourea N1 of L
0.2	0.15	0.14	0.08
0.4	0.14	0.14	0.11
0.6	0.1	0.05	0.13
0.8	0.1	0.05	0.14
1	0.07	0.03	0.17
1.2	0.06	0.04	0.15
2			
5	0.01	0.01	0.07

Table 3.3. ¹H NMR Chemical shift differences of TEAI protons and N1 proton of **L** with equivalents

Tetraethyl ammonium bromide (TEABr)

No. of equiv.	¹ H NMR Δδ (ppm)		
	methylene	methyl	Thiourea N1 of L
0.2	0.21	0.12	0.11
0.4	0.2	0.11	0.18
0.6	0.18	0.09	0.26
0.8	0.15	0.08	0.3
1	0.13	0.07	0.35
1.2	0.13	0.06	0.37
2	0.09	0.05	0.42
5	0.01	0	0.38

Table 3.4. ¹H NMR Chemical shift differences of TEABr protons and N1 proton of **L** with equivalents

Tetraethyl ammonium chloride (TEACl)

No. of equiv.	¹ H NMR Δδ (ppm)		
	methylene	methyl	Thiourea N1 of L
0.2	0.27	0.12	0.13
0.4	0.25	0.12	0.3
0.6	0.26	0.12	0.49
0.8	0.24	0.12	0.61
1	0.22	0.11	0.64
1.2	0.2	0.1	0.71
2	0.14	0.07	0.87
5	0.05	0.03	0.93

Table 3.5. ¹H NMR Chemical shift differences of TEACl protons and N1 proton of **L** with equivalents

Tetraethyl ammonium fluoride (TEAF)

No. of equiv.	$^1\text{H NMR } \Delta\delta$ (ppm)		
	methylene	methyl	Thiourea N1 of L
0.2	0.24	0.12	0.1
0.4	0.24	0.11	0.21
0.6	0.23	0.11	0.33
0.8	0.22	0.11	0.45
1	0.2	0.11	0.57
1.2	0.2	0.11	0.73
2	0.18	0.12	1.54
5	0.11	0.08	

Table 3.6. $^1\text{H NMR}$ Chemical shift differences of TEAF protons and N1 proton of **L** with equivalents

Based on the above data, a plot has been drawn for chemical shift differences of methylene protons of TEA salts in the presence and the absence of **L** versus number of equivalents of TEA salts.

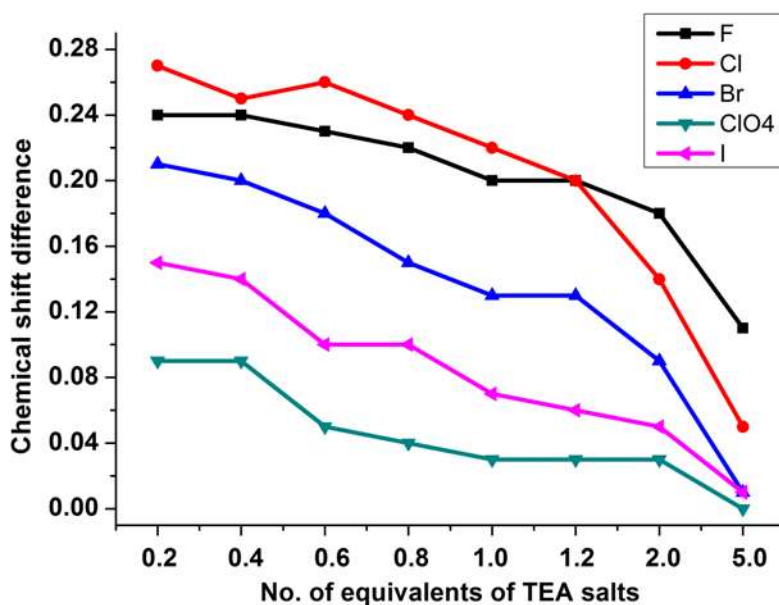


Figure 3.22. Plot showing chemical shift differences of methylene protons of TEAX in presence of **L** versus number of equivalents of TEAX.

From the plot, it is apparent that as the number of equivalents of TEA salts increases the chemical shift difference decreases suggesting the ion pair binding is inversely proportional to the number of TEAX equivalents. This is probably due to increase in the polarity of the solvent that causes stabilization of salts by solvation. Among the different TEA salts the fluoride and chloride salts show strong binding compared to the remaining salts as indicated by the chemical shift difference. Also the receptor (**L**) N1 proton shift is high with TEAF and TEACl where as TEAI and TEAClO₄ causes less shift. From these observations it can be concluded that the receptor **L** is selective for TEAF and TEACl ion pairs.

3.4.3. Amino acid binding studies

Based on the ion pair binding studies of **L**, we further investigated the possible binding of zwitter ionic amino acids to the receptor **L** predicting that the ammonium cation of amino acid can be stabilized by CTV cavity where as the Thiourea groups of **L** stabilizes the acid group.(Figure 3.23)

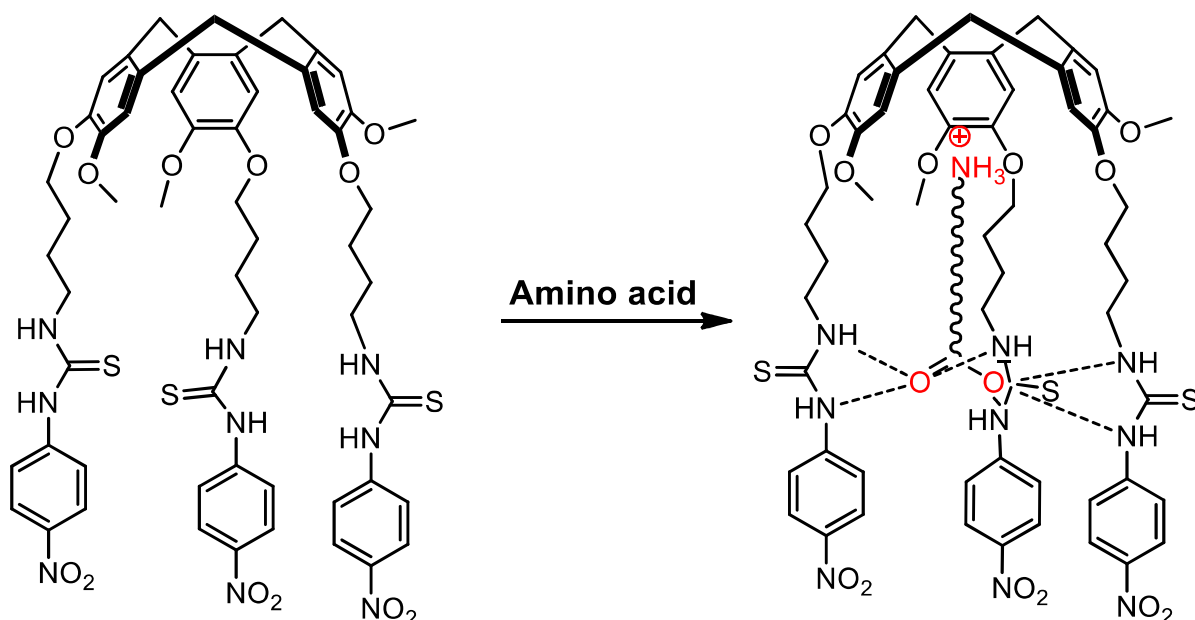


Figure 3.23. Predicted binding of amino acid to **L**.

Initially we performed ^1H NMR studies with different amino acids in 10% $\text{D}_2\text{O}/\text{DMSO-d}_6$. None of these showed chemical shift difference in the presence of **L** indicating no binding. But interestingly, we observed a colour change from pale yellow to red on addition of arginine to the receptor **L**. Therefore we conducted UV-Vis studies with various amino acids (0.2 M in H_2O) in 5% $\text{H}_2\text{O}/\text{DMSO}$ at $[\text{L}] = 1.42 \times 10^{-5}$ M. As expected, arginine shows new absorption peak at 487 nm. (Figure 3.24)

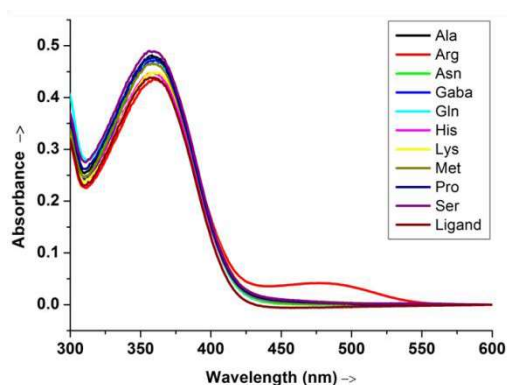


Figure 3.24. UV-Vis titration of **L** with various amino acids.

Then UV titration experiments were performed at $[\text{L}] = 1.42 \times 10^{-5}$ M in 5% $\text{H}_2\text{O}/\text{DMSO}$ with $[\text{Arg}] = 0.2$ M in H_2O . The new absorption peak appeared at $[\text{Arg}] = 1.39 \times 10^{-4}$ M and the saturation point was reached at $[\text{Arg}] = 4.3 \times 10^{-3}$ M.

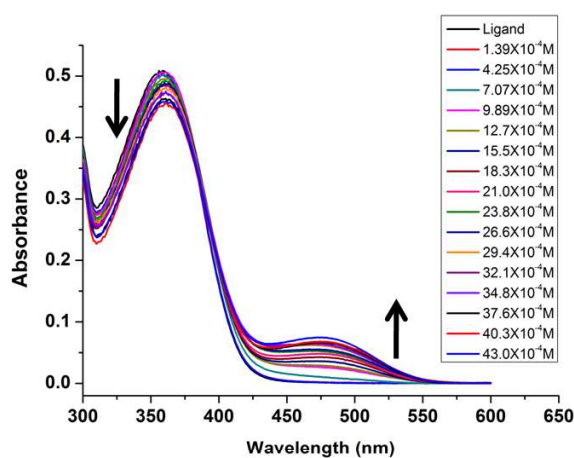


Figure 3.25. UV-Vis titration plot of **L** with arginine in 5% $\text{H}_2\text{O}/\text{DMSO}$.

Further we did ^1H NMR studies by adding 0.2 M Arginine in H_2O to 0.00313 M 5% $\text{H}_2\text{O}/\text{DMSO-d}_6$ (0.5 mL). After adding 0.2 equiv. of arginine to **L**, the protons corresponding to the thiourea moiety were disappeared completely indicating the deprotonation. As a result of this, colour is changing to red by Internal Charge Transfer (ICT) mechanism. (Figure 3.26)

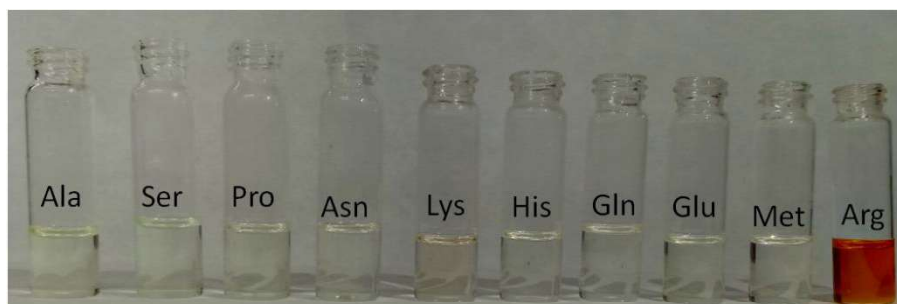


Figure 3.26. 5% $\text{H}_2\text{O}/\text{DMSO}$ solution of **L** (1.42×10^{-4} M) in presence of various amino acids

3.5. Summary

Thiourea functionalized CTG host was synthesized and its receptor properties were studied. Studies shows that it act as colorimetric sensor for F^- , CN^- anions in DMSO and for arginine in 5% $\text{H}_2\text{O}/\text{DMSO}$. Also the host acts as ion pair receptor for tetraethyl ammonium salts in non-polar solvents.

3.6. Experimental Section

Materials: Reagent grade and metal salts were acquired from Aldrich and used as received. All solvents, were procured from Merck Chemicals, India. Solvents were purified prior to use following standard procedures.

3.6.1. Synthesis of (4-(4-bromobutoxy)-3-methoxyphenyl)methanol (**2**)

Vanillyl alcohol (5g, 32.45 mmol) was dissolved in 30 mL of dry acetone and anhydrous K_2CO_3 (5.4g, 38.94mmol) was added under N_2 atmosphere, to this solution 1, 4-dibromo butane (35.031 g, 162.25 mmol) was added and refluxed overnight. The reaction

mixture was filtered and solvent was evaporated under reduced pressure. The residue was purified by column chromatography using (silica 100-200), (20%Hexane+80%EtOAc) as eluent, resulted in a sticky liquid. (8.33g, 74%)¹H NMR (400 MHz, CDCl₃) δ 6.90 (s, 1H), 6.83 (m, *J* = 2.2 Hz, 2H), 4.57 (s, 2H), 4.02 (t, *J* = 6.2 Hz, 2H), 3.83 (s, 3H), 3.48 (t, *J* = 6.6 Hz, 2H), 2.11 – 2.01 (m, 3H), 1.96 (m, *J* = 12.7, 6.3 Hz, 2H).¹³C NMR (100 MHz, CDCl₃) δ 149.65, 147.84, 134.09, 119.43, 113.26, 111.03, 77.48, 77.16, 76.84, 68.22, 65.18, 55.97, 33.59, 29.51, 27.90.

3.6.2. Synthesis of 2,7,12-tris(4-bromobutoxy)-3,8,13-trimethoxy-10,15-dihydro-5H-tribenzo[a,d,g][9]annulene (CTG-BuBr (3))

CTG-BuBr was prepared following similar procedure.¹⁸ The alkylated vanillyl alcohol (5) (6.93 g, 23.98 mmol) was dissolved in dry acetonitrile 15 mL under N₂ atmosphere, to this solution Sc(OTf)₃(118mg, 0.239mmol) was added and kept at 70°C for overnight. The solution was evaporated under reduced pressure to this DCM was added and washed with water the DCM layer was dried under anhydrous Na₂SO₄ and the DCM was evaporated under reduced pressure. The crude product purified by column chromatography (silica 100-200) DCM as eluent yielded a white coloured solid (3.66g, 56.37 %).¹H NMR (400 MHz, CDCl₃) δ: 6.85 (s, 1H), 6.82 (s, 1H), 4.75 (d, *J* = 13.8 Hz, 1H), 4.11 – 3.94 (m, 2H), 3.82 (s, 3H), 3.53 (d, *J* = 13.8 Hz, 1H), 3.50 – 3.43 (m, 2H), 2.10 – 2.00 (m, 2H), 1.94 (m, 2H).¹³C NMR (100 MHz, CDCl₃) δ 148.48, 147.17, 132.50, 132.03, 115.66, 113.96, 77.48, 77.16, 76.84, 68.48, 56.42, 36.59, 33.64, 29.51, 27.97.¹³C NMR (100 MHz, CDCl₃) δ 148.32, 147.03, 132.37, 131.92, 115.48, 113.80, 77.34, 77.16, 76.98, 68.68, 56.20, 51.15, 36.42, 26.49, 25.73. ESI-MS *m/z* 837.030

3.6.3. Synthesis of 2,7,12-tris(4-azidobutoxy)-3,8,13-trimethoxy-10,15-dihydro-5H-tribenzo[a,d,g][9]annulene (CTG-BuN₃ (4))

Compound **3** (1.58g, 1.95 mmol) was dissolved in dry DMF 10 mL under N₂ atmosphere, to this solution NaN₃ (1.26g, 19.5mmol) was added and stirred at 70 °C for 12 hours. The solvent was evaporated under reduced pressure and dissolved in DCM, washed with water. The organic layer was evaporated under reduced pressure and the crude product was purified by column chromatography (silica 100-200) (98% DCM + 2% MeOH) as eluent yielded a semi solid (1.24 g, 91%). ¹H NMR (700 MHz, CDCl₃) δ 6.86 (s, 1H), 6.84 (s, 1H), 4.74 (d, *J* = 13.8 Hz, 1H), 4.12 – 3.94 (m, 1H), 3.84 (s, 1H), 3.54 (d, *J* = 13.8 Hz, 1H), 3.42 – 3.30 (m, 1H), 1.94 – 1.86 (m, 1H), 1.79 (m, 1H). ESI-MS *m/z* 722.312

3.6.4 4,4',4''-((3,8,13-trimethoxy-10,15-dihydro-5H-tribenzo[a,d,g][9]annulene-2,7,12-triyl)tris(oxy))tris(butan-1-amine) (CTG-BuNH₂) (5**)**

Compound **4** (1 g, 1.43 mmol) dissolved in dry THF was slowly added to the LiAlH₄ (0.265 g, 7.15 mmol) suspended in THF at 0 °C. After addition the reaction was stirred at room temperature for 24 h. Then the reaction was quenched by the sequential addition of EtOAc, MeOH and little H₂O. The resultant aluminium salts were filtered off via celite and evaporated the solvent to get the title compound **5** as a semi solid. This was used for the next step without any further purification.

3.6.5 1,1',1''-(((3,8,13-trimethoxy-10,15-dihydro-5H-tribenzo[a,d,g][9]annulene-2,7,12-triyl)tris(oxy))tris(butane-4,1-diyl))tris(3-(4-nitrophenyl)thiourea) (L**)**

To the compound **5** from the above step dissolved in dry DMF, 4-nitrophenyl isothiocyanate (0.902 g, 5.005 mmol) was added and stirred for 24 h at room temperature. Then the solvent was evaporated at reduced pressure to get a yellow coloured residue. This was subjected to column chromatography (silica 230-400) with 2% MeOH + DCM as eluent to obtain the title compound (**L**) as yellow solid. (0.598 g, 37%). ¹H NMR (400 MHz, DMSO-d₆) δ 10.07 (s, 1H), 8.28 (s, 1H), 8.16 (d, *J* = 8.8 Hz, 2H), 7.80 (d, *J* = 8.8 Hz, 2H), 7.09 (s,

1H), 7.06 (s, 1H), 4.69 (d, $J = 13.1$ Hz, 1H), 3.96 (m, 2H), 3.62 – 3.46 (m, 3H), 1.71 (s, 4H).
 ^{13}C NMR (175 MHz, DMSO) δ 179.98, 147.59, 146.44, 141.67, 132.24, 132.05, 124.51, 120.28, 115.11, 113.85, 68.18, 55.91, 54.92, 43.53, 40.02, 39.88, 39.76, 39.64, 39.52, 39.40, 39.28, 39.16, 35.04, 26.29, 24.96. HRMS m/z 1184.369 $[\text{M} + \text{Na}]^+$ (calc 1184.365)

3.7. References

1. Beer, P. D.; Gale, P. A., *Angew. Chem. Int. Ed.* **2001**, *40*, 486-516.
2. Kim, S. K.; Sessler, J. L., *Chem. Soc. Rev.* **2010**, *39*, 3784-3809.
3. McConnell, A. J.; Beer, P. D., *Angew. Chem. Int. Ed.* **2012**, *51*, 5052-5061.
4. Coquiere, D.; Le Gac, S.; Darbost, U.; Seneque, O.; Jabin, I.; Reinaud, O., *Org. Biomol. Chem.* **2009**, *7*, 2485-2500.
5. Hardie, M. J., *Chem. Soc. Rev.* **2010**, *39*, 516-527.
6. Henkelis, J. J.; Hardie, M. J., *Chem. Commun.* **2015**, *51*, 11929-11943.
7. Gale, P. A., *Coord. Chem. Rev.* **2003**, *240*, 191-221.
8. Holman, K. T.; Halihan, M. M.; Jurisson, S. S.; Atwood, J. L.; Burkhalter, R. S.; Mitchell, A. R.; Steed, J. W., *J. Am. Chem. Soc.* **1996**, *118*, 9567-9576.
9. Gawenis, J. A.; Holman, K. T.; Atwood, J. L.; Jurisson, S. S., *Inorg. Chem.* **2002**, *41*, 6028-6031.
10. Fairchild, R. M.; Holman, K. T., *J. Am. Chem. Soc.* **2005**, *127*, 16364-16365.
11. Zhang, S.; Echegoyen, L., *J. Am. Chem. Soc.* **2005**, *127*, 2006-2011.
12. Reynes, O.; Maillard, F.; Moutet, J.-C.; Royal, G.; Saint-Aman, E.; Stanciu, G.; Dutasta, J.-P.; Gosse, I.; Mulatier, J.-C., *J. Organomet. Chem.* **2001**, *637*, 356-363.
13. T. Moriuchi-Kawakami, J. S. a. Y. S., *Anal. Sci.*, **2009**, *25*, 449.
14. Dam, H. H.; Reinhoudt, D. N.; Verboom, W., *New J. Chem.* **2007**, *31*, 1620-1632.
15. Abrahams, B. F.; FitzGerald, N. J.; Hudson, T. A.; Robson, R.; Waters, T., *Angew. Chem. Int. Ed.* **2009**, *48*, 3129-3132.

16. Hardie, M. J.; Ahmad, R.; Sumbly, C. J., *New J. Chem.* **2005**, *29*, 1231-1240.
17. Satha, M. P.; Illa, M. G.; Ghosh, A.; Purohit, C. S., *ChemistrySelect* **2016**, *1*, 1630-1635.
18. Brotin, T.; Roy, V.; Dutasta, J.-P., *J. Org. Chem.* **2005**, *70*, 6187-6195.

3.8. Spectral data

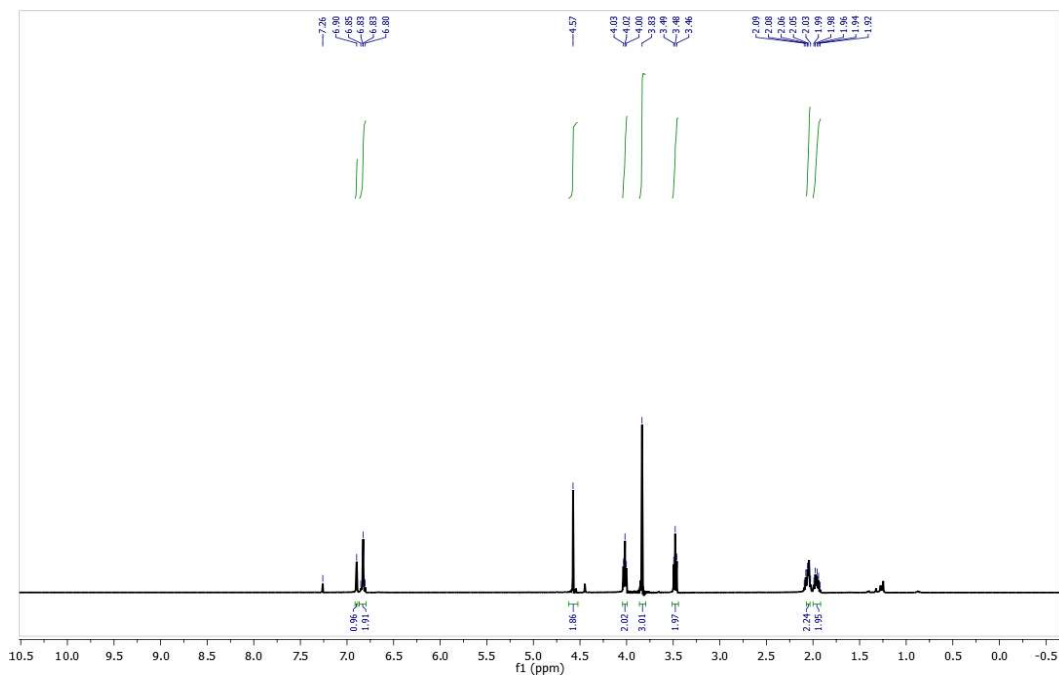


Figure 3.27. ^1H NMR spectrum of compound 2

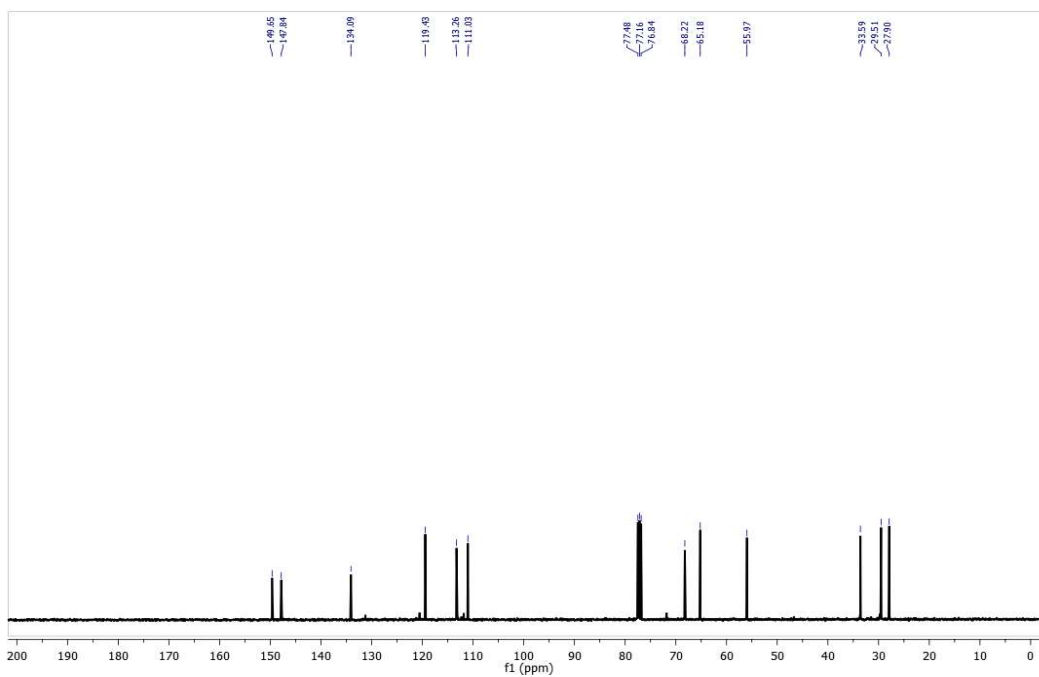


Figure 3.28. ^{13}C NMR spectrum of compound 2

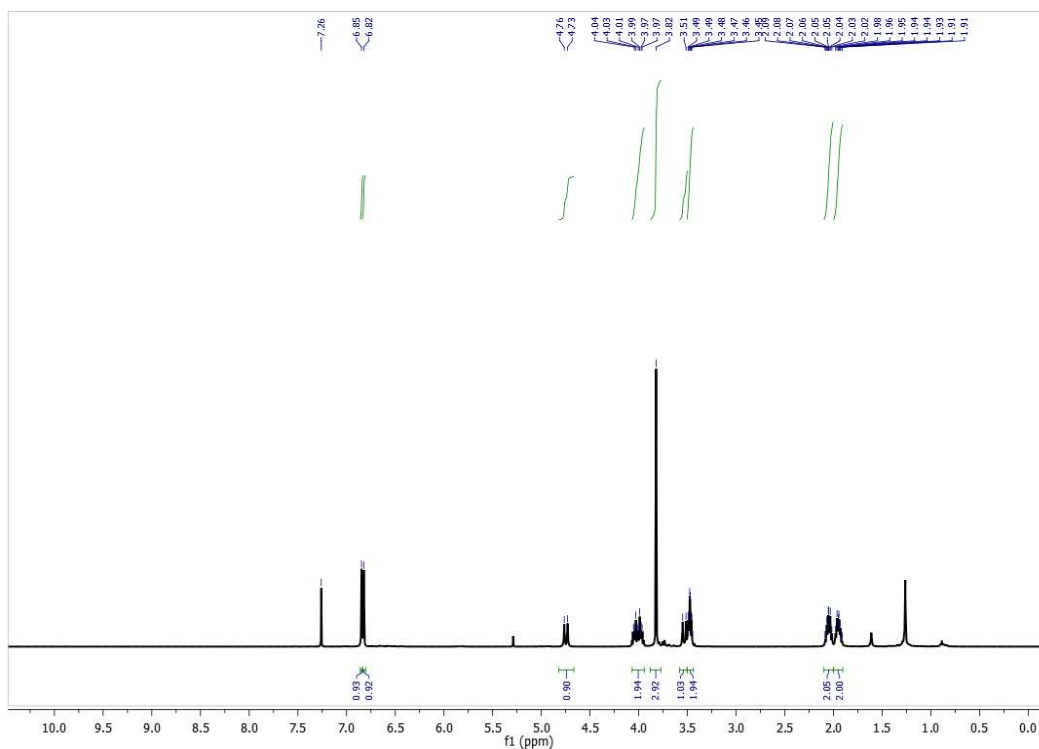


Figure 3.29. ^1H NMR spectrum of compound 3

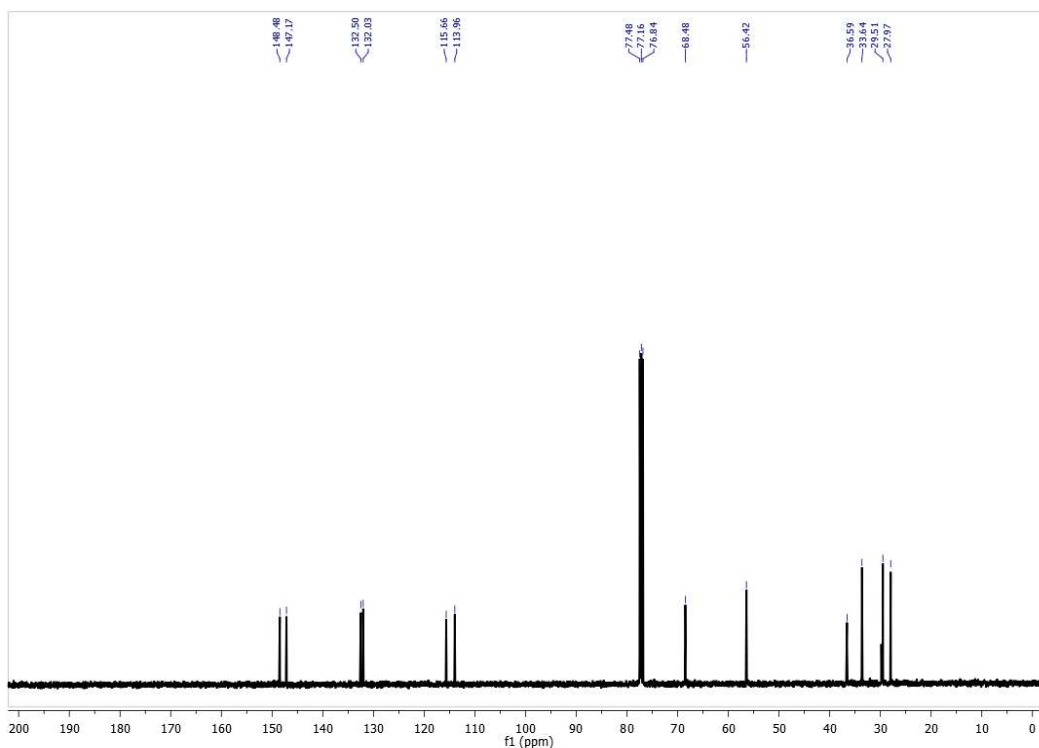


Figure 3.30. ^{13}C NMR spectrum of compound 3

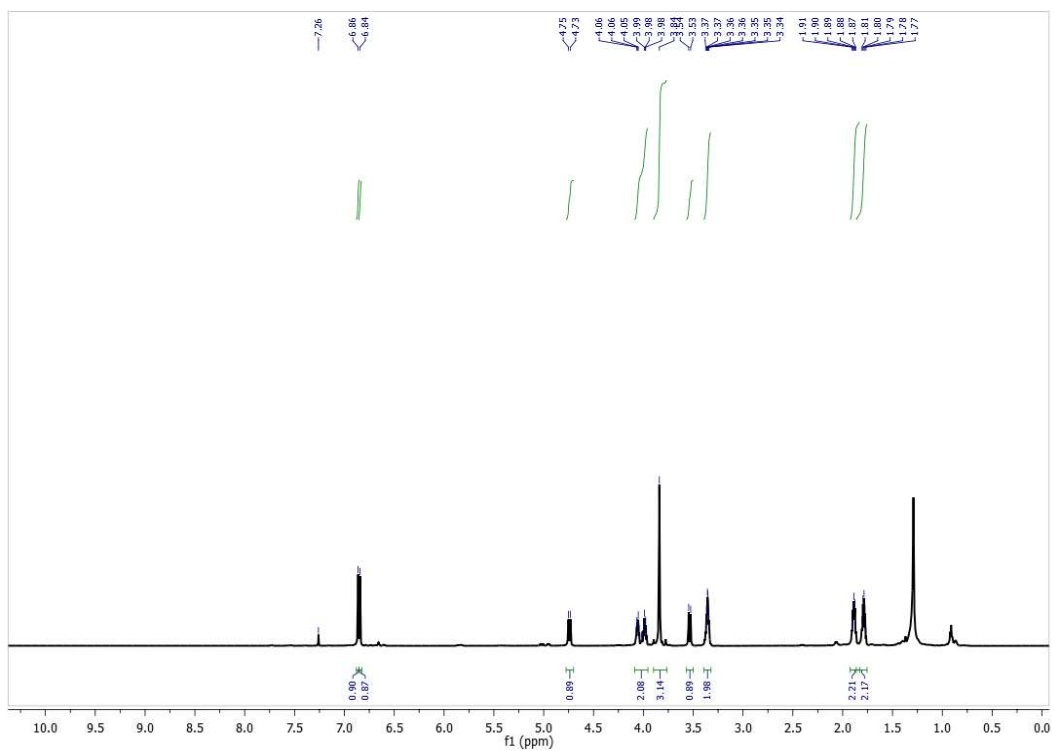


Figure 3.31. ^1H NMR spectrum of compound 4

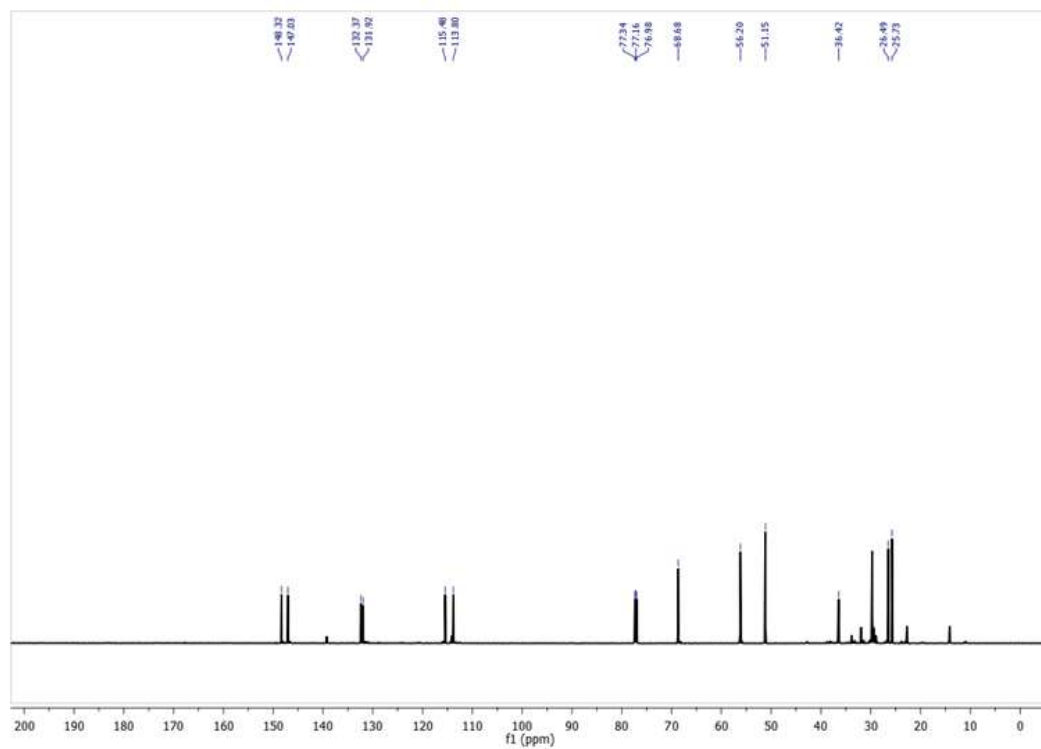


Figure 3.32. ^{13}C NMR spectrum of compound 4

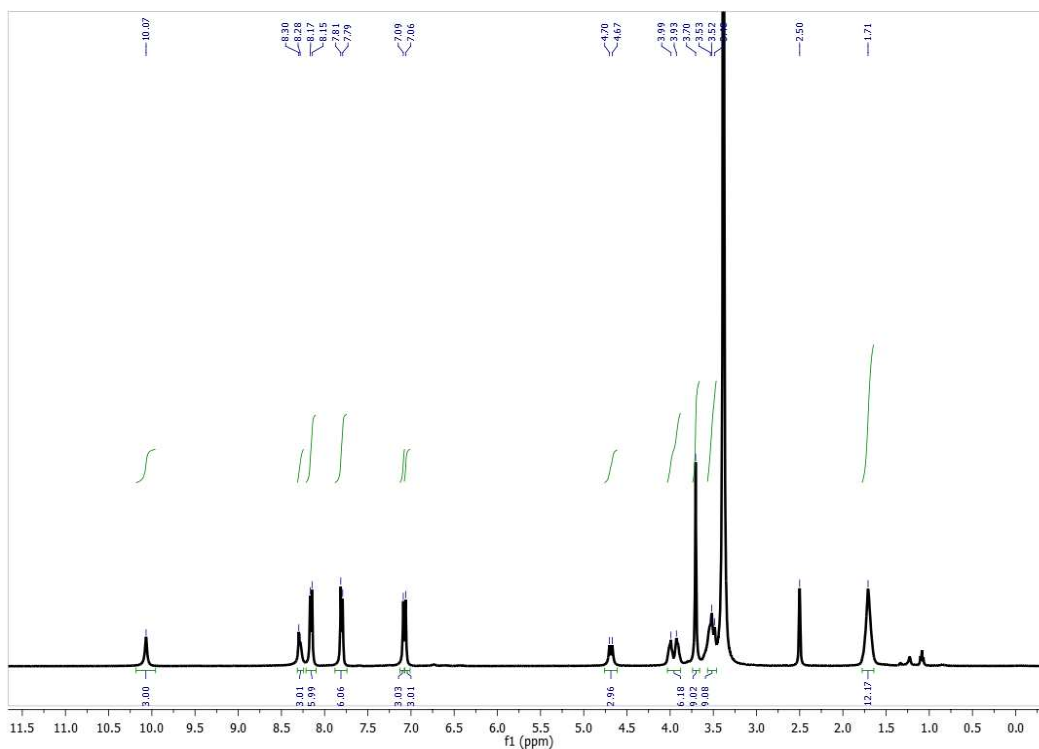


Figure 3.33. (a) ^1H NMR spectrum of compound **L**

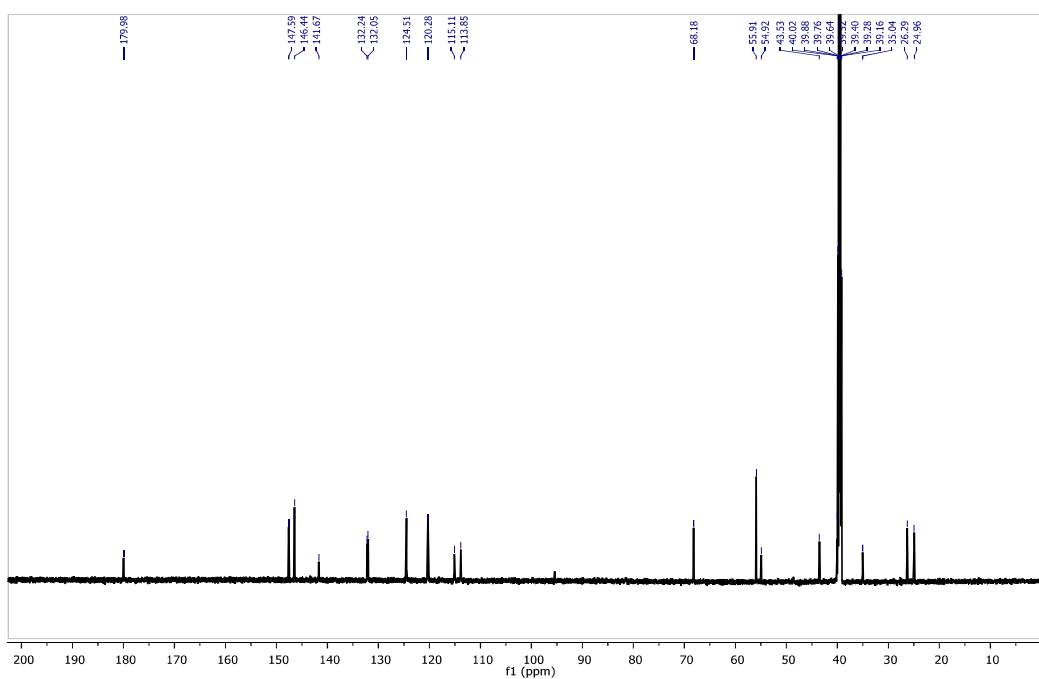


Figure 3.33. (b) ^{13}C NMR spectrum of compound **L**

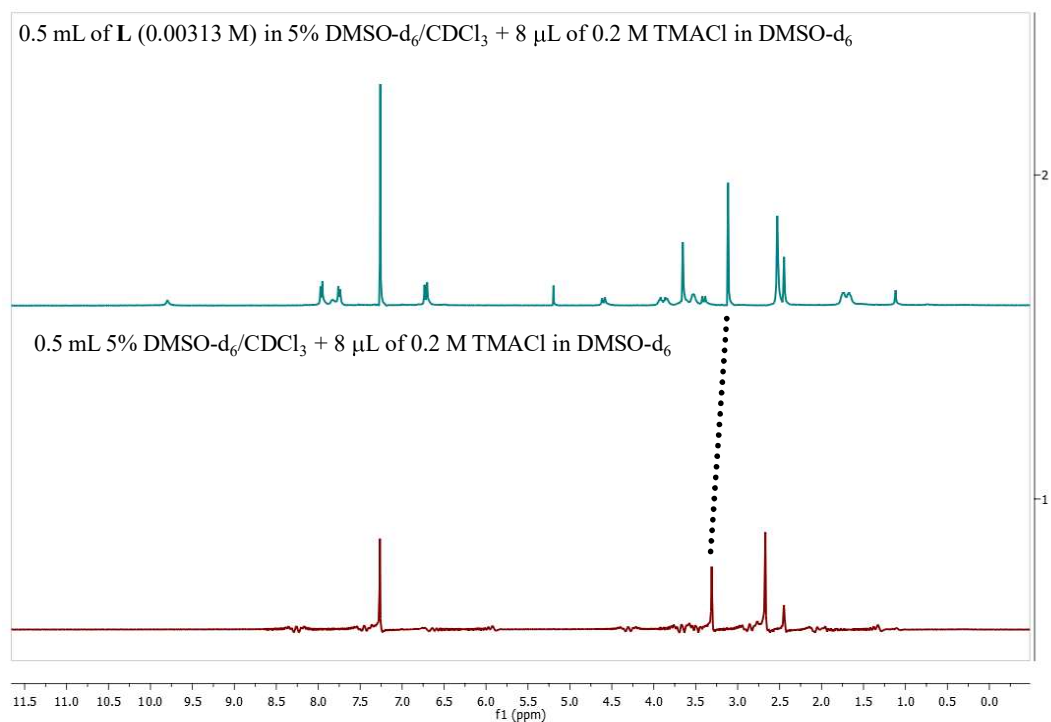


Figure 3.34. ^1H NMR spectra showing shift of peak corresponding to methyl groups of *TMACl* in the presence of **L**

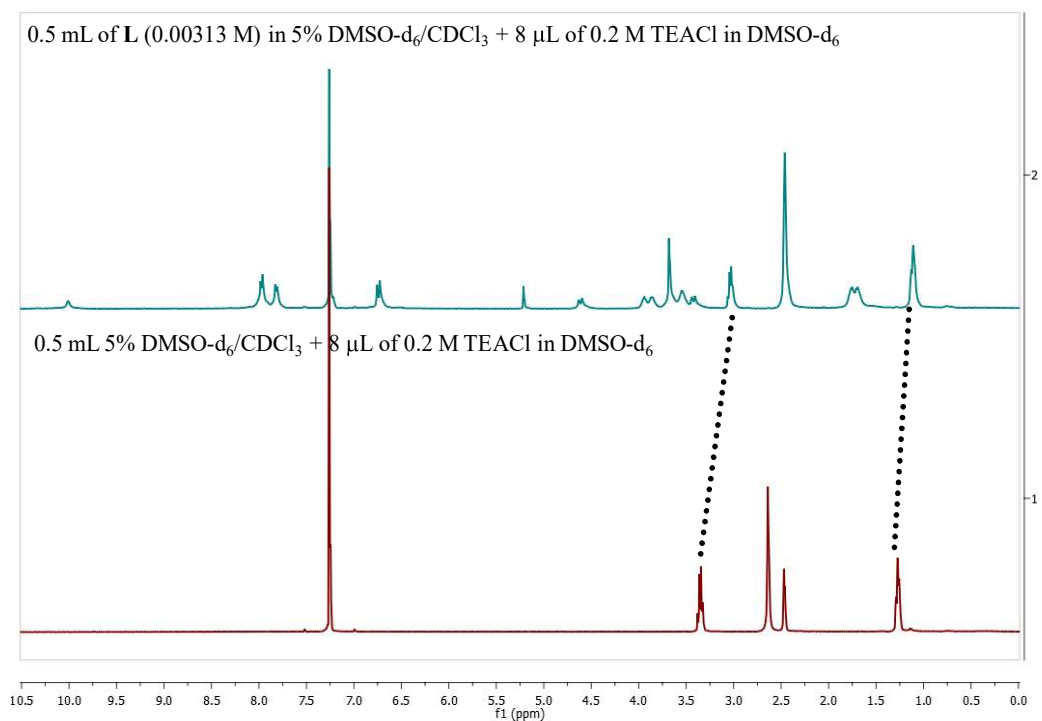


Figure 3.35. ^1H NMR spectra showing shift of peak corresponding to ethyl groups of *TEACl* in the presence of **L**

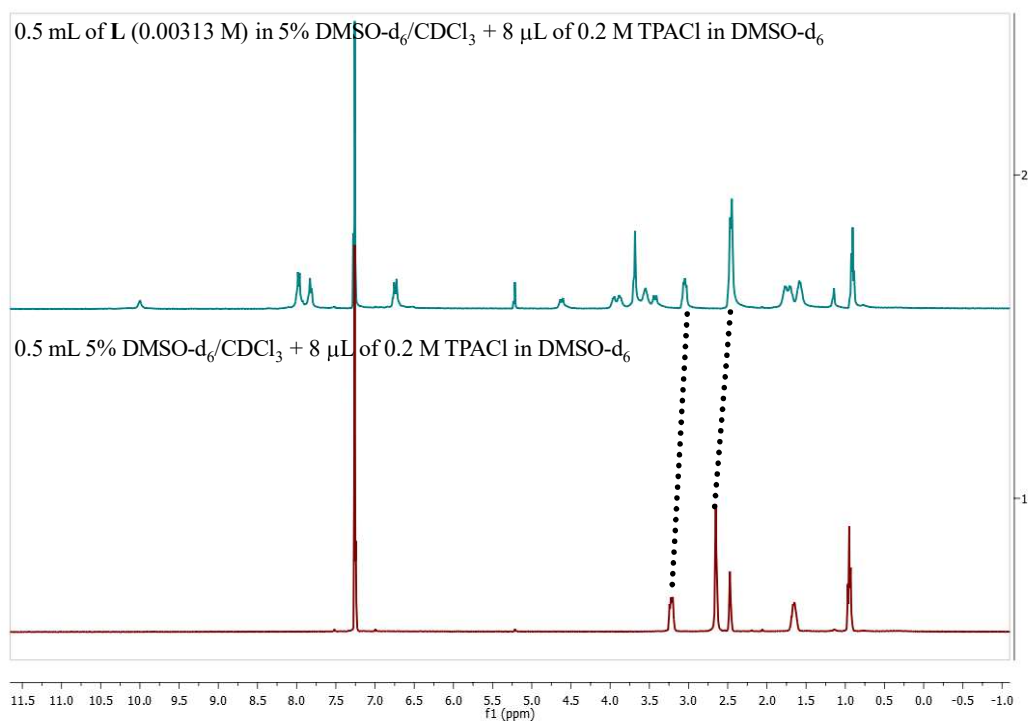


Figure 3.36. ^1H NMR spectra showing shift of peak corresponding to methylene groups of TPACl in the presence of **L**

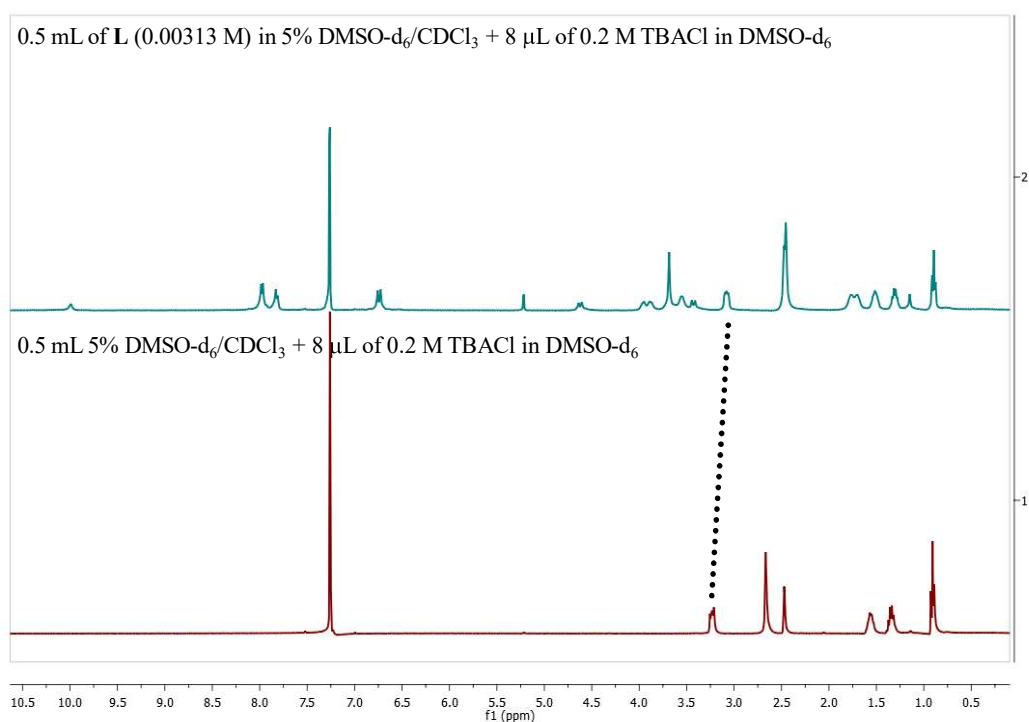


Figure 3.37. ^1H NMR spectra showing minor shift of peak corresponding to N-methylene group of TBACl in the presence of **L**

^1H NMR titrations of **L** with TEAF salt

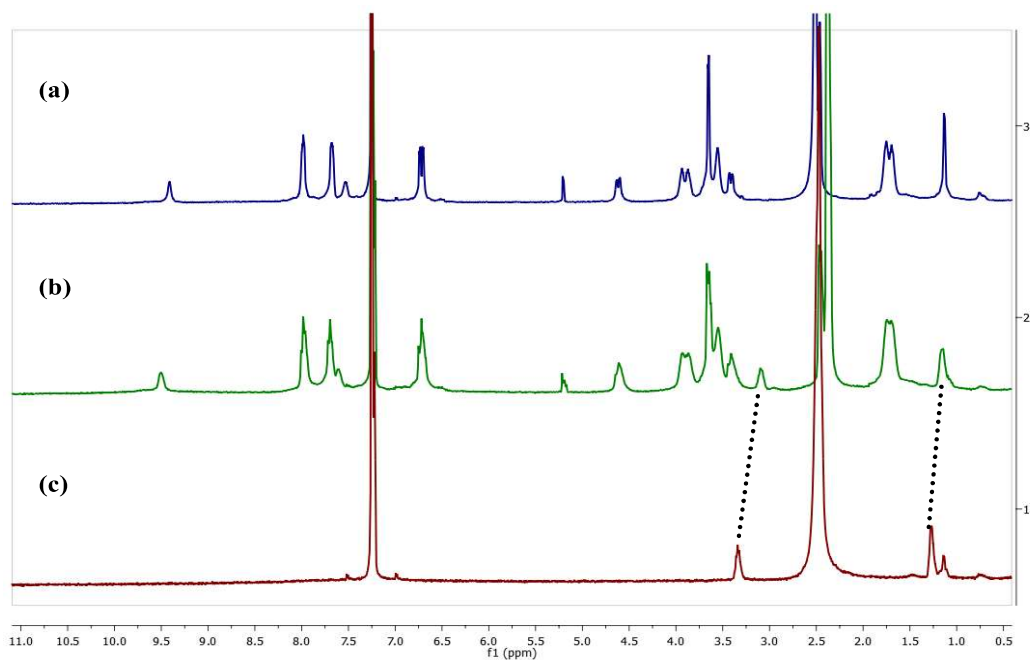


Figure 3.38.(a) 0.5 mL of **L** (0.00313 M) in 5% DMSO- d_6 /CDCl $_3$ + 3 μL DMSO- d_6 . (b) 0.5 mL of **L** (0.00313 M) in 5% DMSO- d_6 /CDCl $_3$ + 0.2 equiv. 0.1 M TEAF in DMSO- d_6 . (3 μL) (c) 0.5 mL 5% DMSO- d_6 /CDCl $_3$ + 3 μL 0.1 M TEAF in DMSO- d_6 .

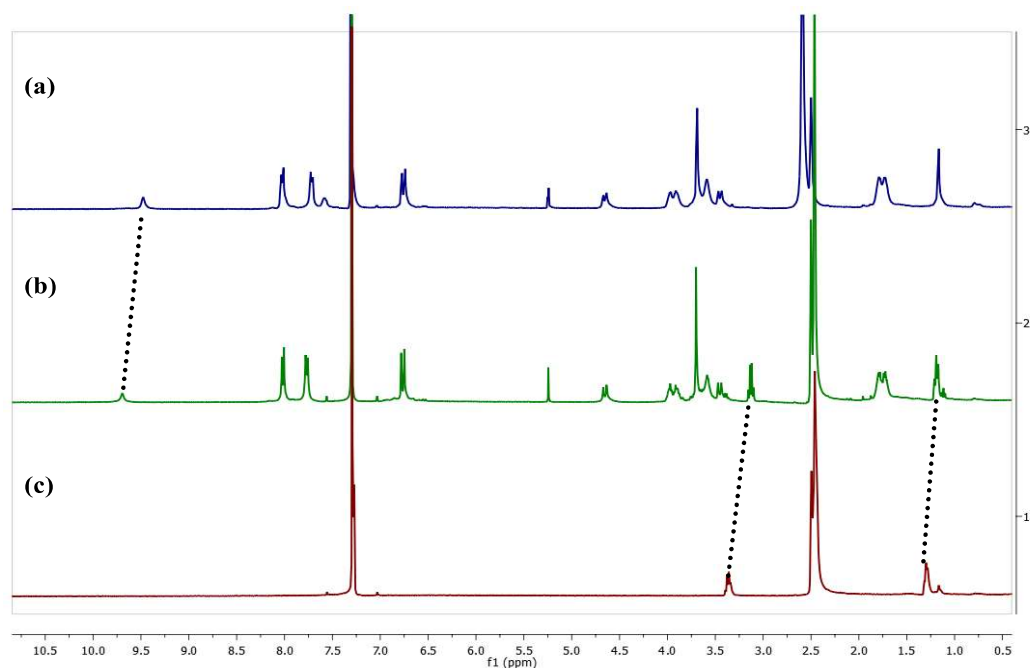


Figure 3.39.(a) 0.5 mL of **L** (0.00313 M) in 5% DMSO- d_6 /CDCl $_3$ + 6 μL DMSO- d_6 . (b) 0.5 mL of **L** (0.00313 M) in 5% DMSO- d_6 /CDCl $_3$ + 0.4 equiv. 0.1 M TEAF in DMSO- d_6 . (6 μL) (c) 0.5 mL 5% DMSO- d_6 /CDCl $_3$ + 6 μL 0.1 M TEAF in DMSO- d_6 .

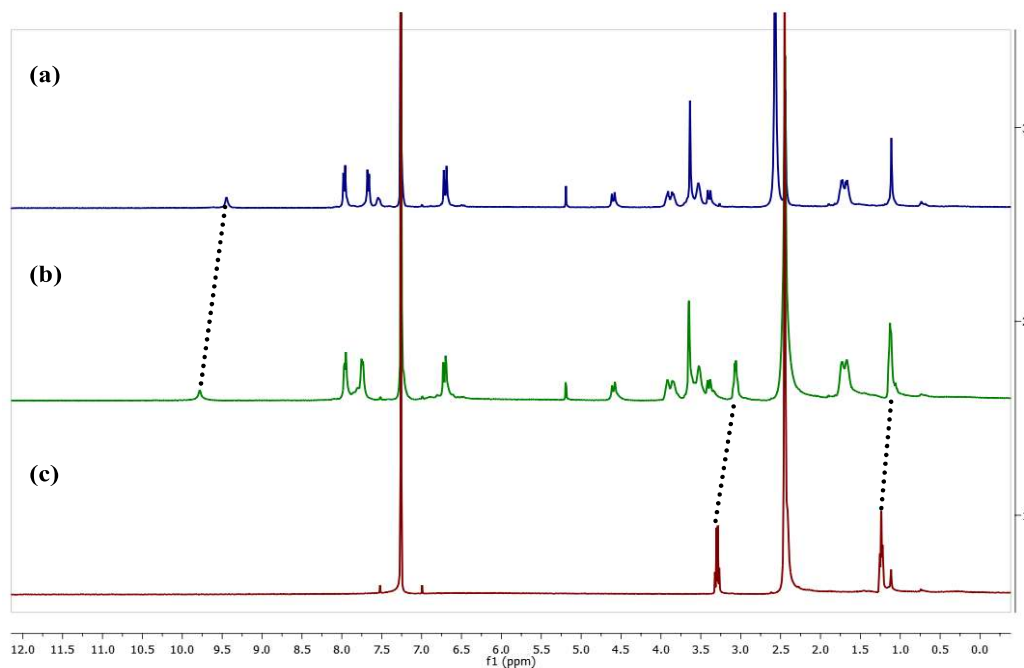


Figure 3.40.(a)0.5 mL of **L** (0.00313 M) in 5% DMSO-d₆/CDCl₃ + 9μL DMSO-d₆. (b) 0.5 mL of **L** (0.00313 M) in 5% DMSO-d₆/CDCl₃ + 0.6 equiv. 0.1 M TEA in DMSO-d₆. (9μL)(c)0.5 mL 5% DMSO-d₆/CDCl₃ + 9μL 0.1 M TEA in DMSO-d₆.

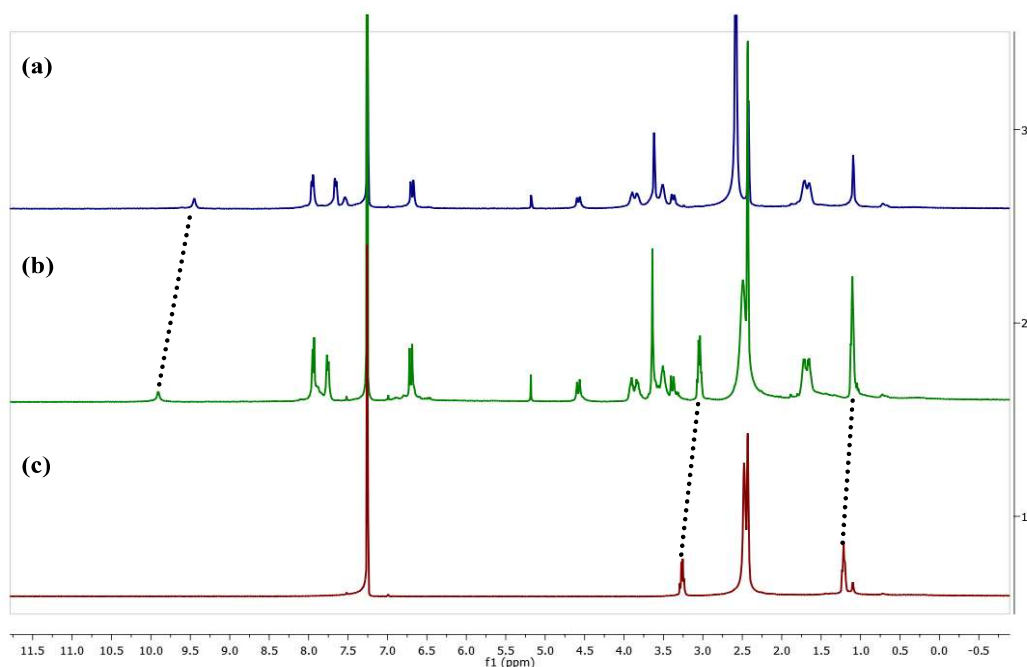


Figure 3.41.(a)0.5 mL of **L** (0.00313 M) in 5% DMSO-d₆/CDCl₃ + 11μL DMSO-d₆. (b) 0.5 mL of **L** (0.00313 M) in 5% DMSO-d₆/CDCl₃ + 0.8 equiv. 0.1 M TEA in DMSO-d₆. (11μL)(c)0.5 mL 5% DMSO-d₆/CDCl₃ + 11μL 0.1 M TEA in DMSO-d₆

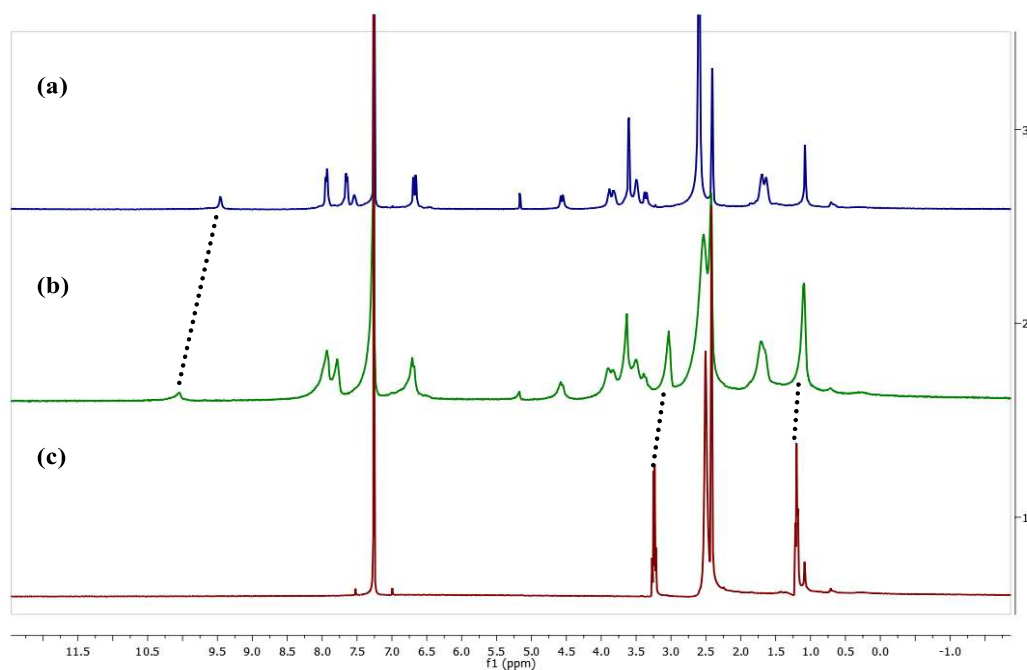


Figure 3.42.(a)0.5 mL of **L** (0.00313 M) in 5% DMSO- d_6 /CDCl $_3$ + 14 μ L DMSO- d_6 . (b) 0.5 mL of **L** (0.00313 M) in 5% DMSO- d_6 /CDCl $_3$ + 1 equiv. 0.1 M TEAFinDMSO- d_6 . (14 μ L)(c)0.5 mL 5% DMSO- d_6 /CDCl $_3$ + 14 μ L 0.1 M TEAFinDMSO- d_6 .

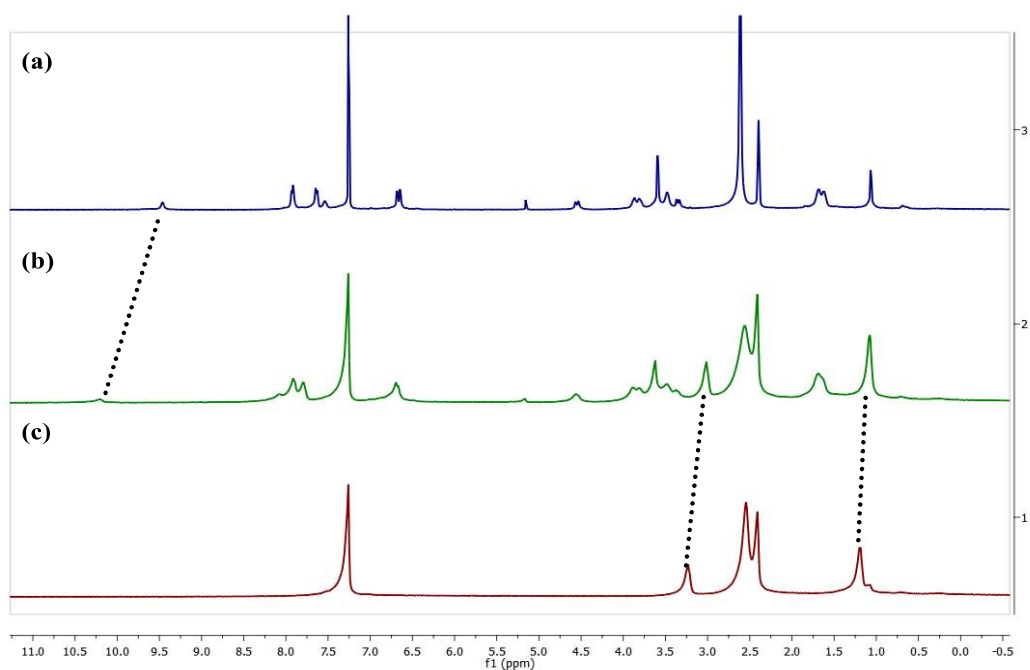


Figure 3.43.(a)0.5 mL of **L** (0.00313 M) in 5% DMSO- d_6 /CDCl $_3$ + 17 μ L DMSO- d_6 . (b) 0.5 mL of **L** (0.00313 M) in 5% DMSO- d_6 /CDCl $_3$ + 1.2 equiv. 0.1 M TEAFinDMSO- d_6 . (17 μ L)(c)0.5 mL 5% DMSO- d_6 /CDCl $_3$ + 17 μ L 0.1 M TEAFinDMSO- d_6

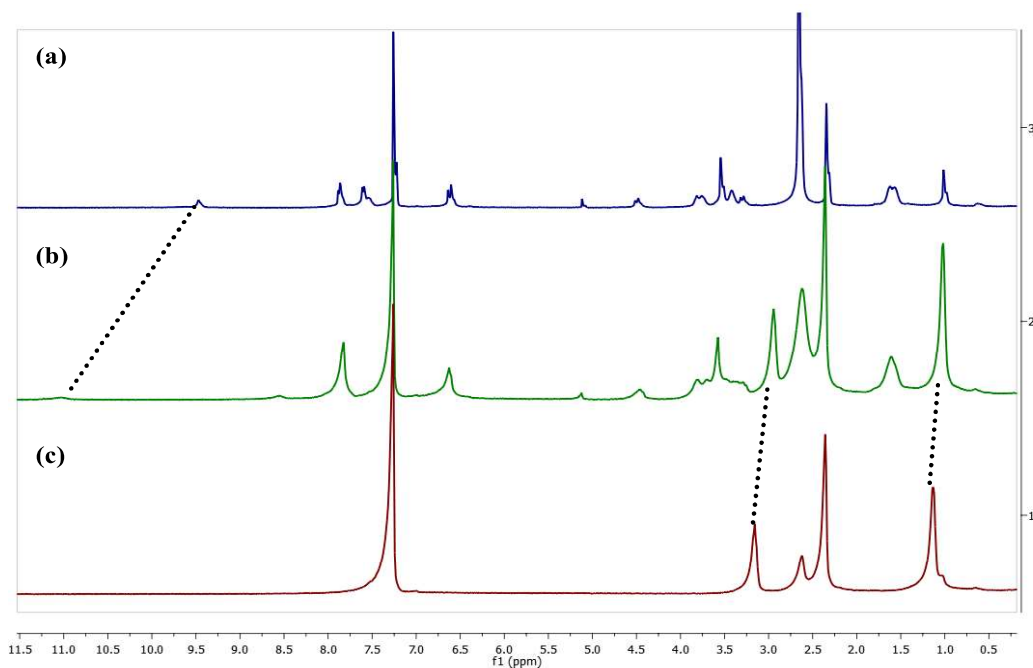


Figure 3.44.(a)0.5 mL of **L** (0.00313 M) in 5% DMSO- d_6 /CDCl $_3$ + 20 μ L DMSO- d_6 . (b) 0.5 mL of **L** (0.00313 M) in 5% DMSO- d_6 /CDCl $_3$ + 2 equiv. 0.1 M TEAFinDMSO- d_6 . (20 μ L)(c)0.5 mL 5% DMSO- d_6 /CDCl $_3$ + 20 μ L 0.1 M TEAFinDMSO- d_6 .

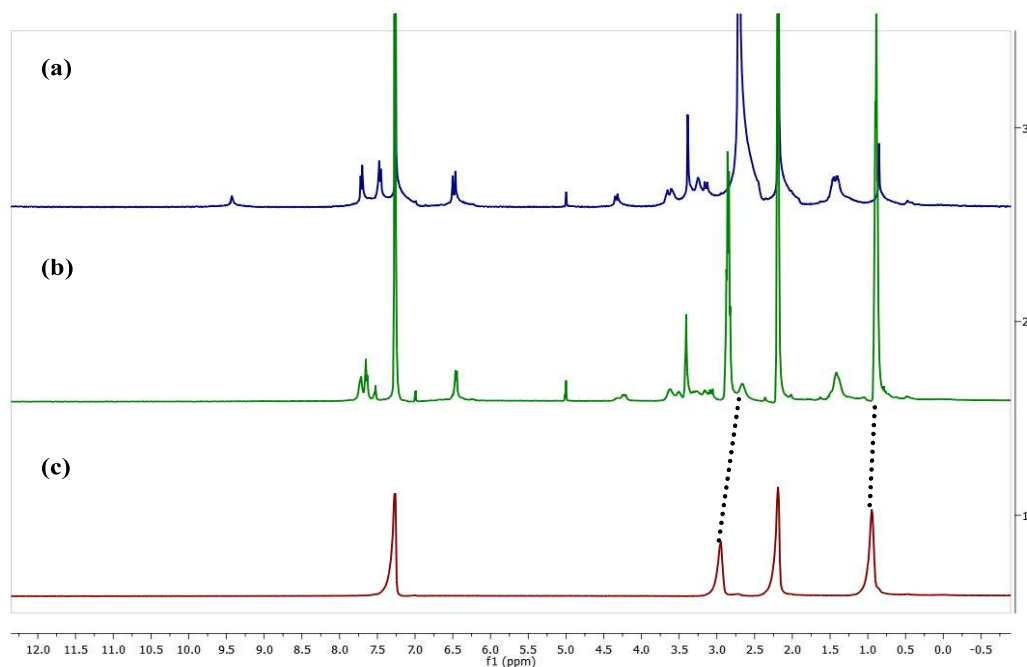


Figure 3.45.(a)0.5 mL of **L** (0.00313 M) in 5% DMSO- d_6 /CDCl $_3$ + 23 μ L DMSO- d_6 . (b) 0.5 mL of **L** (0.00313 M) in 5% DMSO- d_6 /CDCl $_3$ + 5 equiv. 0.1 M TEAFinDMSO- d_6 . (23 μ L)(c)0.5 mL 5% DMSO- d_6 /CDCl $_3$ + 23 μ L 0.1 M TEAFinDMSO- d_6 .

^1H NMR titrations of **L** with TEACl salt

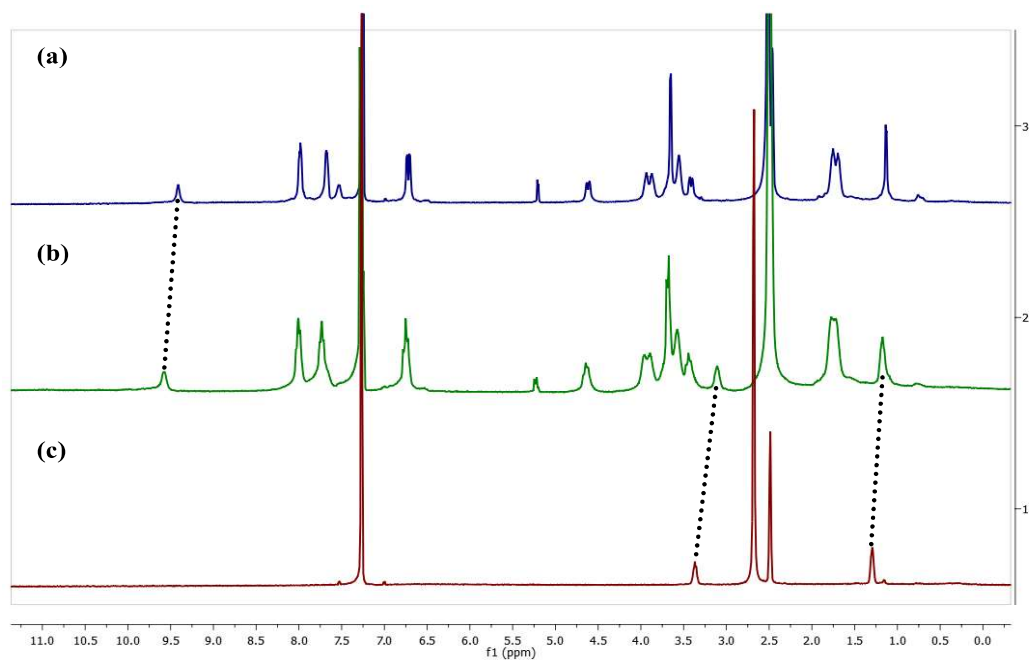


Figure 3.46.(a) 0.5 mL of **L** (0.00313 M) in 5% DMSO- d_6 /CDCl $_3$ + 3 μL DMSO- d_6 . (b) 0.5 mL of **L** (0.00313 M) in 5% DMSO- d_6 /CDCl $_3$ + 0.2 equiv. 0.1 M TEAClinDMSO- d_6 . (3 μL) (c) 0.5 mL 5% DMSO- d_6 /CDCl $_3$ + 3 μL 0.1 M TEAClinDMSO- d_6 .

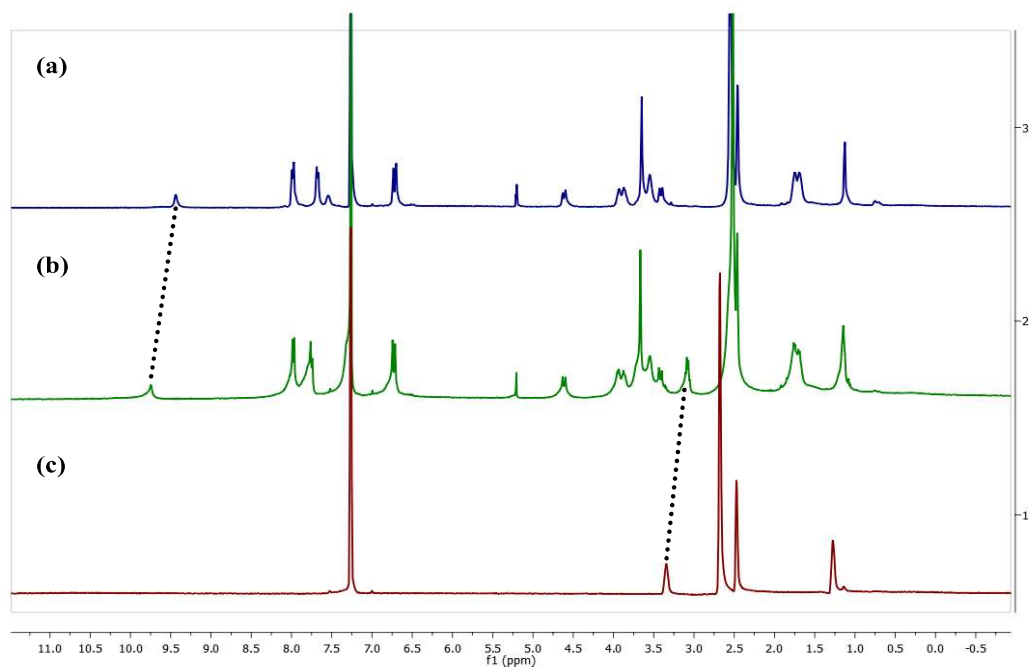


Figure 3.47.(a) 0.5 mL of **L** (0.00313 M) in 5% DMSO- d_6 /CDCl $_3$ + 6 μL DMSO- d_6 . (b) 0.5 mL of **L** (0.00313 M) in 5% DMSO- d_6 /CDCl $_3$ + 0.4 equiv. 0.1 M TEAClinDMSO- d_6 . (6 μL) (c) 0.5 mL 5% DMSO- d_6 /CDCl $_3$ + 6 μL 0.1 M TEAClinDMSO- d_6 .

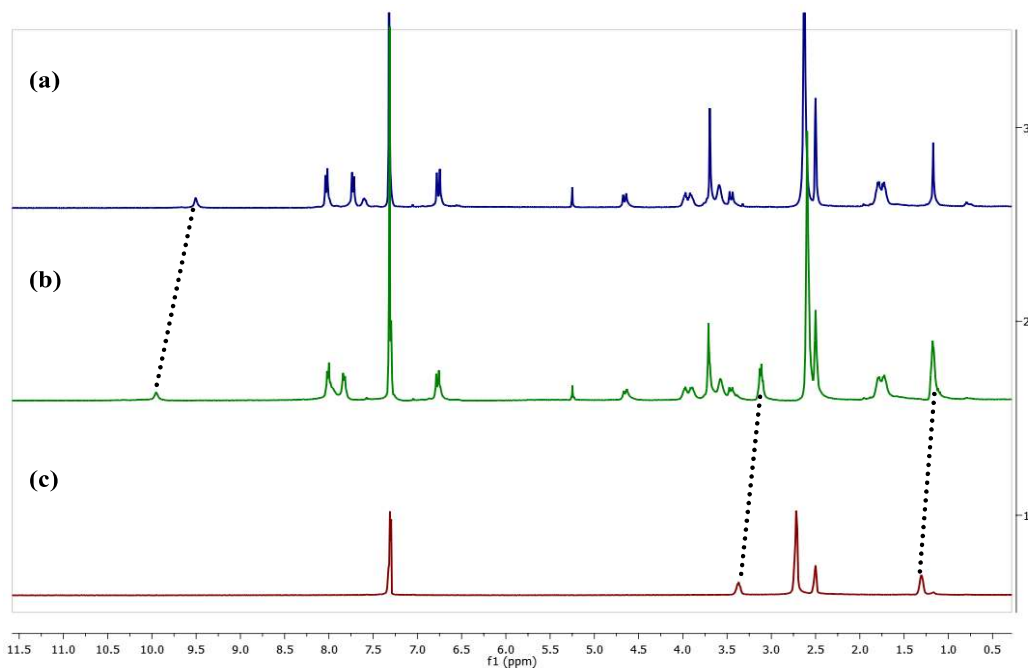


Figure 3.48.(a)0.5 mL of **L** (0.00313 M) in 5% DMSO-d₆/CDCl₃ + 9μL DMSO-d₆. (b) 0.5 mL of **L** (0.00313 M) in 5% DMSO-d₆/CDCl₃ + 0.6 equiv. 0.1 M TEAClinDMSO-d₆. (9μL)(c)0.5 mL 5% DMSO-d₆/CDCl₃ + 9μL 0.1 M TEAClinDMSO-d₆.

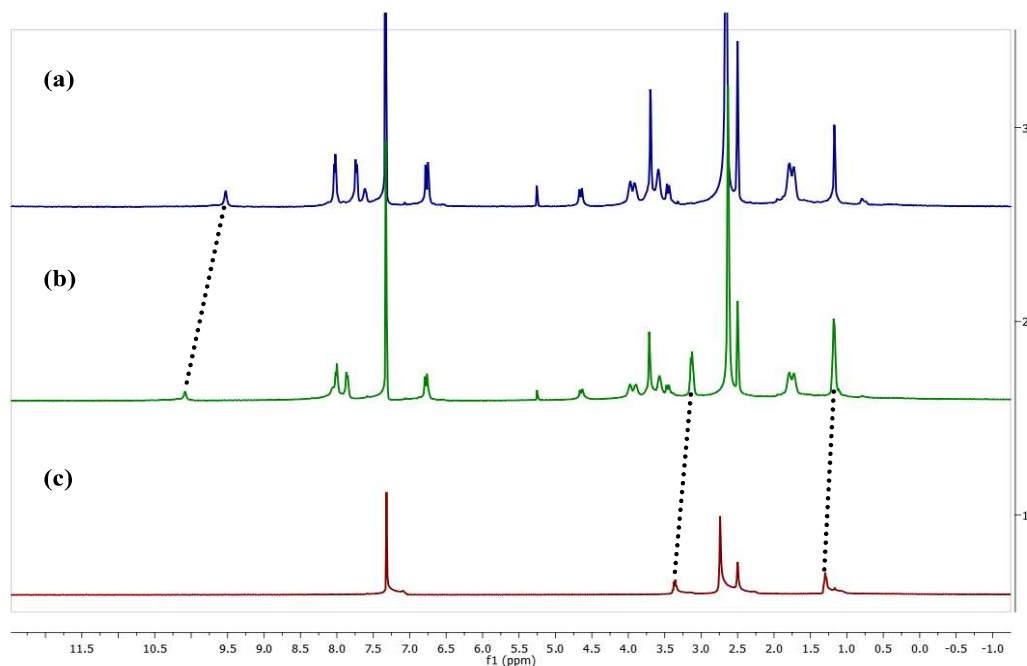


Figure 32.49.(a)0.5 mL of **L** (0.00313 M) in 5% DMSO-d₆/CDCl₃ + 11μL DMSO-d₆. (b) 0.5 mL of **L** (0.00313 M) in 5% DMSO-d₆/CDCl₃ + 0.8 equiv. 0.1 M TEAClinDMSO-d₆. (11μL)(c)0.5 mL 5% DMSO-d₆/CDCl₃ + 11μL 0.1 M TEAClinDMSO-d₆

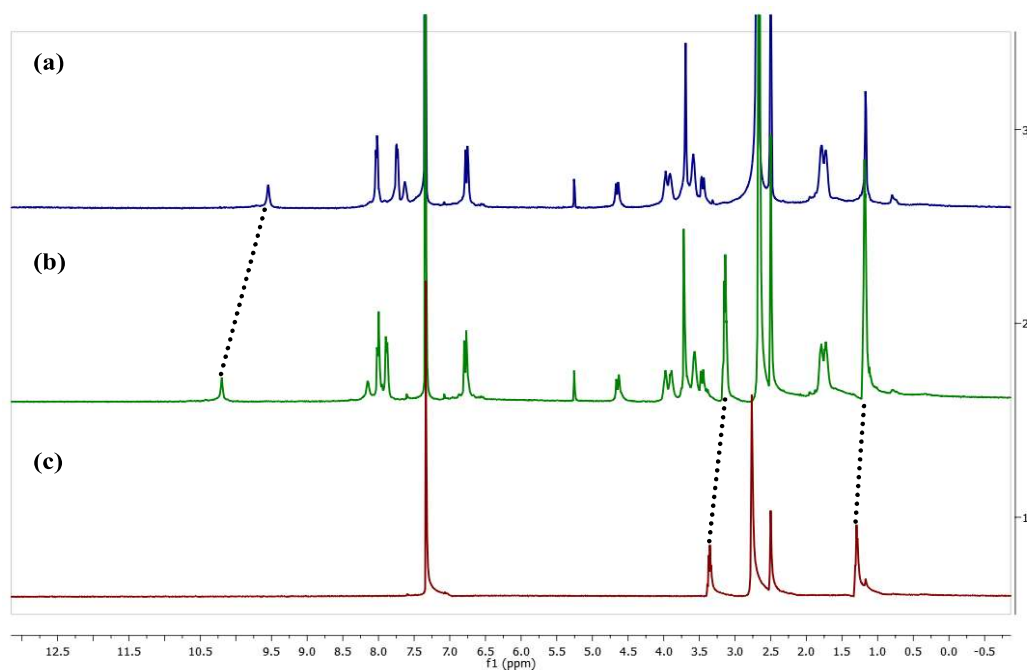


Figure 3.50.(a)0.5 mL of **L** (0.00313 M) in 5% DMSO- d_6 /CDCl $_3$ + 14 μ L DMSO- d_6 . (b) 0.5 mL of **L** (0.00313 M) in 5% DMSO- d_6 /CDCl $_3$ + 1 equiv. 0.1 M TEAClinDMSO- d_6 . (14 μ L)
(c)0.5 mL 5% DMSO- d_6 /CDCl $_3$ + 14 μ L 0.1 M TEAClinDMSO- d_6 .

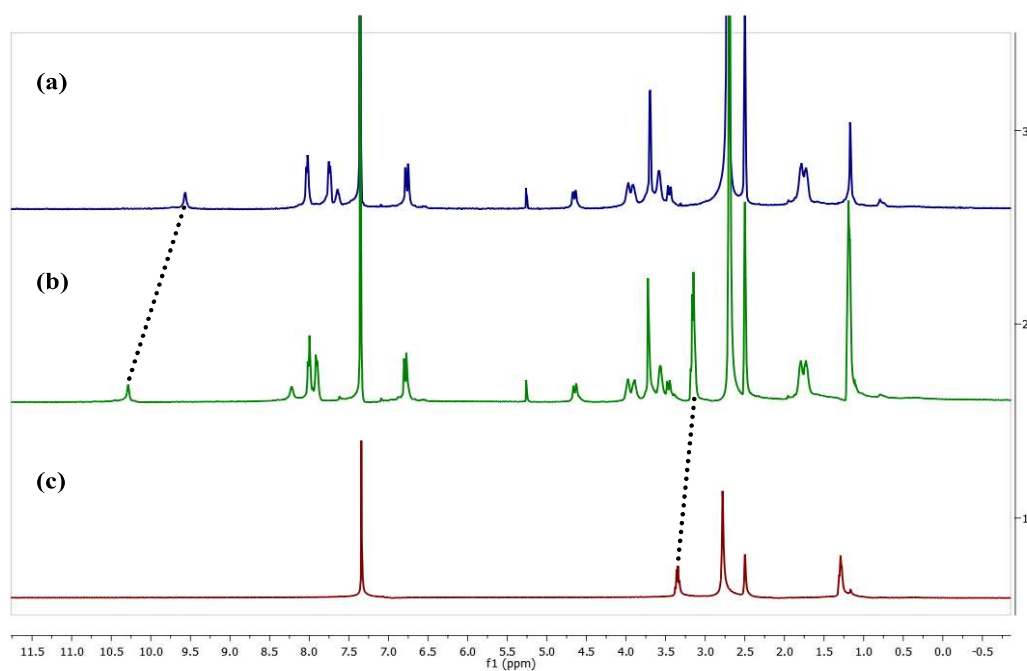


Figure 3.51.(a)0.5 mL of **L** (0.00313 M) in 5% DMSO- d_6 /CDCl $_3$ + 17 μ L DMSO- d_6 . (b) 0.5 mL of **L** (0.00313 M) in 5% DMSO- d_6 /CDCl $_3$ + 1.2 equiv. 0.1 M TEAClinDMSO- d_6 . (17 μ L)
(c)0.5 mL 5% DMSO- d_6 /CDCl $_3$ + 17 μ L 0.1 M TEAClinDMSO- d_6

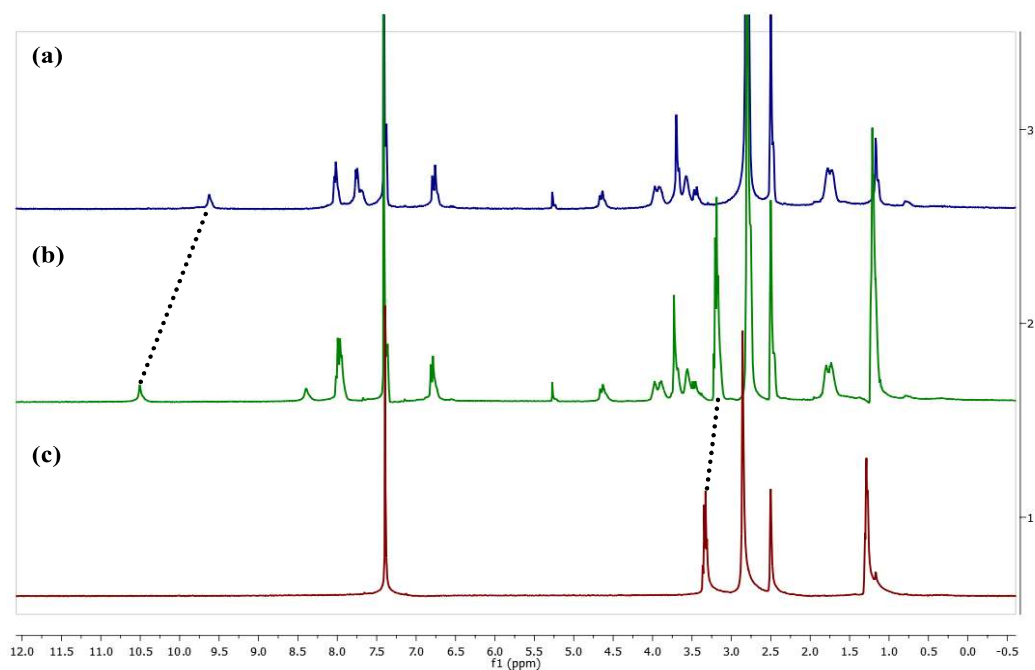


Figure 3.52.(a) 0.5 mL of **L** (0.00313 M) in 5% DMSO- d_6 /CDCl $_3$ + 20 μ L DMSO- d_6 . (b) 0.5 mL of **L** (0.00313 M) in 5% DMSO- d_6 /CDCl $_3$ + 2 equiv. 0.1 M TEAClinDMSO- d_6 . (20 μ L) (c) 0.5 mL 5% DMSO- d_6 /CDCl $_3$ + 20 μ L 0.1 M TEAClinDMSO- d_6 .

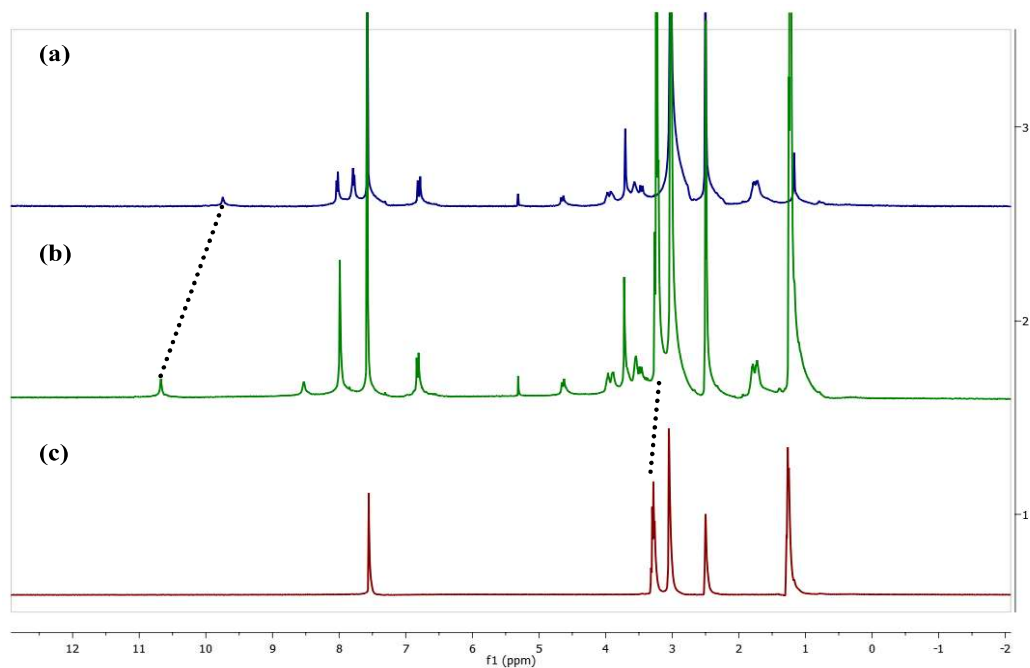


Figure 3.53.(a) 0.5 mL of **L** (0.00313 M) in 5% DMSO- d_6 /CDCl $_3$ + 23 μ L DMSO- d_6 . (b) 0.5 mL of **L** (0.00313 M) in 5% DMSO- d_6 /CDCl $_3$ + 5 equiv. 0.1 M TEAClinDMSO- d_6 . (23 μ L) (c) 0.5 mL 5% DMSO- d_6 /CDCl $_3$ + 23 μ L 0.1 M TEAClinDMSO- d_6 .

^1H NMR titrations of **L** with TEABr salt

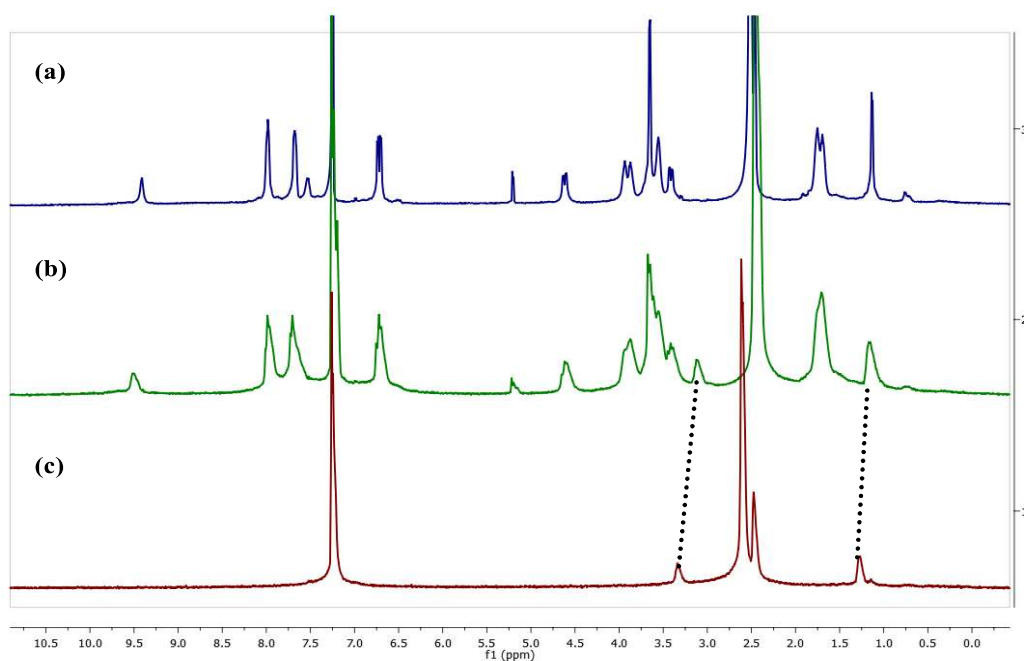


Figure 3.54.(a) 0.5 mL of **L** (0.00313 M) in 5% DMSO- d_6 /CDCl $_3$ + 3 μL DMSO- d_6 . (b) 0.5 mL of **L** (0.00313 M) in 5% DMSO- d_6 /CDCl $_3$ + 0.2 equiv. 0.1 M TEABr in DMSO- d_6 . (3 μL) (c) 0.5 mL 5% DMSO- d_6 /CDCl $_3$ + 3 μL 0.1 M TEABr in DMSO- d_6 .

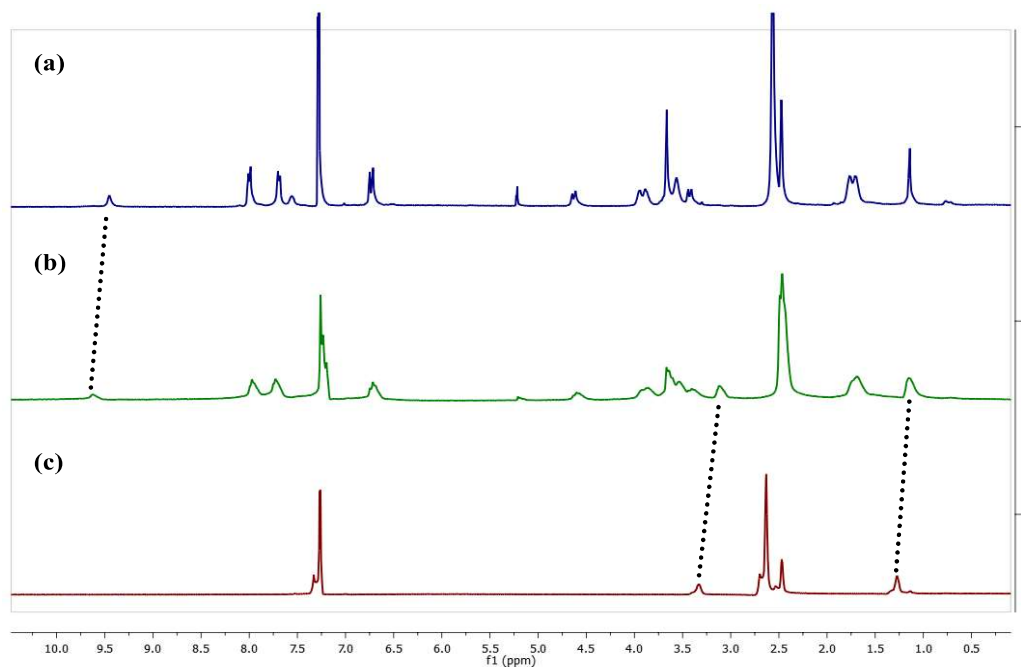


Figure 3.55.(a) 0.5 mL of **L** (0.00313 M) in 5% DMSO- d_6 /CDCl $_3$ + 6 μL DMSO- d_6 . (b) 0.5 mL of **L** (0.00313 M) in 5% DMSO- d_6 /CDCl $_3$ + 0.4 equiv. 0.1 M TEABr in DMSO- d_6 . (6 μL) (c) 0.5 mL 5% DMSO- d_6 /CDCl $_3$ + 6 μL 0.1 M TEABr in DMSO- d_6 .

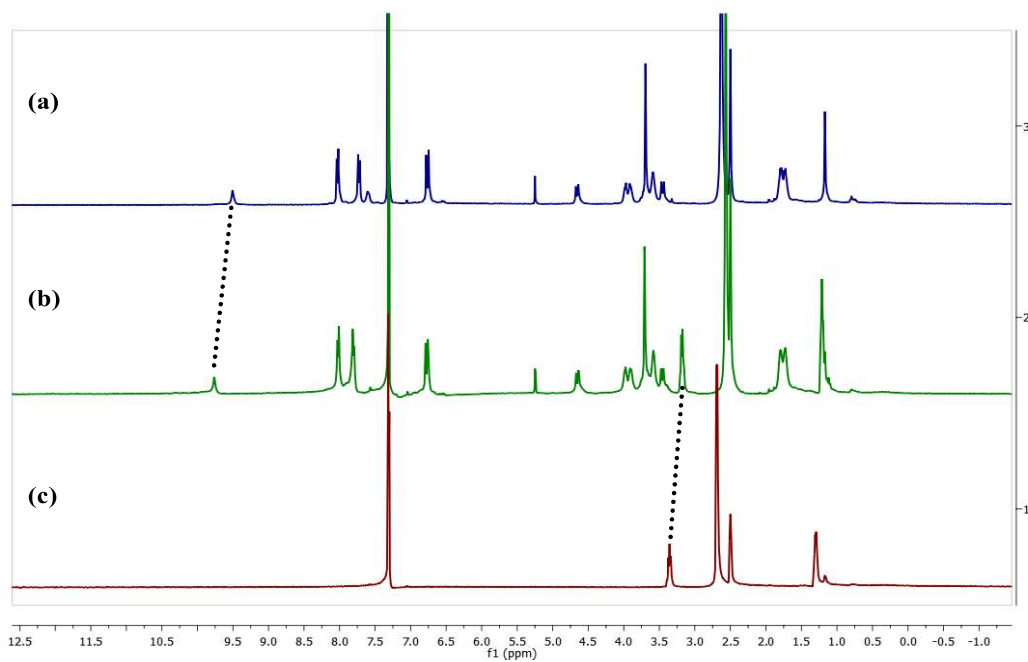


Figure 3.56.(a) 0.5 mL of **L** (0.00313 M) in 5% DMSO- d_6 /CDCl $_3$ + 9 μ L DMSO- d_6 . (b) 0.5 mL of **L** (0.00313 M) in 5% DMSO- d_6 /CDCl $_3$ + 0.6 equiv. 0.1 M TEABrinDMSO- d_6 . (9 μ L)(c) 0.5 mL 5% DMSO- d_6 /CDCl $_3$ + 9 μ L 0.1 M TEABrinDMSO- d_6 .

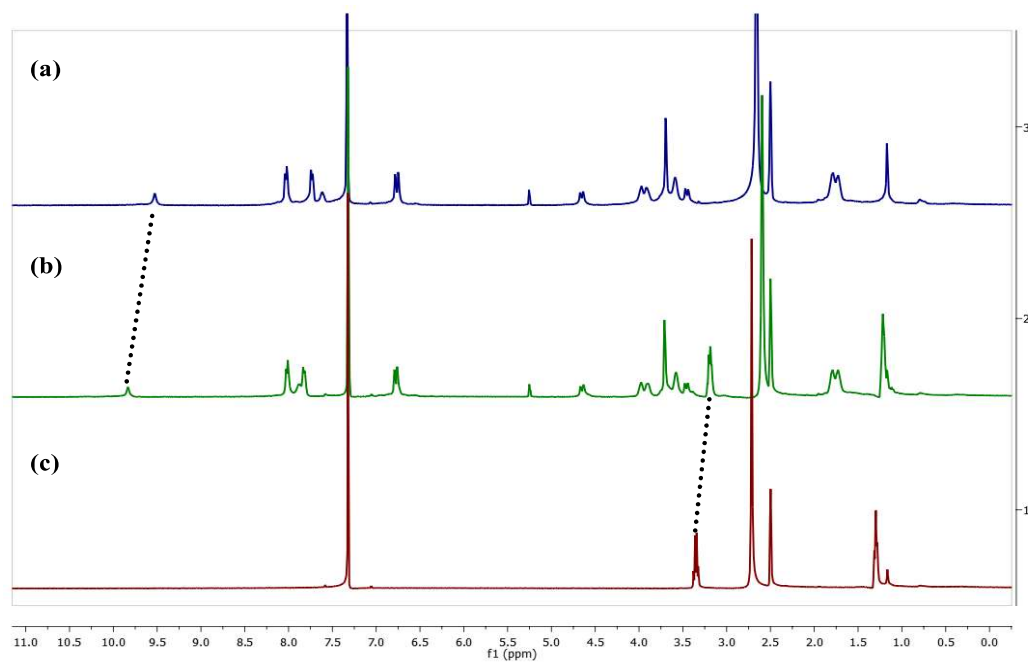


Figure 3.57.(a) 0.5 mL of **L** (0.00313 M) in 5% DMSO- d_6 /CDCl $_3$ + 11 μ L DMSO- d_6 . (b) 0.5 mL of **L** (0.00313 M) in 5% DMSO- d_6 /CDCl $_3$ + 0.8 equiv. 0.1 M TEABrinDMSO- d_6 . (11 μ L)(c) 0.5 mL 5% DMSO- d_6 /CDCl $_3$ + 11 μ L 0.1 M TEABrinDMSO- d_6

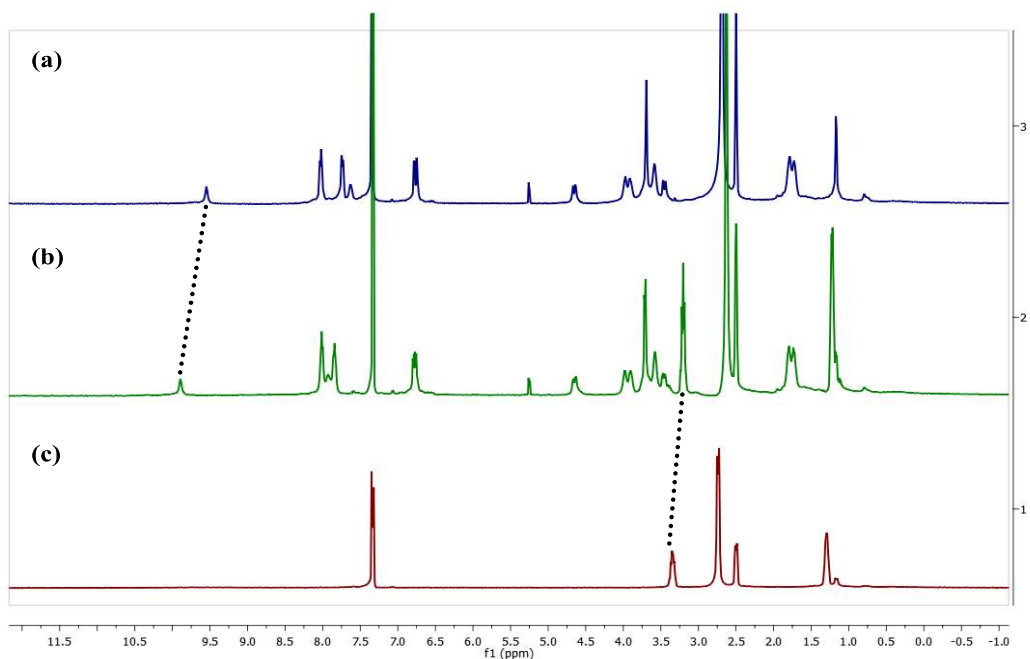


Figure 3.58.(a) 0.5 mL of **L** (0.00313 M) in 5% DMSO- d_6 /CDCl $_3$ + 14 μ L DMSO- d_6 . (b) 0.5 mL of **L** (0.00313 M) in 5% DMSO- d_6 /CDCl $_3$ + 1 equiv. 0.1 M TEABrinDMSO- d_6 . (14 μ L) (c) 0.5 mL 5% DMSO- d_6 /CDCl $_3$ + 14 μ L 0.1 M TEABrinDMSO- d_6

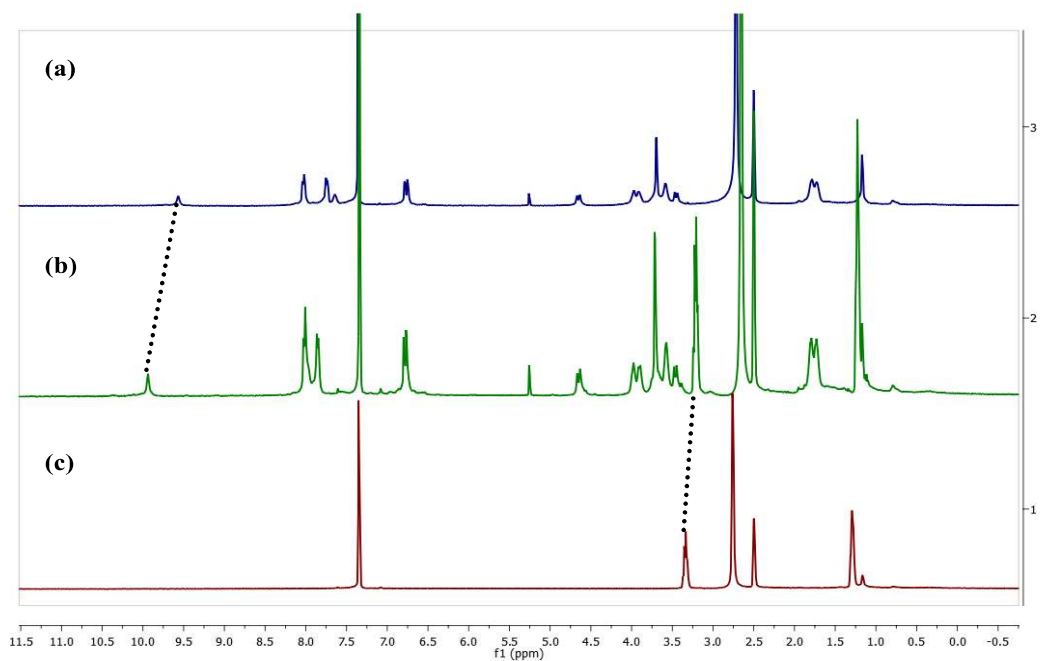


Figure 3.59.(a) 0.5 mL of **L** (0.00313 M) in 5% DMSO- d_6 /CDCl $_3$ + 17 μ L DMSO- d_6 . (b) 0.5 mL of **L** (0.00313 M) in 5% DMSO- d_6 /CDCl $_3$ + 1.2 equiv. 0.1 M TEABrinDMSO- d_6 . (17 μ L) (c) 0.5 mL 5% DMSO- d_6 /CDCl $_3$ + 17 μ L 0.1 M TEABrinDMSO- d_6

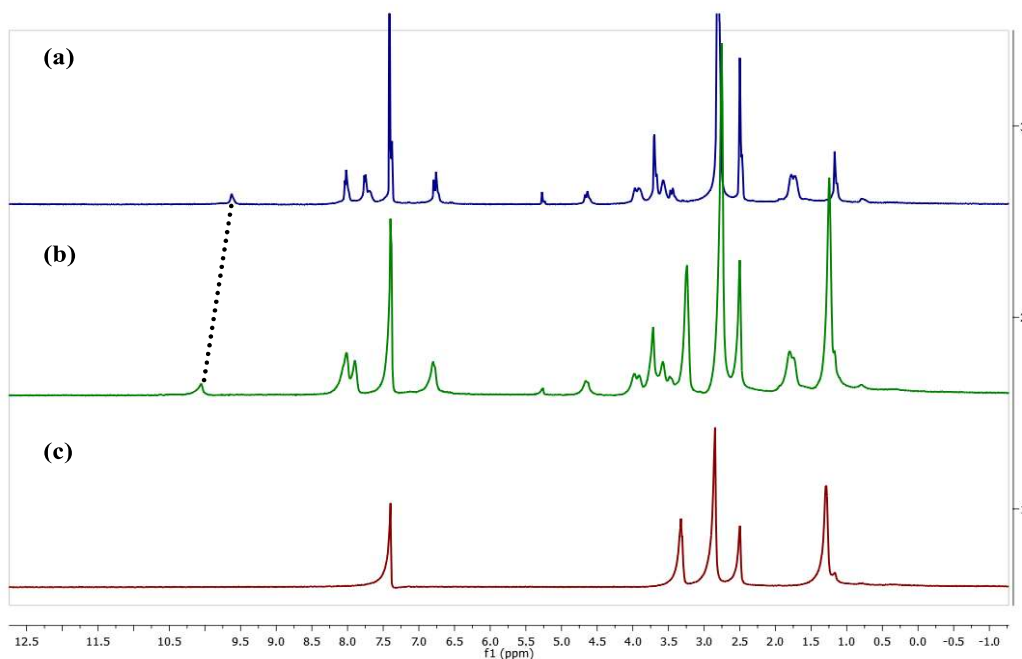


Figure 3.60.(a) 0.5 mL of **L** (0.00313 M) in 5% DMSO- d_6 /CDCl₃ + 20 μ L DMSO- d_6 . (b) 0.5 mL of **L** (0.00313 M) in 5% DMSO- d_6 /CDCl₃ + 2 equiv. 0.1 M TEABrinDMSO- d_6 . (20 μ L) (c) 0.5 mL 5% DMSO- d_6 /CDCl₃ + 20 μ L 0.1 M TEABrinDMSO- d_6 .

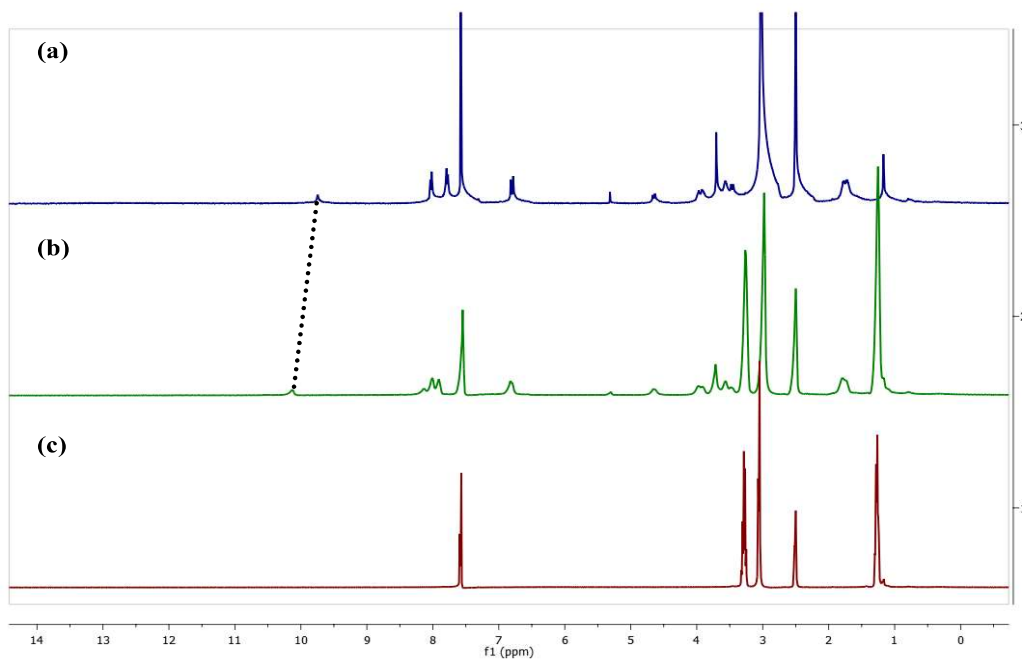


Figure 3.61.(a) 0.5 mL of **L** (0.00313 M) in 5% DMSO- d_6 /CDCl₃ + 23 μ L DMSO- d_6 . (b) 0.5 mL of **L** (0.00313 M) in 5% DMSO- d_6 /CDCl₃ + 5 equiv. 0.1 M TEABrinDMSO- d_6 . (23 μ L) (c) 0.5 mL 5% DMSO- d_6 /CDCl₃ + 23 μ L 0.1 M TEABrinDMSO- d_6 .

^1H NMR titrations of **L** with TEAI salt

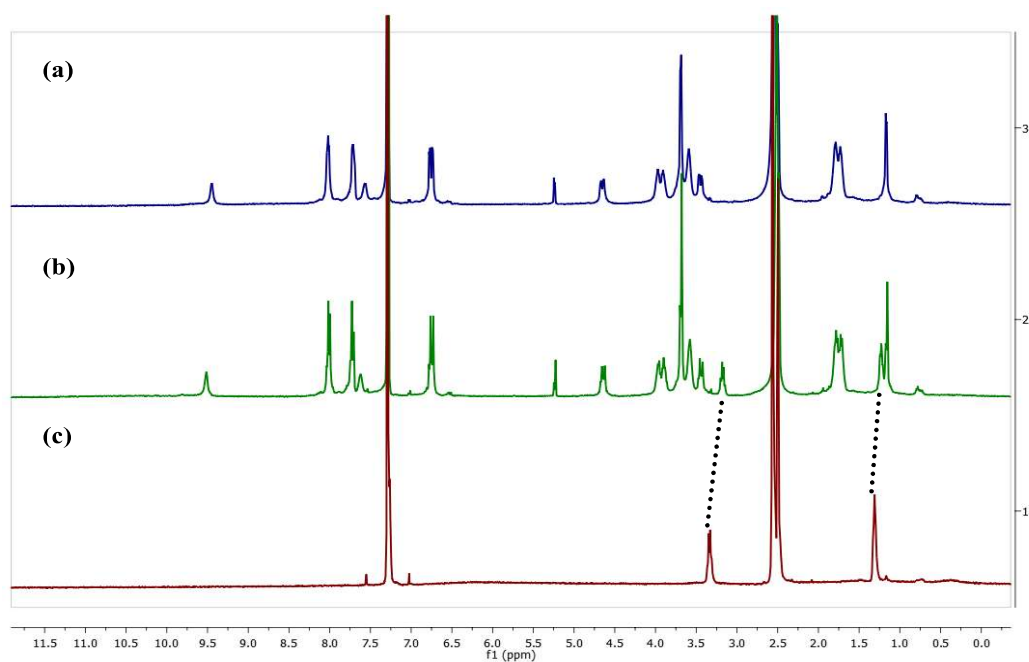


Figure 3.62.(a) 0.5 mL of **L** (0.00313 M) in 5% DMSO- d_6 /CDCl $_3$ + 3 μL DMSO- d_6 . (b) 0.5 mL of **L** (0.00313 M) in 5% DMSO- d_6 /CDCl $_3$ + 0.2 equiv. 0.1 M TEAI in DMSO- d_6 . (3 μL) (c) 0.5 mL 5% DMSO- d_6 /CDCl $_3$ + 3 μL 0.1 M TEAI in DMSO- d_6 .

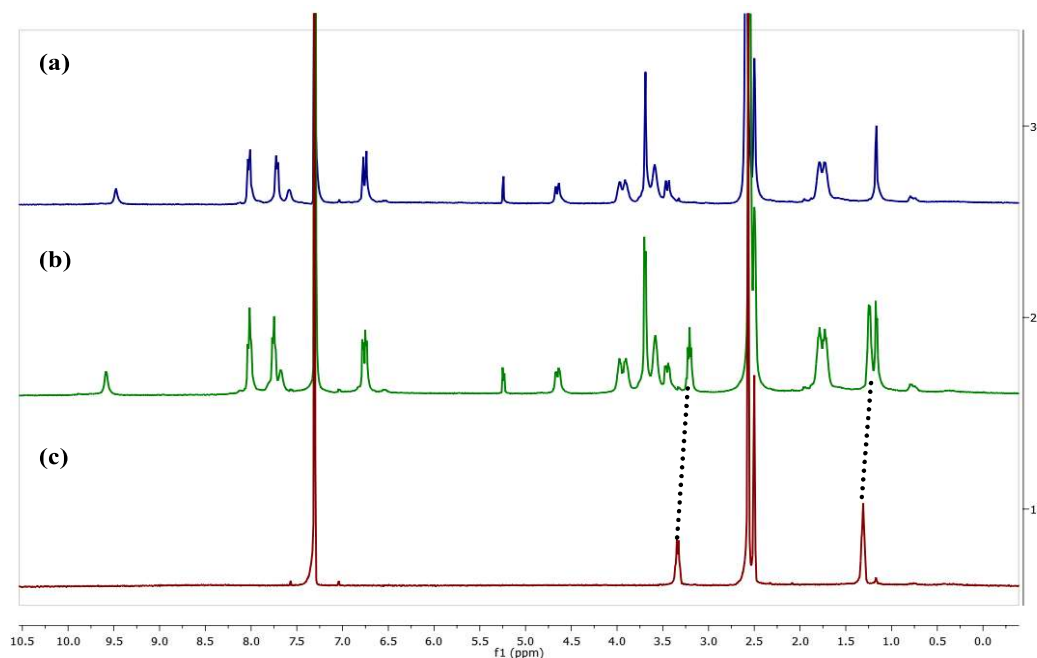


Figure 3.63.(a) 0.5 mL of **L** (0.00313 M) in 5% DMSO- d_6 /CDCl $_3$ + 6 μL DMSO- d_6 . (b) 0.5 mL of **L** (0.00313 M) in 5% DMSO- d_6 /CDCl $_3$ + 0.4 equiv. 0.1 M TEAI in DMSO- d_6 . (6 μL) (c) 0.5 mL 5% DMSO- d_6 /CDCl $_3$ + 6 μL 0.1 M TEAI in DMSO- d_6 .

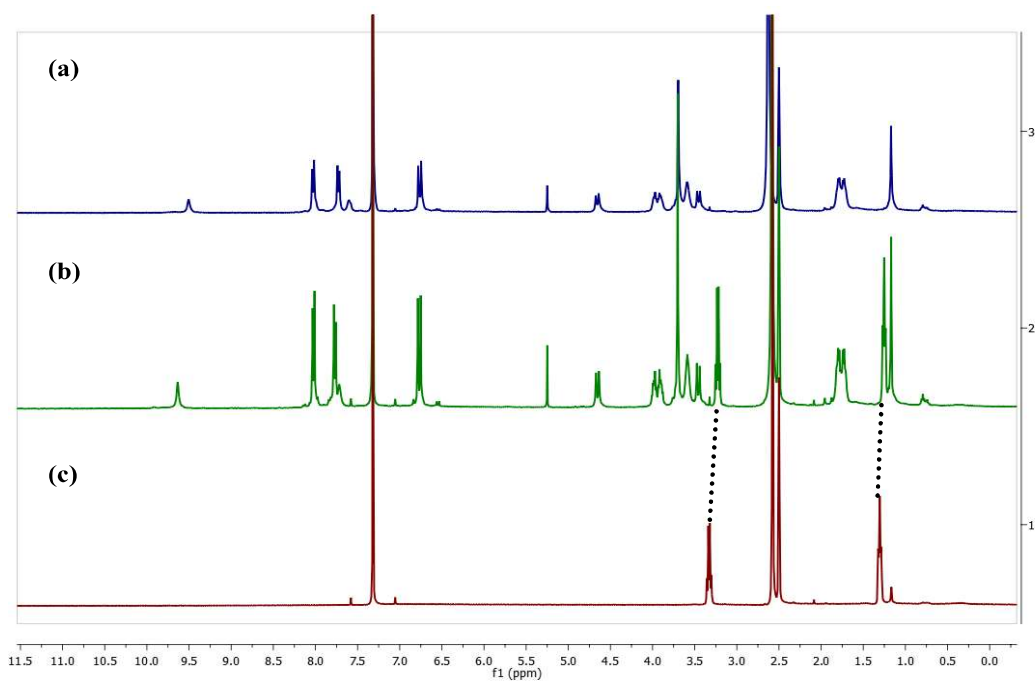


Figure 3.64.(a)0.5 mL of **L** (0.00313 M) in 5% DMSO-d₆/CDCl₃ + 9μL DMSO-d₆. (b) 0.5 mL of **L** (0.00313 M) in 5% DMSO-d₆/CDCl₃ + 0.6 equiv. 0.1 M TEA in DMSO-d₆. (9μL)(c)0.5 mL 5% DMSO-d₆/CDCl₃ + 9μL 0.1 M TEA in DMSO-d₆.

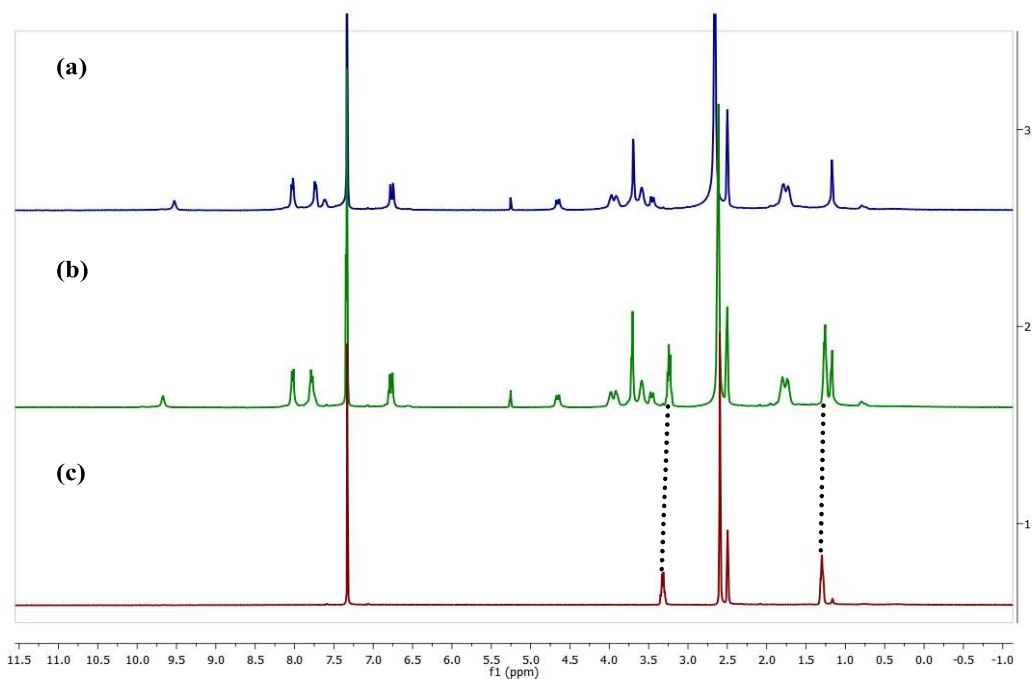


Figure 3.65.(a)0.5 mL of **L** (0.00313 M) in 5% DMSO-d₆/CDCl₃ + 11μL DMSO-d₆. (b) 0.5 mL of **L** (0.00313 M) in 5% DMSO-d₆/CDCl₃ + 0.8 equiv. 0.1 M TEA in DMSO-d₆. (11μL)(c)0.5 mL 5% DMSO-d₆/CDCl₃ + 11μL 0.1 M TEA in DMSO-d₆.

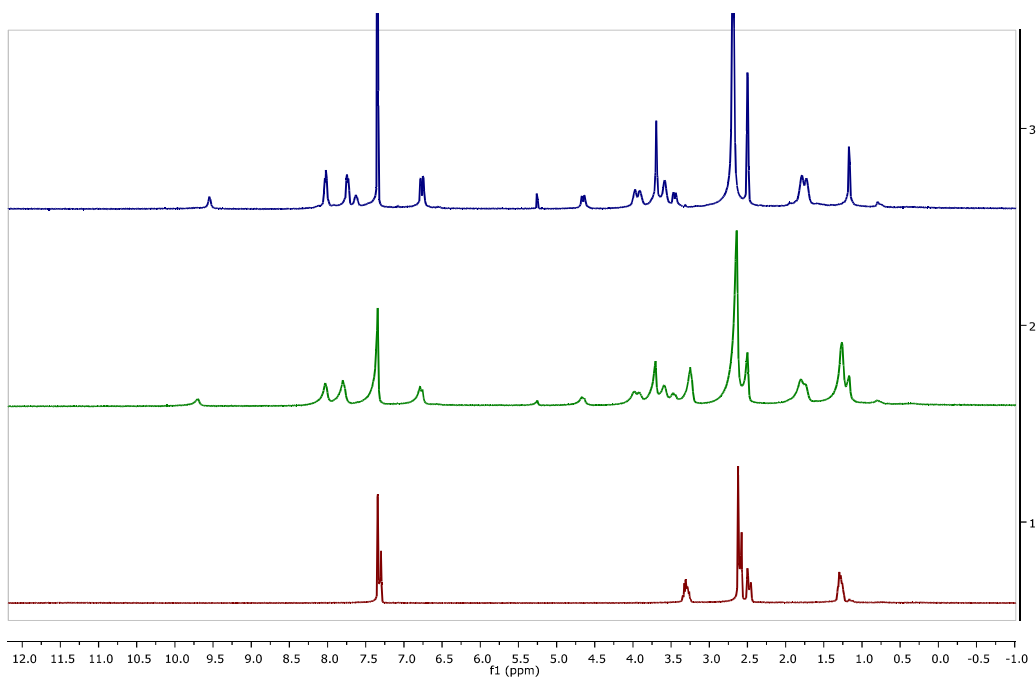


Figure 3.66.(a)0.5 mL of **L** (0.00313 M) in 5% DMSO- d_6 /CDCl $_3$ + 14 μ L DMSO- d_6 . (b) 0.5 mL of **L** (0.00313 M) in 5% DMSO- d_6 /CDCl $_3$ + 1 equiv. 0.1 M TEA in DMSO- d_6 . (14 μ L) (c)0.5 mL 5% DMSO- d_6 /CDCl $_3$ + 14 μ L 0.1 M TEA in DMSO- d_6 .

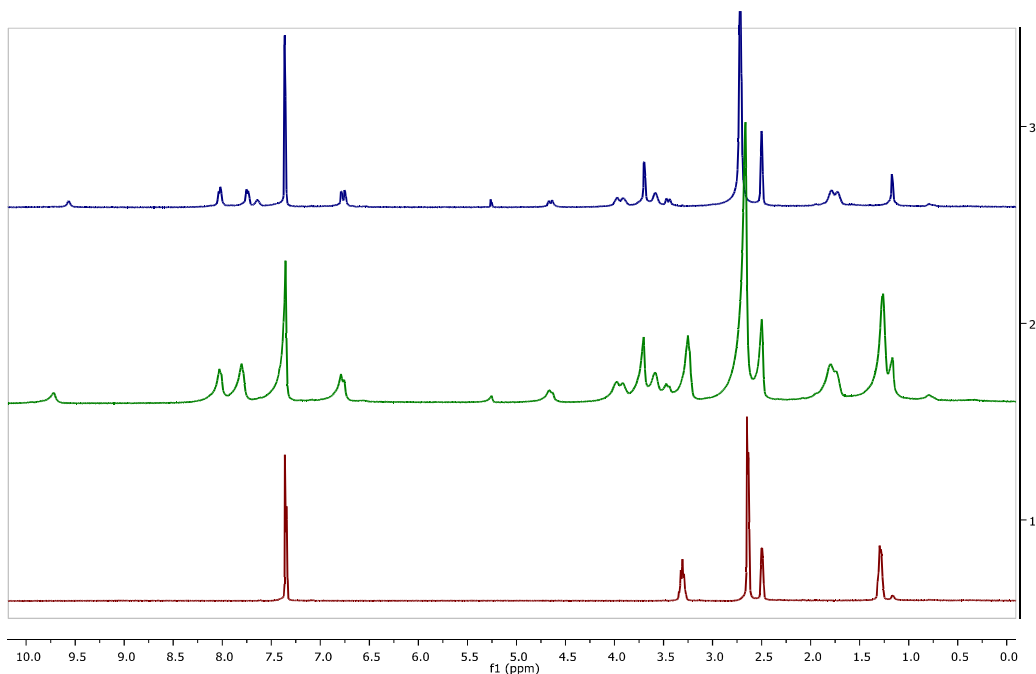


Figure 3.67.(a)0.5 mL of **L** (0.00313 M) in 5% DMSO- d_6 /CDCl $_3$ + 17 μ L DMSO- d_6 . (b) 0.5 mL of **L** (0.00313 M) in 5% DMSO- d_6 /CDCl $_3$ + 1.2 equiv. 0.1 M TEA in DMSO- d_6 . (17 μ L) (c)0.5 mL 5% DMSO- d_6 /CDCl $_3$ + 17 μ L 0.1 M TEA in DMSO- d_6

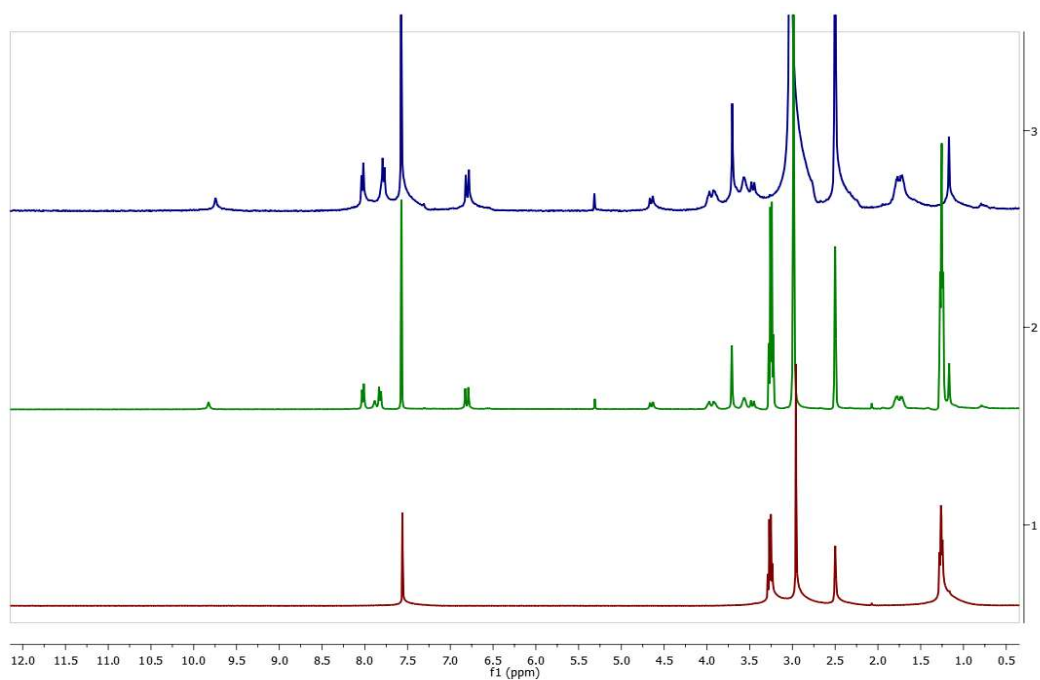


Figure 3.68.(a) 0.5 mL of **L** (0.00313 M) in 5% DMSO- d_6 /CDCl $_3$ + 23 μ L DMSO- d_6 . (b) 0.5 mL of **L** (0.00313 M) in 5% DMSO- d_6 /CDCl $_3$ + 5 equiv. 0.1 M TEA in DMSO- d_6 . (23 μ L) (c) 0.5 mL 5% DMSO- d_6 /CDCl $_3$ + 23 μ L 0.1 M TEA in DMSO- d_6 .

^1H NMR titrations of **L** with TEAClO_4 salt

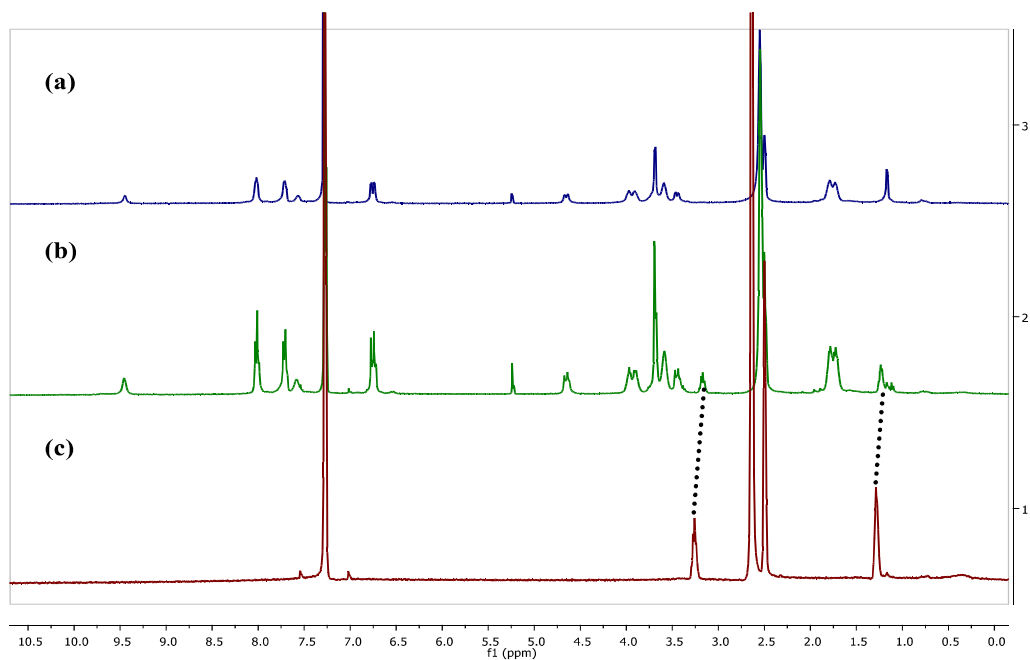


Figure 3.69.(a) 0.5 mL of **L** (0.00313 M) in 5% $\text{DMSO-d}_6/\text{CDCl}_3$ + 3 μL DMSO-d_6 . (b) 0.5 mL of **L** (0.00313 M) in 5% $\text{DMSO-d}_6/\text{CDCl}_3$ + 0.2 equiv. 0.1 M TEAClO_4 in DMSO-d_6 . (3 μL) (c) 0.5 mL 5% $\text{DMSO-d}_6/\text{CDCl}_3$ + 3 μL 0.1 M TEAClO_4 in DMSO-d_6 .

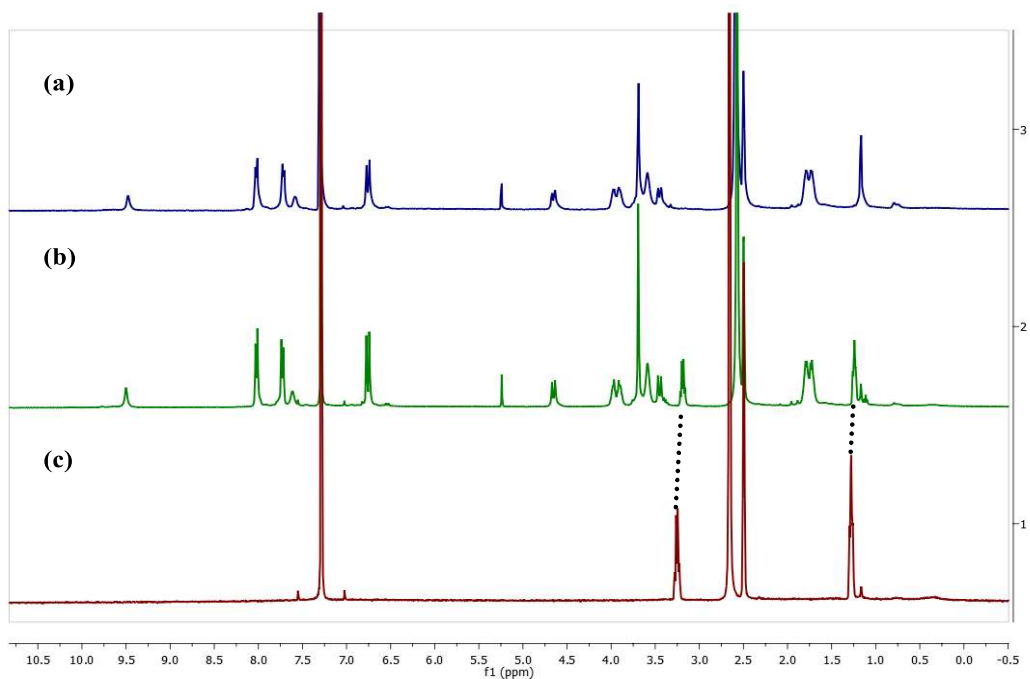


Figure 3.70.(a) 0.5 mL of **L** (0.00313 M) in 5% $\text{DMSO-d}_6/\text{CDCl}_3$ + 6 μL DMSO-d_6 . (b) 0.5 mL of **L** (0.00313 M) in 5% $\text{DMSO-d}_6/\text{CDCl}_3$ + 0.4 equiv. 0.1 M TEAClO_4 in DMSO-d_6 . (6 μL) (c) 0.5 mL 5% $\text{DMSO-d}_6/\text{CDCl}_3$ + 6 μL 0.1 M TEAClO_4 in DMSO-d_6 .

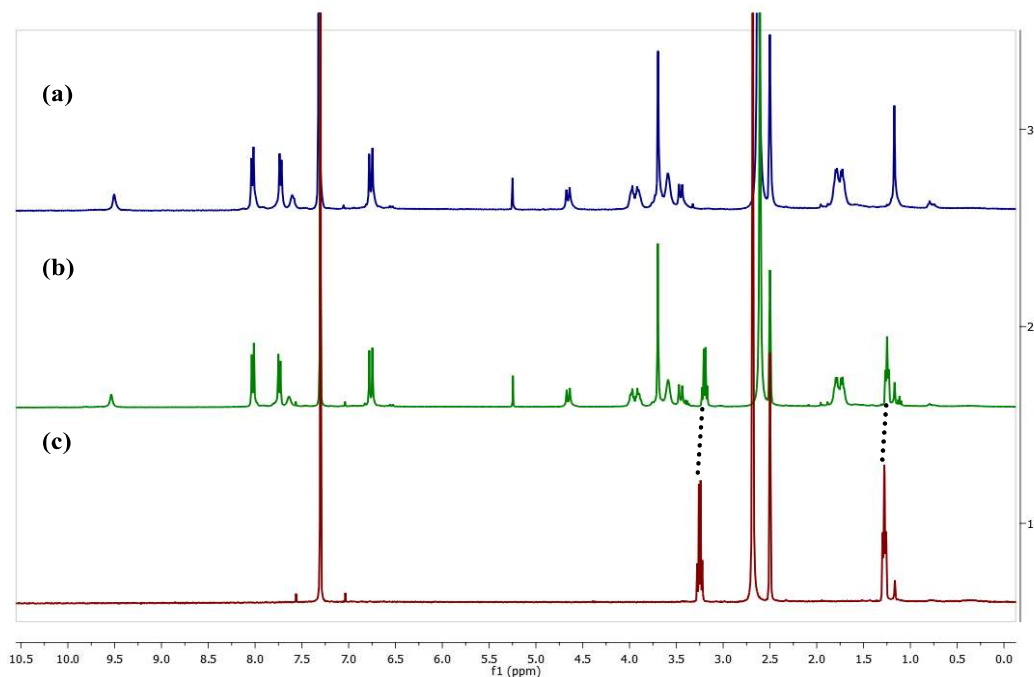


Figure 3.71.(a)0.5 mL of **L** (0.00313 M) in 5% DMSO- d_6 /CDCl $_3$ + 9 μ L DMSO- d_6 . (b) 0.5 mL of **L** (0.00313 M) in 5% DMSO- d_6 /CDCl $_3$ + 0.6 equiv. 0.1 M TEAClO $_4$ inDMSO- d_6 . (9 μ L)(c)0.5 mL 5% DMSO- d_6 /CDCl $_3$ + 9 μ L 0.1 M TEAClO $_4$ inDMSO- d_6 .

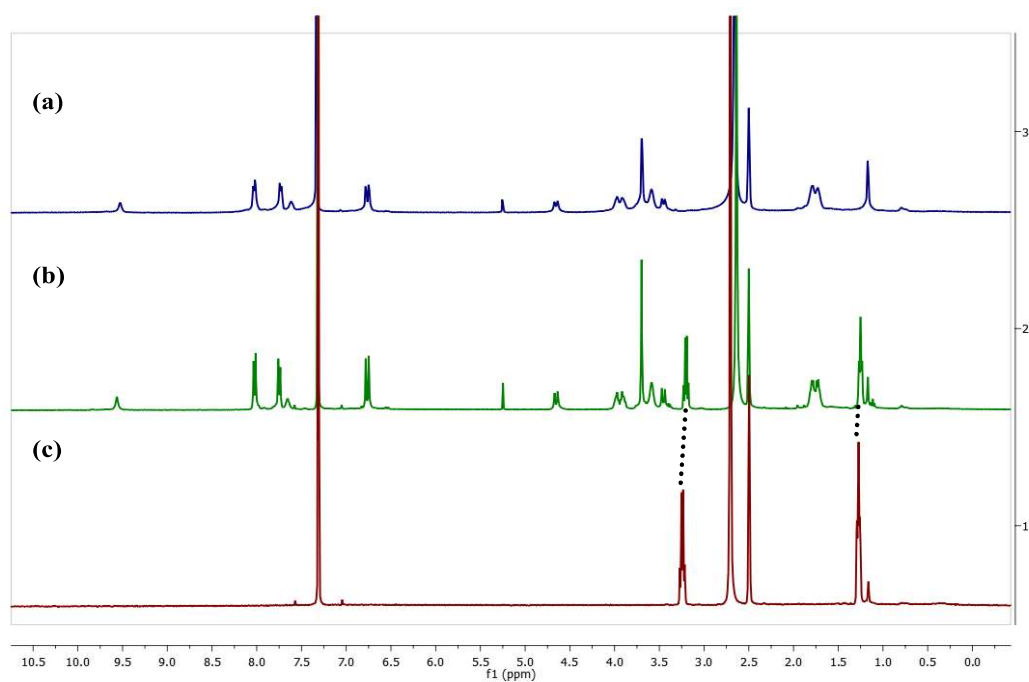


Figure 3.72.(a)0.5 mL of **L** (0.00313 M) in 5% DMSO- d_6 /CDCl $_3$ + 11 μ L DMSO- d_6 . (b) 0.5 mL of **L** (0.00313 M) in 5% DMSO- d_6 /CDCl $_3$ + 0.8 equiv. 0.1 M TEAClO $_4$ inDMSO- d_6 . (11 μ L)(c)0.5 mL 5% DMSO- d_6 /CDCl $_3$ + 11 μ L 0.1 M TEAClO $_4$ inDMSO- d_6 .

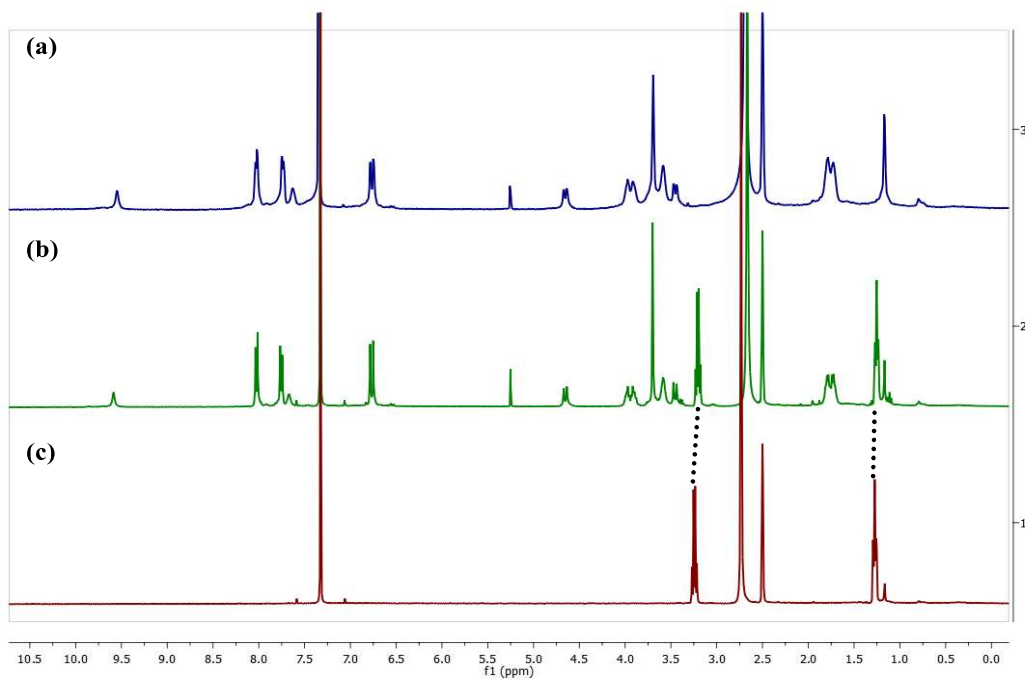


Figure 3.73.(a) 0.5 mL of **L** (0.00313 M) in 5% DMSO- d_6 /CDCl $_3$ + 14 μ L DMSO- d_6 . (b) 0.5 mL of **L** (0.00313 M) in 5% DMSO- d_6 /CDCl $_3$ + 1 equiv. 0.1 M TEAClO $_4$ in DMSO- d_6 . (14 μ L) (c) 0.5 mL 5% DMSO- d_6 /CDCl $_3$ + 14 μ L 0.1 M TEAClO $_4$ in DMSO- d_6 .

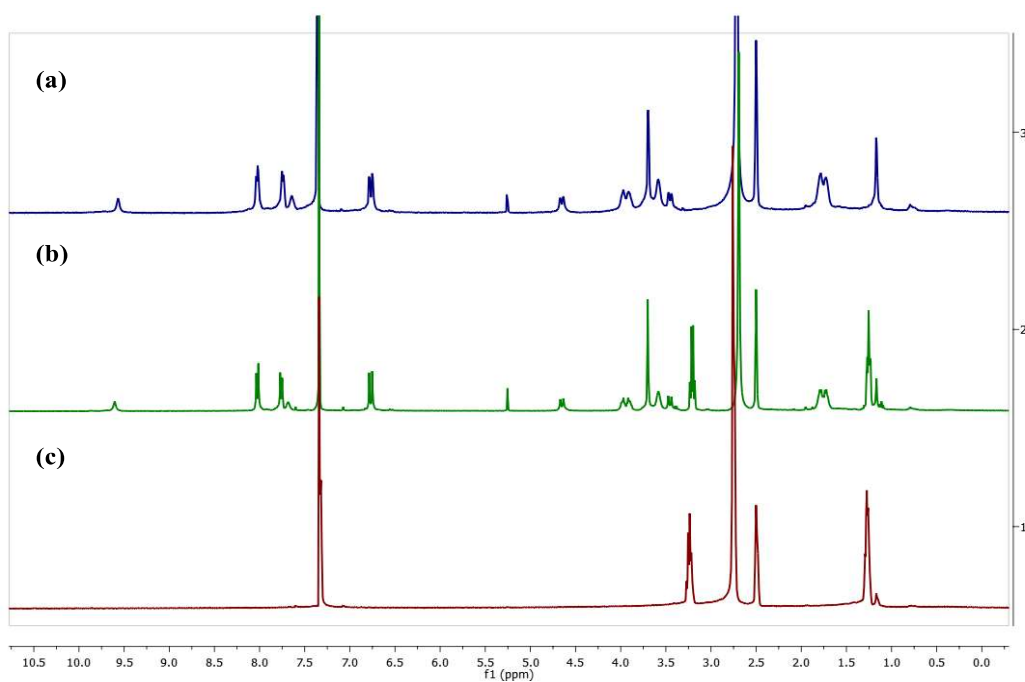


Figure 3.74.(a) 0.5 mL of **L** (0.00313 M) in 5% DMSO- d_6 /CDCl $_3$ + 17 μ L DMSO- d_6 . (b) 0.5 mL of **L** (0.00313 M) in 5% DMSO- d_6 /CDCl $_3$ + 1.2 equiv. 0.1 M TEAClO $_4$ in DMSO- d_6 . (17 μ L) (c) 0.5 mL 5% DMSO- d_6 /CDCl $_3$ + 17 μ L 0.1 M TEAClO $_4$ in DMSO- d_6 .

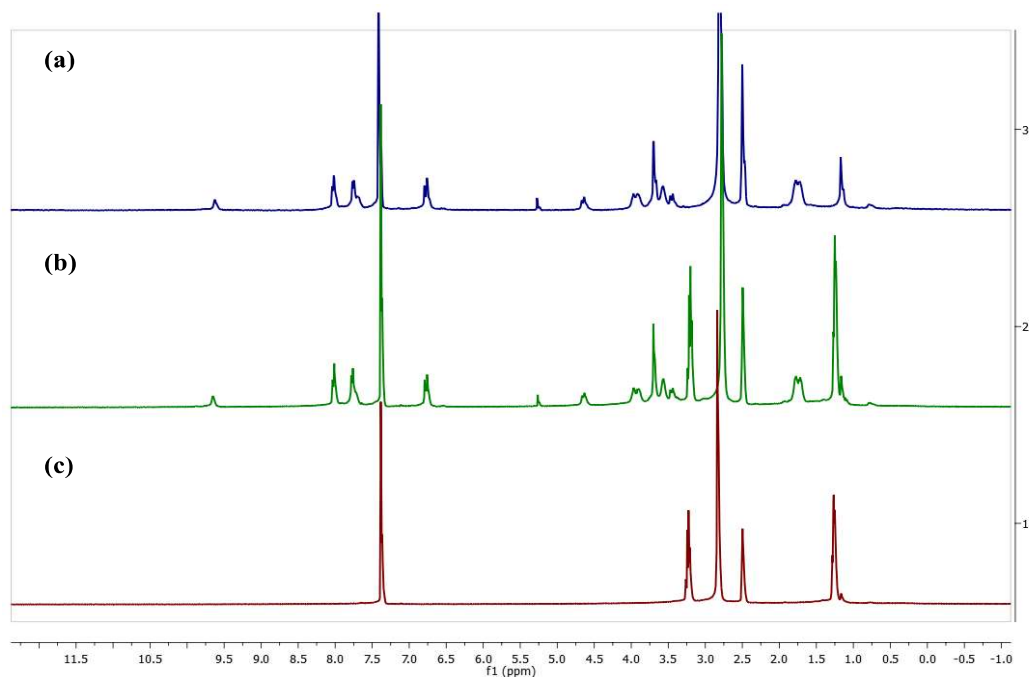


Figure 3.75.(a)0.5 mL of **L** (0.00313 M) in 5% DMSO- d_6 /CDCl $_3$ + 20 μ L DMSO- d_6 . (b) 0.5 mL of **L** (0.00313 M) in 5% DMSO- d_6 /CDCl $_3$ + 2 equiv. 0.1 M TEAClO $_4$ inDMSO- d_6 . (20 μ L)(c)0.5 mL 5% DMSO- d_6 /CDCl $_3$ + 20 μ L 0.1 M TEAClO $_4$ inDMSO- d_6 .

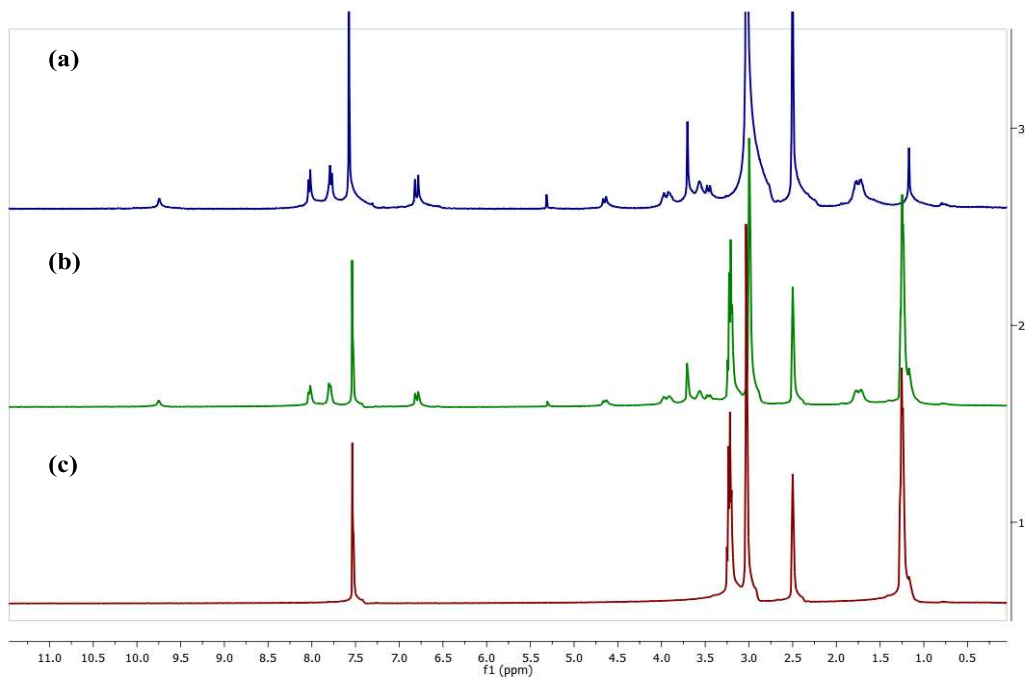


Figure 3.76.(a)0.5 mL of **L** (0.00313 M) in 5% DMSO- d_6 /CDCl $_3$ + 23 μ L DMSO- d_6 . (b) 0.5 mL of **L** (0.00313 M) in 5% DMSO- d_6 /CDCl $_3$ + 5 equiv. 0.1 M TEAClO $_4$ inDMSO- d_6 . (23 μ L)(c)0.5 mL 5% DMSO- d_6 /CDCl $_3$ + 23 μ L 0.1 M TEAClO $_4$ inDMSO- d_6 .

^1H NMR titrations of **L** with Arginine

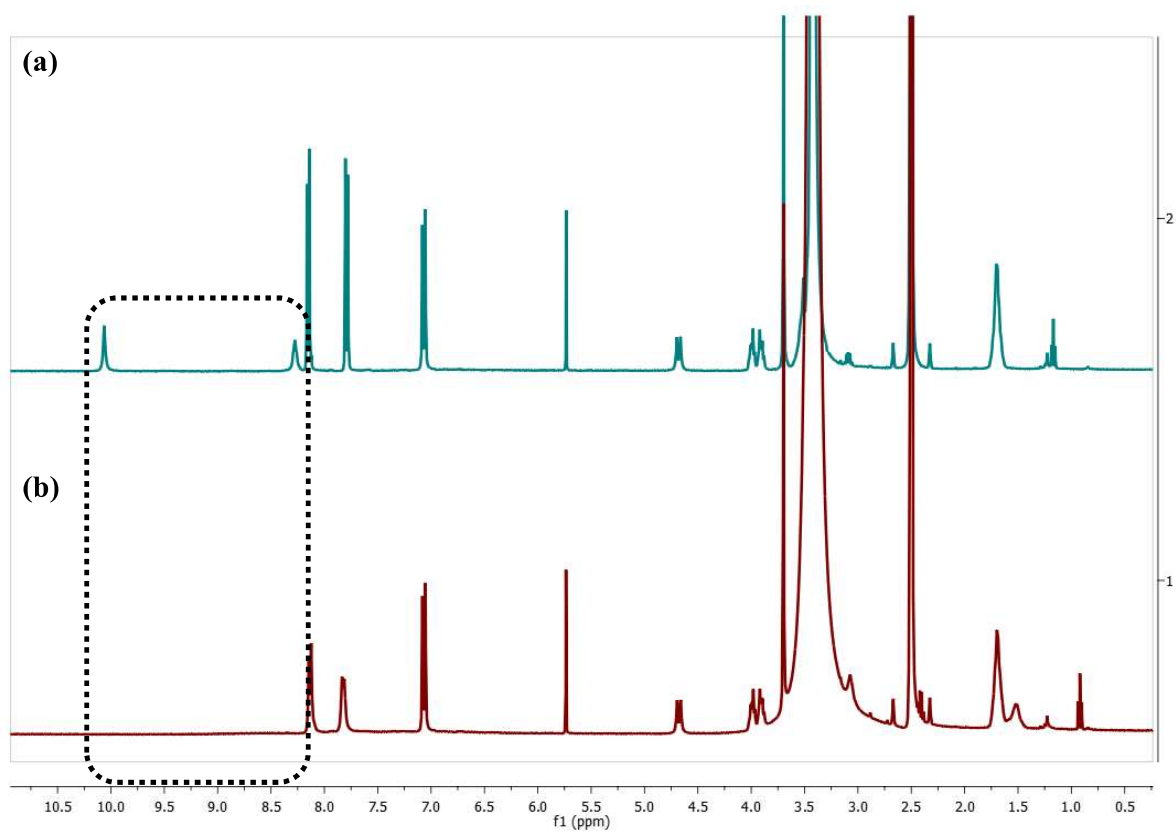


Figure 3.77. (a) **L** (0.00313 M) in 5% $\text{H}_2\text{O}/\text{DMSO-d}_6$ (0.5 mL); (b) **L** (0.00313 M) in 5% $\text{H}_2\text{O}/\text{DMSO-d}_6$ (0.5 mL) + 0.2 equiv. of 0.2 M arginine in H_2O

Figure 3.78.ESI-Mass Spectrum of **3**

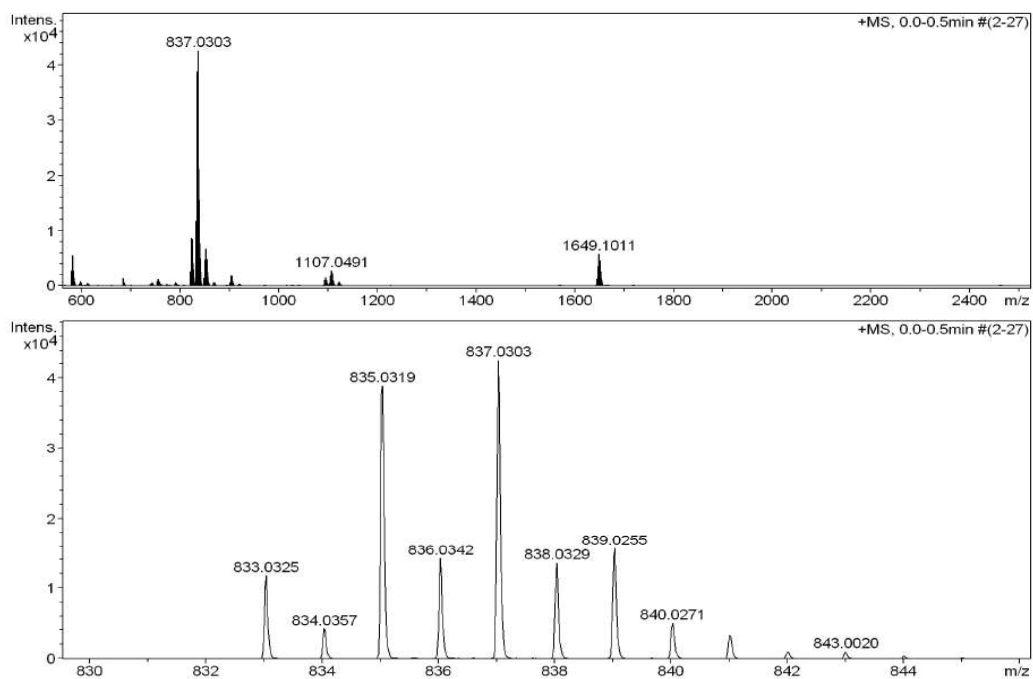


Figure 3.79.ESI-Mass Spectrum of **4**

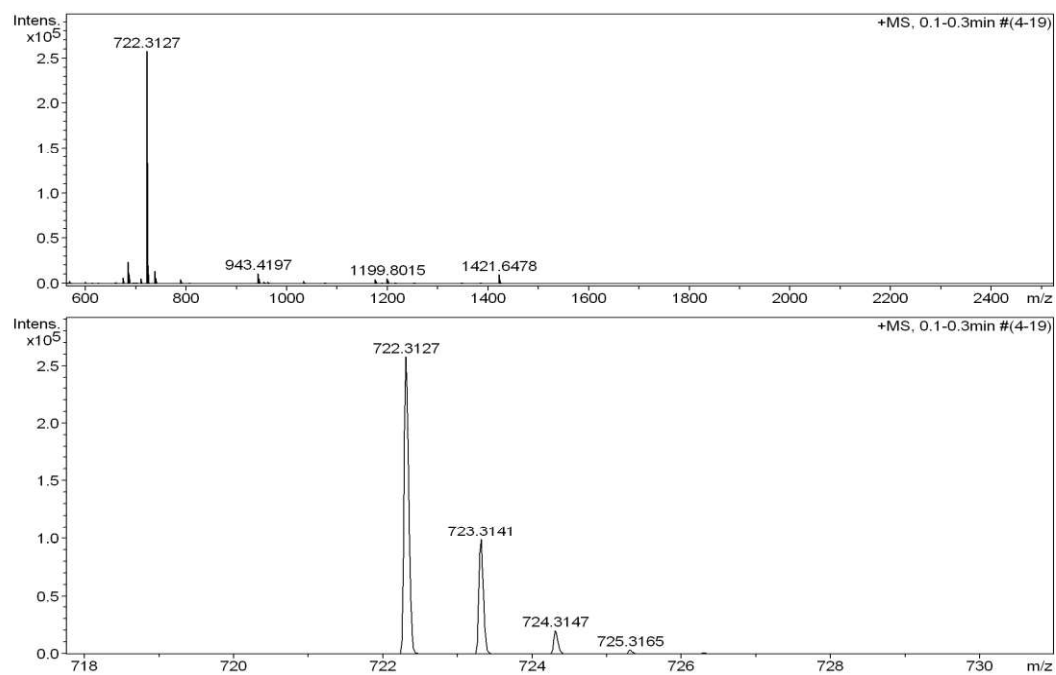
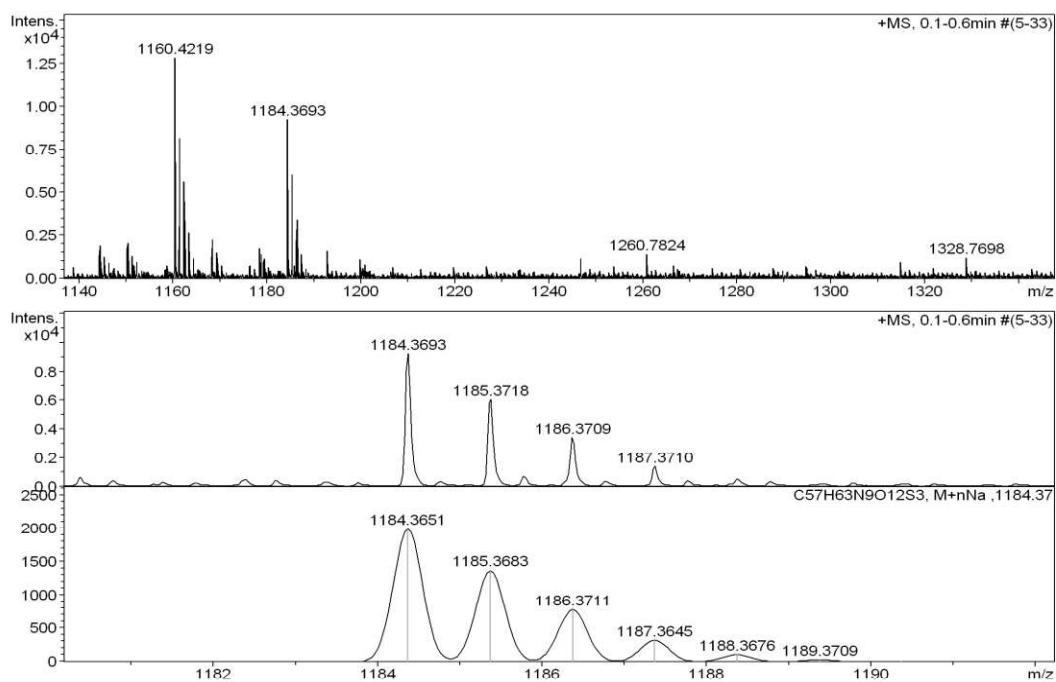


Figure 3.80.ESI-Mass Spectrum of L

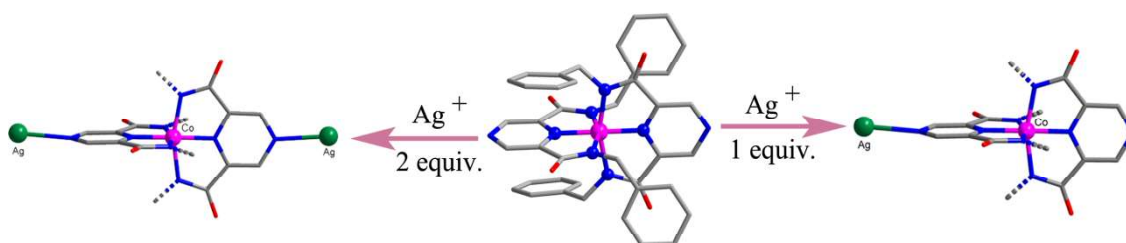


Chapter-4
Consecutive Introduction of Ag(I) to an Anionic Homoleptic Co(III)
Complex: Variable Ag(I) Coordination Mode

4.1. Abstract	191
4.2. Introduction.	193
4.3. Results and Discussion.	201
4.4. Conclusion.	210
4.5. Experimental section.	211
4.6. References.	214
4.7. Spectral Data.	217
4.8. Crystal Data.	222

4.1. Abstract

Although the pyridine-2,6-diamide ligand is widely reported, coordination chemistry of the analogous pyrazine-2,6-diamide ligand has not been reported to date. To study the complexation behavior, we have synthesized N,N'-dibenzylpyrazine-2,6-dicarboxamide and the heterometallic complexes were in a stepwise manner. After dimerisation with Co(III) complexation, two ring nitrogen atoms are freely available. These two free pyrazine nitrogen atoms were studied for their coordination with Ag(I), resulting in three heterometallic complexes, $C_{40}H_{34}AgCoN_8O_5$, $C_{42}H_{38}Ag_3CoN_{10}O_{11}$ and $C_{42}H_{53}AgCoN_9O_{13}$. The mode of coordination could be controlled by varying the metal to ligand ratio and varying the counter anion. Moreover, we found conditions that make the ligand to either coordinate or not coordinate to Ag^+ . Some of these complexes also display the rare organometallic (C–Ag) bond.



4.2. Introduction

Coordination polymers (CPs) are the polymers whose repeating units are coordination complexes. CPs received considerable attention during the past decade because of their structural diversities and versatile properties such as optical, magnetic, electrical, catalysis, luminescence, conduction, separation, sensing, catalysis and storage.¹⁻⁹ CPs are classified into two types homometallic and heterometallic complexes. In contrast to homometallic complexes, Synthesis of heterometallic complexes are challenging. Heterometallic complexes can be synthesized by a one pot method and in a stepwise manner. Although one pot method is synthetically ideal which requires simple mixing of suitable organic ligand with suitable metal salt, the major disadvantage of this method is the formation of a statistical formation of homo and heterometallic metal complexes. The most promising method for the synthesis of heterometallic complexes is stepwise strategy which requires a metalloligand as a building block.¹⁰⁻¹¹(Figure 4.1)

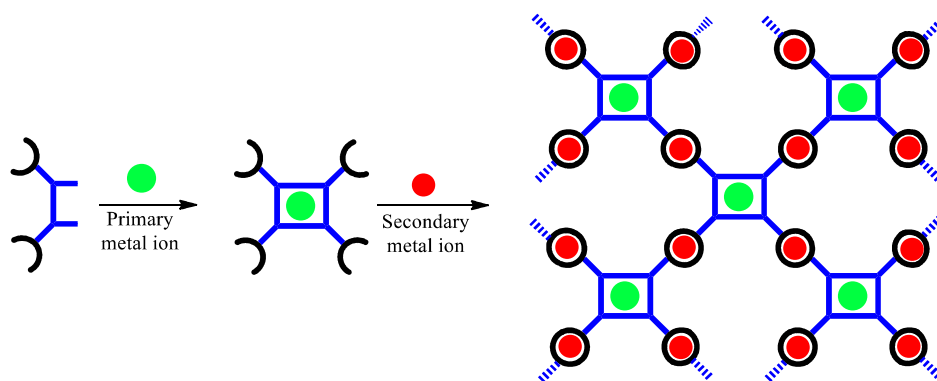


Figure 4.1. Schematic representation of Heterometallic complex by stepwise manner

A metalloligand is a coordination complex having a vacant coordinating sites which are able to coordinate to secondary metal ions resulting a heterometallic architecture. The advantages¹¹ of this approach over conventional approach are , (a) Metalloligands are

conformational rigid which offers meticulous control over the placement of appended functional groups resulting a highly ordered structures. (b) By the interplay of both metalloligands and spacers, The pore size and pore environments of the resulting complexes can be rationally fine tuned. (c) Metalloligands which offers vacant coordinating sites for the secondary metal ion facilitates in placing two or more metal ions in the close proximity.

Metalloligands can be mono¹², di⁴, polynuclear¹³⁻¹⁴ depends on the judicious choice of ligand and the metal salt used. The resultant heterometallic architecture was governed by the nature of secondary metal ion used to form either 1D, 2D or 3D coordination polymers. Among many ligands¹⁰, amide based ligands were also successfully employed in the preparation of heterometallic complexes. In particular pyridine based ligands are well studied. This is for the reason that in the presence of primary metal ion amide ligand forms structurally rigid scaffold subsequently places the appended functional groups in geometrically particular direction.

Rajeev gupta and co-workers have extensively utilized pyridine amide based ligands and their metalloligands for the assembly of discrete as well as network homo- and heterometallic architectures.^{10, 15, 11} They synthesized variety of pyridine amide metalloligands that offers appended pyridine rings which differ in the nitrogen atom position such as 2-pyridyl, 3-pyridyl, 4-pyridyl groups. (Figure 4.2)

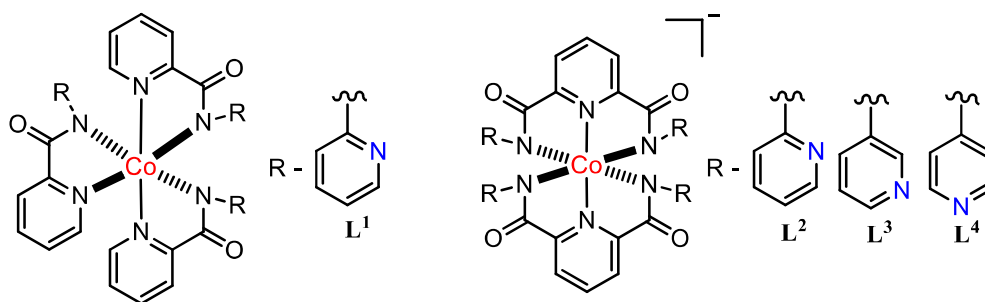


Figure 4.2. *Pyridine amide based metalloligands*

The metalloligands L^1 - L^4 were synthesised by deprotonating corresponding ligands HL_1 , H_2L^{2-4} in the presence of Co(II) salt under inert conditions followed by exposing to molecular oxygen. The deprotonated amide ligands are octahedrally connected to Co(III) ion with uncoordinated pyridine rings, two in case of L^1 and four in case of L^{2-4} . The two pyridine rings which are in proximity as in case of L^1 , L^2 , reacts with M(II) (M – Zn, Cd, Hg, Fe) forms a cleft resulting a discrete heterometallic complex.¹⁶⁻¹⁹(Figure 4.3 & 4.4)

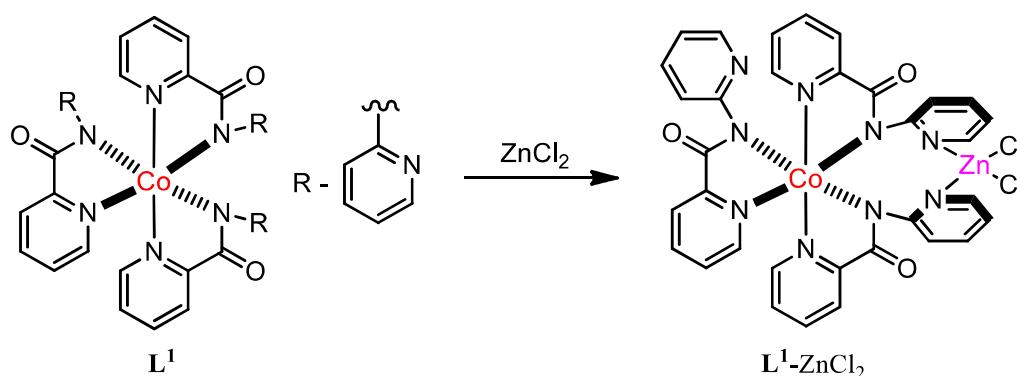


Figure 4.3. Synthesis of discrete heteromonometallic complex from metalloligand L^1 .

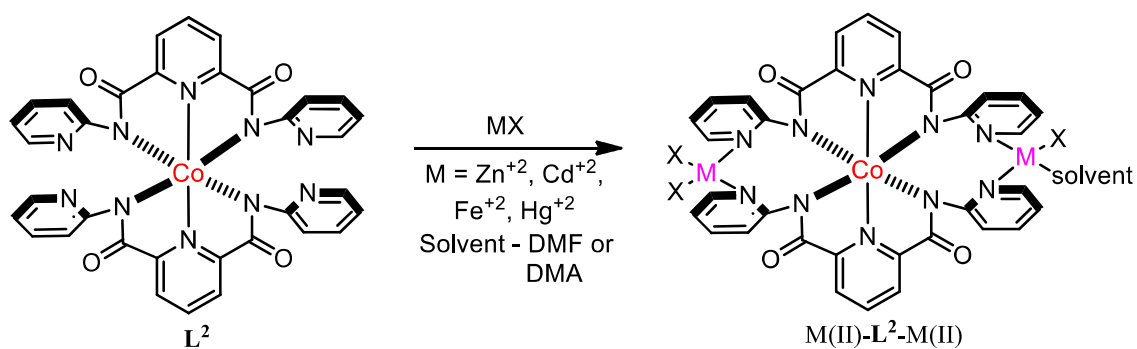
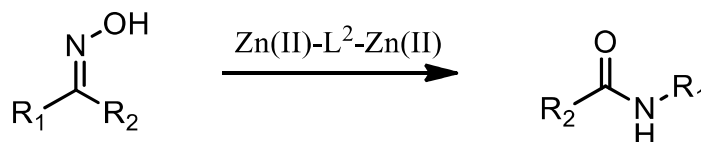


Figure 4.4. Synthesis of discrete heterobimetallic complex from metalloligand L^2 .

The heterometallic complex $Zn(II)$ - L^2 - $Zn(II)$ has a lewis acidic $Zn(II)$ ions in its periphery and was found to be effective in the Beckmann rearrangement which is the conver-

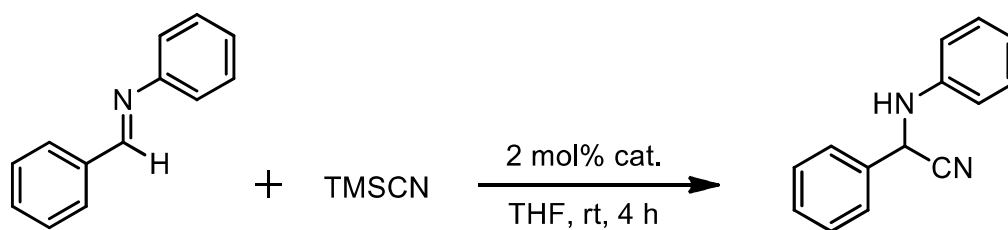
-sion of aldoxime or ketoxime to corresponding amides in the presence of acid. Only ZnCl_2 was ineffective for this conversion shows the importance of heterometallic complex.¹⁶ (Scheme 4.1)



Scheme 4.1. Beckmann rearrangement catalysed by Zn(II) heterobimetallic complex of L^2

A range of aldoximes and ketoximes investigated were found to be successful. Aldoximes undergo conversion to only primary amides without traces of nitrile and aldehyde which are common by-products in this reaction shows the advantage of heterometallic complex. Also the heterometallic complex $\text{Cd(II)-L}^2\text{-Cd(II)}$ was found to be ineffective for this conversion shows the uniqueness of $\text{Zn(II)-L}^2\text{-Zn(II)}$ complex. Most importantly this complex can be reused which is tested eight times without significant drop of conversion as well as yield.

The catalytic activity of $\text{Cd(II)-L}^2\text{-Cd(II)}$ complex was found to be effective for strecker reaction which is the acid promoted cyanation of imines to get α -aminonitriles (Scheme 4.2). These are the important precursors for the synthesis of α -amino acids and other heterocyclic compounds. Interestingly the heterometallic complex $\text{Zn(II)-L}^2\text{-Zn(II)}$ is almost ineffective for this conversion.¹⁷



Scheme 4.2. Strecker reaction catalysed by Cd(II)-L²-Cd(II) complex

The methods required for strecker reaction are often use of expensive reagents, strong acidic and harsh conditions, high catalyst loading, prolong reaction time that leads to several by-products. But with Cd(II)-L²-Cd(II) complex the reaction requires low catalyst loading (2 mol%), less reaction time (4 h) and takes place at room temperature. This shows the potential application of these type of heterometallic complexes in the catalysis.

While the metalloligands L³, L⁴ that contains uncoordinated 3-pyridyl, 4-pyridyl groups respectively, when treated with M(II) (M – Zn, Cd,) salts forms 2D networks instead of discrete heterometallic complexes as in the case of L¹.²⁰⁻²¹(Figure 4.5 & 4.6)

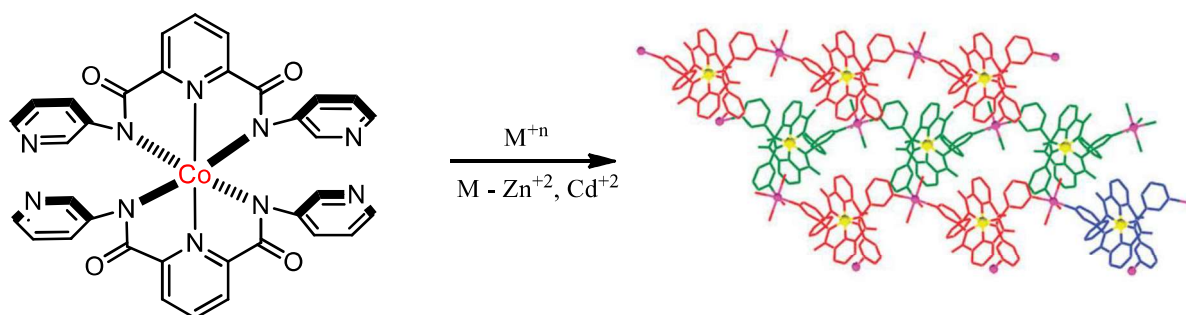


Figure 4.5. Coordination of metalloligand L³ with Cd(II) ions resulting 2D network

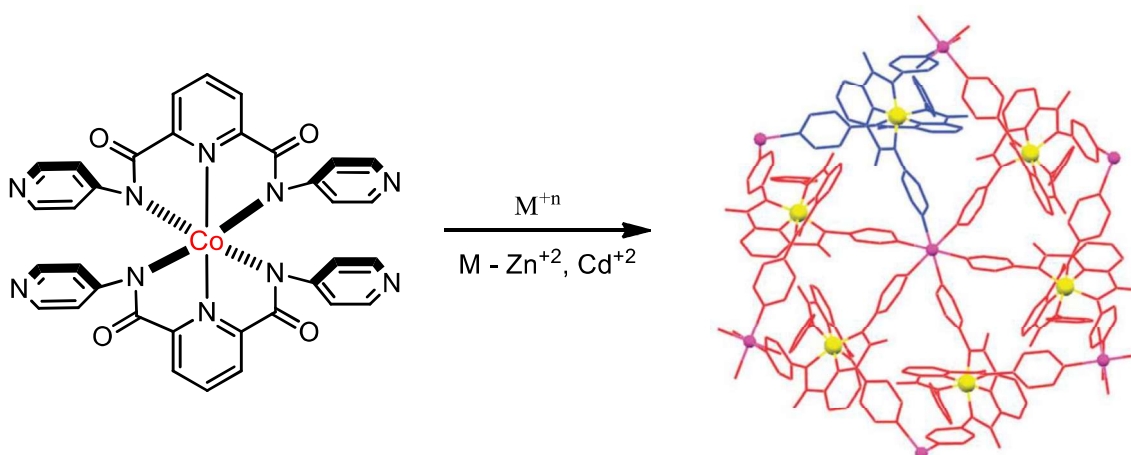
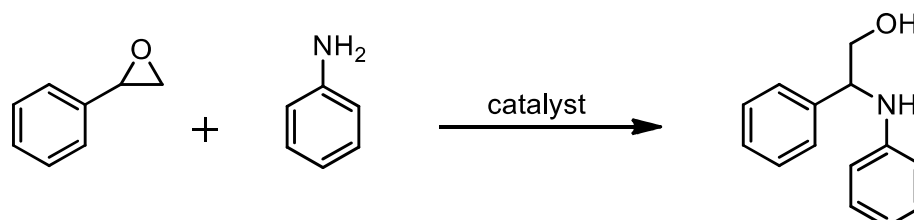


Figure 4.6. Coordination of L³ with Zn(II) ions resulting hexagonal network

The 2D networks in the both cases resulted due to the coordination of Zn(II) in such

away that each metalloligand connected to four different Zn(II) ions. Both the 2D networks are moderately porous and contains lewis acidic secondary metal ions. The catalytic applications of these networks were investigated and are found to be effective in the ring opening reaction of epoxides with anilines to form amino alcohols.²¹ (Scheme 4.3)



Scheme 4.3. Epoxide ring opening reaction catalysed by 2D network of L^3 .

Further the reaction takes place under solvent-free conditions and the catalyst was used several times without losing the catalytic activity.

Although pyridine based amide ligands were comprehensively studied, but the analogue pyrazine amide ligands were less explored. For example sally brooker's group have synthesized N,N-bis[2-(2-pyridyl)ethyl]pyrazine-2,3-dicarboxamide ligand and demonstrated that it forms $[2 \times 2]$ molecular grid Cu(II), Ni(II) salts in the presence of base.²² (Figure 4.7)

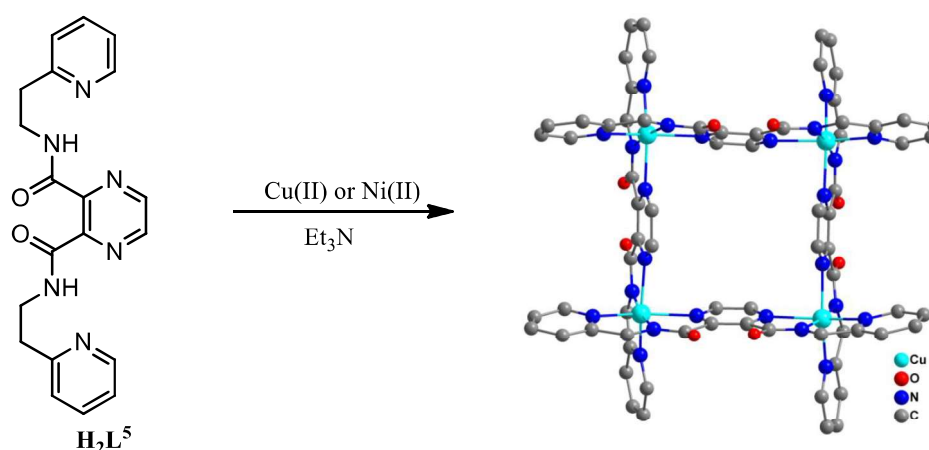


Figure 4.7. Ni(II) or Cu(II) coordination with $[L^5]^{2-}$ resulting $[2 \times 2]$ molecular grid

Similarly same group has showed that its isomer the pyrazine-2,5-diamide also forms [2 x 2] grid with Co(II) salts in the presence of base.²³

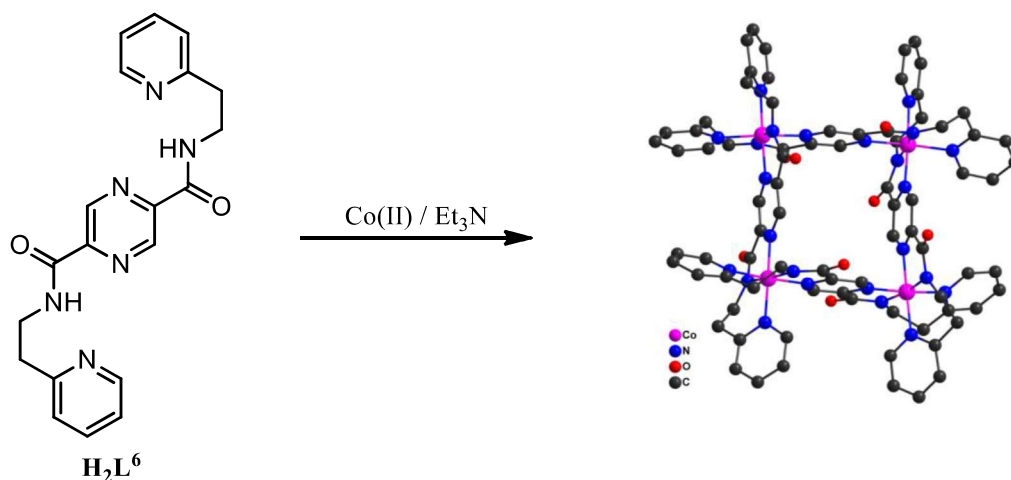


Figure 4.8. Coordination of Co(III) with $[\text{L}^6]^{-2}$ resulting [2 x 2] molecular grid.

Another report by Sally Brooker and co-workers showed the synthesis and mode of coordination of pyridine appended pyrazine-2-carboxamideligand (Figure 4.9).²⁴ This ligand in the presence of Ag(I) ion forms a metallomacrocyclic structure whereas with Co(II) salt in presence of

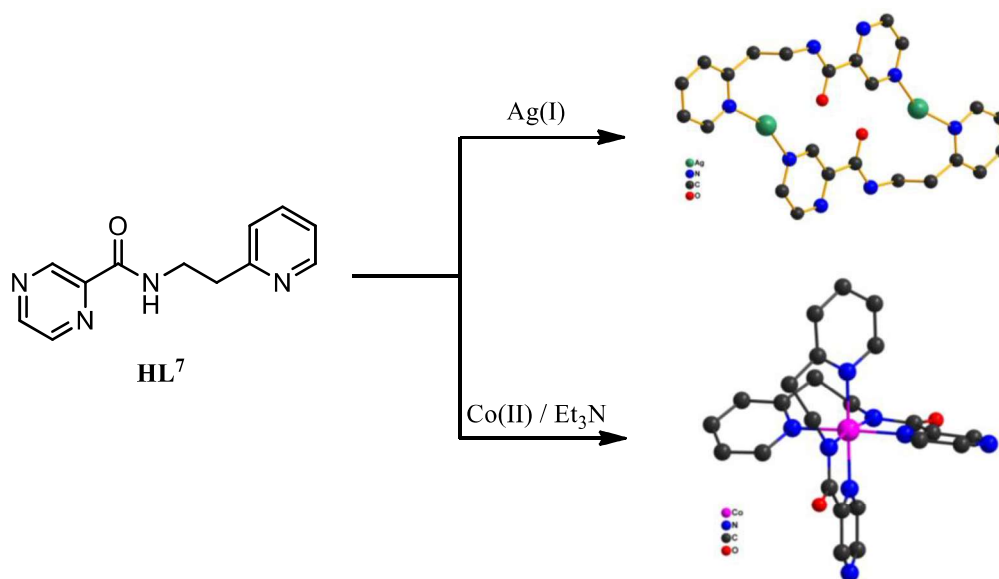


Figure 4.9. Synthesis of $\text{Ag}_2(\text{HL}^7)_2$ and $\text{Co}(\text{L}^7)_2$ from HL^7

base forms Co(III) complex. Attempts to make a heterometallic coordination polymer by adding 1:1 ratio of Ag(I) to Co(III) complex was unsuccessful but indeed resulted a 2:1 Co(III) / Ag(I) discrete heterometallic complex (Figure 4.10). Polymerisation did not formed even after adding 10 equivalents of Ag(I) salt.

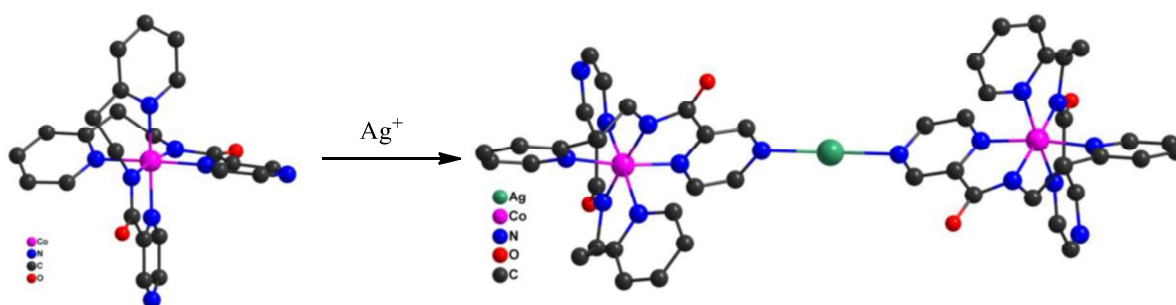


Figure 4.10. Coordination of Ag^+ ion with $Co(L^7)_2$ resulting a discrete heterometallic complex

Based on this literature report we have designed and synthesized N,N'-Dibenzylpyrazine-2,6-dicarboxamide (**1**) ligand for the first time. This ligand has two types of binding sites, one is tridentate anionic site which results by deprotonating two amide protons and another one is monodentate pyrazine ring nitrogen atom (Figure 4.11). We have utilized this ligand to form heterometallic coordination complexes with Co(III) and Ag(I).

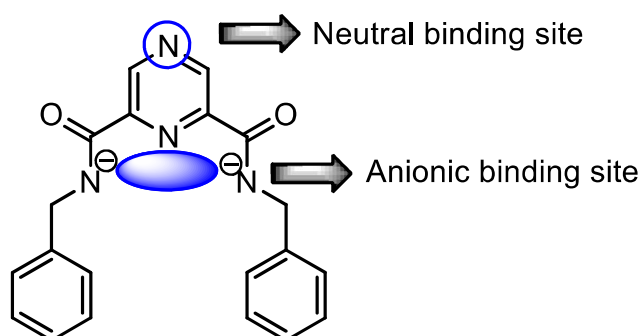
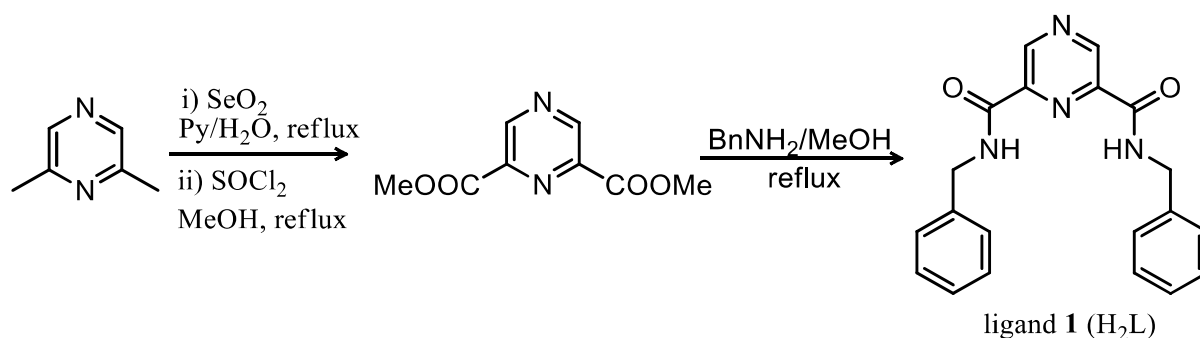


Figure 4.11. Structure of pyrazine-2,6-diamide showing different type of binding sites

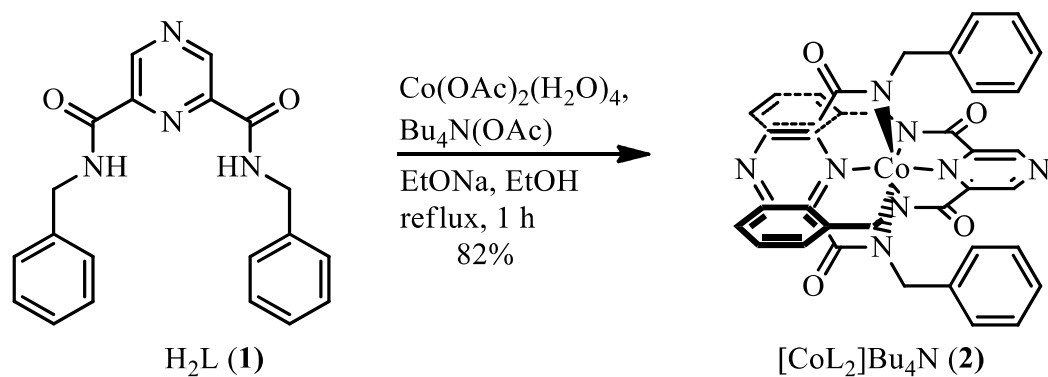
4.3. Results and Discussion



Scheme 4.4. Synthesis of ligand 1

Compound 1 was synthesized in two steps from 2,6-dimethylpyrazine. It was first oxidized with SeO_2 and an esterification reaction was performed with methanol. The dimethylester of pyrazine-2,6-dicarboxylate was then reacted with benzyl amine in methanol to obtain the product 1 (Scheme 4.4). 1 was purified by column chromatography using ethyl acetate as the eluent and characterized by mass and NMR spectroscopy. Deprotonation of the amide protons makes 1 a suitable tridentate ligand for coordination with metals that prefer octahedral or square planar coordination. We chose cobalt, which prefers an octahedral geometry in both Co(II) and Co(III) complexes. This type of amide ligand is known to stabilize the higher oxidation state of cobalt, i.e., Co(III).²⁵ We metalated 1, following a literature procedure.²⁶⁻²⁸ In brief, deprotonation of the amide protons was performed with sodium ethoxide ($\text{NaH} + \text{EtOH}$) in ethanol. It was then metalated with $\text{Co}(\text{OAc})_2$ and the subsequent air oxidation obtained $[\text{CoL}_2]\text{Bu}_4\text{N}$ (2) (Scheme 4.5).

The compound was characterized by ^1H NMR and mass spectroscopy. The ^1H NMR spectra clearly shows the absence of the amide protons, suggesting the coordination of the metal centre to the amide nitrogen atoms. Moreover, a peak corresponding to the counter



Scheme 4.5. Synthesis of cobalt complex $[\text{CoL}_2]\text{Bu}_4\text{N}$ from H_2L

Cation tetrabutyl ammonium was found in the NMR. High resolution mass spectroscopy in $-ve$ mode clearly shows the molecular ion peak at $m/z = 747.1870$ (calc. m/z 747.1873).

A crystal suitable for an X-ray diffraction study was grown by slow evaporation after making a near saturated solution of the compound in acetonitrile. The crystal belonged to $\bar{4}$ space group in tetragonal crystal system. The cobalt atom lies at a site having four-fold-inversion symmetry with a distorted octahedral geometry that contains four amide and two Pyrazine nitrogen atoms coordinating to it (Figure 4.12). Out of them, two pyrazine and two amide nitrogen atoms are making a distorted square, whereas the other two coordinate through the axial positions. The pyrazine nitrogen atoms, N1 and N2, lie on a two-fold axis, whereas the central N4 atom in the counter cation Bu_4N lies at a site with four-fold-inversion symmetry. The Co–N1 distance is 1.846(3) Å and the Co–N3 distance is 1.959(3) Å; the other coordinating atoms are symmetry generated. The bond angles are 180° for N1–Co–N1#5 and $\sim 81^\circ$ for N1–Co–N3. In the crystal lattice, the tetrabutyl ammonium ion is packed between the anionic parts (Figure 4.13).

The anionic part of the molecule has two pyrazine nitrogen atoms free. Therefore, this molecule can be utilized to bind other metals to form heterometallic complexes. These

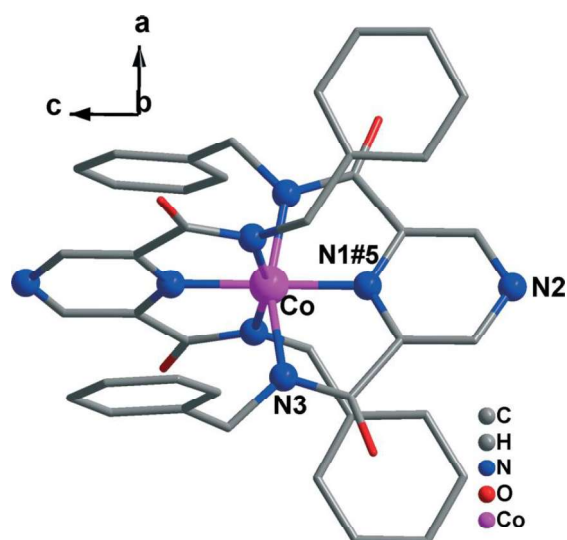


Figure 4.12. Anionic part of **2**, showing the coordination around of Co(III) atom. The cationic part and hydrogen atoms were omitted for clarity. The atom labelled as N1#5 is at equivalent position $(0.5 + y, 0.5 - x, 0.5 - z)$.

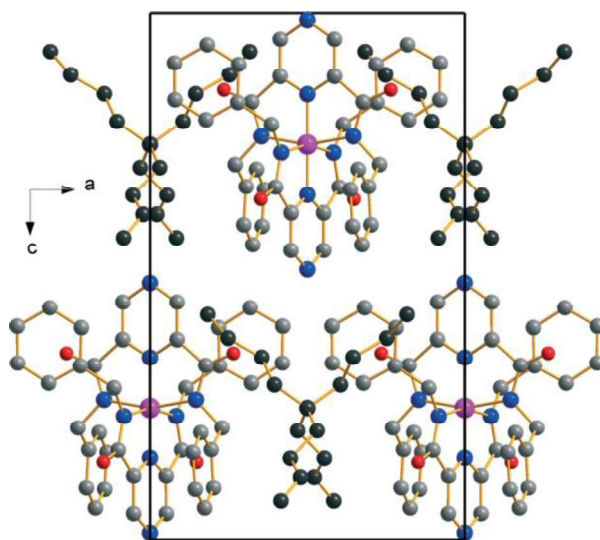


Figure 4.13. Unit cell of complex **2**. Tetrabutyl ammonium cations are shown in black.

binding sites are less nucleophilic because of the strong electron withdrawing nature of the amide groups. Therefore, we have chosen the Ag^+ ion, which is soft, to study the coordination chemistry of **2**. Ag(I) complexes are attracting a great deal of attention due to

their possible use as antimicrobial agents or as antibiotics,²⁶⁻²⁷ new topological uniqueness in their complexes,²⁹ biologically relevant coordination complexes,³⁰ and photo active materials.³¹

Ag(I) generally forms coordination compounds with 2, 3 and 4 coordination number with a preference to the tetracoordination mode.³² Some Ag(I) complexes have coordination numbers of 5, 6, and 7.³³ Ag(I) also forms organometallic compounds with different modes of coordination ranging from η^1 to η^6 with aromatic rings in suitable ligand systems. The challenge, however, remains to design organosilver(I) complexes bearing aromatic ligands attached with coordinating groups.³⁴⁻³⁵ To study the coordination behaviour of complex **2**, we tried to metallate it with Ag(I). For a quick insight into the complex formation, we obtained mass spectra with a 1 : 2 ratio of complex **2** and silver nitrate. It clearly reveals the existence of three types of complexes (Figure 4.14). The peak at m/z 857.07 ($C_{40}H_{32}CoN_8O_4Ag$) suggests one silver ion coordinates with complex **2**, while two silver coordination (m/z 962.96, $C_{40}H_{32}CoN_8O_4Ag_2$) and three silver coordination at m/z 1131.85 ($C_{40}H_{32}CoN_9O_7Ag_3$) are also present. From the spectra, it could be suggested that the two silver coordination (m/z 962.96) is most stable among all the complexes under the mass spectroscopic conditions. This could be due to the two symmetrical nitrogens present in the molecule. Both proton and carbon NMR spectra, however, do not show any relevant shifts.

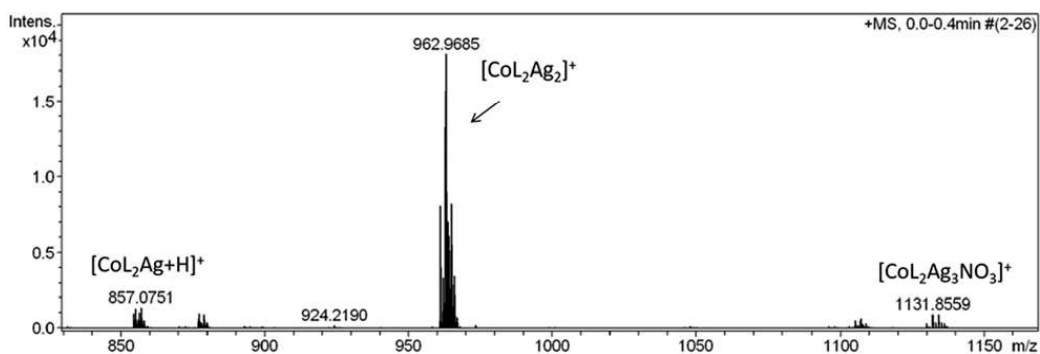


Figure 4.14. ESI MS spectra of cobalt complex **2** after adding 2 equivalents of $AgNO_3$.

The complex $[\text{CoL}_2]\text{Ag}(\text{H}_2\text{O})$ **3** (Figure 4.15) crystallized in the monoclinic crystal system with the space group $\text{P}2_{1/n}$. The asymmetric unit contains only one silver atom, Ag1, which is tetrahedrally coordinated to pyrazine N2 (2.381(2) Å), two amide oxygen atoms O2 (2.312(2) Å) and O4 (2.269(2) Å), and two benzene carbons C32 (2.527(4) Å), C33 (2.658(5) Å) resulting in a η^2 bond. The Ag–C distances (2.5–2.6 Å) are comparable to those reported in the literature;³⁴⁻³⁵ however, the shortest distances are also reported to be 2.3–2.4 Å.³⁶⁻³⁷ To our surprise, pyrazine N4, which is symmetrical to N2, is not coordinated.

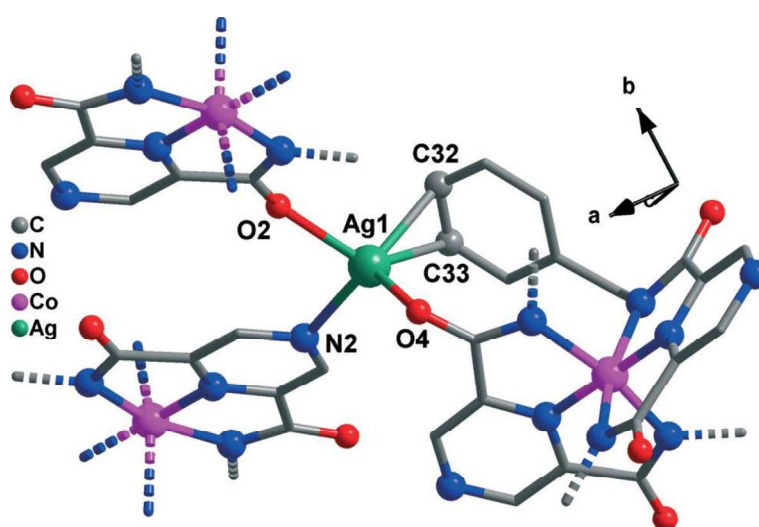


Figure 4.15. Crystal structure of complex **3** showing coordination around Ag^+ . Hydrogen atoms and groups which are not coordinated to Ag^+ are omitted for clarity.

A simplified packing diagram of this complex is shown in Figure 4.16. Due to the coordination of silver and the Ag–C bond, the lattice is making a 2D polymeric structure.

As the complex was not forming a coordination polymer, it might be possible to obtain crystals coordinated to both the free nitrogen atoms in complex **2**. To achieve this, we tried to put two equivalents of AgNO_3 with respect to complex **2**. The crystallization was carried out in acetonitrile with a few drops of ethanol as in the previous case.

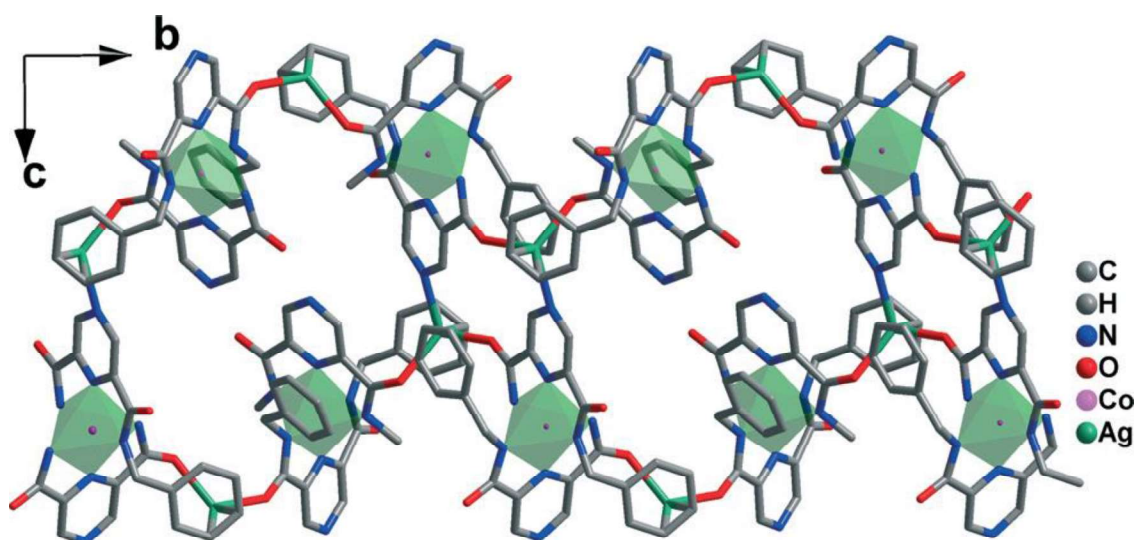


Figure 4.16. Packing diagram of complex 3. Hydrogen atoms and benzyl groups, which are not coordinated are omitted for clarity.

The complex, $[\text{CoL}_2]\text{Ag}_3(\text{NO}_3)_2(\text{EtOH})$ (**4**) crystallized in the triclinic crystal system with a $P\bar{1}$ space group. The overall structure of complex **2**, even in this case, is retained. To our surprise, there are three silver atoms in the asymmetric unit of **4**, indicating that not all of complex **2** took part in the reaction, some was left in the solution. Two of them are coordinated as expected to the nitrogen atoms in pyrazine which were free in complex **2** (Figure 4.17 & 4.18)

The coordination sphere of Ag1 is filled with pyrazine N4(2.385(4) Å), two amide oxygen atoms, O1 (2.346(4) Å) and O2(2.316(4) Å), O8 (2.575(5) Å) of the nitrate ion and Ag3 coordinated with pyrazine N2 (2.384(4) Å), oxygen atom O5(2.375(7) Å) of the nitrate ion, oxygen O11 (2.485(1) Å) of ethanol, and one amide oxygen, O4 (2.322(3) Å). The other silver ion, Ag2, is coordinated to one amide oxygen, O3 (2.247(4)Å), two nitrate oxygen, O5 (2.469(7) Å) and O9 (2.446(5) Å), and one benzene carbon atom (C24–Ag2 = 2.735(5) Å) making a η^1 bond³⁴⁻³⁵

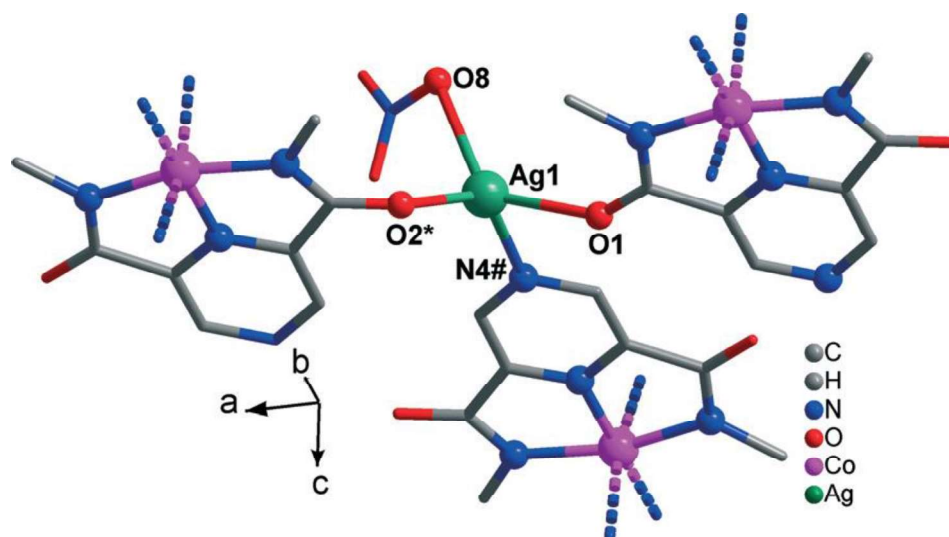


Figure 4.17. Coordination around Ag^+ (Ag1) in complex 4. Hydrogen atoms and groups which are not coordinated to Ag^+ are omitted for clarity. Symbols * and # indicate atoms at equivalent positions $(x - 1, y, z)$ and $(1 - x, 1 - y, -z)$, respectively.

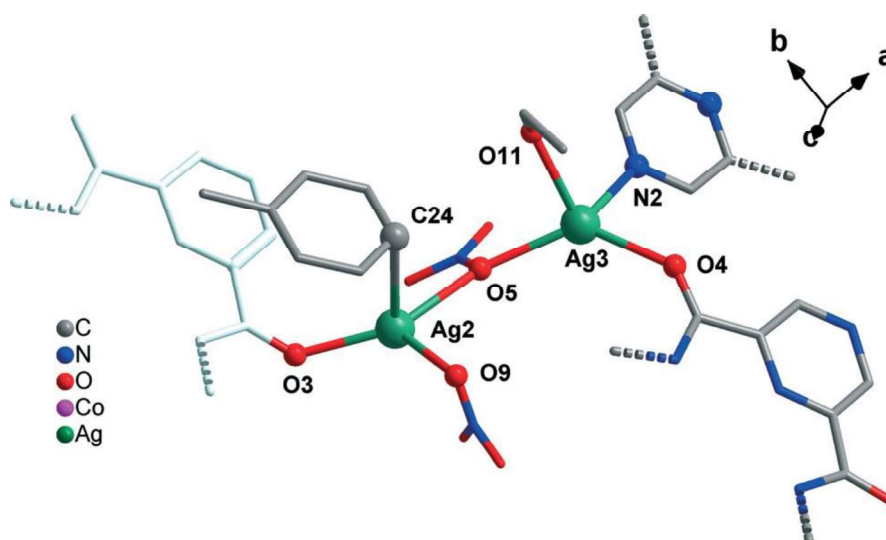


Figure 4.18. Coordination around Ag^+ (Ag2 and Ag3) in complex 4. Hydrogen atoms and groups which are not coordinated to Ag^+ are omitted for clarity.

It may be noted here that the η^1 bond of silver and benzene systems are rare because it is tantamount to form a σ -bond.³⁴ The shortest Ag–Ag distance in this crystal is between Ag2 and Ag3#2,³⁸ which are connected by a μ -oxobridge (O5 of the nitrate ion). It is surprising that the Ag(I) coordination did not make a linear polymeric structure even after both the pyrazine nitrogen atoms were coordinated to a highly symmetrical molecule. However, a three dimensional polymeric structure is formed due to Ag1–C24 and Ag1–O3 and bridging nitrate anions (Figure 4.19).

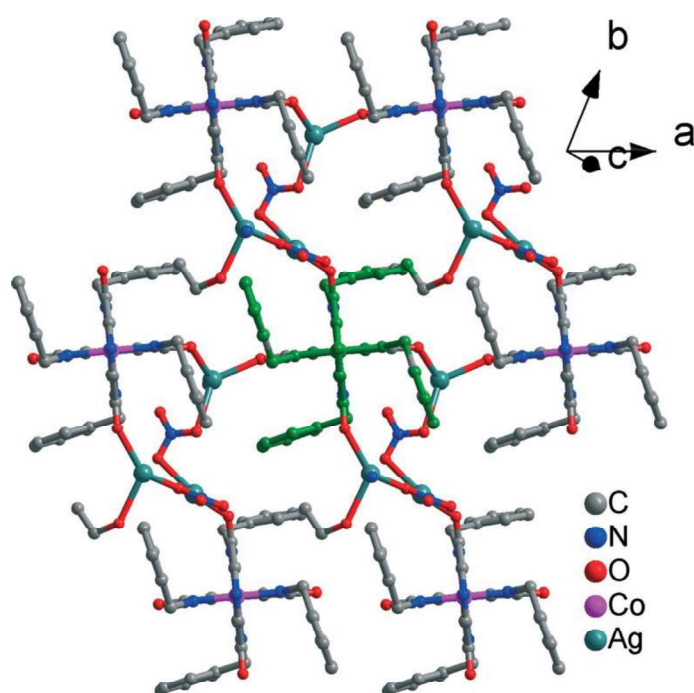


Figure 4.19. Packing diagram of complex 4. Hydrogen atoms are omitted for clarity.

As the stoichiometric ratio of Ag(I) used in the synthesis of complex 3 and complex 4 was only 1 and 2 equivalent, respectively, we decided to crystallize the complex 2 with an excess of silver ions to observe if there were any new coordination complexes obtained. Thus, we tried crystallization with 4 equivalents of AgNO₃ with respect to complex 2. We got crystals by employing a similar method as with complex 3 synthesis. However, initial investigation during data collection, it was noted that the cell parameter were exactly same as

that of complex **3**. This confirms that the crystal obtained were the same as complex **3** and no data was collected further.

There are few cases in the literature wherein silver ion acts as counter cations. In these cases, there was no free coordination site for Ag(I) to coordinate.³⁹⁻⁴¹ In these cases, Ag(I) is coordinated to solvents such as MeCN, MeOH, EtOH and H₂O. In our case, there is a tetrabutyl ammonium ion acting as a counter cation to complex **2**. Therefore, our next target was to replace the ammonium cation with a silver cation. However, as there are coordination sites, it might be difficult. We tried to crystallize complex **2** with different Ag(I) salts other than nitrate anion, such as AgClO₄, AgPF₆ and AgBF₄, in acetonitrile. We could crystallize a complex with AgClO₄. The complex [CoL₂]Ag(MeCN)(H₂O)·4H₂O **5** crystallized in the triclinic crystal system with a $P\bar{1}$ space group. The asymmetric unit contains only one silver ion and no perchlorate ion was found. This Ag(I) cation is acting as a counter cation, which is linearly coordinated to solvent molecules acetonitrile and water (Figure 4.20). The bonds are smaller

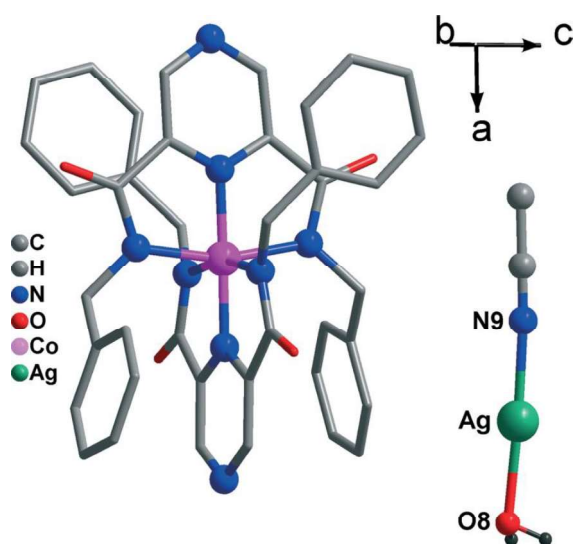


Figure 4.20. Crystal structure of complex **5**. The non-coordinated water molecules are not shown and hydrogen atoms of the [CoL₂] moiety are omitted for clarity.

than those in complex **3** and **4** with distances N9 (2.086(7) Å) and O8 (2.124(6) Å). The asymmetric unit has a further four water molecules (O5, O6, O7, O9) in general positions

Figure 4.21 shows the packing diagram of complex **5** as viewed from crystallographic a-axis. The solvents that are coordinating to the silver ion remain perpendicular to the axis, there by not visible. It can be clearly observed that the silver ions are packed between the cobalt complexes as in the case of complex **2**. Apart from silver ions, a few water molecules are filling the lattice space.

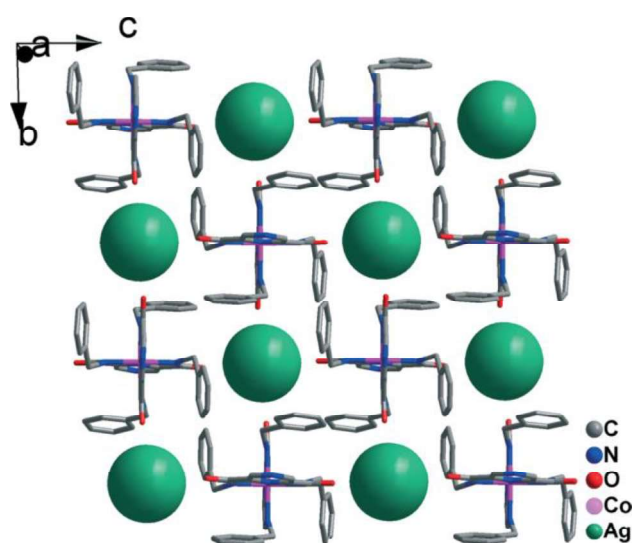


Figure 4.21. Packing diagram of complex **5**. Water, acetonitrile and hydrogen atoms are omitted for clarity.

4.4. Conclusion

In conclusion, we have for the first time studied a Pyrazine 2,6-diamide ligand for making heterometallic complexes by a stepwise synthesis method. We successfully isolated two heterometallic complexes with one $[\text{CoL}_2]\text{Ag}(\text{H}_2\text{O})$ and two $[\text{CoL}_2]\text{Ag}_3(\text{NO}_3)_2(\text{EtOH})$ Ag(I) ions coordinated, wherein a third silver cation is attached by an oxo-bridge with a nitrate oxygen and has a η^1 coordination to the phenyl ring.

We could also find conditions that make the ligand not coordinate to Ag^+ , thereby, unexpected complexes wherein Ag(I) acts as a counter cation could be crystallized.

4.5. Experimental section

4.5.1. Materials

Reagent grade chemicals were acquired from Aldrich and used as received. All solvents were procured from Merck Limited, India. Solvents were purified and dried prior to use following standard procedures. All the X-ray data was collected at room temperature. For complex 4, with a heavy atom in the structure, it was not possible to see a clear electron-density peak in difference-map plots which would correspond with an acceptable location for the ethanol O11 H atom, the refinement was completed with no allowance for this H atom in the model.

4.5.2. Physical measurements

NMR spectra were obtained using a Bruker 400 MHz instrument. Single crystals X-ray diffraction studies were performed on a Bruker 4-circle Kappa APEX-II diffractometer equipped with a CCD detector, the X-ray source being $\text{Mo K}\alpha$ (wavelength 0.71073 Å) at room temperature. Data collection was monitored with Apex II software and pre-processing was carried out with SADABS integrated with Apex II. Mass spectra were obtained in a Bruker micrOTOF-Q II spectrometer using methanol as a solvent without adding any acid. Elemental analysis was performed at SAIF at CDRI, Lucknow.

Dimethyl pyrazine-2,6-dicarboxylate.

Synthesized by following the procedure used for oxidation of 2,5-dimethylpyrazine.⁴² To a solution of 2,6-dimethylpyrazine (1 g, 9.25 mmol) in pyridine and water (10 : 1, 20 mL), selenium dioxide (5.132 g, 46.25 mmol) was added and the mixture was heated to reflux for 12 h. After a few minutes, the mixture turns brown-red, whereas selenium gradually

precipitated as a green solid. The reaction mixture was allowed to cool to room temperature then filtered. The precipitate was then washed with ammonium hydroxide (10 mL). The combined filtrates were evaporated to dryness in vacuum to get a crude brownish solid of pyrazine-2,6-dicarboxylic acid ammonium salt. The crude solid was then suspended in methanol and an excess of thionyl chloride (3.38 mL, 46.25 mmol) was added drop wise at 0 °C, then the mixture was refluxed for 3h. After this time, the reaction mixture was cooled to room temperature, neutralized with saturated Na₂CO₃ aqueous solution and extracted with chloroform (3 × 50 mL). The combined organic phases were dried with anhydrous Na₂SO₄ and the solvent was removed to get a crude residue, which was then subjected to SiO₂ column chromatography with hexane/EtOAc (1 : 1) as the eluent to get the titled compound as a white solid (1.184 g, 65.25%). ¹H-NMR (400 MHz, CDCl₃) δ = 9.47(s), 4.06(s). ¹³C-NMR (100 MHz, CDCl₃) δ = 163.9, 148.8, 148.7, 142.9, 53.5. ESI-HRMS: m/z 197.0585 [M + H]⁺ (calc. m/z 197.0557).

N,N'-Dibenzylpyrazine-2,6-dicarboxamide(H₂L).

Dimethylpyrazine-2,6-dicarboxylate (1 g, 5.1 mmol) was refluxed with 1.23 mL (11.22 mmol) of benzylamine in 10 mL methanol for 2 h. Then, the mixture was cooled and the solvent was evaporated to get a crude residue, which was subjected to short pad column chromatography with EtOAc as the eluent to get the titled compound as a pale yellow solid (1.69 g, 96%). ¹H-NMR (400 MHz, (CD₃)₂SO) δ = 9.88 (1H, t, J = 6.0 Hz), 9.40 (1H, s), 7.34 (4H, d, J = 4.1 Hz), 7.30–7.21 (1H, m), 4.63 (2H, d, J = 6.2 Hz). ¹³C NMR (101 MHz, (CD₃)₂SO) δ = 162.3, 145.7, 142.4, 138.9, 128.4, 127.0, 126.9, 42.1. ESI-HRMS: m/z 347.1551 [M + H]⁺ (calc. 347.1503). Elemental analysis (%) calcd for C₂₀H₁₈N₄O₂: C 69.35, H 5.24, N 16.17, found: C 69.05, H 5.31, N 16.25.

[CoL₂]Bu₄N(2).

Synthesized by following the procedure used for pyridine derivative.²⁸ To H₂L (1 g, 2.9 mmol) in ethanol(10 mL), Bu₄N(OAc) (0.379 g, 1.45 mmol) and Co(OAc)₂·(H₂O)₄(0.361 g, 1.45 mmol) were added and then refluxed under a nitrogen atmosphere to obtain a clear pale pink solution. To this was added a solution of sodium ethoxide in dry ethanol, generated by the careful addition of NaH (0.26 g of 60% dispersion in oil, 6.38 mmol) to dry ethanol, resulting in a colour change to deep purple. Upon exposure to air, the solution turned to green after which it was refluxed further for one hour. The solvent was evaporated and the residue was subjected to SiO₂ column chromatography with dcm/acetone(3 : 1) as the eluent to obtain the titled compound as a dark brown solid (1.177 g, 82%). The ¹H-NMR (400 MHz, CD₃CN)δ = 8.70 (s, 1H), 7.02–6.99 (m, 3H), 6.39 (d, J = 7.0 Hz, 2H), 3.30 (s, 2H), 3.09–3.04 (m, 2H), 1.63–1.55 (m, 2H), 1.37–1.31 (m, 2H), 0.96 (t, J = 7.3 Hz, 3H). ¹³C NMR (101 MHz, CD₃CN)δ = 168.1, 152.6, 143.8, 141.5, 128.6, 127.5, 126.9, 59.35, 59.3, 59.3, 47.3, 32.6, 31.6, 30.5, 30.4, 30.3, 30.0, 24.3, 23.4, 20.3, 20.3, 14.3, 13.7. ESI-HRMS (–ve mode) m/z M[–] = 747.1870 (calc. 747.1873). Elemental analysis (%) calcd for C₅₆H₆₈CoN₉O₄: C 67.93, H 6.92, N 12.73; found: C 67.85, H 6.99, N 12.85. The brown coloured crystals suitable for X-ray studies were grown by slow evaporation from acetonitrile.

[CoL₂]Ag·(H₂O) (3).

To [CoL₂]Bu₄N (0.20 g, 0.2 mmol) in 5 mL of acetonitrile added to a round bottom flask, AgNO₃ (0.034 g, 0.2 mmol) was added and sonicated for few minutes. This resulted in a turbid solution. It was stirred for two more hours. Then, the volume of the solvent was reduced to about 1 mL and the precipitate that formed was filtered. For growing single crystals for X-ray studies, 5 mg of this solid was taken and dissolved in 1 mL of acetonitrile

with a few drops of methanol and kept for slow evaporation. Brown coloured crystals good enough for X-ray studies appeared within a few days. Elemental analysis (%) calcd for $C_{40}H_{32}AgCoN_8O_4$: C 56.16, H 3.77, N 13.10; found: C 56.06, H 3.81, N 12.92. $[CoL_2]Ag_3(NO_3)_2(EtOH)$ (**4**). A similar procedure as for complex **5** was followed, with 2 equivalent of $AgNO_3$. Elemental analysis (%) calcd for $C_{42}H_{32}Ag_3CoN_{10}O_{10}$: C 40.19, H 2.7, N 11.72; found: C 40.32, H 2.65, N 11.55. $[CoL_2]Ag(CH_3CN)(H_2O) \cdot 4H_2O$ (**5**). To $[CoL_2]Bu_4N$ (0.020 g, 0.02 mmol) in 1 mL of acetonitrile added in a vial, $AgClO_4$ (0.009 g, 0.04 mmol) was added, sonicated for few minutes and kept for slow evaporation. Brown coloured crystals appeared within few days were suitable for X-ray analysis. Elemental analysis (%) calcd for $C_{40}H_{32}AgCoN_8O_4$: C 56.16, H 3.77, N 13.10; found: C 56.21, H 3.95, N 13.31.

4.6. References

1. Harriman, A.; Ziessel, R., *Coord. Chem. Rev.* **1998**, *171*, 331.
2. Schelter, E. J.; Prosvirin, A. V.; Dunbar, K. R., *J. Am. Chem. Soc.* **2004**, *126*, 15004.
3. Vreshch, V. D.; Lysenko, A. B.; Chernega, A. N.; Howard, J. A. K.; Krautscheid, H.; Sieler, J.; Domasevitch, K. V., *Dalton Trans.* **2004**, 2899.
4. Cho, S.-H.; Ma, B.; Nguyen, S. T.; Hupp, J. T.; Albrecht-Schmitt, T. E., *Chem. Commun.* **2006**, 2563.
5. Cooke, M. W.; Hanan, G. S., *Chem. Soc. Rev.* **2007**, *36*, 1466.
6. Engelhardt, L. P.; Muryn, C. A.; Pritchard, R. G.; Timco, G. A.; Tuna, F.; Winpenny, R. E. P., *Angew. Chem. Int. Ed.* **2008**, *47*, 924.
7. Koshevoy, I. O.; Lin, Y.-C.; Chen, Y.-C.; Karttunen, A. J.; Haukka, M.; Chou, P.-T.; Tunik, S. P.; Pakkanen, T. A., *Chem. Commun.* **2010**, *46*, 1440.
8. Sun, D.; Wang, D.-F.; Zhang, N.; Huang, R.-B.; Zheng, L.-S., *Cryst. Growth Des.* **2010**, *10*, 5031.

9. Sun, D.; Zhang, L.; Lu, H.; Feng, S.; Sun, D., *Dalton Trans.* **2013**,42, 3528.
10. Kumar, G.; Gupta, R., *Chem. Soc. Rev.* **2013**,42, 9403.
11. Srivastava, S.; Gupta, R., *CrystEngComm* **2016**,18, 9185.
12. Fenton, H.; Tidmarsh, I. S.; Ward, M. D., *Dalton Trans.* **2010**,39, 3805.
13. Sun, D.; Wang, D.-F.; Han, X.-G.; Zhang, N.; Huang, R.-B.; Zheng, L.-S., *Chem. Commun.* **2011**,47, 746.
14. Sun, D.; Zhang, L.; Yan, Z.; Sun, D., *Chem. Asian J.* **2012**,7, 1558.
15. Kumar, P.; Gupta, R., *Dalton Trans.* **2016**,45, 18769.
16. Mishra, A.; Ali, A.; Upreti, S.; Gupta, R., *Inorg Chem* **2008**,47, 154.
17. Mishra, A.; Ali, A.; Upreti, S.; Whittingham, M. S.; Gupta, R., *Inorg Chem* **2009**,48, 5234.
18. Kumar, G.; Singh, A. P.; Gupta, R., *Eur. J. Inorg. Chem.* **2010**,2010, 5103.
19. Singh, A. P.; Gupta, R., *Eur. J. Inorg. Chem.* **2010**,2010, 4546.
20. Singh, A. P.; Ali, A.; Gupta, R., *Dalton Trans.* **2010**,39, 8135.
21. Singh, A. P.; Kumar, G.; Gupta, R., *Dalton Trans.* **2011**,40, 12454.
22. Klingele, J.; Boas, J. F.; Pilbrow, J. R.; Moubaraki, B.; Murray, K. S.; Berry, K. J.; Hunter, K. A.; Jameson, G. B.; Boyd, P. D. W.; Brooker, S., *Dalton Trans.* **2007**, 633.
23. Hausmann, J.; Brooker, S., *Chem. Commun.* **2004**, 1530.
24. Hellyer, R. M.; Larsen, D. S.; Brooker, S., *Eur. J. Inorg. Chem.* **2009**,2009, 1162.
25. Hausmann, J.; Jameson, G. B.; Brooker, S., *Chem. Commun.* **2003**, 2992.
26. Balogh, L.; Swanson, D. R.; Tomalia, D. A.; Hagnauer, G. L.; McManus, A. T., *Nano Lett.* **2001**,1, 18.
27. Kascatan-Nebioglu, A.; Panzner, M. J.; Tessier, C. A.; Cannon, C. L.; Youngs, W. J., *Coord. Chem. Rev.* **2007**,251, 884.

28. Leigh, D. A.; Lusby, P. J.; McBurney, R. T.; Morelli, A.; Slawin, A. M. Z.; Thomson, A. R.; Walker, D. B., *J. Am. Chem. Soc.* **2009**,*131*, 3762.
29. Batten, S. R.; Robson, R., *Angew. Chem. Int. Ed.* **1998**,*37*, 1460.
30. Purohit, C. S.; Verma, S., *J. Am. Chem. Soc.* **2006**,*128*, 400.
31. Xu, F.-B.; Weng, L.-H.; Sun, L.-J.; Zhang, Z.-Z.; Zhou, Z.-F., *Organometallics* **2000**,*19*, 2658.
32. Carvajal, M. A.; Novoa, J. J.; Alvarez, S., *J. Am. Chem. Soc.* **2004**,*126*, 1465.
33. Holloway, C. E.; Melnik, M.; Nevin, W. A.; Liu, W., *J. Coord. Chem.* **1995**,*35*, 85.
34. Lindeman, S. V.; Rathore, R.; Kochi, J. K., *Inorg Chem* **2000**,*39*, 5707.
35. Deng, Z.-P.; Li, M.-S.; Zhu, Z.-B.; Huo, L.-H.; Zhao, H.; Gao, S., *Organometallics* **2011**,*30*, 1961.
36. Sun, D.; Zhang, N.; Xu, Q.-J.; Huang, R.-B.; Zheng, L.-S., *J. Organomet. Chem.* **2010**,*695*, 1598.
37. Li, Y.-H.; Sun, D.; Hao, H.-J.; Zhao, Y.; Huang, R.-B.; Zheng, L.-S., *Dalton Trans.* **2012**,*41*, 2289.
38. Symmetry transformations #2: $x + 1, y - 1, z$.
39. Zhao, L.; Wong, W.-Y.; Mak, T. C. W., *Chem. Eur. J.* **2006**,*12*, 4865.
40. Li, B.; Zang, S.-Q.; Li, H.-Y.; Wu, Y.-J.; Mak, T. C. W., *J. Organomet. Chem.* **2012**,*708–709*, 112.
41. Li, H.; Han, Y.-F.; Lin, Y.-J.; Guo, Z.-W.; Jin, G.-X., *J. Am. Chem. Soc.* **2014**,*136*, 2982.
42. Zhang, C. Y.; Tour, J. M., *J. Am. Chem. Soc.* **1999**,*121*, 8783.

4.7. Spectral data

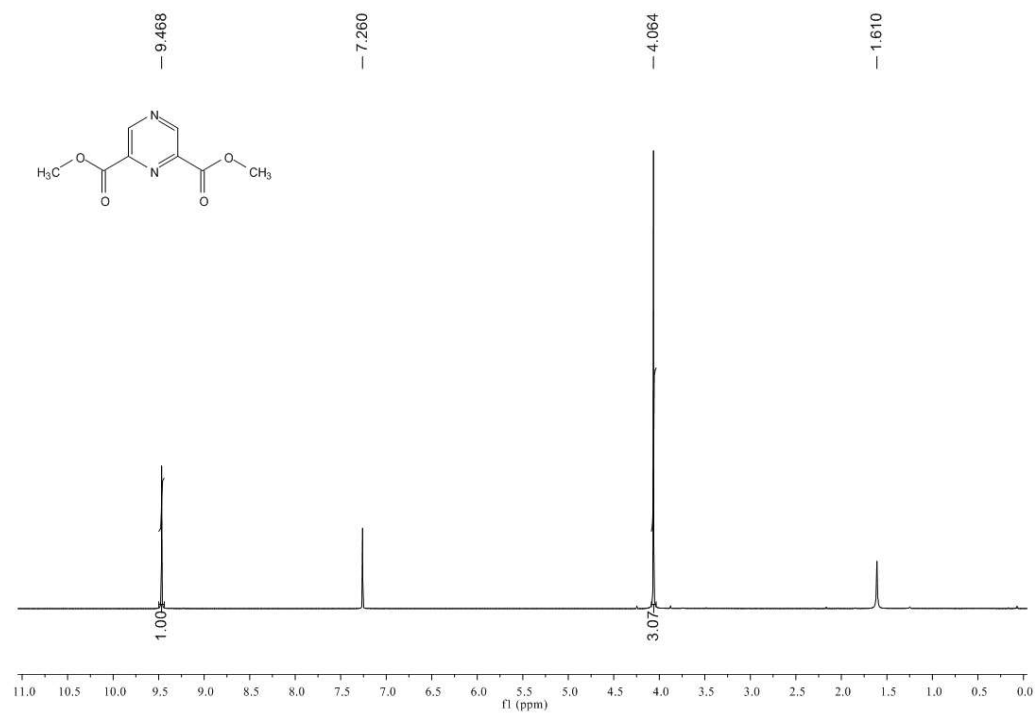


Figure 4.22. ¹H NMR of Dimethyl pyrazine-2,6-dicarboxylate

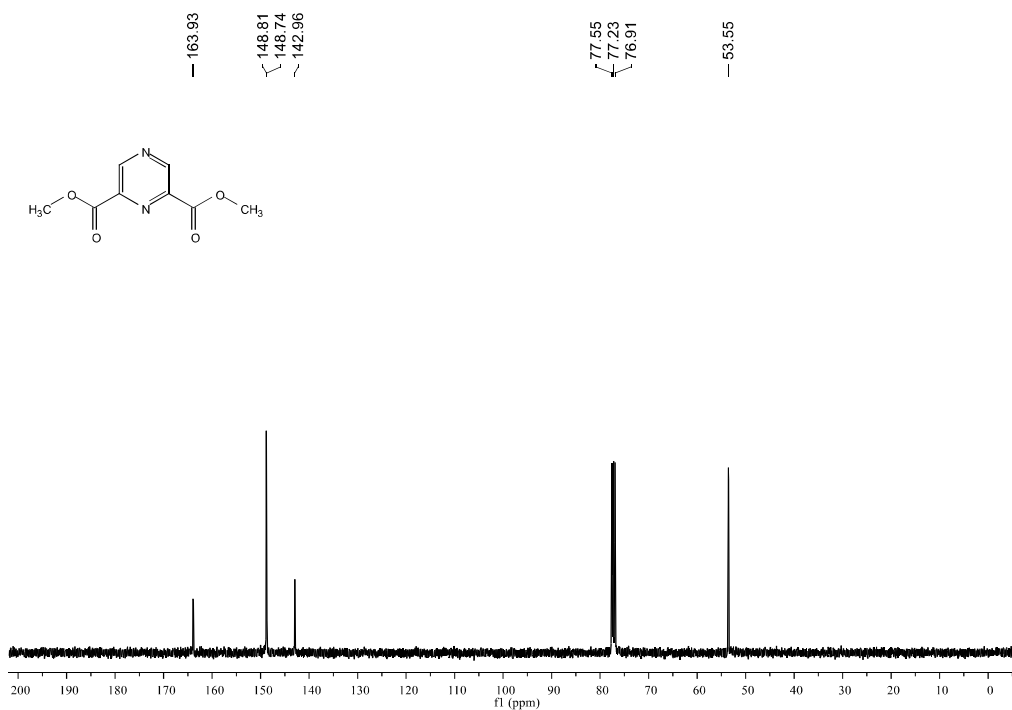


Figure 4.23. ¹³C NMR of Dimethyl pyrazine-2,6-dicarboxylate

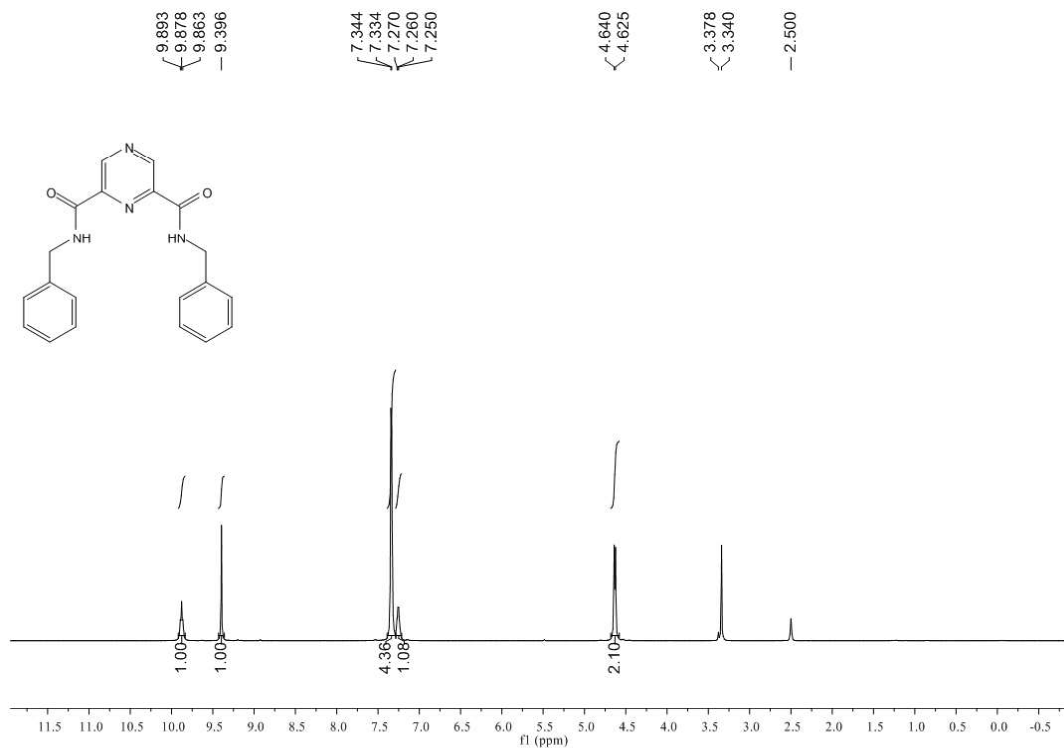


Figure 4.24. ¹H NMR of Compound 1

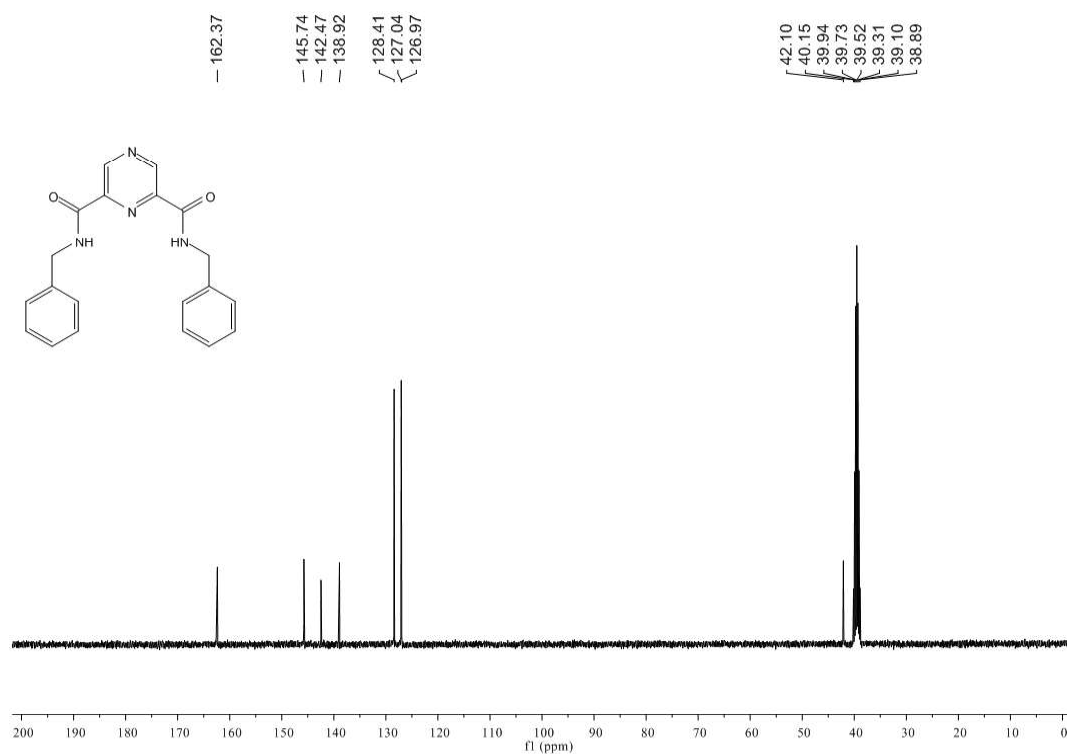


Figure 4.25. ¹³C NMR of Compound 1

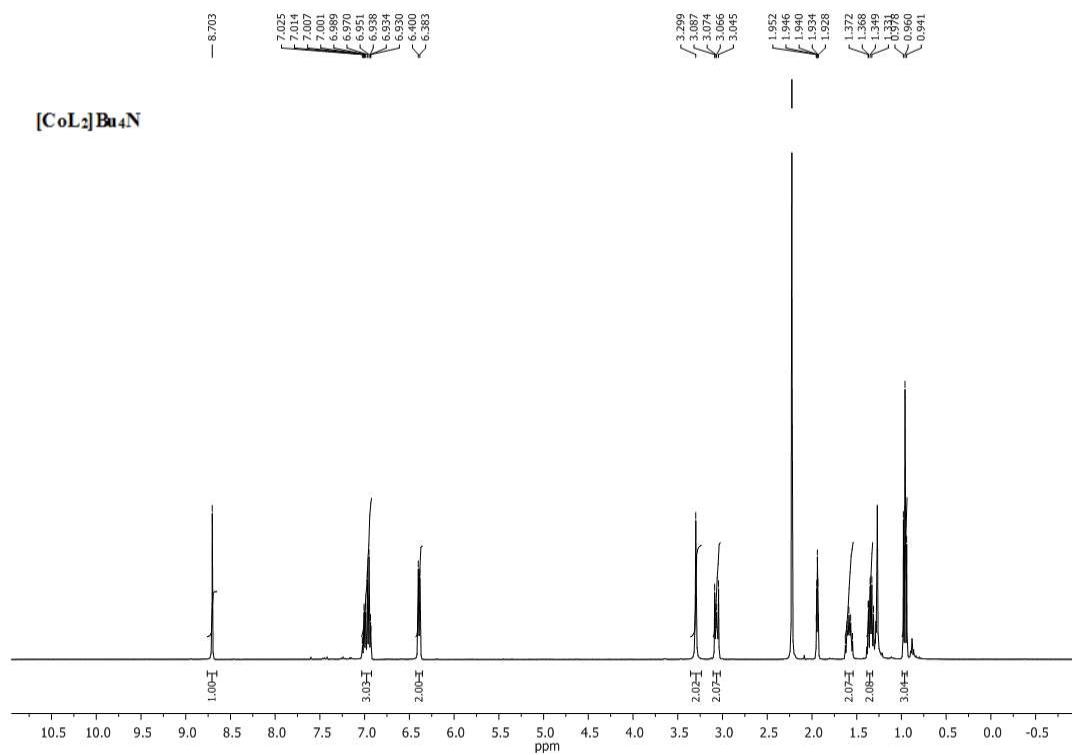


Figure 4.26. ¹H NMR of [CoL₂]Bu₄N

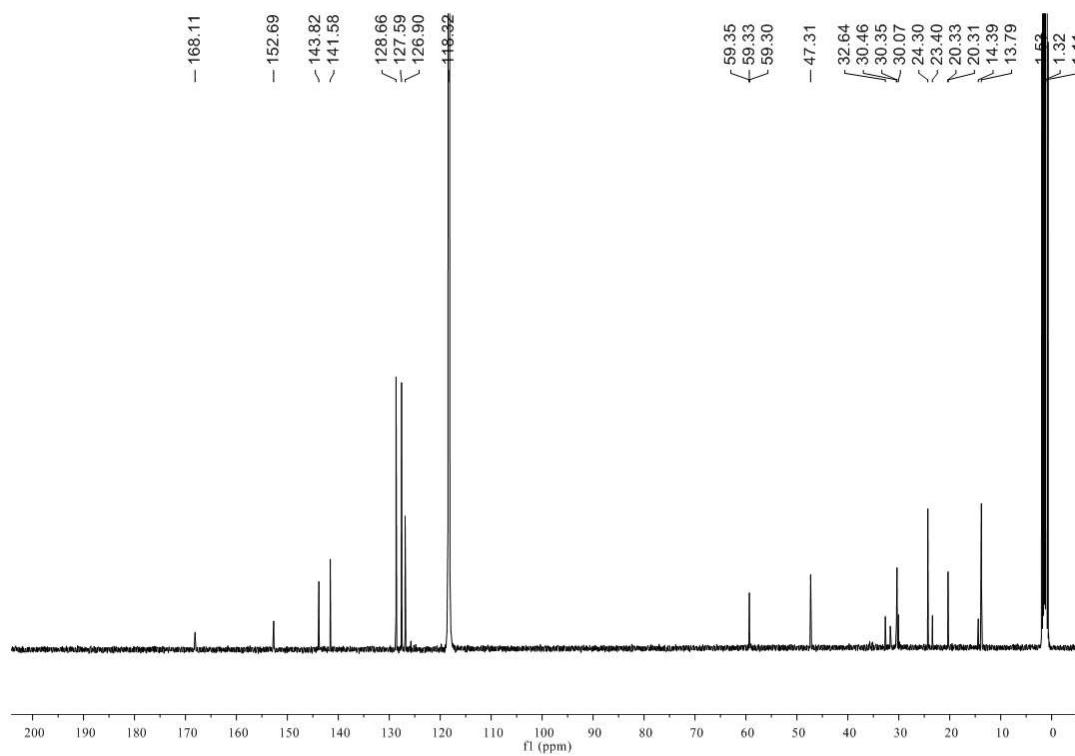


Figure 4.27. ¹³C NMR of [CoL₂]Bu₄N

Mass Spectra

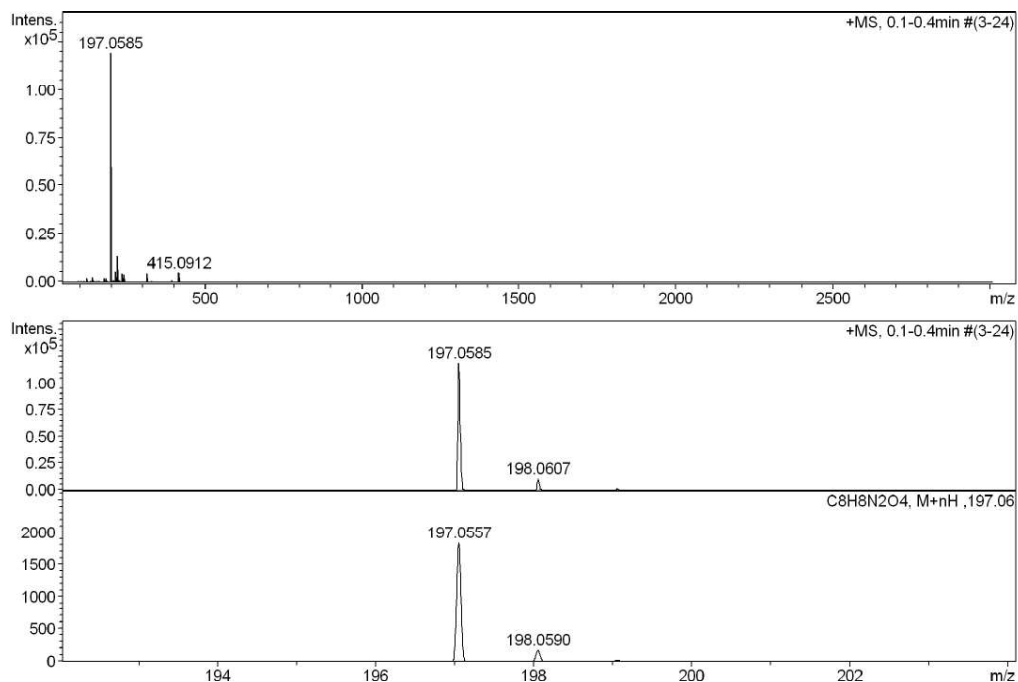


Figure 4.28. ESI-MS spectrum of Dimethyl pyrazine-2,6-dicarboxylate

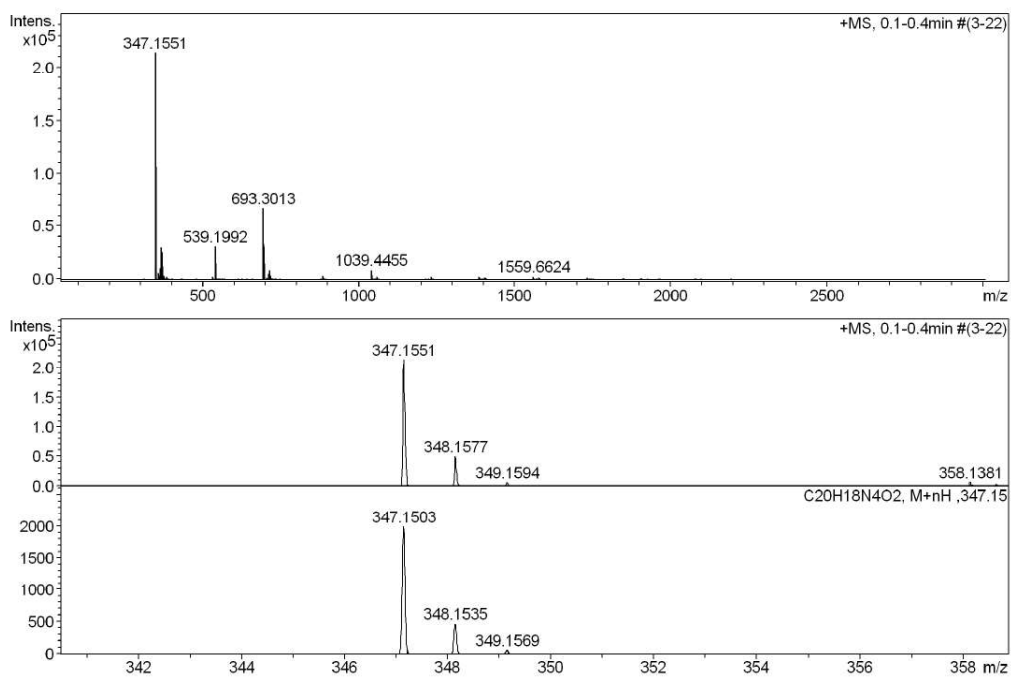


Figure 4.29. ESI-MS spectrum of compound 1

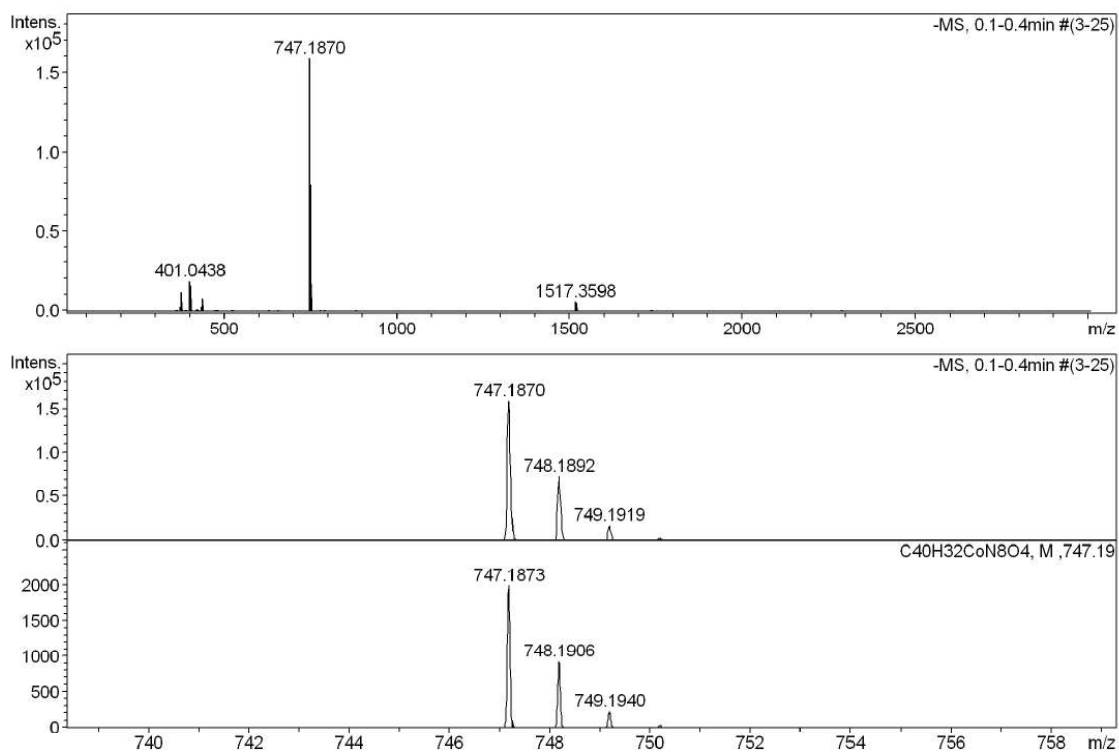


Figure 4.30. ESI-MS spectrum of $[\text{CoL}_2]\text{Bu}_4\text{N}$

4.8. Crystal Data

Table 4.1. Summary of crystal data

Compound	2	3	4	5
Empirical formula	$C_{14}H_{17}Co_{0.25}N_{2.2}O_8$	$C_{40}H_{34}AgCoN_8O_5$	$C_{42}H_{37}Ag_3CoN_{10}O_{11}$	$C_{42}H_{45}AgCoN_9O_9$
Formula weight	247.53	873.55	1240.36	986.67
Temperature	296(2) K	296(2) K	296(2) K	296(2) K
Wavelength	0.71073 Å	0.71073 Å	0.71073 Å	0.71073 Å
Crystal system	Tetragonal	Monoclinic	Triclinic	Triclinic
Space group	I-4	P2(1)/n	P-1	P-1
a (Å)	11.527(4)	12.288(3)	10.2257(2)	11.595(5)
b (Å)	11.527(4)	16.136(4)	12.3002(2)	13.528(5)
c (Å)	19.263(14)	18.416(5)	19.2829(3)	13.555(5)
α (deg)	90	90	77.1530(10)	88.726(5)
β (deg)	90	98.103(10)	77.7610(10)	83.438(5)
γ (deg)	90	90	72.0520(10)	77.730(5)
Volume (Å ³)	2559.5(5)	3615(2)	2222.51(7)	2064.0(14)
Z	8	4	2	2
Density (calculated) mg/mm ³	1.285	1.605	1.853	1.588
Absorption coefficient mm ⁻¹	0.391	1.059	1.741	0.945
F(000)	1052	1776	1230	1012
θ max	27.11°	27.14°	27.89°	25.71°
Reflections collected	16546	44063	32308	20010
Independent reflections	2840	7995	10611	7689
Goodness of fit	1.028	1.030	1.044	1.092
Final R indices [I>2σ(I)]	R1 = 0.0524, wR2 = 0.1433	R1 = 0.0375, wR2 = 0.0874	R1 = 0.0557, wR2 = 0.1432	R1 = 0.0808, wR2 = 0.2241
R indices (all data)	R1 = 0.0683, wR2 = 0.1604	R1 = 0.0616, wR2 = 0.1007	R1 = 0.0877, wR2 = 0.1662	R1 = 0.1047, wR2 = 0.2440
CCDC numbers	1421277	1421396	1421276	1421278

Table 4.2. Bond lengths and Bond angles of [CoL₂]Bu₄N, 3

Bond lengths		Bond angles	
C(1)-N(2)	1.354(5)	N(2)-C(1)-C(2)	121.1(4)
C(2)-N(1)	1.330(4)	N(1)-C(2)-C(3)	112.5(3)
C(2)-C(3)	1.515(6)	N(3)-C(3)-C(2)	110.0(3)
C(3)-O(1)	1.233(4)	N(3)-C(4)-C(5)	113.9(3)
C(5)-C(6)	1.377(7)	N(1)#5-Co(1)-N(3)#6	81.21(8)
C(5)-C(10)	1.390(7)	N(1)-Co(1)-N(3)#6	98.79(8)
C(6)-C(7)	1.381(7)	N(1)#5-Co(1)-N(3)#5	81.21(8)
C(7)-C(8)	1.343(13)	N(3)#6-Co(1)-N(3)#5	162.43(16)
C(8)-C(9)	1.415(14)	N(1)-Co(1)-N(3)	81.21(8)
C(9)-C(10)	1.404(9)	N(3)#5-Co(1)-N(3)	91.34(2)
C(11)-C(12)	1.485(8)	N(3)#6-Co(1)-N(3)#1	91.34(2)
C(11)-N(4)	1.518(5)	N(3)#5-Co(1)-N(3)#1	91.34(2)
C(12)-C(13)	1.461(9)	C(1)-C(2)-C(3)	128.2(4)
C(13)-C(14)	1.343(10)	C(6)-C(5)-C(10)	119.7(4)
N(1)-C(2)#1	1.330(4)	C(8)-C(7)-C(6)	121.7(7)
N(3)-Co(1)	1.959(3)	C(7)-C(8)-C(9)	118.9(6)
N(4)-C(11)#4	1.518(5)	C(10)-C(9)-C(8)	120.0(7)
Co(1)-N(3)#5	1.959(3)	C(5)-C(10)-C(9)	119.1(7)
C(1)#1-N(2)-C(1)	117.9(5)	C(13)-C(12)-C(11)	114.6(6)
C(11)#2-N(4)-C(11)#3	112.2(5)	C(14)-C(13)-C(12)	129.0(10)
C(11)#2-N(4)-C(11)#4	108.1(2)	C(2)-N(1)-C(2)#1	121.5(4)
C(11)-N(4)-C(11)#4	112.2(5)	C(2)-N(1)-Co(1)	119.3(2)
C(11)#3-N(4)-C(11)#4	108.1(2)	C(2)#1-N(1)-Co(1)	119.3(2)
O(1)-C(3)-N(3)	129.3(4)	C(1)#1-N(2)-C(1)	117.9(5)
O(1)-C(3)-C(2)	120.6(4)	C(3)-N(3)-C(4)	117.3(3)

Symmetry transformations used to generate equivalent atoms:

#1: -x+1,-y,z #2: -y+1/2,x+1/2,-z+1/2 #3: y-1/2,-x+1/2,-z+1/2 #4: -x,-y+1,z

#5: y+1/2,-x+1/2,-z+1/2 #6: -y+1/2,x-1/2,-z+1/2

Table 4.3. Bond lengths and Bond angles of 4

Bond lengths		Bond angles	
C(1)-N(1)	1.336(3)	N(1)-C(1)-C(2)	118.7(3)
C(1)-C(2)	1.379(4)	N(1)-C(1)-C(6)	111.8(2)
C(1)-C(6)	1.503(4)	N(2)-C(2)-C(1)	121.5(3)
C(3)-N(1)	1.334(3)	N(1)-C(3)-C(5)	113.0(2)
C(3)-C(4)	1.382(4)	N(2)-C(4)-C(3)	121.7(3)
C(4)-N(2)	1.337(4)	N(6)-C(5)-C(3)	110.9(2)
C(5)-O(2)	1.249(3)	N(3)-C(7)-C(11)	112.2(2)
C(5)-N(6)	1.327(3)	N(3)-C(7)-C(10)	118.0(3)
C(6)-O(1)	1.237(3)	N(3)-C(8)-C(9)	118.1(3)
C(6)-N(5)	1.335(4)	N(3)-C(8)-C(12)	112.4(2)
C(7)-N(3)	1.331(4)	N(4)-C(9)-C(8)	121.9(3)
C(7)-C(11)	1.487(4)	N(4)-C(10)-C(7)	122.1(3)
C(8)-C(9)	1.387(4)	N(7)-C(11)-C(7)	112.3(2)
C(8)-C(12)	1.500(4)	N(8)-C(12)-C(8)	110.4(3)
C(9)-N(4)	1.338(4)	N(7)-C(14)-C(15)	117.8(2)
C(12)-O(3)	1.236(4)	N(5)-C(28)-C(29)	113.5(2)
C(14)-C(15)	1.504(4)	N(8)-C(35)-C(36)	114.0(3)

C(15)-C(20)	1.371(5)	N(1)-Co(1)-N(3)	175.58(10)
C(15)-C(16)	1.385(5)	N(1)-Co(1)-N(5)	81.39(10)
C(16)-C(17)	1.372(5)	N(3)-Co(1)-N(5)	102.34(10)
C(17)-C(18)	1.342(7)	N(3)-Co(1)-N(8)	81.08(10)
C(18)-C(119)	1.377(7)	N(1)-Co(1)-N(7)	96.22(10)
C(20)-C(119)	1.386(6)	N(5)-Co(1)-N(7)	89.93(10)
C(21)-N(6)	1.459(3)	N(1)-Co(1)-N(6)	81.34(10)
C(21)-C(22)	1.509(4)	N(3)-Co(1)-N(6)	95.03(10)
C(22)-C(23)	1.372(5)	N(7)-Co(1)-N(6)	94.39(10)
C(22)-C(27)	1.391(5)	N(2)#4-Ag(1)-C(32)	112.13(14)
C(23)-C(24)	1.387(5)	N(2)#4-Ag(1)-C(33)	89.16(12)
C(26)-C(27)	1.386(6)	C(9)-C(8)-C(12)	129.5(3)
C(29)-C(30)	1.382(4)	C(16)-C(15)-C(14)	118.9(3)
C(29)-C(34)	1.385(4)	C(17)-C(16)-C(15)	121.4(4)
C(31)-C(32)	1.366(6)	C(18)-C(17)-C(16)	119.3(4)
C(32)-Ag(1)	2.527(4)	C(17)-C(18)-C(119)	121.1(4)
C(33)-Ag(1)	2.658(5)	C(15)-C(20)-C(119)	119.9(4)
C(36)-C(41)	1.375(5)	C(27)-C(22)-C(21)	119.3(3)
C(36)-C(37)	1.383(5)	C(22)-C(23)-C(24)	120.9(4)
C(38)-C(39)	1.342(7)	C(25)-C(24)-C(23)	119.9(5)
N(2)-Ag(1)#1	2.381(2)	C(26)-C(27)-C(22)	120.0(4)
N(8)-Co(1)	1.952(2)	C(30)-C(29)-C(34)	118.4(3)
O(2)-Ag(1)#2	2.312(2)	C(30)-C(29)-C(28)	120.4(3)
O(4)-Ag(1)	2.269(2)	C(34)-C(29)-C(28)	121.1(3)
Ag(1)-N(2)#4	2.381(2)	C(32)-C(31)-C(30)	119.9(4)
		C(31)-C(32)-C(33)	120.0(4)
		C(31)-C(32)-Ag(1)	103.2(3)
Bond Angles			
C(36)-C(41)-C(40)	119.9(4)	C(34)-C(33)-Ag(1)	107.3(2)
C(18)-C(119)-C(20)	119.7(4)	C(29)-C(34)-C(33)	119.6(4)
C(1)-N(1)-Co(1)	119.62(19)	C(41)-C(36)-C(37)	119.3(3)
C(4)-N(2)-C(2)	118.1(3)	C(41)-C(36)-C(35)	121.1(3)
C(4)-N(2)-Ag(1)#1	112.83(19)	C(37)-C(36)-C(35)	119.6(3)
C(2)-N(2)-Ag(1)#1	127.22(19)	C(38)-C(37)-C(36)	119.9(4)
C(7)-N(3)-Co(1)	118.35(19)	C(39)-C(38)-C(37)	121.1(4)
C(6)-N(5)-Co(1)	116.49(18)	C(38)-C(39)-C(40)	119.9(4)
C(28)-N(5)-Co(1)	125.69(19)	O(2)-C(5)-N(6)	130.2(3)
C(5)-N(6)-C(21)	117.5(2)	O(2)-C(5)-C(3)	118.9(2)
C(5)-N(6)-Co(1)	115.81(18)	O(1)-C(6)-N(5)	127.9(3)
C(21)-N(6)-Co(1)	126.34(18)	O(1)-C(6)-C(1)	121.4(3)
C(11)-N(7)-C(14)	116.6(2)	O(4)-C(11)-N(7)	127.5(3)
C(11)-N(7)-Co(1)	114.93(19)	O(4)-C(11)-C(7)	120.1(3)
C(14)-N(7)-Co(1)	125.67(18)	O(3)-C(12)-N(8)	129.1(3)
C(12)-N(8)-C(35)	118.0(3)	O(3)-C(12)-C(8)	120.4(3)
C(12)-N(8)-Co(1)	116.69(19)	O(4)-Ag(1)-O(2)#3	106.73(8)
C(35)-N(8)-Co(1)	124.5(2)	O(4)-Ag(1)-N(2)#4	117.74(9)
C(5)-O(2)-Ag(1)#2	144.55(19)	O(2)#3-Ag(1)-N(2)#4	94.14(8)
C(11)-O(4)-Ag(1)	119.96(18)	O(4)-Ag(1)-C(32)	116.88(11)
C(32)-Ag(1)-C(33)	30.58(14)	O(2)#3-Ag(1)-C(32)	105.62(12)

Symmetry transformations used to generate equivalent atoms:

#1: $x-1/2, -y+1/2, z-1/2$ #2: $-x+3/2, y-1/2, -z+3/2$ #3: $-x+3/2, y+1/2, -z+3/2$ #4: $x+1/2, -y+1/2, z+1/2$

N(3)-Co(1)-N(5)	98.12(16)	N(8)-C(6)-C(3)	111.2(4)
N(1)-Co(1)-N(8)	98.49(16)	N(1)-C(7)-C(8)	118.4(4)
N(3)-Co(1)-N(8)	81.05(15)	N(1)-C(7)-C(11)	112.2(4)
N(5)-Co(1)-N(8)	92.36(16)	C(8)-C(7)-C(11)	129.3(4)
N(1)-Co(1)-N(6)	81.57(15)	N(2)-C(8)-C(7)	121.1(5)
N(8)-Co(1)-N(6)	90.97(16)	N(1)-C(9)-C(10)	117.3(4)
N(1)-Co(1)-N(7)	98.97(16)	N(1)-C(9)-C(12)	113.0(4)
N(3)-Co(1)-N(7)	81.50(15)	C(10)-C(9)-C(12)	129.7(4)
N(5)-Co(1)-N(7)	90.87(16)	N(2)-C(10)-C(9)	122.2(4)
O(2)#6-Ag(1)-O(1)	103.53(13)	O(3)-C(11)-N(5)	127.7(4)
O(2)#6-Ag(1)-N(4)#5	132.37(14)	O(3)-C(11)-C(7)	121.0(4)
O(1)-Ag(1)-N(4)#5	87.58(13)	N(5)-C(11)-C(7)	111.3(4)
O(2)#6-Ag(1)-O(8)	102.85(16)	O(4)-C(12)-N(6)	130.0(4)
O(1)-Ag(1)-O(8)	130.77(17)	O(4)-C(12)-C(9)	118.9(4)
N(4)#5-Ag(1)-O(8)	103.84(17)	N(6)-C(12)-C(9)	111.1(4)
O(3)-Ag(2)-O(9)#7	119.73(16)	N(6)-C(27)-C(28)	113.1(4)
C(5)-O(1)-Ag(1)	144.0(3)	C(7)-N(1)-C(9)	122.4(4)
C(11)-O(3)-Ag(2)	131.9(3)	C(7)-N(1)-Co(1)	119.4(3)
C(12)-O(4)-Ag(3)	140.4(3)	C(9)-N(1)-Co(1)	118.2(3)
C(12)-N(6)-C(27)	118.7(4)	C(10)-N(2)-C(8)	118.6(4)
C(12)-N(6)-Co(1)	116.0(3)	C(10)-N(2)-Ag(3)#4	116.6(3)
C(27)-N(6)-Co(1)	125.3(3)	C(8)-N(2)-Ag(3)#4	124.8(3)
C(5)-N(7)-C(20)	118.4(4)	C(1)-N(3)-C(3)	122.2(4)
C(5)-N(7)-Co(1)	115.6(3)	C(1)-N(3)-Co(1)	118.5(3)
C(11)-N(5)-C(13)	117.1(4)	C(3)-N(3)-Co(1)	119.2(3)
C(11)-N(5)-Co(1)	115.7(3)	C(4)-N(4)-C(2)	118.6(4)
C(13)-N(5)-Co(1)	126.6(3)	C(4)-N(4)-Ag(1)#5	126.1(3)
		C(2)-N(4)-Ag(1)#5	115.1(3)

Symmetry transformations used to generate equivalent atoms:

#1: x+1,y,z #2: x+1,y-1,z #3: x,y-1,z #4: -x+1,-y+1,-z+1 #5: -x+1,-y+1,-z

#6: x-1,y,z #7: x,y+1,z #8: x-1,y+1,z

Table 4.5. Bond lengths and Bond angles of 6

Bond lengths		Bond angles	
C(1)-N(1)	1.324(8)	N(1)-C(1)-C(2)	122.0(5)
C(2)-N(2)	1.322(7)	N(2)-C(2)-C(1)	118.0(5)
C(2)-C(9)	1.499(8)	N(2)-C(2)-C(9)	113.0(4)
C(3)-N(2)	1.328(7)	C(1)-C(2)-C(9)	128.7(5)
C(3)-C(4)	1.398(8)	N(2)-C(3)-C(4)	116.6(5)
C(3)-C(10)	1.497(8)	N(2)-C(3)-C(10)	113.0(5)
C(4)-N(1)	1.329(8)	C(4)-C(3)-C(10)	130.3(5)
C(5)-C(11)	1.499(8)	N(3)-C(5)-C(6)	118.2(5)
C(6)-N(4)	1.330(8)	N(3)-C(5)-C(11)	111.7(5)
C(7)-N(3)	1.330(7)	N(4)-C(6)-C(5)	121.9(6)
C(8)-N(4)	1.329(8)	N(3)-C(7)-C(8)	117.6(5)
C(9)-O(1)	1.247(7)	C(8)-C(7)-C(12)	130.0(5)
C(9)-N(7)	1.332(7)	N(4)-C(8)-C(7)	122.6(6)
C(11)-O(4)	1.253(7)	O(1)-C(9)-N(7)	128.0(5)
C(11)-N(8)	1.320(7)	O(1)-C(9)-C(2)	120.8(5)
C(12)-O(3)	1.251(6)	N(7)-C(9)-C(2)	111.1(4)

C(12)-N(6)	1.330(7)	O(2)-C(10)-N(5)	128.1(5)
C(13)-N(6)	1.456(7)	O(2)-C(10)-C(3)	121.0(5)
C(13)-C(17)	1.505(8)	N(5)-C(10)-C(3)	110.9(4)
C(14)-N(8)	1.468(7)	N(8)-C(11)-C(5)	111.9(5)
C(14)-C(23)	1.505(8)	O(3)-C(12)-N(6)	127.6(5)
C(15)-N(5)	1.460(7)	N(6)-C(13)-C(17)	114.4(4)
C(19)-C(20)	1.357(10)	N(5)-C(15)-C(29)	114.5(4)
C(26)-C(27)	1.389(11)	C(22)-C(17)-C(13)	122.0(5)
C(27)-C(28)	1.367(10)	C(19)-C(18)-C(17)	120.4(6)
C(29)-C(30)	1.377(8)	C(20)-C(19)-C(18)	120.1(6)
C(32)-C(33)	1.359(11)	C(20)-C(21)-C(22)	119.9(6)
C(35)-C(40)	1.381(8)	C(24)-C(23)-C(28)	117.7(6)
C(36)-C(37)	1.397(9)	C(24)-C(23)-C(14)	119.6(5)
C(37)-C(38)	1.378(10)	C(25)-C(24)-C(23)	120.9(7)
N(2)-Co	1.849(4)	C(27)-C(28)-C(23)	121.0(7)
N(6)-Co	1.977(4)	C(30)-C(29)-C(34)	118.7(6)
N(7)-Co	1.962(4)	C(30)-C(29)-C(15)	122.1(5)
N(8)-Co	1.963(4)	C(34)-C(29)-C(15)	119.2(5)
N(9)-Ag(2)	2.086(7)	C(31)-C(30)-C(29)	120.7(6)
N(3)-Co-N(2)	178.95(19)	C(33)-C(34)-C(29)	120.2(6)
N(3)-Co-N(7)	97.34(18)	C(36)-C(35)-C(40)	119.5(6)
N(2)-Co-N(7)	81.71(18)	C(36)-C(35)-C(16)	121.9(5)
N(5)-Co-N(7)	163.65(18)	C(40)-C(35)-C(16)	118.5(5)
N(3)-Co-N(8)	81.55(18)	C(35)-C(36)-C(37)	120.2(6)
N(7)-Co-N(8)	91.49(18)	C(38)-C(37)-C(36)	120.2(6)
N(5)-Co-N(6)	90.09(18)	C(39)-C(38)-C(37)	119.1(7)
N(9)-Ag(2)-O(8)	176.2(3)	C(38)-C(39)-C(40)	121.0(7)
C(12)-N(6)-Co	114.7(4)	N(9)-C(42)-C(41)	178.1(7)
C(13)-N(6)-Co	126.2(4)	C(1)-N(1)-C(4)	117.7(5)
C(9)-N(7)-C(16)	116.8(4)	C(2)-N(2)-C(3)	123.0(5)
C(9)-N(7)-Co	115.4(4)	C(2)-N(2)-Co	118.7(4)
C(16)-N(7)-Co	126.5(4)	C(3)-N(2)-Co	118.2(4)
C(11)-N(8)-C(14)	117.7(4)	C(7)-N(3)-C(5)	121.7(5)
C(11)-N(8)-Co	115.7(4)	C(7)-N(3)-Co	119.1(4)
C(14)-N(8)-Co	125.6(4)	C(5)-N(3)-Co	119.2(4)
C(42)-N(9)-Ag(2)	175.5(7)	C(8)-N(4)-C(6)	117.8(5)

Chapter-5

Attempted Synthesis of [3]catenane

5.1. Abstract	233
5.2. Introduction	234
5.3. History of catenanes	234
5.3.1. catenane synthesis by template directed method	236
5.4. Properties and applications	238
5.5. Motivation	239
5.6. Literature reports for the synthesis of [3]catenanes	240
5.7. Our approach to [3]catenanes	243
5.8. Results and discussion	245
5.9. Summary	252
5.10. Experimental section	253
5.11. References	263
5.12. Spectral data	266

5.1. Abstract

A new approach is designed for the synthesis of [3]catenanes by the cleavage of handcuff catenane. A handcuff catenane is composed of bis-macrocycle threaded by single macrocycle. We have synthesised alkyne appended handcuff catenane by the synthesis of bis-rotaxane followed by the cyclisation. Attempts to cleave alkyne bond of handcuff catenane furnishes macrocycle rather than [3]catenane.

5.2 Introduction

Catenanes are the class of Mechanically Interlocked Molecules (MIMs) composed of two or more mechanically interlocked macrocyclic components (Figure 5.1). Other examples of MIMs include rotaxanes, catenanes, molecular knots and molecular borromean rings.¹⁻³ These cannot be separated without breaking the covalent bond of at least one macrocycle. The name catenane is derived from Latin word *catena* meaning “chain”. The nomenclature for these compounds is [n]catenane, where ‘n’ is the number of mechanically interlocked macrocycles.

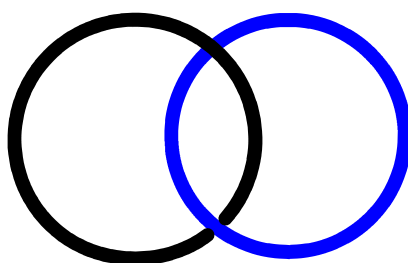


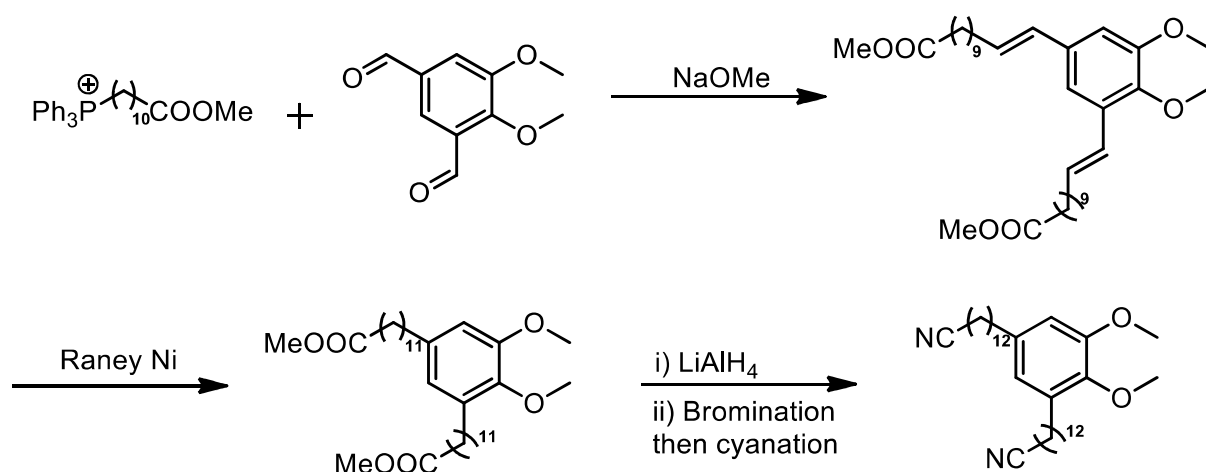
Figure 5.1. *Cartoon representation of [2]catenane*

5.3. History of catenanes

Although pioneering work⁴⁻⁷ has been done on the macrocyclic chemistry in early 1930's, the existence of catenanes which constitutes macrocycles are not known until the appearance of report by H. Frisch *et al.*, in 1953. In that report they proposed that the liquid/waxy nature of polysiloxanes is due to presence of large interlocked macrocycles.⁸ Following this report, Luttringhaus and Cramer made an unsuccessful attempt to synthesise catenane by ring closing an inclusion complex.⁹

The first synthesis of [2]catenane came into reality in 1960 by the seminal publication of Wassermann.¹⁰ The synthetic strategy includes the acyloin condensation of diester in the presence of a deuterated macrocycle. The product isolated was less than 1% yield (0.0001%)

and was characterised by IR spectroscopy. Appearance of the C-D IR stretching frequency in the newly formed product that corresponds to a deuterated macrocycle considered as an evidence for the formation of [2]catenane. Following year Frisch and Wasserman discussed¹⁰ the limitations of the statistical method and proposed directed strategy for the synthesis of interlocked molecules. Schill and Luttringhaus made a first successful attempt at the synthesis of catenane by directed strategy via a covalent bond.¹¹ The decisive step in their strategy is the positioning of alkyl chlorides above and below the macrocycle possessing amine group. Then intramolecular cyclisation followed by cleavage of aryl nitrogen bond cleavage furnished [2]catenane (Figure 5.2). This was the most elegant illustration for the synthesis of catenane that remained for next 20 years. Similarly, this strategy was successfully extended to synthesise [3]catenane but it results in an inseparable mixture of translational isomers.¹² Schill's investigation for alternative synthetic routes was unsuccessful.



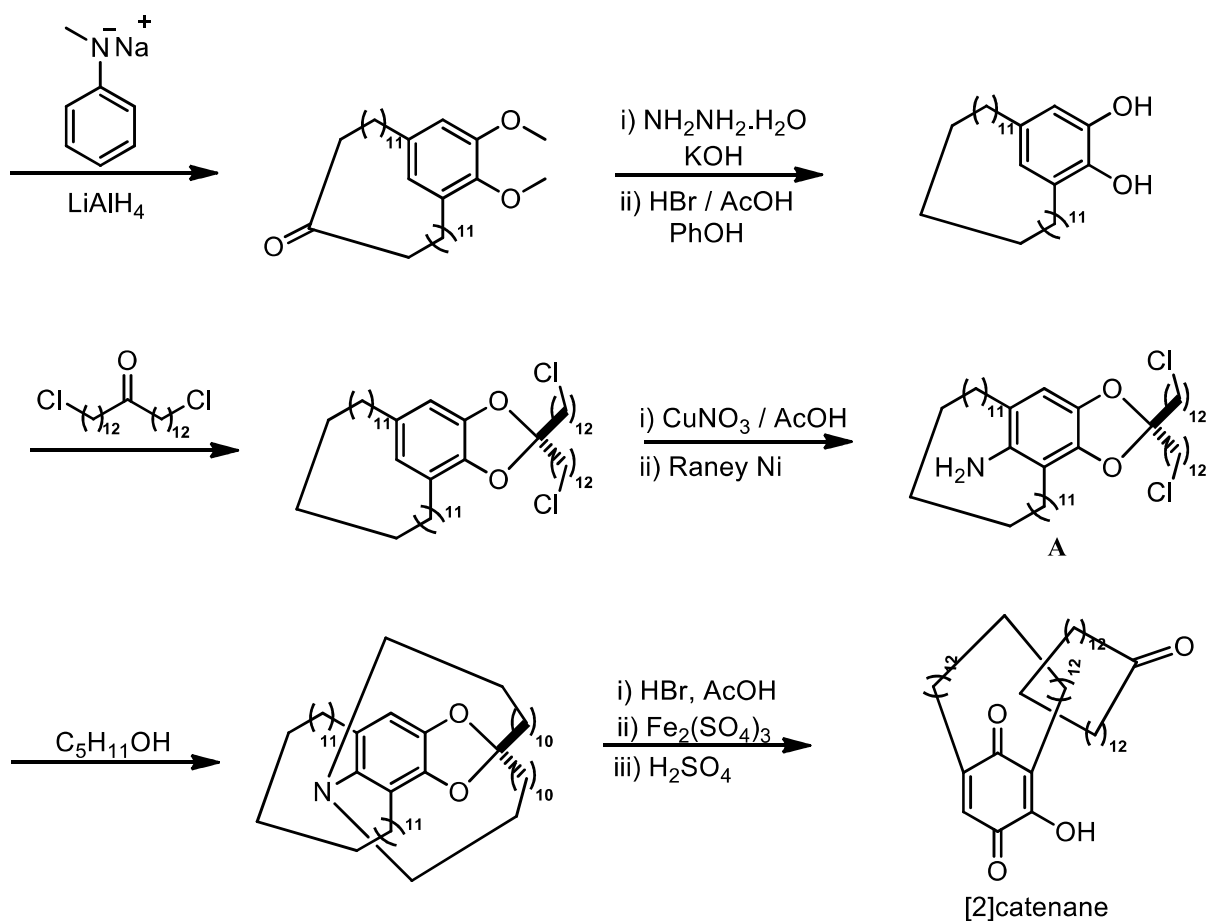


Figure 5.2. Schill's covalent directed [2]catenane

5.3.1 Catenane synthesis by template-directed method

Despite the fact that Schill's directed approach is superior to statistical method, it has its limitations such as lengthy procedures, inseparable isomers, harsh conditions, low yields made catenanes less exploited.¹³ Nearly 20 years later, Sauvage's landmark paper¹⁴ changed the situation and a new era has begun for the synthesis of interlocked molecules. Sauvage addressed this problem by making use of a template. According to D.H.Busch, "A chemical template organizes an assembly of atoms or molecules with respect to one or more geometric loci, in order to achieve a particular linking of atoms."¹⁵⁻¹⁶

Sauvage's group employed metal ion as template that organizes ligand in a particular direction which in turn generates a molecular crossing points. They demonstrated this by using hydroxy-functionalized 2,9-diphenyl-1,10-phenanthroline ligand which forms tetrahedral complex with Cu(I) ion creating a cross point. Williamson ether macrocyclisation of hydroxyl groups of the resultant complex affords metallo[2]catenane in 19% yield. The Cu(I) ion was quantitatively removed using KCN furnishes [2]catenane. (Figure 5.3)

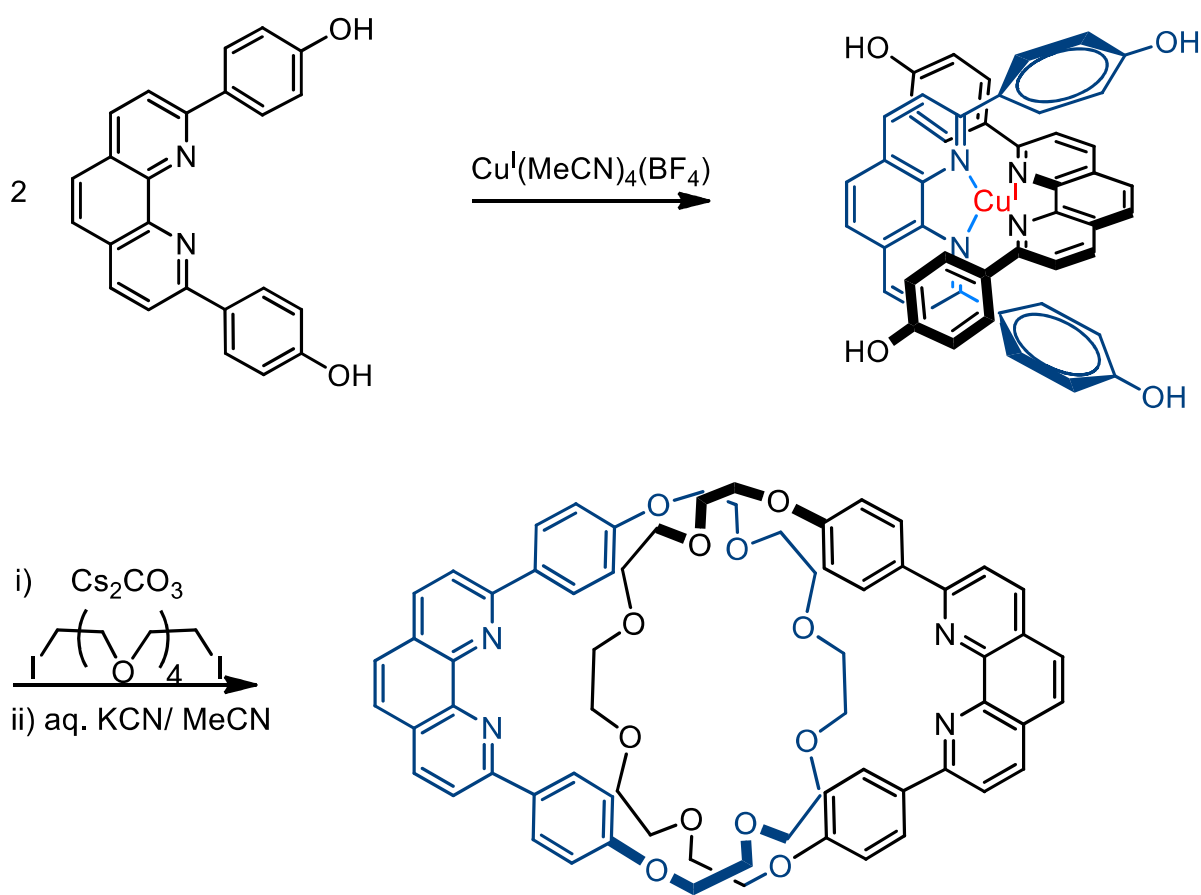


Figure 5.3. Sauvage's first metal template synthesis of [2]catenane.

Further yield was increased up to 42% by using a macrocyclic precursor.¹⁷ Adopting an efficient macrocyclisation reaction such as RCM (Ring-Closing olefin Metathesis) enables catenane synthesis up to 92%.¹⁸

Inspired from this pioneering work, many reports emanated with a variety of metal templates such as octahedral,¹⁹⁻²⁰ square planar,²¹ trigonal bipyramidal²² and linear geometry.²³ Later many other fascinating templates which utilizes non-covalent interactions were developed that includes π - π interactions,²⁴⁻²⁵ hydrogen bonding,²⁶⁻²⁷ halogen bonding,²⁸ anions,²⁹ hydrophobic interaction,³⁰ ion-pairing³¹ etc for the synthesis of mechanically interlocked molecules.

5.4. Properties and applications

Catenanes have a unique feature of independent motion (rotation and translation) of one ring with respect to the other ring³² made them attractive candidates for variety of applications such as molecular machines, molecular switches (Figure 5.4 & 5.5), memory devices, drug delivery, anion receptors (Figure 5.6), switchable surfaces to name a few.

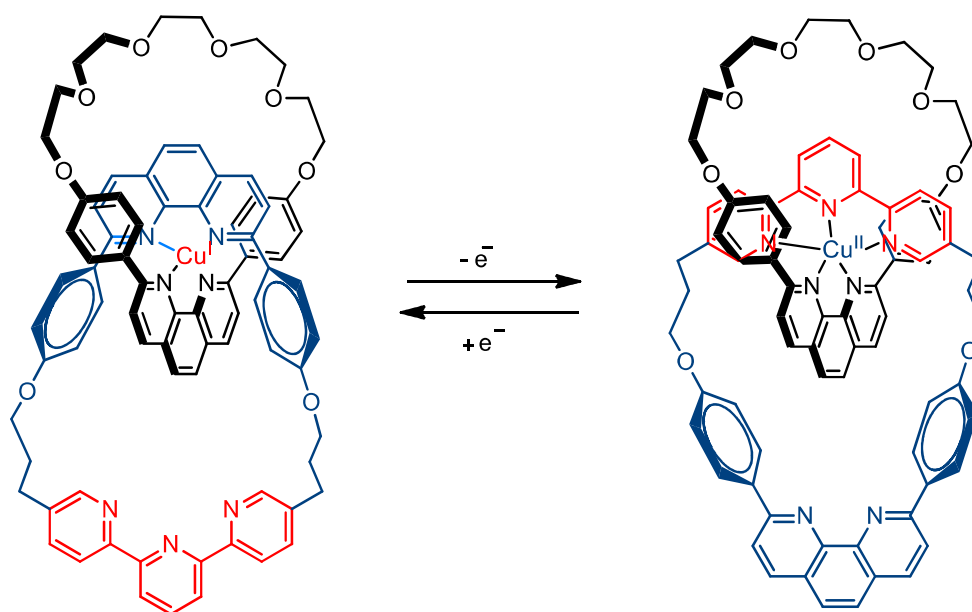


Figure 5.4. *Sauvage's molecular switch controlled by oxidation state of copper ion.*³³

Apart from these, catenanes are anticipated to contribute remarkable properties when incorporated into polymeric material. Polymeric catenanes are expected to have a low

activation energies for viscous flow, large loss moduli and also effects on elasticity, friction, impact resistance etc.³⁴ But unfortunately these properties were not properly studied experimentally because of difficulty in synthesis of [n]catenanes ($n > 2$).

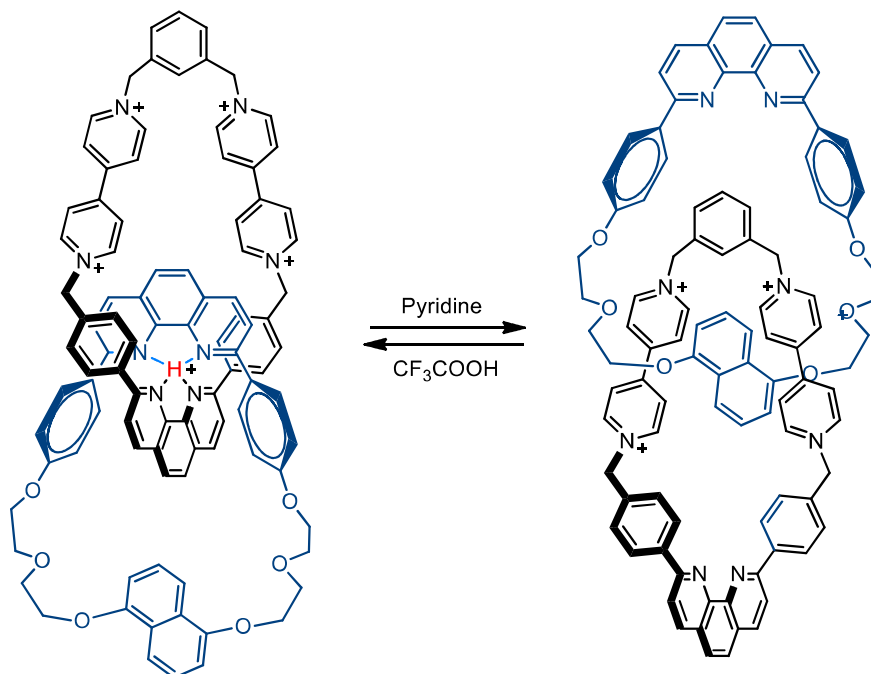


Figure 5.5. Sauvage's pH controlled molecular switch

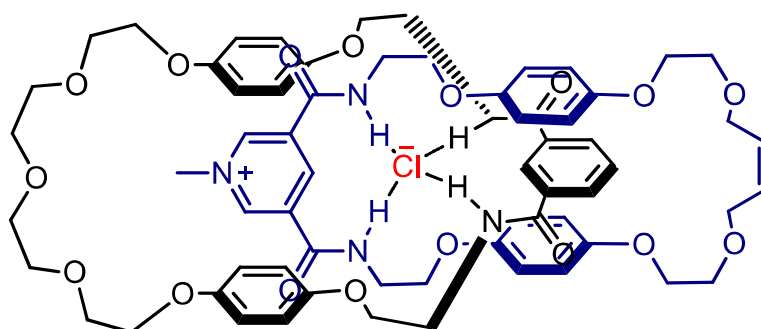


Figure 5.6. Beer's [2]catenane anion receptor.³⁵

5.5. Motivation

Although substantial work has been done for the synthesis of [2]catenanes, challenges still remain for higher order catenane ($n > 2$) synthesis. For instance there are only two

reports known in the literature for [4]- and [5]catenane synthesis.³⁶⁻³⁷ Even for [3]catenane synthesis, less number of reports documented compared to that of [2]catenane. In order to synthesize polycatenanes, novel strategies are highly desirable. Keeping this in mind, we have designed a new approach for synthesis of [3]catenanes.

5.6. Literature reports for the synthesis of [3]catenane

First report of [3]catenane includes Schill's covalent directed approach which is tedious multistep synthesis.¹² Later sauvage extended his metal template method to construct [3]catenane. The synthetic scheme involves the joining of two metallo pseudo[2]rotaxanes by Williamson ether condition followed by demetallation with KCN but it suffers from less yield (2%).³⁸ Enhancement of yield was observed up to 23% when replacing Williamson ether synthesis with oxidative coupling of alkynes for intermolecular cyclisation (Figure 5.7).³⁹

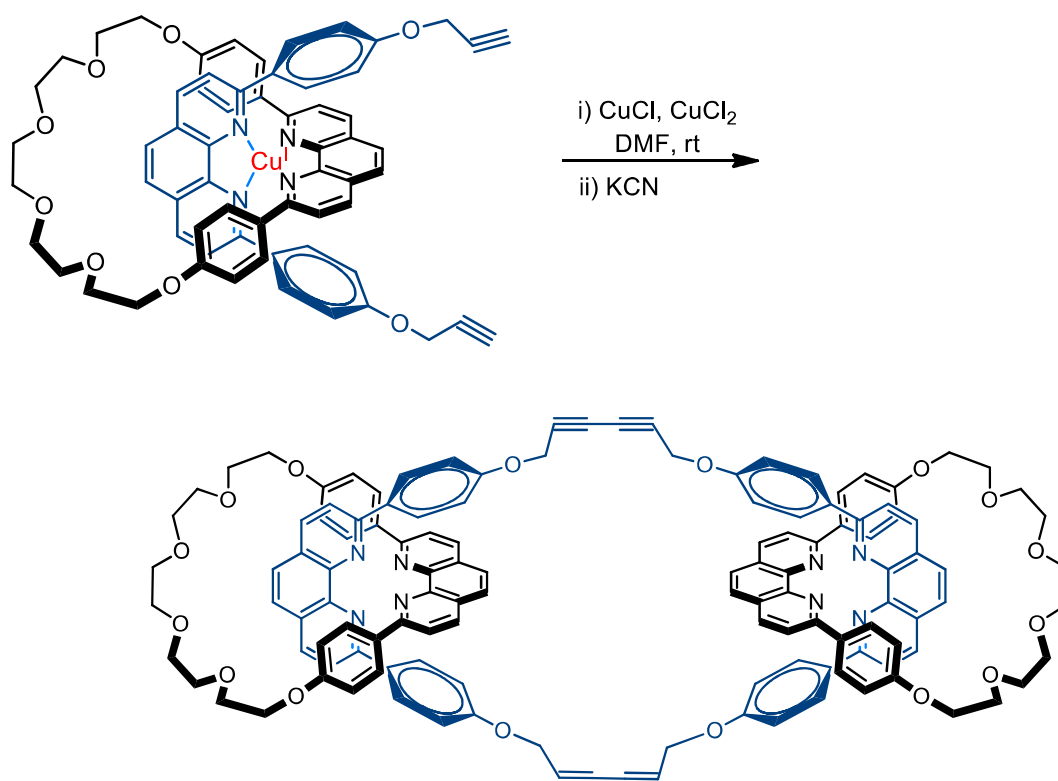


Figure 5.7. Sauvage's metal template synthesis of [3]catenane.

In 1991, Stoddart's group reported the synthesis of [3]catenane by linking electron rich macrocycles with tetracationic cyclophane utilizing π - π interaction.⁴⁰

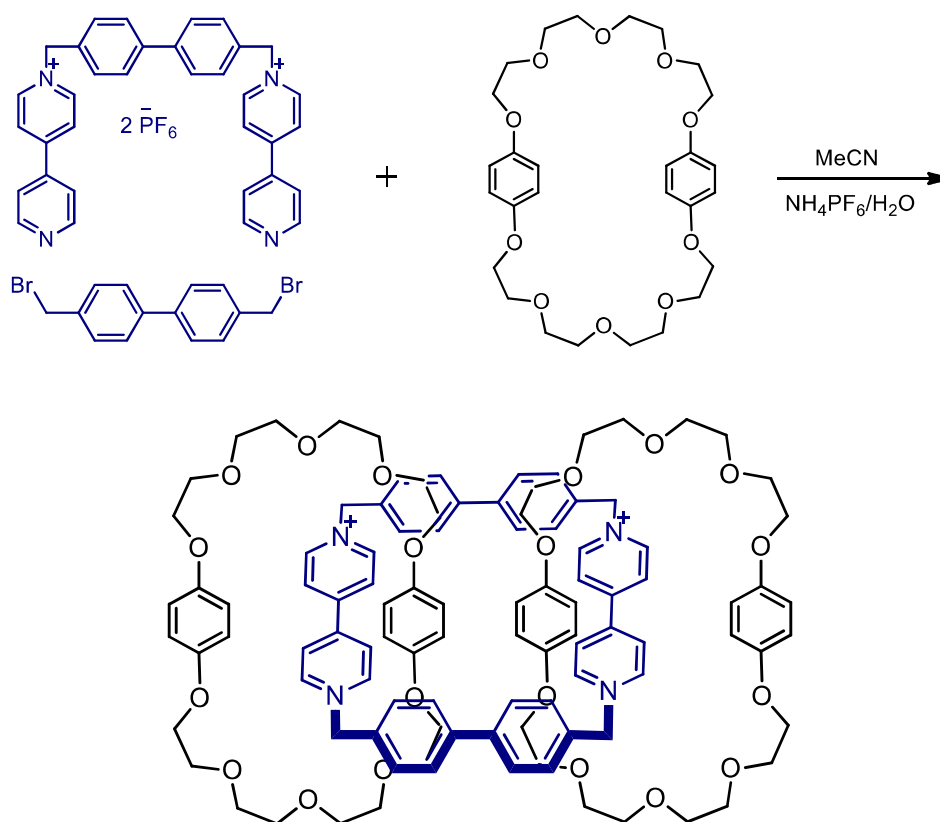
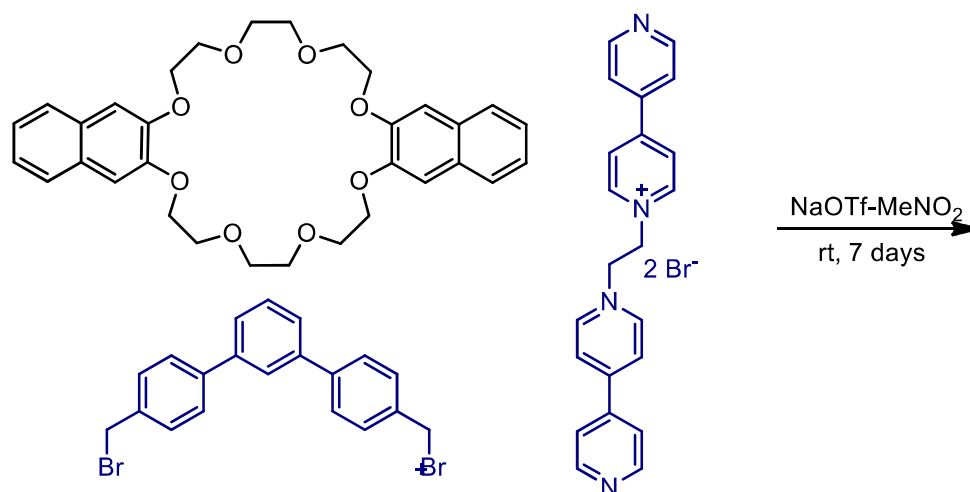


Figure 5.8. Stoddart's donor/acceptor [3]catenane.

Host-guest interaction was also utilized as a template for the assembly of [3]catenane promoted by dipyrindinium ethane, dibenzo-24-crown-8 ether recognition motif (Figure 5.9).⁴¹



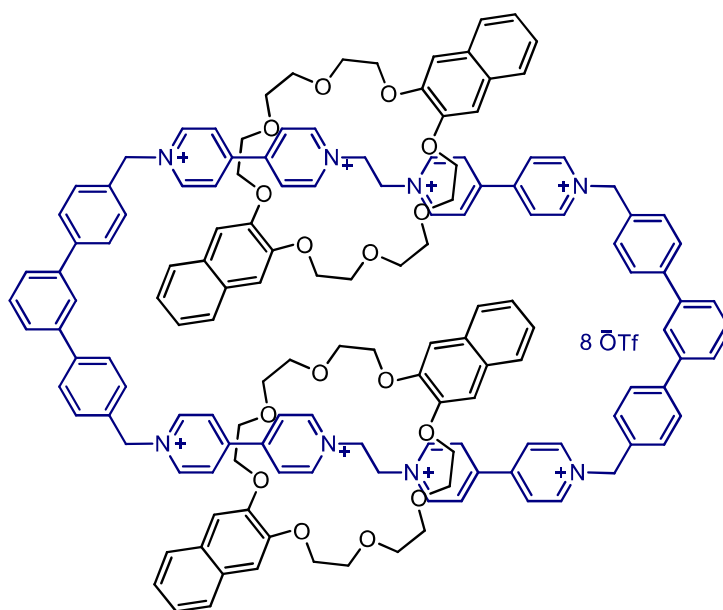


Figure 5.9. Host-guest interactions template [3]catenane.

Fujita *et al* demonstrated the self-assembly of [3]catenane from twelve components during the formation of thermodynamically stable product [2]catenane by DOSY-NMR (Figure 5.10).⁴² Mayer's group proposed and employed double ring closure strategy for the synthesis of [3]catenane (Figure 5.11).⁴³

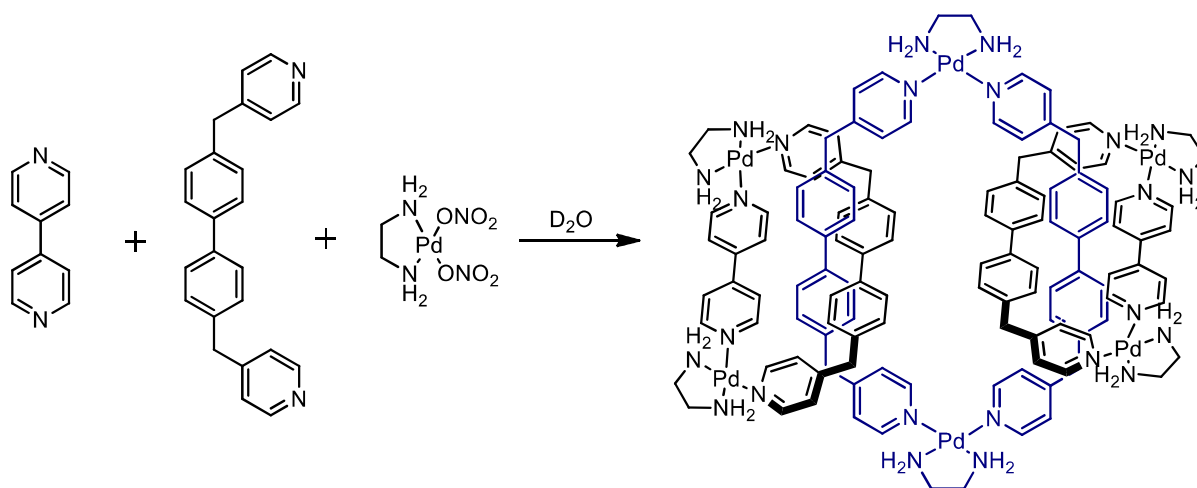


Figure 5.10. Fujita's Pd(II) [3]catenane.

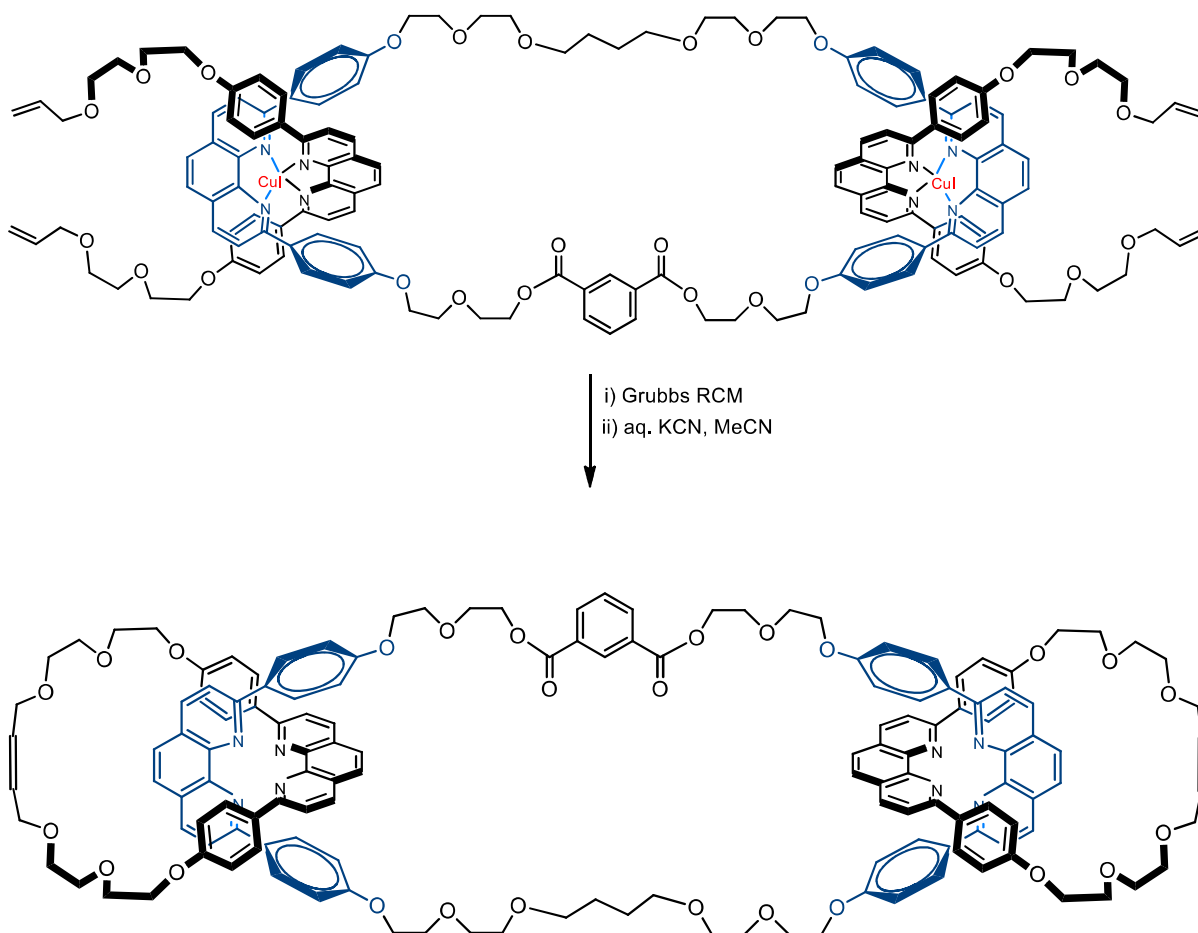


Figure 5.11. Meyer's double ring closing strategy for [3]catenane synthesis.

Apart from these, Leigh's amide based [3]catenane molecular rotor, Sanders dynamic combinatorial synthesis of [3]catenane are also known along with few reports based on above mentioned strategies but with different templates were documented in the literature.⁴⁴⁻⁴⁷

5.7. Our approach to [3]catenane

Previous methods for [3]catenanes synthesis includes (a) dimerisation of pseudo[2]rotaxane. (b) Double ring closure reaction of pseudo[3]rotaxanes. (c) Single ring closure of pseudo[3]rotaxanes. Our approach is to cleave Handcuff catenane to get [3]catenane. (Figure 5.12)

Handcuff catenane is a mechanically interlocked compound composed of bis-macrocycle threaded through the single macrocycle.

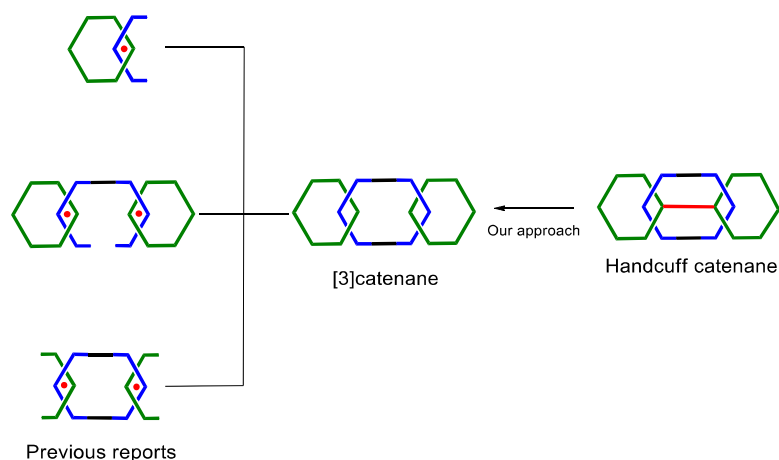


Figure 5.12.Cartoon representation of previous reports and our approach of [3]catenane synthesis.

First of this type was reported by Sauvage *et al* in 2005.⁴⁸ Later Beer's group reported the same by anion template method.⁴⁹

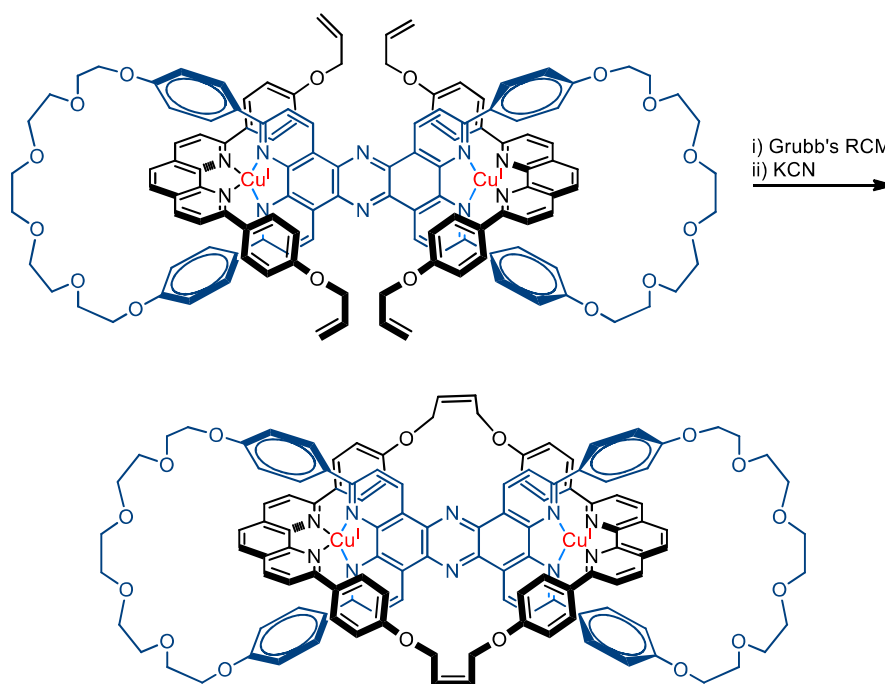


Figure 5.13.Sauvage's Handcuff catenane.

Our design of making handcuff catenane is based on the Stoddart's method of synthesizing rotaxane by clipping approach.⁵⁰ In 2001 Stoddart and co-workers inspired by dibenzo-24-crown-8, dibenzylammonium recognition motif, demonstrated that dibenzylammonium salt having a bulky stoppers templates the macrocyclic imine formation of pyridine-2,6-dicarbaldehyde and tetraethylene glycol bis(2-aminophenyl)ether resulting the [2]rotaxanes. (Figure 5.14)

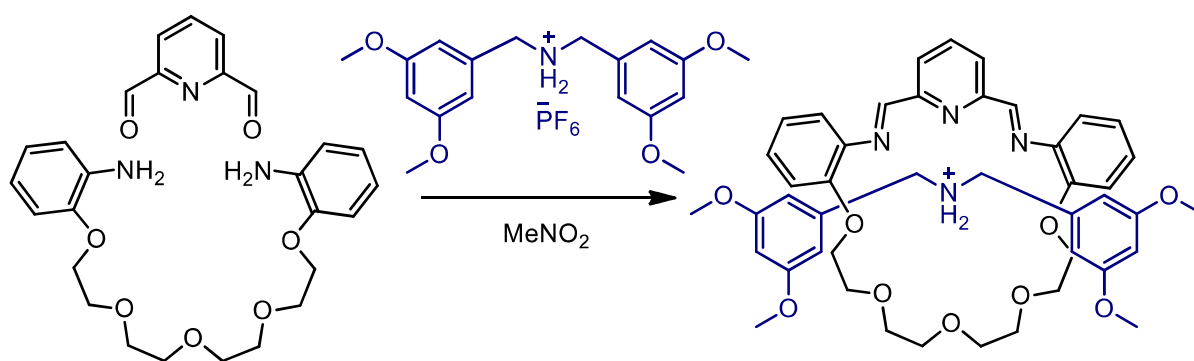


Figure 5.14. Stoddart's [2]rotaxane by clipping.

We adopted this strategy for the synthesis of alkyne connected bis-[2]rotaxane which undergo intramolecular Williamson ether reaction to form alkyne appended Handcuff catenane. The final step is to cleave alkyne bond to get [3]catenane.

5.8. Results and Discussion

The required precursors are 4,4'-(ethyne-1,2-diyl)bis(pyridine-2,6-dicarbaldehyde) (**1**), tetraethyleneglycol bis(2-aminophenyl)ether (**2**) and a template dibenzylammonium salt (**3.HBF₄**) (Figure 5.15). The methoxy and benzyloxy groups of the template serve as bulky stoppers during the rotaxane formation. While the allyl groups provide hydroxy functional groups after the formation of bis-[2]rotaxanes by deallylation. These hydroxy group were connected to get Handcuff catenane.

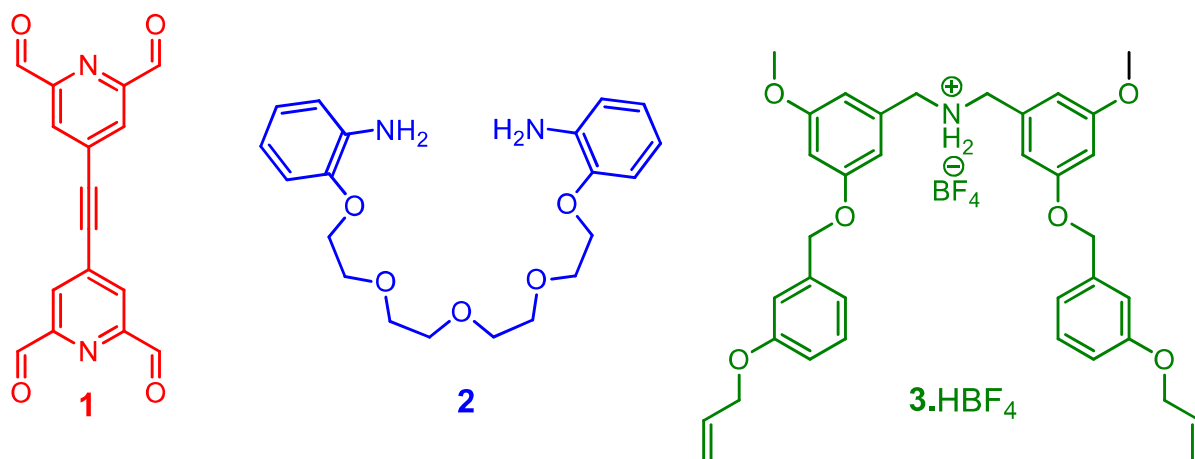
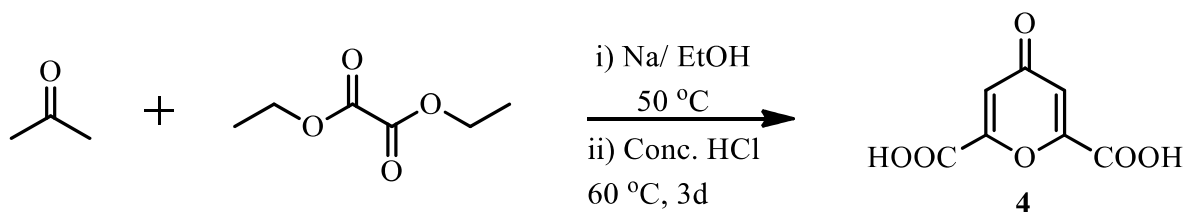
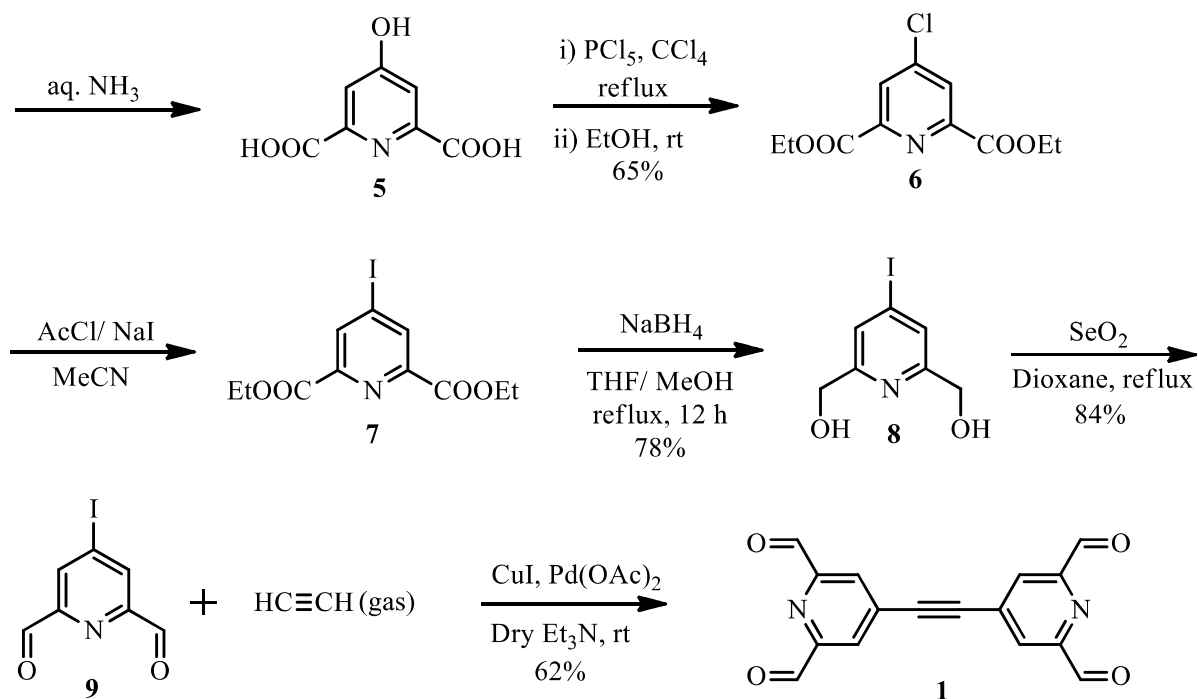


Figure 5.15. *Precursors for the synthesis of handcuff catenane.*

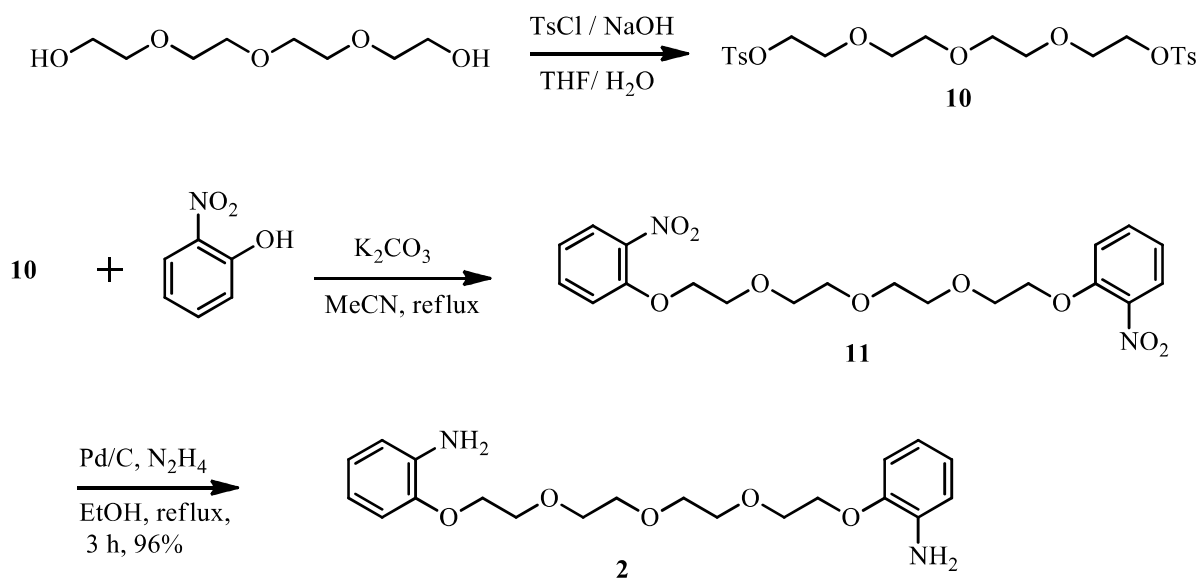
The tetra aldehyde **1** was synthesised from 4-iodopyridine-2,6-dicarbaldehyde (**9**). **9** was prepared by following literature reports starting with a reaction between diethyl oxalate and acetone in the presence of sodium in ethanol as a solvent at 50 °C for 1 h followed by addition of conc.HCl and continued till 3 days stirring at 60 °C to obtain chelidonic acid (**4**) as a yellow precipitate. This was treated with aqueous ammonia followed by acidification with conc.HCl gives chelidamic acid (**5**). The reaction of **5** with PCl_5 in CCl_4 at 80 °C for 5 h followed by the slow addition of ethanol with 1 h reflux yields diethyl 4-chloropyridinedicarboxylate (**6**). The chloro derivative **6** was converted to iodo derivative (**7**) by sonicating with acetyl chloride and sodium iodide in acetonitrile. Reduction of **7** with sodium borohydride gives 4-iodopyridine-2,6-dimethanol (**8**) which in turn oxidation with SeO_2 results 4-iodopyridine-2,6-dicarbaldehyde (**9**). This dialdehyde **9** undergo sonogoshira coupling with acetylene gas to form tetra aldehyde (**1**). (Scheme 5.1)





Scheme 5.1. Synthesis of tetra aldehyde **1**.

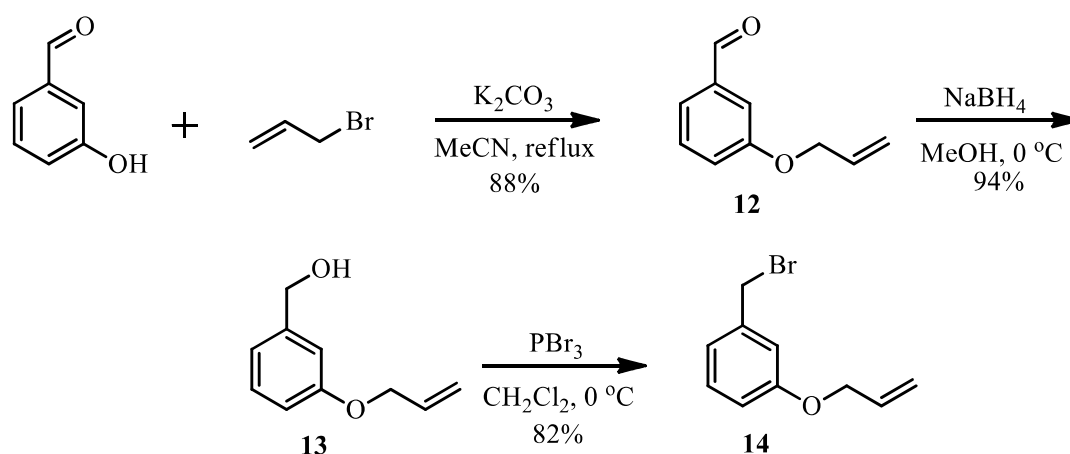
The diamine precursor tetraethylene glycol bis(2-aminophenyl)ether (**2**) was synthesized according to the literature procedure. Tetraethylene glycol was ditosylated with tosylchloride to get **10**. This was refluxed with 2-nitrophenol in the presence of K_2CO_3 in

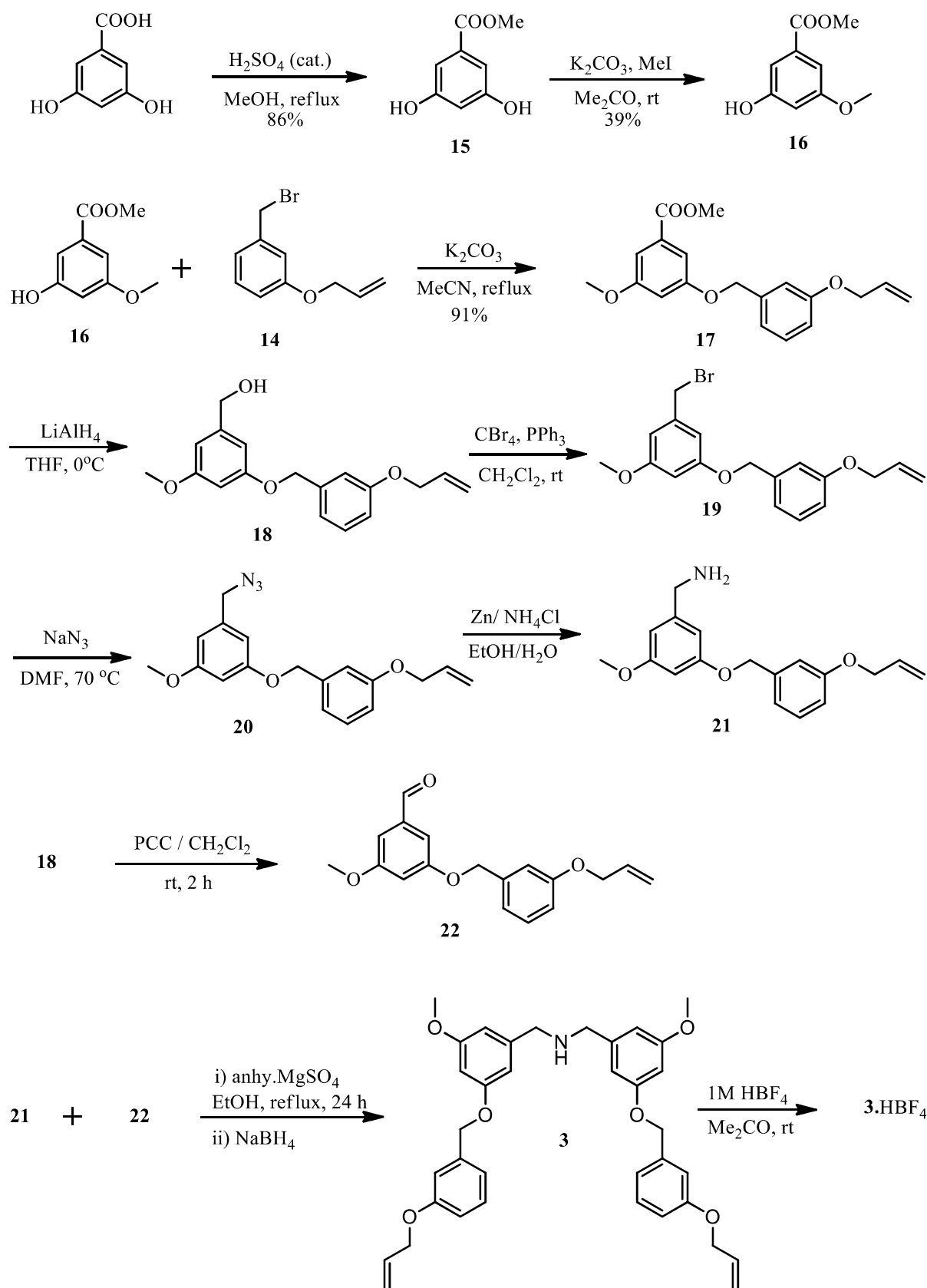


Scheme 5.2. Synthesis of diamine **2**

acetonitrile gives dinitro derivative **11**. Reducing the nitro groups of **11** with Pd/C and hydrazine hydrate in ethanol produces diamine **2**. (Scheme 5.2)

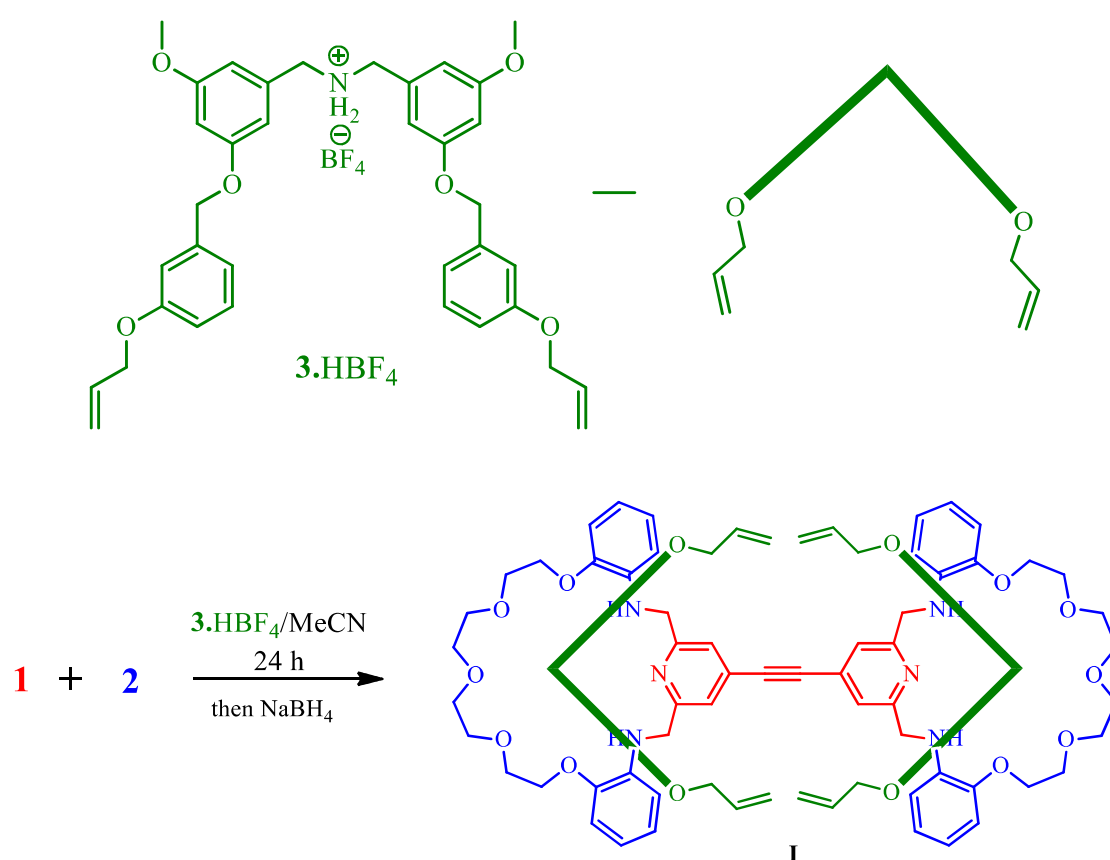
The dibenzyl ammonium salt template **3.HBF₄** was prepared according to the following scheme. Initially 3-allyloxybenzyl bromide (**15**) was synthesised from 3-hydroxybenzaldehyde by performing allylation with allyl bromide, then sodium borohydride reduction followed by bromination with PBr₃. The dibenzyl ammonium core was synthesised from 3,5-dihydroxybenzoic acid. Esterification of this acid gives ester **16** which undergo mono methylation with methyl iodide in acetone to produce **17**. The mono hydroxy derivative **17** was functionalised with **15** in the presence of K₂CO₃ in acetonitrile yields methyl 3-((3-(allyloxy)benzyl)oxy)-5-methoxybenzoate **18**. Lithium aluminium hydride reduction of **17** gives 3-((3-(allyloxy)benzyl)oxy)-5-methoxyphenyl)methanol **19**. Portion of this was converted to corresponding amine **22** by treating **18** with CBr₄/PPh₃ to get bromo derivative **19**, then azidation followed by reduction with Zn/NH₄Cl. Another portion of **19** was converted to corresponding aldehyde **23** using PCC oxidation. Condensation of **22** and **23** in the presence of anhydrous MgSO₄ which was subsequently reduced with sodium borohydride affords dibenzylamine **3**. Finally template **3.HBF₄** was obtained by treating **3** with 1M HBF₄ in acetone. (Scheme 5.3)





Scheme 5.3. Synthetic scheme for template 3.HBF₄

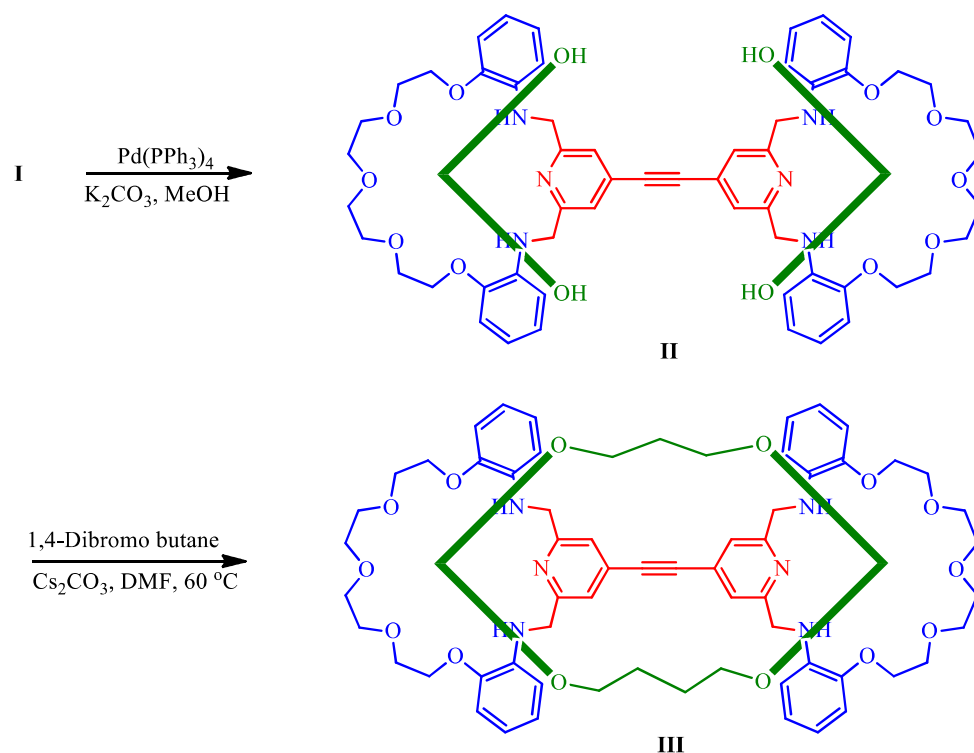
After making necessary precursors we attempted to prepare bis[2]rotaxane by mixing tetra aldehyde **1** with two equivalents of both diamine **2** and ammonium salt **3.HBF₄** in acetonitrile, followed by sodium borohydride reduction results in a sticky liquid product (Scheme 5.4). This was subjected to column chromatography but unable to get pure product. ProtonNMR spectrum of this product was not clean but mass spectral analysis shows the peak at m/z 1073.008 $[M + H]^{+2}$ that corresponds to our desired bis[2]rotaxane **I**. So, we moved to next step without any further purification.



Scheme 5.4. *Synthesis of bis-rotaxane I*

The allyl groups of bis[2]rotaxane **I** were cleaved by $\text{Pd}(\text{PPh}_3)_4$ in the presence of base K_2CO_3 to get corresponding hydroxy bis[2]rotaxane **II**. This tetra hydroxy derivative undergo Williamson ether intramolecular cyclisation with 1,4-dibromo butane in the presence of base Cs_2CO_3 furnishes handcuff catenane **III** (Scheme 5.5). Both the products **II** and **III** were

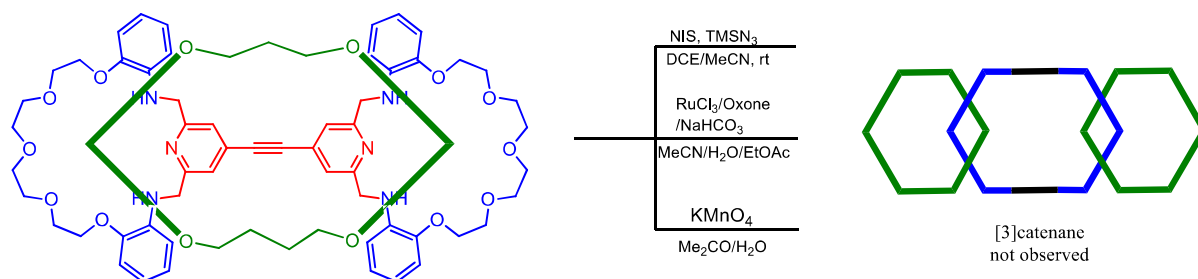
characterized by ESI-mass spectral analysis but their corresponding proton NMRs were complicated due to the difficulty in purification.



Scheme 5.5. *Synthesis of handcuff catenane III.*

After successfully synthesizing Handcuff catenane **III**, we made an effort to cleave alkyne bond by employing known methods in the literature to furnish the target [3]catenane. Initially, we performed a metal free method of alkyne cleavage⁵¹ by treating **III** with N-iodosuccinimide and trimethylsilyl azide in acetonitrile at $80\text{ }^\circ\text{C}$. The mass spectral analysis shows the peak at $1111.5314\text{ }m/z$ corresponds to the macrocycle **IV** (Figure 5.16) that passes through the bis-macrocycle of handcuff catenane. Further, no peak found in the spectrum corresponds to [3]catenane suggests that during the reaction the bis-macrocycle of the handcuff catenane undergoes cleavage elsewhere other than alkyne site resulting the slippage of the macrocycle **IV**. Attempts to cleave with other methods such as KMnO_4 oxidation,

$\text{RuCl}_3/\text{oxone}$ were also unsuccessful resulting a decomposed products which was confirmed by mass analysis (Scheme 5.6).



Scheme 5.6. Attempted methods to cleave alkyne bond of handcuff catenane.

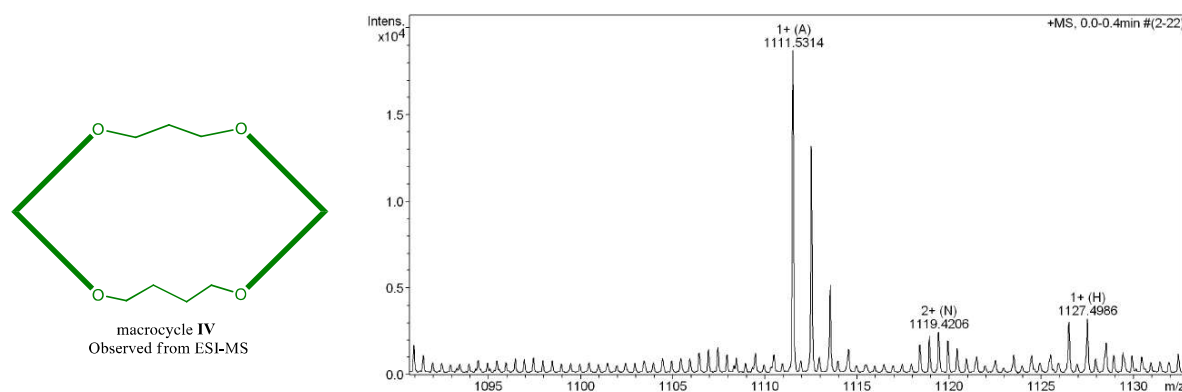


Figure 5.16. ESI-Mass spectrum of macrocycle IV.

5.9 Summary

We have designed a new approach to synthesize [3]catenane by the cleavage of handcuff catenane. For this, we synthesized alkyne appended handcuff catenane by first making bis rotaxanes by clipping approach followed by cyclisation. Attempts to cleave handcuff catenane to furnish [3]catenane was unsuccessful so far.

5.10. Experimental Section

Materials: Reagent grade and metal salts were acquired from Aldrich and used as received. All solvents, were procured from Merck Chemicals, India. Solvents were purified prior to use following standard procedures.

5.10.1. Chelidonic acid (4) :

Sodium pieces (2.35 g, 0.102 mol) were carefully dissolved in 36 mL of dry ethanol. To this, a mixture of dry acetone (3.8 mL, 0.05 mol) and diethyloxalate (14.4 mL, .106 mol) was added slowly over a period of 15 min. During the course of addition, yellow precipitate started to form. This was kept for 1 h at 60 °C. Then 20 mL of 36% HCl and 10 mL of H₂O were sequentially added, and continued stirring for 24 h at 50 °C. One third volume of the reaction mixture was reduced and to this 30 mL of H₂O and 5 mL 36% HCl were added and the stirring was continued at 50 °C. After 72 h, the precipitate formed was filtered, washed with cold water and then with acetone to obtain **4** as off white solid (83%). ¹H NMR (400 MHz, DMSO) δ 7.55 (s, 1H), 6.89 (s, 1H), 2.50 (s, 1H). ¹³C NMR (100 MHz, DMSO) δ 179.67, 160.98, 155.25, 118.22, 40.15, 39.94, 39.73, 39.52, 39.31, 39.10, 38.89.

5.10.2. Chelidamic acid (5):

To the compound **4** (5.0 g, 24.8 mmol), 50 mL 28% aq.NH₃ was added slowly at 0 °C. The reaction mixture was stirred at rt for 48 h, during this time the suspension turns to orange colour. Ammonia solution was evaporated to dryness and dissolved in 50 mL of water. This solution was acidified with 36% HCl and the formed precipitate was filtered, washed with cold water, acetone to get **5** as off white solid (92%). ¹H NMR (400 MHz, DMSO) δ 7.54 (s, 1H). ¹³C NMR (100 MHz, DMSO) δ 168.24, 164.94, 148.61, 114.83, 39.76, 39.64, 39.52, 39.40, 39.28, 39.16.

5.10.3. Diethyl 4-chloropyridine-2,6-dicarboxylate (6):

To the compound **5** (6.45 g, 35.24 mmol) in CCl_4 (40 mL), PCl_5 (20.02 g, 96 mmol) was added and was heated under reflux for 4 h. Then the reaction mixture was cooled down, dry ethanol was slowly added and stirred at rt for 1 h. The reaction mixture was neutralized by adding saturated aq. NaHCO_3 solution and extracted with dichloromethane (3 x 100 mL). The organic extracts were evaporated under reduced pressure and subjected to column chromatography with 10% EtOAc/hexane as eluent to get title compound **6** as white solid (6.44 g, 71%). ^1H NMR (700 MHz, CDCl_3) δ 8.24 (s, 1H), 4.68 – 4.32 (t, 2H), 1.43 (q, 3H). ^{13}C NMR (176 MHz, CDCl_3) δ 163.73, 149.91, 146.70, 128.18, 77.34, 77.16, 76.98, 62.83, 14.28. ESI-MS calculated for $\text{C}_{11}\text{H}_{12}\text{ClNO}_4$ $[\text{M} + \text{Na}]^+$ 280.0347, found 280.0371

5.10.4. Diethyl 4-iodopyridine-2,6-dicarboxylate (7):

To the chloro derivative **6** (5.15 g, 65.61 mmol) dissolved in acetonitrile (150 mL), NaI and acetyl chloride were added. The reaction mixture was sonicated for 5 h and was neutralized with saturated aq. NaHCO_3 solution, extracted with dichloromethane. Solvent was evaporated and was passed through short pad of silica gel with 10% EtOAc/hexane as eluent to get **7** as white solid (18.77 g, 82 %). ^1H NMR (700 MHz, CDCl_3) δ 8.56 (s, 1H), 4.42 (t, 2H), 1.38 (q, 3H). ^{13}C NMR (100 MHz, CDCl_3) δ 163.34, 148.68, 136.86, 106.87, 77.34, 77.16, 76.98, 62.64, 14.19. ESI-MS calculated for $\text{C}_{11}\text{H}_{12}\text{INO}_4$ $[\text{M} + \text{H}]^+$ 349.9884, found 349.9858

5.10.5. 4-iodopyridine-2,6-dimethanol (8):

The diester **7** (2 g, 5.73 mmol) in dry THF (25 mL) was added sodium borohydride (1.088 g, 28.65 mmol). To this, dry methanol (5 mL) was added dropwise at 0 °C under N_2 atmosphere. After allowing to room temperature, the reaction mixture was kept at reflux for

12 h. Then the reaction was quenched with sat.NH₄Cl solution and is extracted repeatedly for two days. The organic extracts were evaporated under reduced pressure to get **8** as white crystalline powder which was used for the next step without any further purification.

5.10.6. 4-iodopyridine-2,6-dicarboxaldehyde (**9**) :

A mixture of diol **8** (2.2 g, 8.3 mmol) and selenium dioxide (2.026 g, 18.26 mmol) in dioxane (20 mL) was heated under reflux for 2 h. The formed metallic selenium was filtered while hot and washed with chloroform. The solvent was evaporated under reduced pressure and the residue was subjected to column chromatography (SiO₂) with 5% EtOAc/hexane as eluent to obtain dialdehyde **9** as white solid (1.82 g, 84%). ¹H NMR (700 MHz, CDCl₃) δ 10.07 (s, 1H), 8.48 (s, 1H). ¹³C NMR (175 MHz, CDCl₃) δ 191.23, 152.96, 134.53, 107.59, 77.34, 77.16, 76.98. ESI-MS calculated for C₇H₄INO₂ [M + H]⁺ 261.9359, found 261.9324.

5.10.7. 4,4'-(ethyne-1,2-diyl)bis(pyridine-2,6-dicarbaldehyde) (**1**) :

To the aryl iodide **9** (2.297 g, 8.803 mmol) in dry triethylamine (150 mL), CuI (0.017 g, 1 mol%) and Pd(OAc)₂ (0.020 g, 1 mol%) were added along with PPh₃ (0.046 g, 20 mol%). The reaction mixture was degassed and purged N₂ gas three times. Then acetylene gas was slowly bubbled through the reaction mixture for 12 h with stirring. After **9** was consumed (by TLC), the solid particles were filtered, washed with dichloromethane. The organic extracts were evaporated and the residue was subjected to short pad column chromatography with 5% MeOH/DCM as eluent to obtain tetra aldehyde **1** as white solid (0.759 g, 59 %). ¹H NMR (700 MHz, DMSO) δ 10.11 (s, 1H), 8.41 (s, 1H). ¹³C NMR (175 MHz, DMSO) δ 192.06, 153.05, 131.98, 127.38, 91.34, 40.02, 39.88, 39.76, 39.64, 39.52, 39.40, 39.28, 39.16.

5.10.8. Tetraethylene glycol ditosylate (**10**) :

Tetraethylene glycol (1.94 g, 10 mmol) was dissolved in THF (10 mL). To this, NaOH (1 g, 25 mmol) dissolved in 2.5 mL water was added and stirred at 0 °C. Tosyl chloride (4.7 g, 25 mmol) in 5 mL THF was added dropwise and continued stirring for 3 h. Water was added to the reaction mixture and extracted with dichloromethane. The organic extracts were evaporated and purified by column chromatography with 20% EtOAc/hexane as eluent to get title compound **10** as colourless oil (3.67 g, 73%). ¹H NMR (700 MHz, CDCl₃) δ 7.79 (d, *J* = 7.3 Hz, 1H), 7.34 (d, *J* = 7.8 Hz, 1H), 4.25 – 4.03 (m, 1H), 3.70 – 3.66 (m, 1H), 3.56 (d, *J* = 3.4 Hz, 2H), 2.44 (s, 1H). ¹³C NMR (175 MHz, CDCl₃) δ 144.98, 133.12, 129.98, 128.12, 77.34, 77.16, 76.98, 70.88, 70.68, 69.40, 68.84, 21.79. ESI-MS calculated for C₂₂H₃₀S₂O₉ [M + Na]⁺525.1223, found 525.1259

5.10.9. 1,11-Bis(2-nitrophenoxy)-3,6,9-trioxaundecane (**11**) :

To the mixture of **11** (1.806 g, 3.594 mmol) and 2-nitrophenol (1 g, 7.188 mmol) in the acetonitrile, K₂CO₃ was added and heated under reflux for 12 h. Then the precipitated potassium tosylate was filtered and the solvent was evaporated to get liquid residue. This was subjected to column chromatography with 40% EtOAc/hexane to obtain title compound as a liquid. (1.419 g, 90.5%) ¹H NMR (700 MHz, CDCl₃) δ 7.76 (d, *J* = 8.1 Hz, 1H), 7.47 (t, *J* = 7.9 Hz, 1H), 7.08 (d, *J* = 8.5 Hz, 1H), 6.98 (t, *J* = 7.8 Hz, 1H), 4.26 – 4.16 (m, 2H), 3.88 – 3.83 (m, 2H), 3.73 – 3.67 (m, 2H), 3.66 – 3.58 (m, 2H). ¹³C NMR (175 MHz, CDCl₃) δ 152.26, 140.05, 134.14, 125.49, 120.56, 115.03, 77.34, 77.16, 76.98, 71.04, 70.60, 69.56, 69.25. ESI-MS calculated for C₂₀H₂₄N₂O₉ [M + Na]⁺459.1374, found 459.1396

5.10.10. 2,2'-((((oxybis(ethane-2,1-diyl))bis(oxy))bis(ethane-2,1-diyl))bis(oxy))dianiline (**2**)

To a mixture of **11** (0.5 g, 1.146 mmol), Pd/C (0.122 g, 0.114 mmol), and EtOH (20 mL) was added NH₂NH₂·H₂O (0.976 mL, 16.044 mmol), and the resulting solution was

heated at reflux condition for 3 h. Then the mixture was filtered and concentrated under vacuum to get colourless liquid compound which was used for the next step without further purification. (0.4 g, 92.7%) ^1H NMR (700 MHz, CDCl_3) δ 6.79 (m, 1H), 6.69 (m, 1H), 4.18 – 4.10 (m, 1H), 3.87 – 3.82 (m, 1H), 3.76 – 3.70 (m, 1H), 3.68 (m, 1H), 3.26 (s, 1H). ^{13}C NMR (175 MHz, CDCl_3) δ 146.49, 137.00, 121.96, 118.52, 115.58, 113.09, 77.34, 77.16, 76.98, 70.84, 70.72, 69.91, 68.43. ESI-MS calculated for $\text{C}_{20}\text{H}_{28}\text{N}_2\text{O}_5$ $[\text{M} + \text{H}]^+$ 377.2071, found 377.2053

5.10.11. 3-(allyloxy)benzaldehyde (12)

To a solution of *m*-hydroxybenzaldehyde (4.00 g, 32.76 mmol) in acetonitrile (30 mL) was added allyl bromide (3.2 mL, 4.36 g, 36.03 mmol) and K_2CO_3 (4.980 g, 36.03 mmol). The mixture was stirred at reflux for 18 h. Then the mixture was filtered through Celite and the filtrate was concentrated. The resultant oil was then purified by column chromatography (10% EtOAc–hexane) to afford **13** as a yellow oil product. (4.52 g, 85%). The NMR data is in good agreement with that of literature.

5.10.12. (3-(allyloxy)phenyl)methanol (13)

To the aldehyde **12** (13.13 g, 80.96 mmol) dissolved in methanol, NaBH_4 (3.691 g, 97.15 mmol) was added portion wise at 0 °C. After 15 min, the reaction was quenched with saturated aq. NH_4Cl solution and extracted with DCM. The organic extracts were evaporated to get **14** as a colourless liquid product (12.44 g, 93.61%). ^1H NMR (700 MHz, CDCl_3) δ 7.28 (dd, 1H), 6.93 (m, 2H), 6.86 (d, 1H), 6.08 (m, 1H), 5.44 (d, 1H), 5.31 (d, 1H), 4.62 (s, 2H), 4.54 (d, 2H). ^{13}C NMR (175 MHz, CDCl_3) δ 158.78, 142.61, 133.28, 129.55, 119.34, 117.69, 113.93, 113.16, 77.34, 77.16, 76.98, 68.78, 64.93. ESI-MS calculated for $\text{C}_{10}\text{H}_{12}\text{O}_2$ $[\text{M} + \text{Na}]^+$ 187.0730, found 187.0717

5.10.13. 1-(allyloxy)-3-(bromomethyl)benzene (14)

PBr₃(7.9 mL, 83.07 mmol) was added dropwise to the alcohol **13** (12.4 g, 75.52 mmol) dissolved in DCM at 0 °C. After 10 min the reaction quenched with ice water and extracted with DCM. The DCM extracts were washed with saturated aq.NaHCO₃ and evaporated to get a liquid residue which was purified by short pad flash column chromatography (SiO₂, 60-120 mesh) with 10% EtOAc/hexane as eluent to get title compound **14** as a colourless liquid. (12.95 g, 76%) ¹H NMR (700 MHz, CDCl₃) δ 7.28 (d, *J* = 8.3 Hz, 1H), 7.00 (d, 1H), 6.98 (s, 1H), 6.88 (d, *J* = 8.3 Hz, 1H), 6.08 (m, 1H), 5.45 (d, 1H), 5.32 (d, 1H), 4.57 (d, 2H), 4.48 (s, 2H). ¹³C NMR (175 MHz, CDCl₃) δ 158.88, 139.25, 133.16, 129.91, 121.57, 117.92, 115.45, 115.01, 77.34, 77.16, 76.98, 68.93, 33.59.

5.10.14. methyl 3,5-dihydroxybenzoate (15)

To 3,5-dihydroxybenzoic acid (10 g, 59.47 mmol) in methanol, 6 drops of conc.H₂SO₄ was added and refluxed for 8 h. After cooling to the room temperature, the solvent was reduced and the residue was extracted with DCM by adding saturated aq.NaHCO₃ solution. The organic solvent was evaporated to get ester **15** as white solid.(8.34 g, 86%) ¹H NMR (700 MHz, DMSO) δ 9.63 (s, 1H), 6.81 (s, 1H), 6.44 (s, 1H), 3.78 (s, 2H). ¹³C NMR (175 MHz, DMSO) δ 166.28, 158.57, 131.32, 107.19, 107.11, 52.02, 39.88, 39.76, 39.64, 39.52, 39.40, 39.28.

5.10.15. methyl 3-hydroxy-5-methoxybenzoate (16)

To the mixture of **15** (9.956 g, 61.024 mmol) and K₂CO₃ (9.272 g, 67.13 mmol) in acetone, methyl iodide (3.8 mL, 61.024 mmol) was added at 0 °C. The resultant suspension was stirred at room temperature for 15 h. Then the solid was filtered through celite and washed with EtOAc several times. The organic solvent was evaporated and subjected to

column chromatography with EtOAc/hexane to get title compound **17** as colourless liquid. (4.33 g, 39%) ^1H NMR (700 MHz, CDCl_3) δ 7.19 (s, 1H), 7.11 (s, 1H), 6.64 (s, 1H), 3.89 (s, 3H), 3.78 (s, 2H). ^{13}C NMR (175 MHz, CDCl_3) δ 167.65, 160.88, 157.25, 109.52, 106.95, 77.34, 77.16, 76.98, 55.64, 52.62.

5.10.16. methyl 3-((3-(allyloxy)benzyl)oxy)-5-methoxybenzoate (**17**)

To the mixture of **16** (3.265 g, 17.923 mmol) and K_2CO_3 (2.971g, 21.507 mmol) in acetonitrile, benzyl bromide **15** (4.477 g, 19.715 mmol) was added and refluxed for 2 h. After cooling down, the precipitate was filtered and the solvent was evaporated to get a liquid residue. This was subjected to column chromatography with 10% EtOAc/hexane to afford **17** as a colourless liquid. (5.7 g, 96.8%) ^1H NMR (700 MHz, CDCl_3) δ 7.32 – 7.27 (m, 1H), 7.20 (s, 1H), 7.01 (s, 1H), 6.88 (d,1H), 6.72 (d, 1H), 6.11 – 6.00 (m, 1H), 5.42 (d,1H), 5.29 (d, 1H), 5.04 (s, 1H), 4.55 (d, 1H), 3.90 (s, 2H), 3.81 (s, 2H). ^{13}C NMR (175 MHz, CDCl_3) δ 166.89, 160.72, 159.80, 158.95, 138.16, 133.27, 132.10, 129.75, 119.94, 117.80, 114.48, 113.87, 108.10, 107.55, 106.61, 77.34, 77.16, 76.98, 70.17, 68.87, 55.65, 52.34. ESI-MS calculated for $\text{C}_{19}\text{H}_{20}\text{O}_5$ $[\text{M} + \text{Na}]^+$ 351.1203, found 351.1161.

5.10.17. (3-((3-(allyloxy)benzyl)oxy)-5-methoxyphenyl)methanol (**18**)

To the LiAlH_4 (0.705 g, 18.543 mmol) suspended in dry THF (5 mL), the ester **17** (5.074 g, 15.453 mmol) dissolved in THF was added drop wise at 0 °C. Then the reaction was stirred at rt for 30 min. After completion of starting ester, the reaction was quenched carefully by the sequential addition of EtOAc, methanol and little water. The formed aluminium salts were filtered through celite to get alcohol **18** as colourless liquid. (4.5 g, 97%) ^1H NMR (400 MHz, CDCl_3) δ 7.32 – 7.26 (m, 1H), 7.00 (m, 2H), 6.91 – 6.86 (m, 1H), 6.55 – 6.52 (m, 1H), 6.50 (m, 1H), 6.48 (m, 1H), 6.06 (m, 1H), 5.42 (d, $J = 17.3, 1.6$ Hz, 1H), 5.29 (d, $J = 10.5, 1.4$ Hz, 1H), 5.02 (s, 2H), 4.55 (m, 2H), 4.27 (s, 2H), 3.79 (s, 2H). ^{13}C NMR (100 MHz,

CDCl₃) δ 161.01, 160.16, 158.90, 143.54, 138.55, 133.27, 129.71, 119.92, 117.82, 114.34, 113.86, 105.41, 105.00, 100.55, 77.34, 77.16, 76.98, 69.96, 68.87, 65.26, 55.42. ESI-MS calculated for C₁₈H₂₀O₄ [M + Na]⁺ 323.1254, found 323.1273.

5.10.18. 1-((3-(allyloxy)benzyl)oxy)-3-(bromomethyl)-5-methoxybenzene (19)

To the mixture of alcohol **18** (3.022 g, 10.07 mmol) and CBr₄ (4.006 g, 12.08 mmol) in DCM, PPh₃ (3.168 g, 12.08 mmol) was added portion wise at 0 °C and then stirred at rt for 3 h. Then the solvent was evaporated and the residue was purified by column chromatography with 10% EtOAc/hexane to obtain bromide **19** as colourless liquid. (2.88 g, 79%) ¹H NMR (700 MHz, CDCl₃) δ 7.30 (m, 1H), 7.01 (s, 2H), 6.89 (m, 1H), 6.63 (s, 1H), 6.57 (m, 1H), 6.48 (s, 1H), 6.12 – 6.02 (m, 1H), 5.43 (d, 1H), 5.30 (d, 1H), 5.02 (s, 2H), 4.56 (m, 2H), 4.42 (s, 2H), 3.79 (s, 3H). ¹³C NMR (175 MHz, CDCl₃) δ 160.97, 160.12, 158.96, 139.86, 138.33, 133.29, 129.76, 119.96, 117.84, 114.47, 113.89, 107.88, 107.44, 101.53, 77.34, 77.16, 76.98, 70.08, 68.90, 55.50, 33.72. ESI-MS calculated for C₁₈H₁₉BrO₃ [M + Na]⁺ 385.0410 and 387.0390, found 385.0355 and 387.0335

5.10.19. 1-((3-(allyloxy)benzyl)oxy)-3-(azidomethyl)-5-methoxybenzene (20)

The mixture of bromide **19** (2 g, 5.506 mmol) and NaN₃ (0.43 g, 6.607 mmol) in dry DMF was stirred at 65 °C for overnight. Then the DMF was evaporated and was extracted with DCM after adding water to it. The extracts were evaporated to get azide **20** as pale yellow liquid. (1.758 g, 98%) ¹³C NMR (175 MHz, CDCl₃) δ 160.97, 160.12, 158.96, 139.86, 138.33, 133.29, 129.76, 119.96, 117.84, 114.47, 113.89, 107.88, 107.44, 101.53, 77.34, 77.16, 76.98, 70.08, 68.90, 55.50, 33.72.

5.10.20. (3-((3-(allyloxy)benzyl)oxy)-5-methoxyphenyl)methanamine (21)

To the azide (0.9 g, 2.766 mmol) dissolved in EtOH / H₂O (3:1, 24 mL), Zn dust (0.272 g, 4.15 mmol) and ammonium chloride (0.37 g, 6.92 mmol) were added. The resultant suspension was refluxed for 15 min. After cooling down, aq.NH₃, EtOAc were added and filtered. The filtrate was evaporated to get a oily residue which was used without any further purification.

5.10.21.0 3-((3-(allyloxy)benzyl)oxy)-5-methoxybenzaldehyde (**22**)

To the alcohol **18** (1.9 g, 6.326 mmol) dissolved in DCM, PCC (1.636 g, 7.591 mmol) was added at 0 °C and stirred at rt for 2 h. After completion of reaction, the insoluble solid was filtered through celite and evaporated at reduced pressure to get oily residue. This was purified by column chromatography with 10% EtOAc/hexane to afford aldehyde **22** as colourless liquid. (1.7 g, 90.07%) ¹H NMR (700 MHz, CDCl₃) δ 9.89 (s, 1H), 7.30 (t, 1H), 7.08 (s, 1H), 7.04 – 6.99 (m, 3H), 6.89 (d, 1H), 6.78 (s, 1H), 6.05 (m, 1H), 5.42 (d, 1H), 5.29 (d, 1H), 5.06 (s, 2H), 4.55 (d, 2H), 3.83 (s, 3H). ¹³C NMR (175 MHz, CDCl₃) δ 192.01, 161.37, 160.42, 159.01, 138.51, 137.95, 133.25, 129.85, 119.94, 117.88, 114.54, 113.94, 108.15, 108.08, 107.51, 77.34, 77.16, 76.98, 70.31, 68.92, 55.77. ESI-MS calculated for C₁₈H₁₈O₄ [M + Na]⁺ 321.1097, found 321.1124.

5.10.22. bis(3-((3-(allyloxy)benzyl)oxy)-5-methoxybenzyl)amine (**3**)

The mixture of aldehyde **22** (1.495 g, 5.01 mmol) and amine **21** (1.5 g, 5.01 mmol) in dry EtOH (25 mL) was refluxed in the presence of anhydrous MgSO₄ for 24 h. After cooling down, NaBH₄ (0.38 g, 10.02 mmol) was added portion wise and again refluxed for 1 h. Then the reaction quenched with saturated aq.NH₄Cl solution and was extracted with DCM. The organic extracts were evaporated and the residue was purified by column chromatography with 40% EtOAc/hexane as eluent to furnish **3** as a colourless liquid. (1.941 g, 66.74%) ¹H NMR (700 MHz, CDCl₃) δ 7.28 (d, *J* = 7.8 Hz, 1H), 7.00 (s, 3H), 6.86 (d, *J* = 8.3 Hz, 1H),

6.61 (s, 1H), 6.54 (s, 1H), 6.44 (s, 1H), 6.05 (m, 2H), 5.41 (d, $J = 17.2$ Hz, 2H), 5.28 (d, $J = 10.5$ Hz, 1H), 5.01 (s, 3H), 4.54 (d, $J = 5.0$ Hz, 3H), 3.77 (s, 4H), 3.75 (s, 2H). ^{13}C NMR (175 MHz, CDCl_3) δ 161.02, 160.17, 158.97, 138.63, 133.34, 129.74, 120.02, 117.85, 114.42, 113.92, 107.10, 106.73, 100.32, 77.34, 77.16, 76.98, 70.05, 68.92, 55.50, 52.81. ESI-MS calculated for $\text{C}_{36}\text{H}_{39}\text{NO}_6$ $[\text{M} + \text{H}]^+$ 582.2850, found 582.2970.

5.10.23. Bis-rotaxane (I)

To the mixture of **2** (0.055 g, 0.146 mmol) and **3**. HBF_4 (0.098 g, 0.146 mmol) (prepared by adding 1 M HBF_4 to **3** in acetone) dissolved in acetonitrile, tetraaldehyde **1** (0.021 g, 0.073 mmol) was added and stirred for 24 h at rt. Then sodium borohydride (0.014 g, 0.0365 mmol) was added and stirred further for 1 h. Then the reaction quenched with saturated aq. NH_4Cl solution and was extracted with DCM to get a sticky liquid. This was subjected to column chromatography with 2% aq. NH_3 /5% MeOH/ CHCl_3 to afford pale yellow viscous liquid which was impure. Repeated columns and changing different solvents did not give any better results. Therefore the product was only analysed by mass spectroscopy that corresponds to our desired **I**. We moved to next step without any further purification. ESI-MS 1073.008 m/z $[\text{M} + \text{H}]^{2+}$

5.10.24. Bis-rotaxane (II)

To the mixture compound **I** (0.086 g, 0.04 mmol) and $\text{Pd}(\text{PPh}_3)_4$ (0.002 g, 5 mol%) in MeOH, K_2CO_3 (0.110 g, 0.8 mmol) was added and refluxed for overnight. Then the solvent was evaporated under reduced pressure and the residue was subjected to column chromatography but couldn't get pure product. The compound **II** was characterized by mass spectroscopy. ESI-MS 1984.836 m/z $[\text{M} + \text{H}]^+$

5.10.25. Handcuff catenane (III)

The mixture of compound **II** (0.050 g, 0.0252 mmol), 1,4-dibromobutane (5.9 μ L, 0.051 mmol) and Cs_2CO_3 (0.82 g, 0.252 mmol) in dry DMF was stirred for 24 h at 65 $^\circ\text{C}$. Then the solvent was evaporated and the residue was subjected to column chromatography but unable to get pure product. The compound **III** was confirmed by mass spectroscopy. ESI-MS 1047.498 m/z $[\text{M} + \text{H}]^{2+}$

5.11. References

1. Dietrich-Buchecker, C. O.; Sauvage, J. P., *Chem. Rev.* **1987**,*87*, 795.
2. Amabilino, D. B.; Stoddart, J. F., *Chem. Rev.* **1995**,*95*, 2725.
3. Gil-Ramírez, G.; Leigh, D. A.; Stephens, A. J., *Angew. Chem. Int. Ed.* **2015**,*54*, 6110.
4. L. Ruzićka, M. S., H. Schinz, *Helv. Chim. Acta* **1926**,*9*, 249.
5. K. Ziegler, H. E., H. Ohlinger, *Justus Liebigs Ann. Chem* **1933**,*504*, 94.
6. M. Stoll, J. H., *Helv. Chim. Acta* **1947**,*30*, 815
7. V. Prelog, L. F., M. Kobelt, P. Barman, *Helv. Chim. Acta* **1947**,*30*, 1741
8. Frisch, H.; Martin, I.; Mark, H., *Monatsh. Chem.* **1953**,*84*, 250.
9. A. Lüttringhaus, F. Cramer, H. Prinzbach, F. M. Henglein, *Justus Liebigs Ann. Chem.* **1958**, 613, 185 – 198.
10. Wasserman, E., *J. Am. Chem. Soc.* **1960**, *82*, 4433.
11. Schill, G.; Lüttringhaus, A., *Angew. Chem. Int. Ed* **1964**,*3*, 546.
12. Schill, G.; Zürcher, C., *Angew. Chem. Int. Ed* **1969**,*8*, 988.
13. G. Schill, *Catenanes, Rotaxanes and Knots*, Academic Press, New York, **1971**.
14. Dietrich-Buchecker, C. O.; Sauvage, J. P.; Kintzinger, J. P., *Tetrahedron Lett.* **1983**,*24*, 5095.
15. Busch, D. H.; Stephenson, N. A., *Coord. Chem. Rev.* **1990**,*100*, 119.

16. Busch, D. H., *J Incl Phenom Macrocycl Chem* **1992**,*12*, 389.
17. Dietrich-Buchecker, C. O.; Sauvage, J. P.; Kern, J. M., *J. Am. Chem. Soc.* **1984**,*106*, 3043.
18. Mohr, B.; Sauvage, J.-P.; Grubbs, R. H.; Weck, M., *Angew. Chem. Int. Ed* **1997**,*36*, 1308.
19. Sauvage, J. P.; Ward, M., *Inorg Chem* **1991**,*30*, 3869.
20. Leigh, D. A.; Lusby, P. J.; Teat, S. J.; Wilson, A. J.; Wong, J. K. Y., *Angew. Chem. Int. Ed.* **2001**,*40*, 1538.
21. Fuller, A.-M. L.; Leigh, D. A.; Lusby, P. J.; Slawin, A. M. Z.; Walker, D. B., *J. Am. Chem. Soc.* **2005**,*127*, 12612.
22. Hamann, C.; Kern, J.-M.; Sauvage, J.-P., *Inorg Chem* **2003**,*42*, 1877.
23. Goldup, S. M.; Leigh, D. A.; Lusby, P. J.; McBurney, R. T.; Slawin, A. M. Z., *Angew. Chem. Int. Ed.* **2008**,*47*, 6999.
24. Stoddart, J. F.; Tseng, H.-R., *Proc. Natl. Acad. Sci. U.S.A* **2002**,*99*, 4797.
25. K. E. Griffiths, J. F. S., *Pure Appl. Chem.* **2008**,*80*, 485
26. Hunter, C. A., *J. Am. Chem. Soc.* **1992**,*114*, 5303.
27. Vögtle, F.; Meier, S.; Hoss, R., *Angew. Chem. Int. Ed* **1992**,*31*, 1619.
28. Caballero, A.; Zapata, F.; White, N. G.; Costa, P. J.; Félix, V.; Beer, P. D., *Angew. Chem. Int. Ed.* **2012**,*51*, 1876.
29. Vickers, M. S.; Beer, P. D., *Chem. Soc. Rev.* **2007**,*36*, 211.
30. Fujita, M., *Chem. Soc. Rev.* **1998**,*27*, 417.
31. Nakatani, Y.; Furusho, Y.; Yashima, E., *Angew. Chem. Int. Ed.* **2010**,*49*, 5463.
32. Godt, A., *Eur. J. Org. Chem.* **2004**,*2004*, 1639.

33. Livoreil, A.; Dietrich-Buchecker, C. O.; Sauvage, J.-P., *J. Am. Chem. Soc.* **1994**,*116*, 9399.
34. Pakula, T.; Jeszka, K., *Macromolecules* **1999**,*32*, 6821.
35. Langton, M. J.; Beer, P. D., *Acc. Chem. Res.* **2014**,*47*, 1935.
36. Amabilino, D. B.; Ashton, P. R.; Reder, A. S.; Spencer, N.; Stoddart, J. F., *Angew. Chem. Int. Ed* **1994**,*33*, 1286.
37. Wang, K.; Yee, C.-C.; Au-Yeung, H. Y., *Chem. Sci.* **2016**,*7*, 2787.
38. Sauvage, J. P.; Weiss, J., *J. Am. Chem. Soc.* **1985**,*107*, 6108.
39. Bitsch, F.; Dietrich-Buchecker, C. O.; Khemiss, A. K.; Sauvage, J. P.; Van Dorsselaer, A., *J. Am. Chem. Soc.* **1991**,*113*, 4023.
40. Ashton, P. R.; Brown, C. L.; Chrystal, E. J. T.; Goodnow, T. T.; Kaifer, A. E.; Parry, K. P.; Slawin, A. M. Z.; Spencer, N.; Stoddart, J. F.; Williams, D. J., *Angew. Chem. Int. Ed* **1991**,*30*, 1039.
41. Hubbard, A. L.; Davidson, G. J. E.; Patel, R. H.; Wisner, J. A.; Loeb, S. J., *Chem. Commun.* **2004**, 138.
42. Hori, A.; Kumazawa, K.; Kusukawa, T.; Chand, D. K.; Fujita, M.; Sakamoto, S.; Yamaguchi, K., *Chem. Eur. J.* **2001**,*7*, 4142.
43. Gupta, M.; Kang, S.; Mayer, M. F., *Tetrahedron Lett.* **2008**,*49*, 2946.
44. D. A. Leigh, J. K. Y. W., F. Dehez, F. Zerbetto, *Nature* **2003**,*424*, 174
45. Megiatto, J. D.; Schuster, D. I., *Chem. Eur. J.* **2009**,*15*, 5444.
46. Cougnon, F. B. L.; Jenkins, N. A.; Pantoş, G. D.; Sanders, J. K. M., *Angew. Chem. Int. Ed.* **2012**,*51*, 1443.
47. Wojtecki, R. J.; Wu, Q.; Johnson, J. C.; Ray, D. G.; Korley, L. T. J.; Rowan, S. J., *Chem. Sci.* **2013**,*4*, 4440.
48. Frey, J.; Kraus, T.; Heitz, V.; Sauvage, J.-P., *Chem. Commun.* **2005**, 5310.

49. Evans, N. H.; Serpell, C. J.; Beer, P. D., *Angew. Chem. Int. Ed.* **2011**,*50*, 2507.
50. Glink, P. T.; Oliva, A. I.; Stoddart, J. F.; White, A. J. P.; Williams, D. J., *Angew. Chem. Int. Ed.* **2001**,*40*, 1870.
51. Okamoto, N.; Ishikura, M.; Yanada, R., *Org. Lett.* **2013**,*15*, 2571.

5.12. Spectral data

Figure 5.17 ^1H NMR and ^{13}C NMR spectrum of compound 4

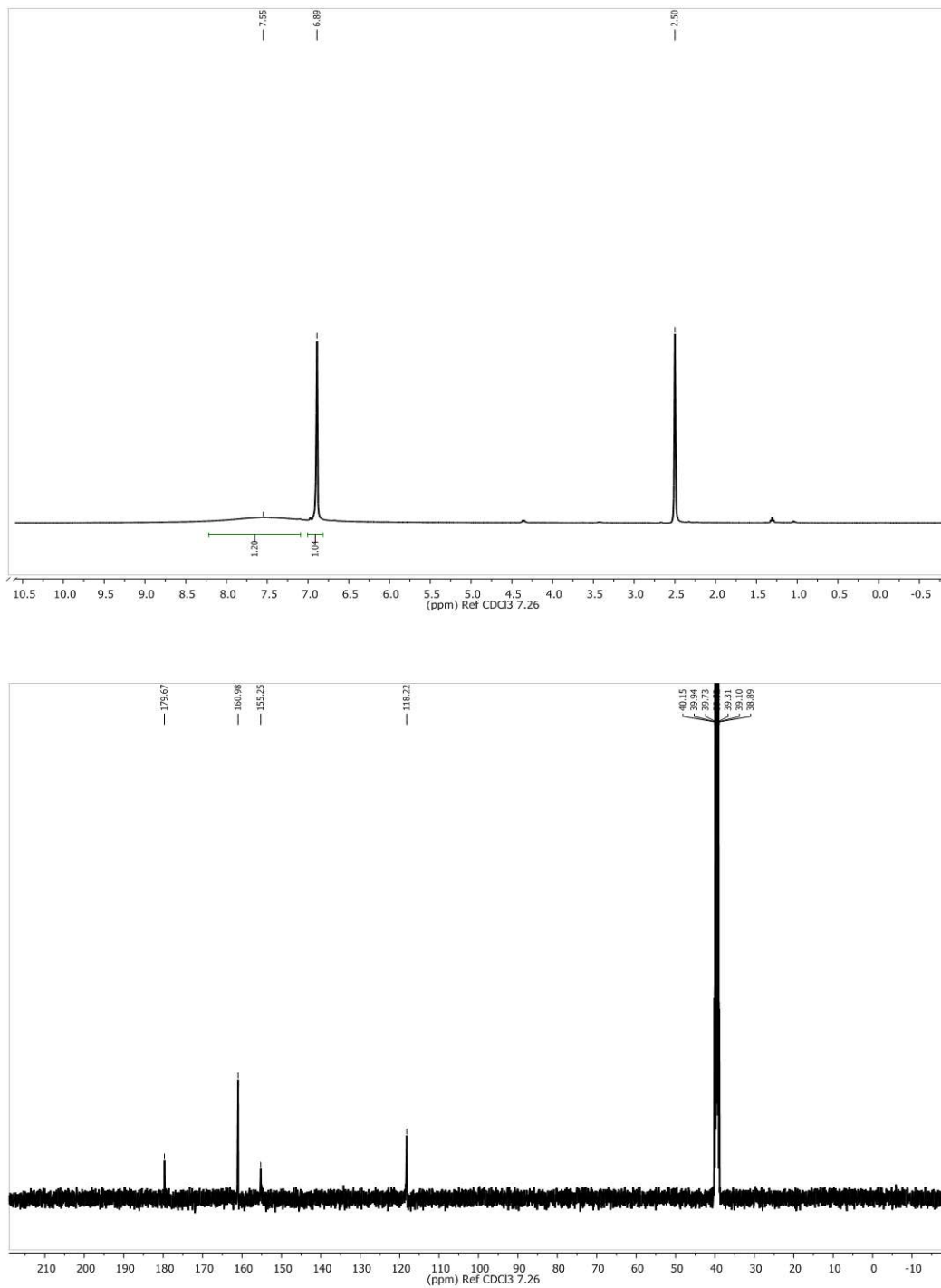


Figure 5.18 ^1H NMR and ^{13}C NMR spectrum of compound 5

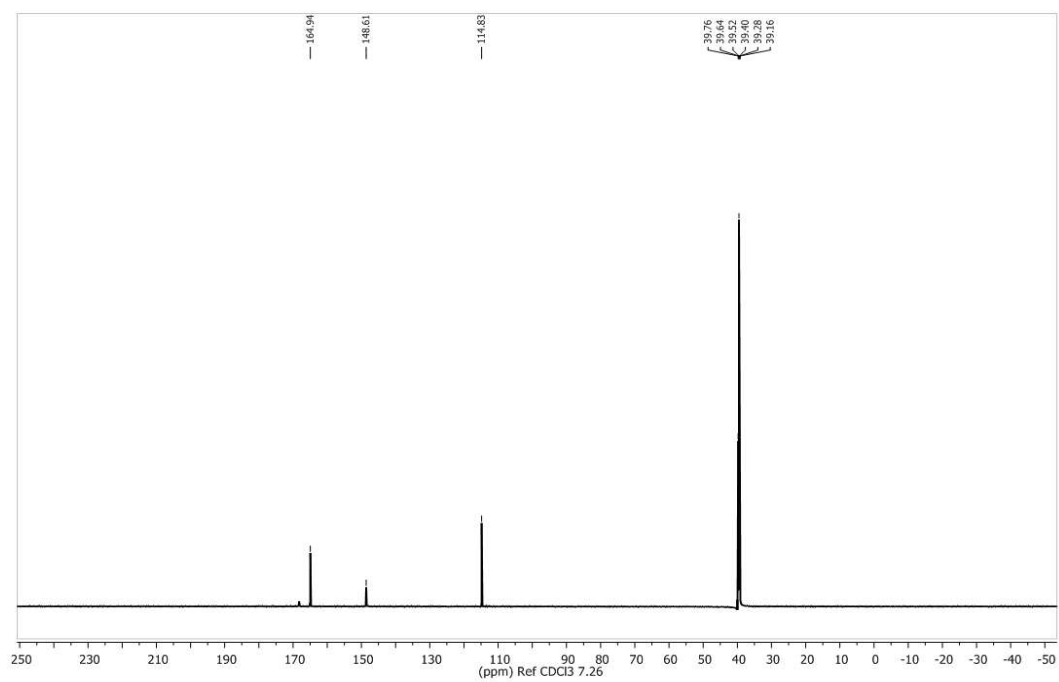
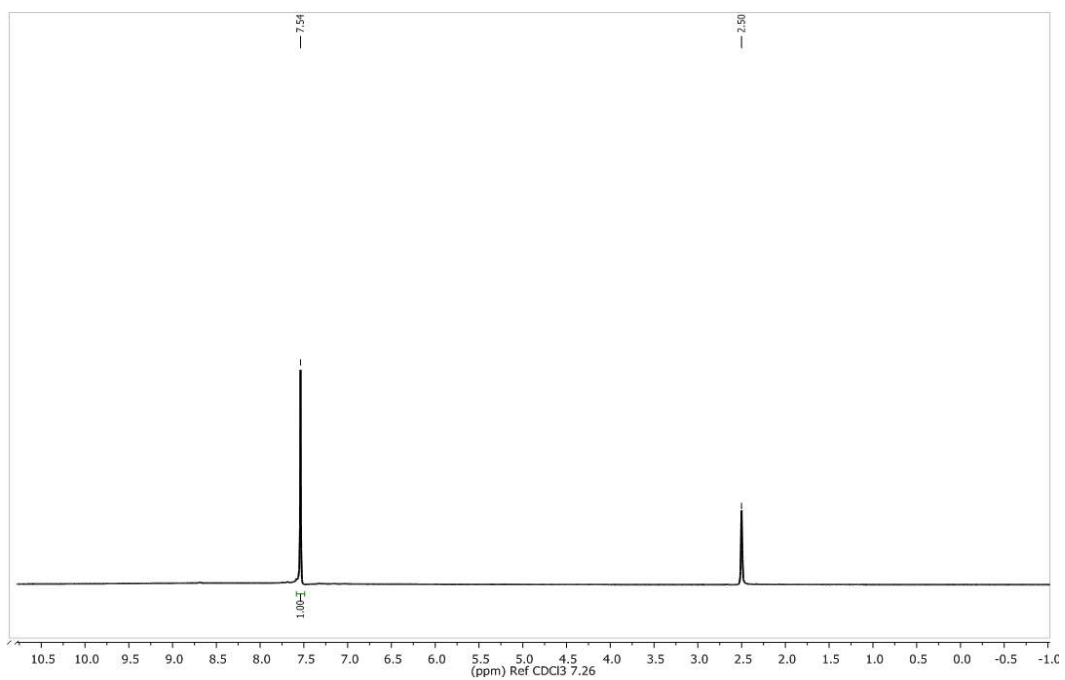


Figure 5.19 ^1H NMR and ^{13}C NMR spectrum of compound 6

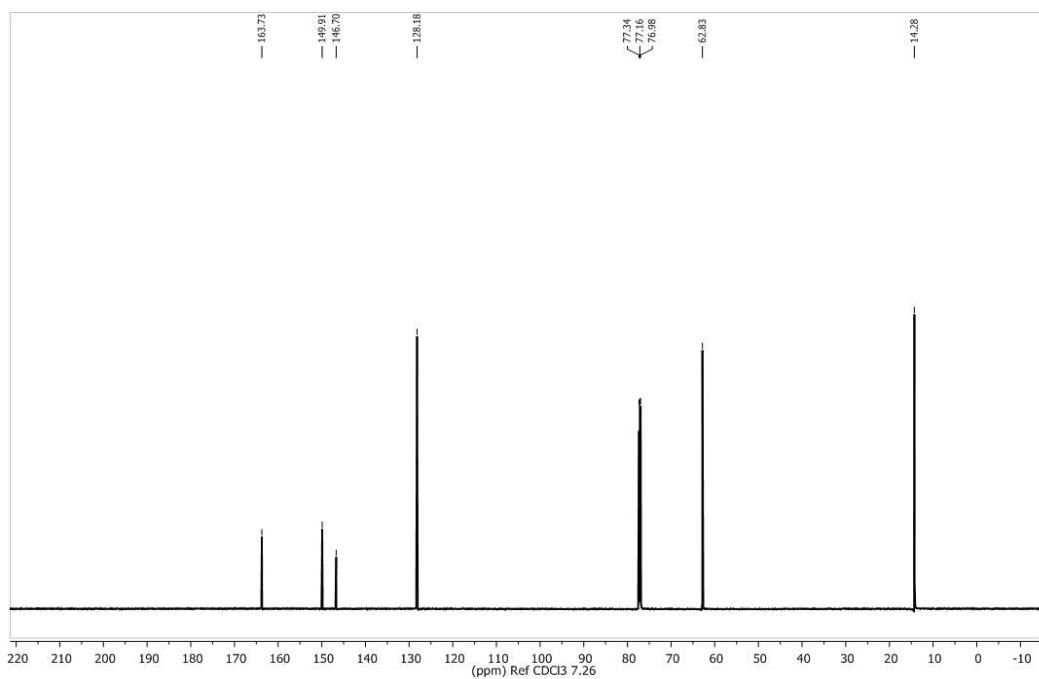
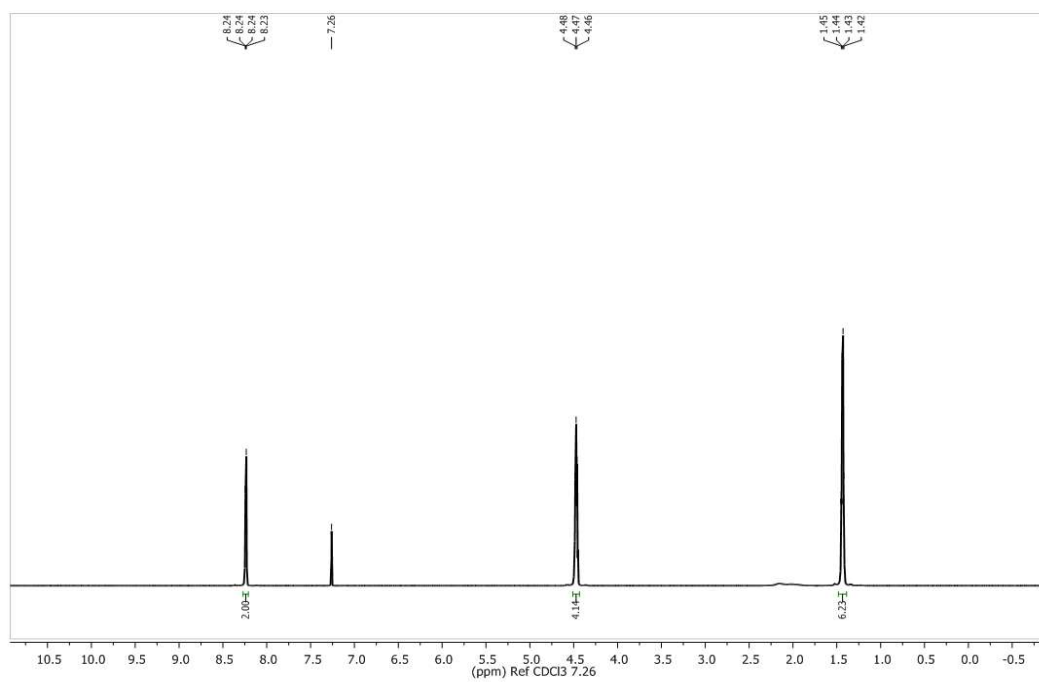


Figure 5.20 ^1H NMR and ^{13}C NMR spectrum of compound 7

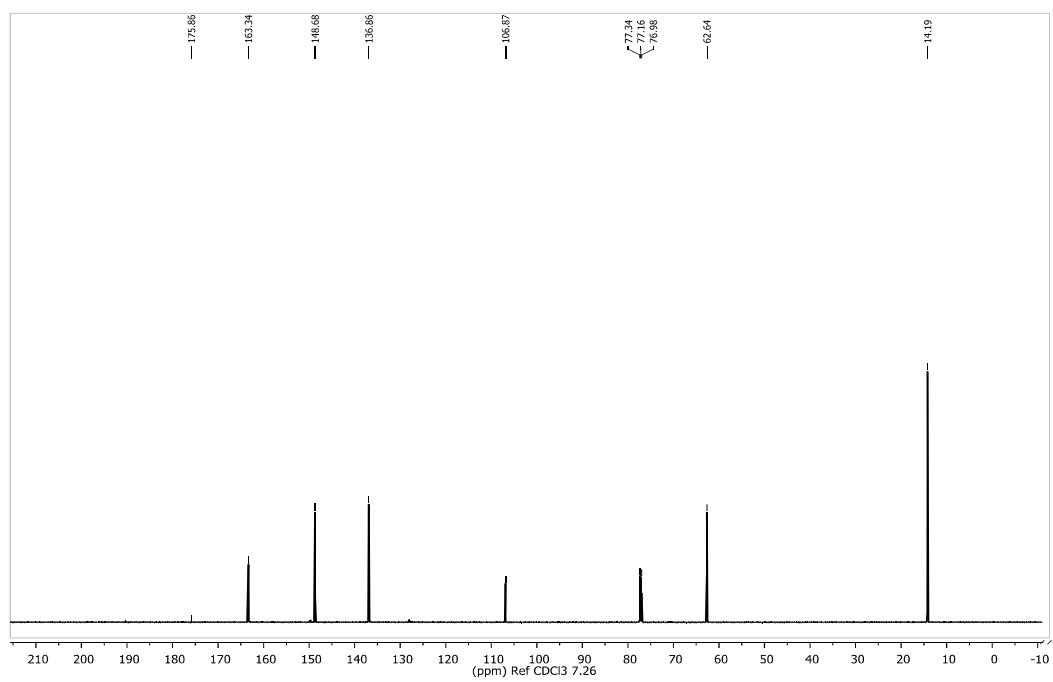
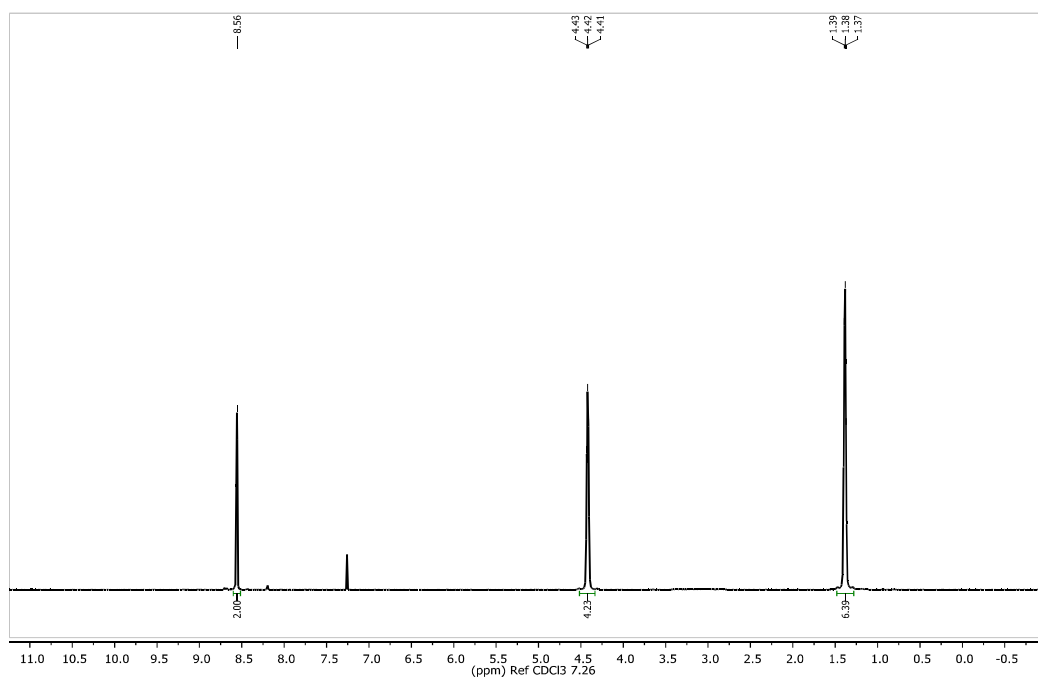


Figure 5.21 ^1H NMR and ^{13}C NMR spectrum of compound 9

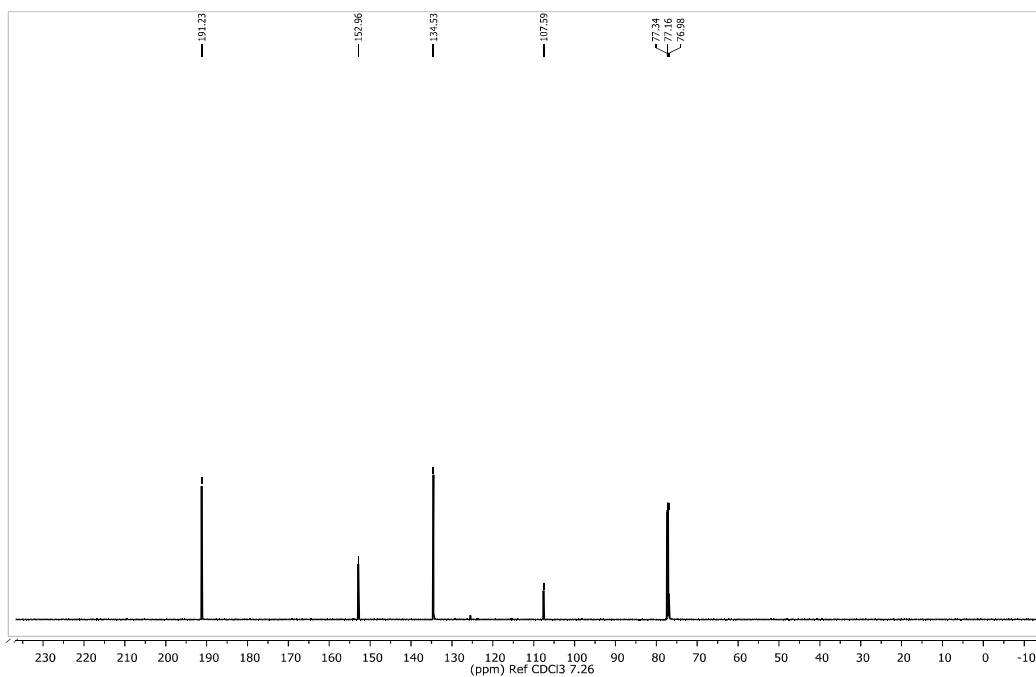
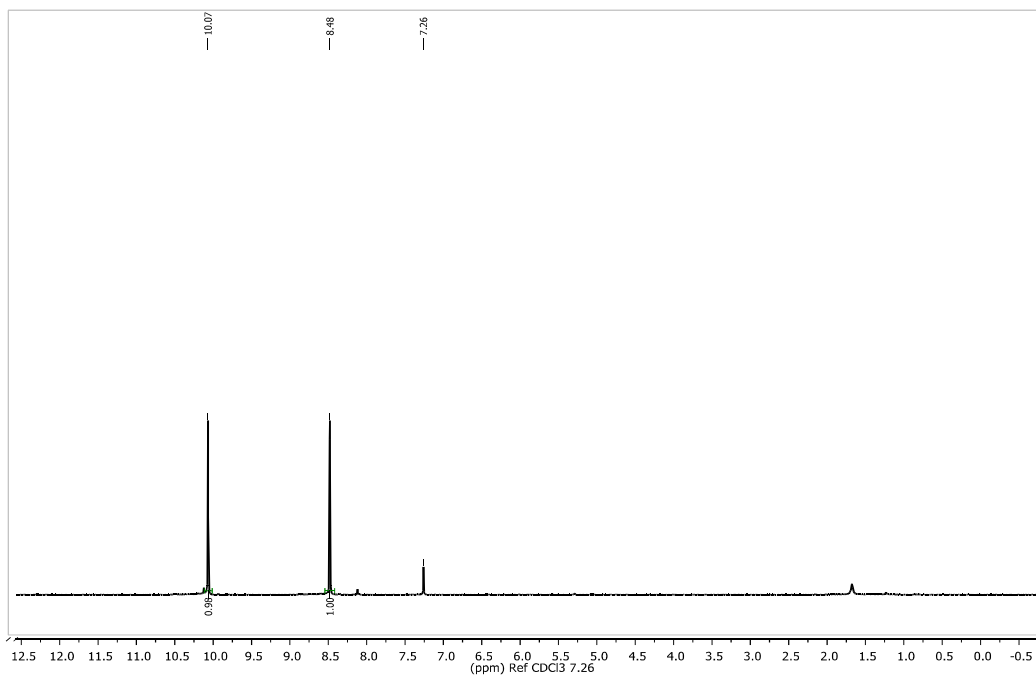


Figure 5.22 ^1H NMR and ^{13}C NMR spectrum of compound 1

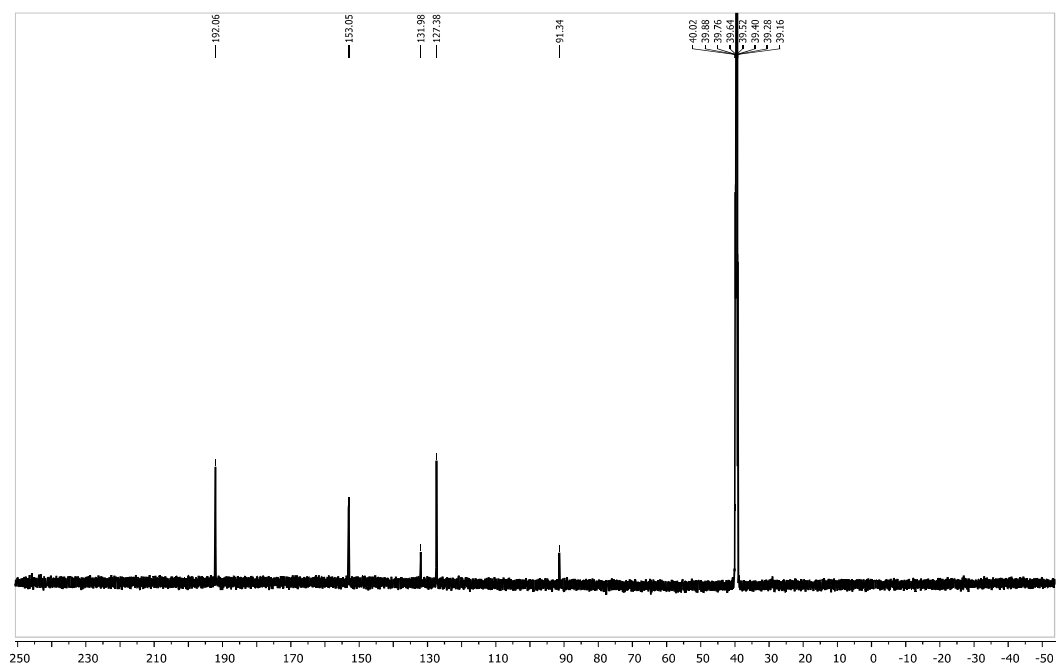
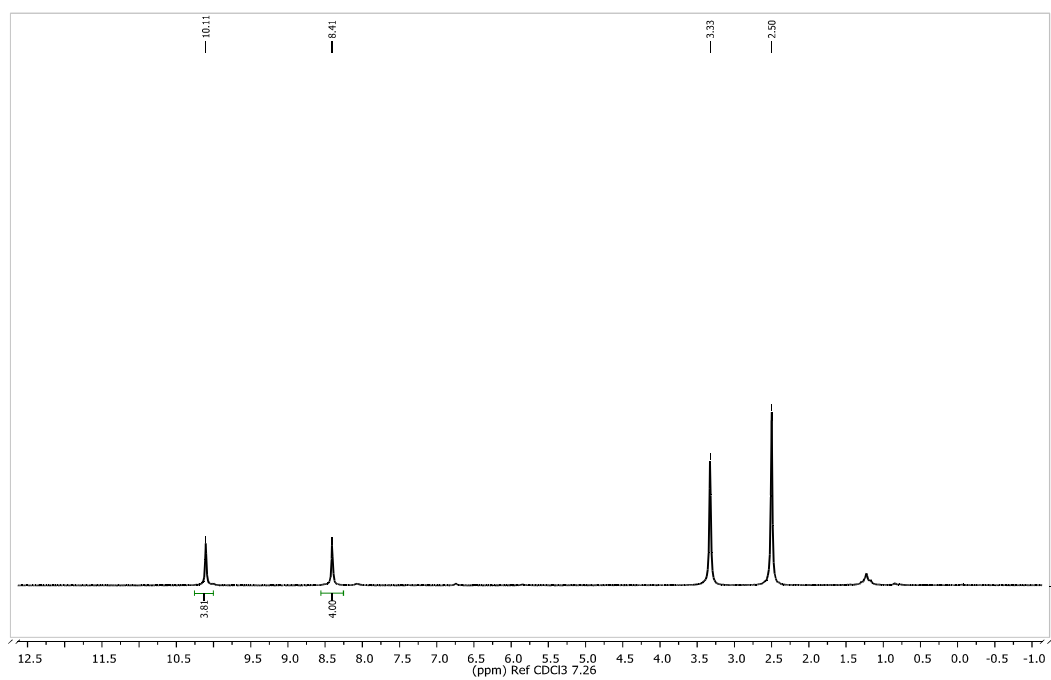


Figure 5.23 ^1H NMR and ^{13}C NMR spectrum of compound 10

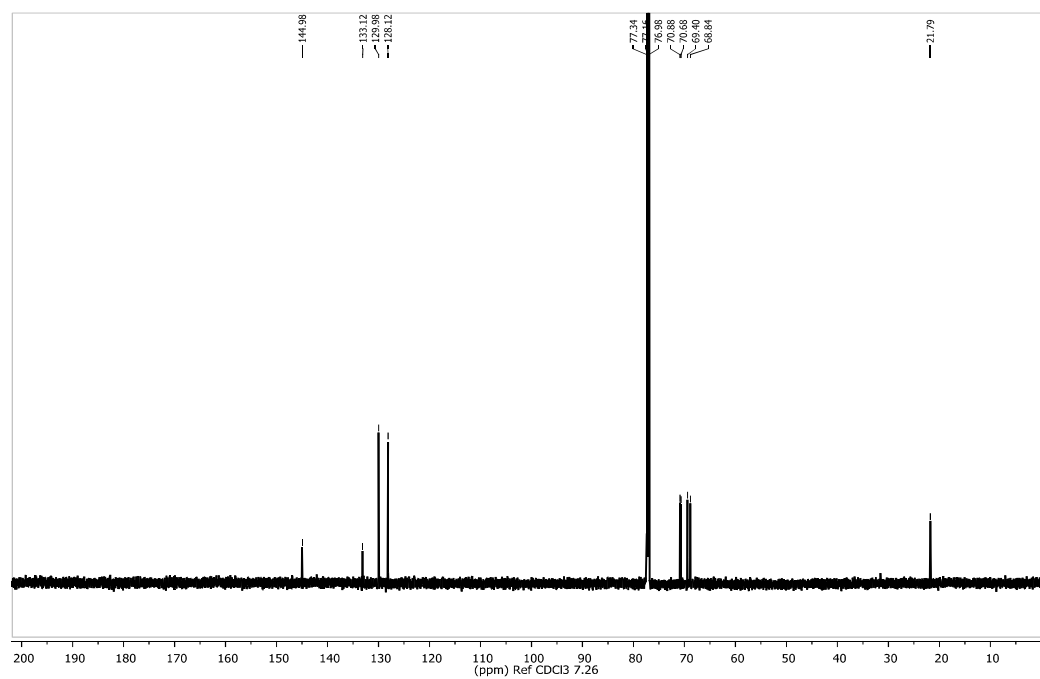
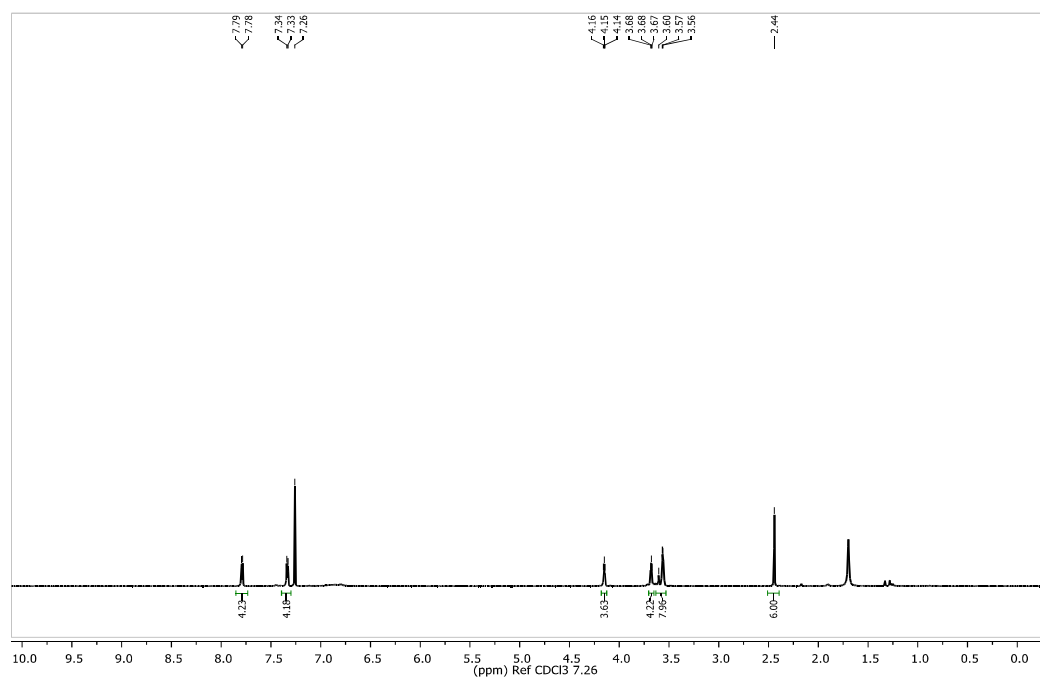


Figure 5.24 ^1H NMR and ^{13}C NMR spectrum of compound 11

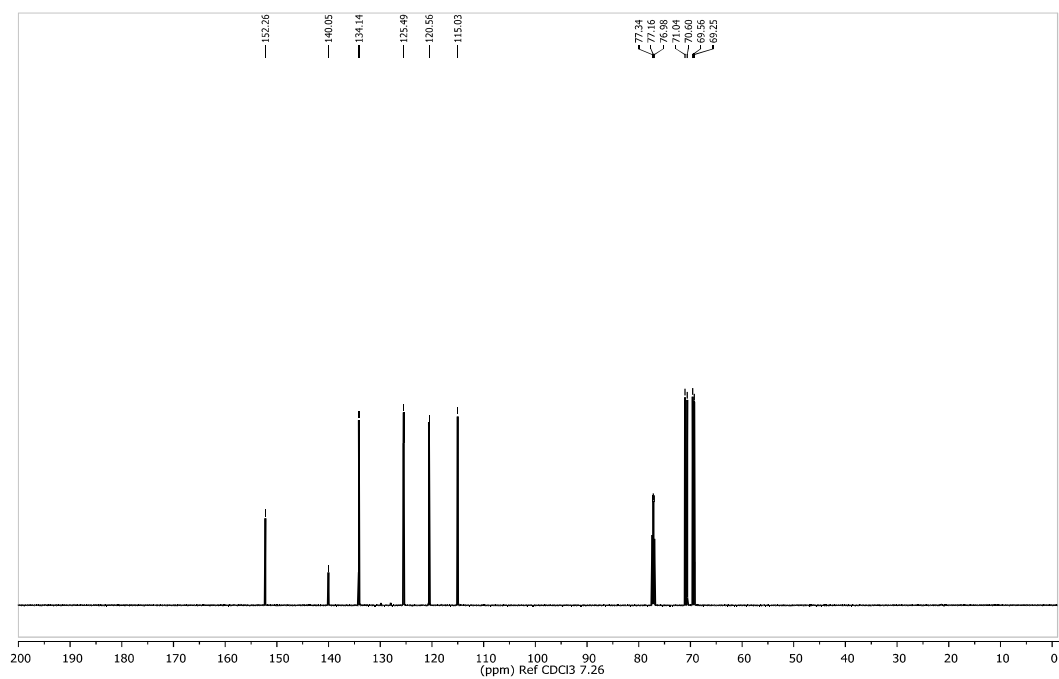
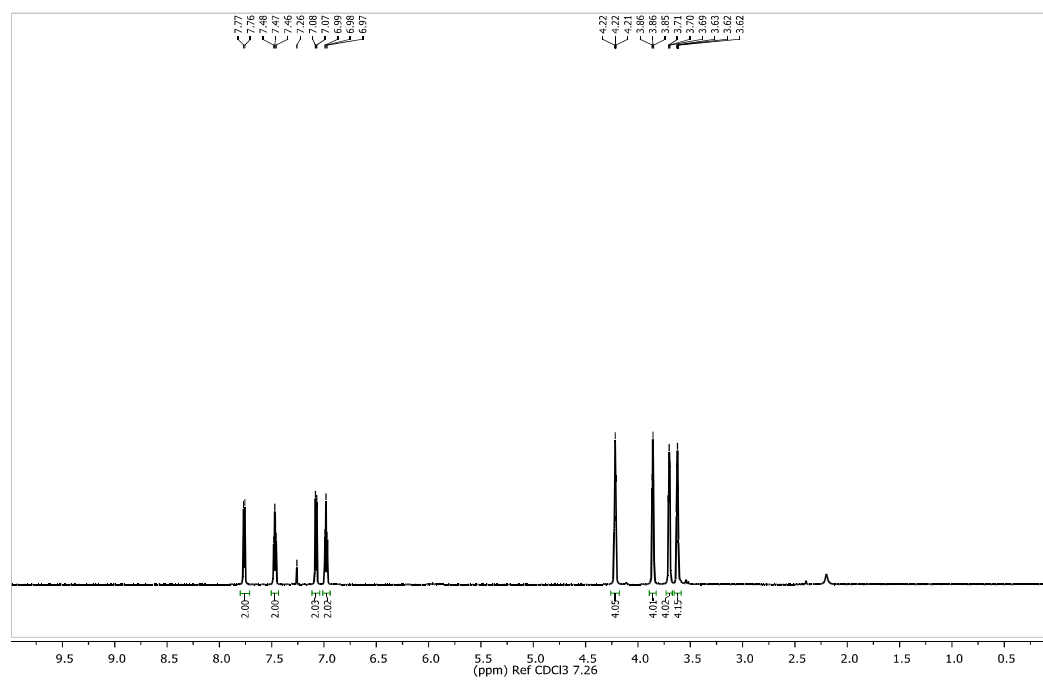


Figure 5.25 ^1H NMR and ^{13}C NMR spectrum of compound 2

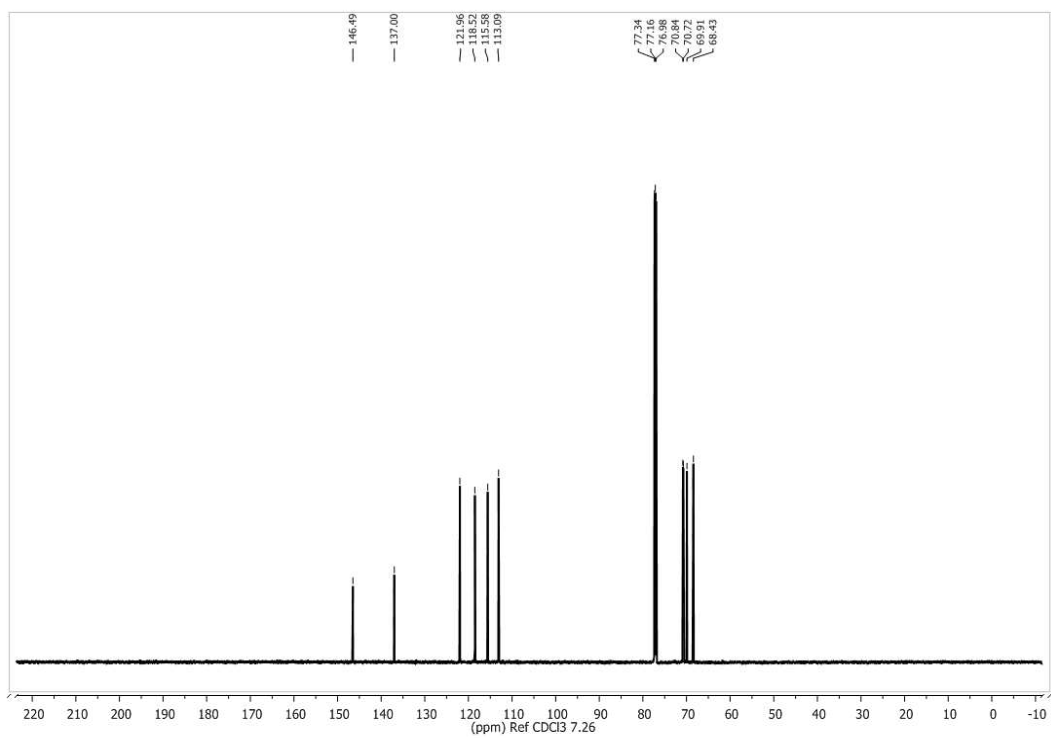
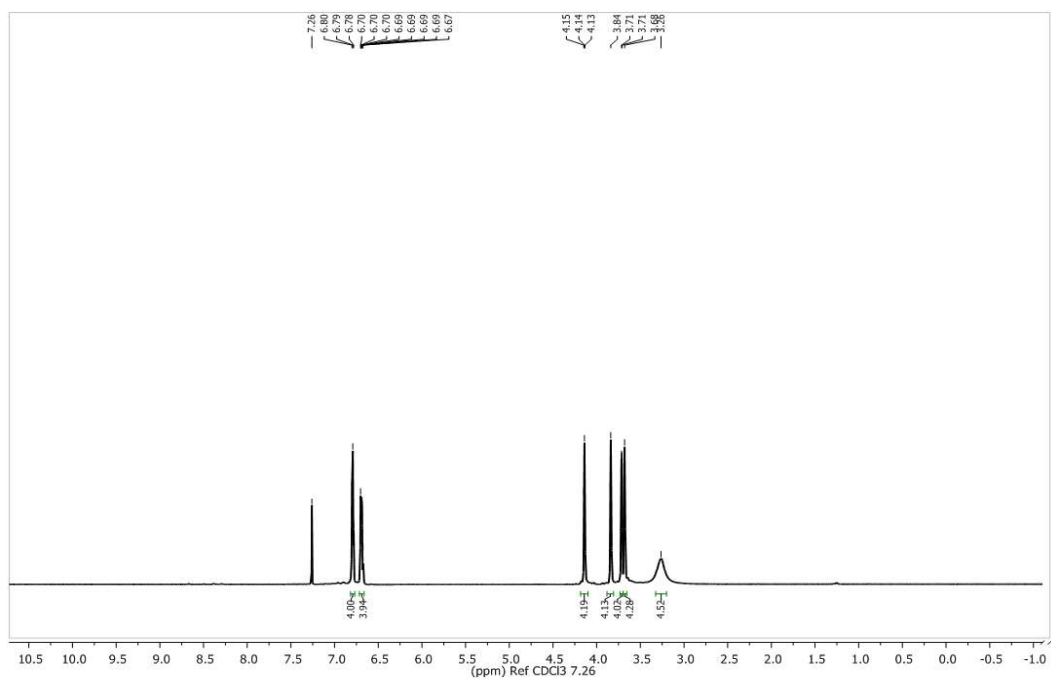


Figure 5.26 ^1H NMR and ^{13}C NMR spectrum of compound 13

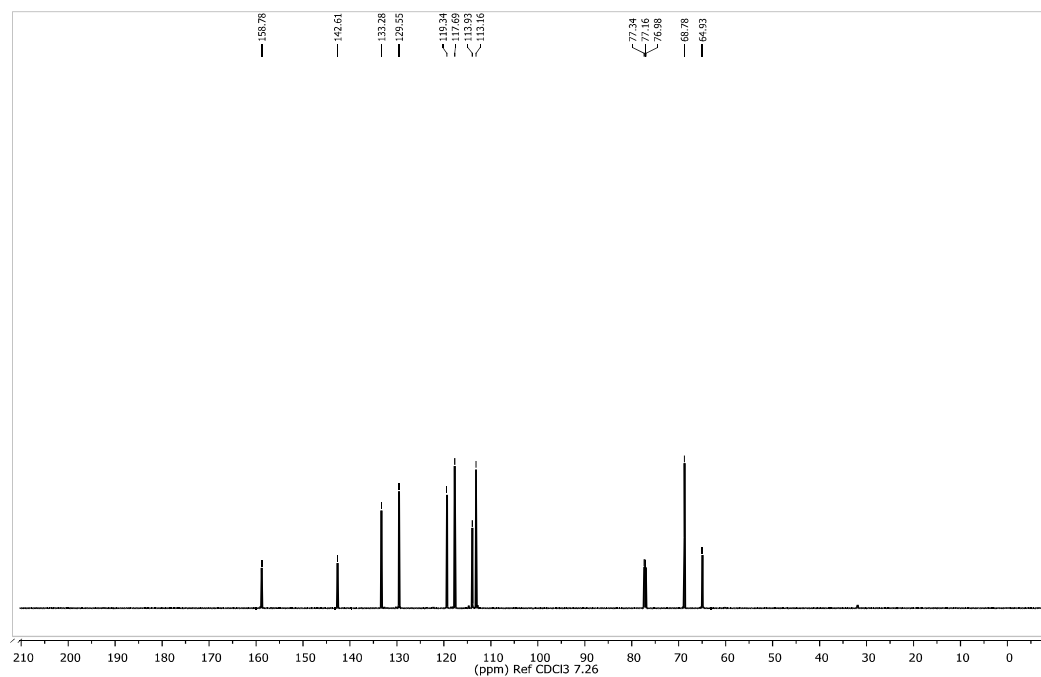
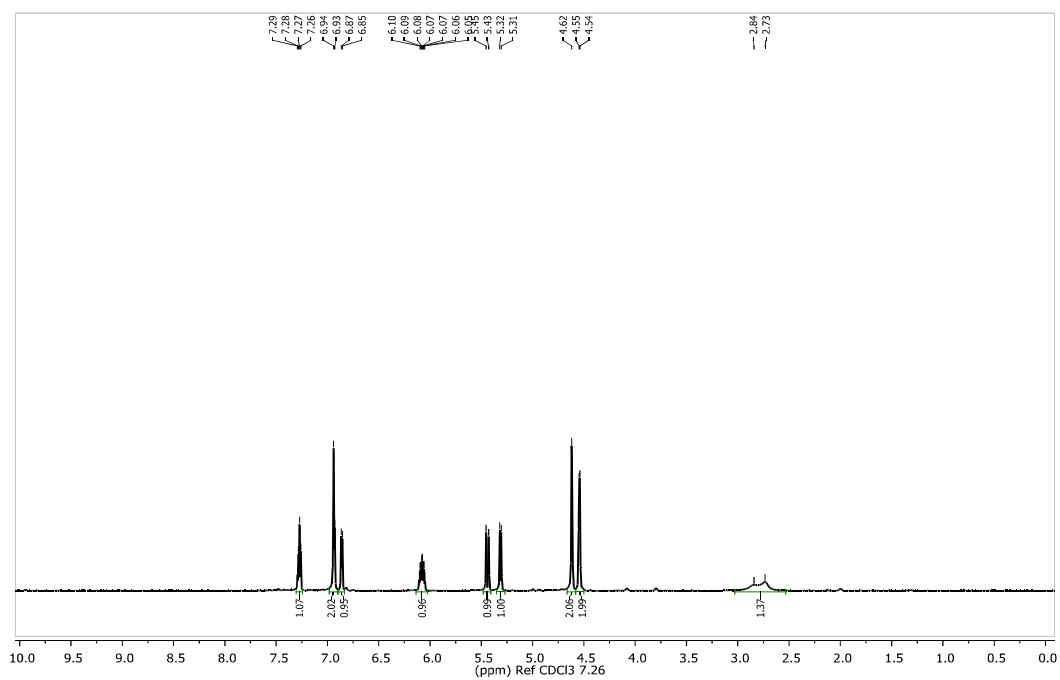


Figure 5.27 ^1H NMR and ^{13}C NMR spectrum of compound 14

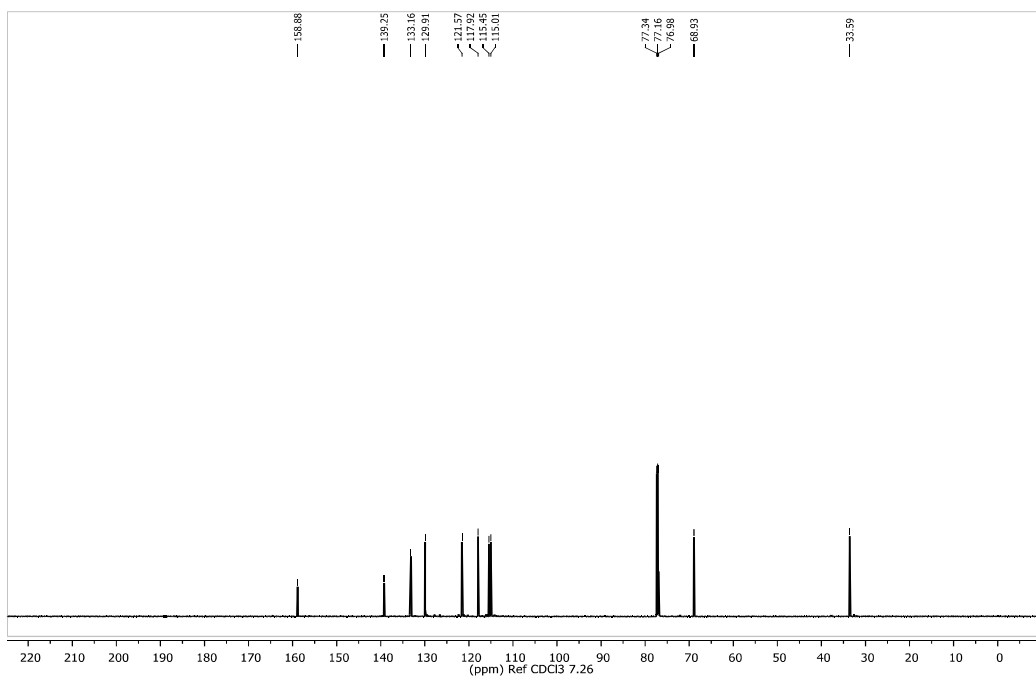
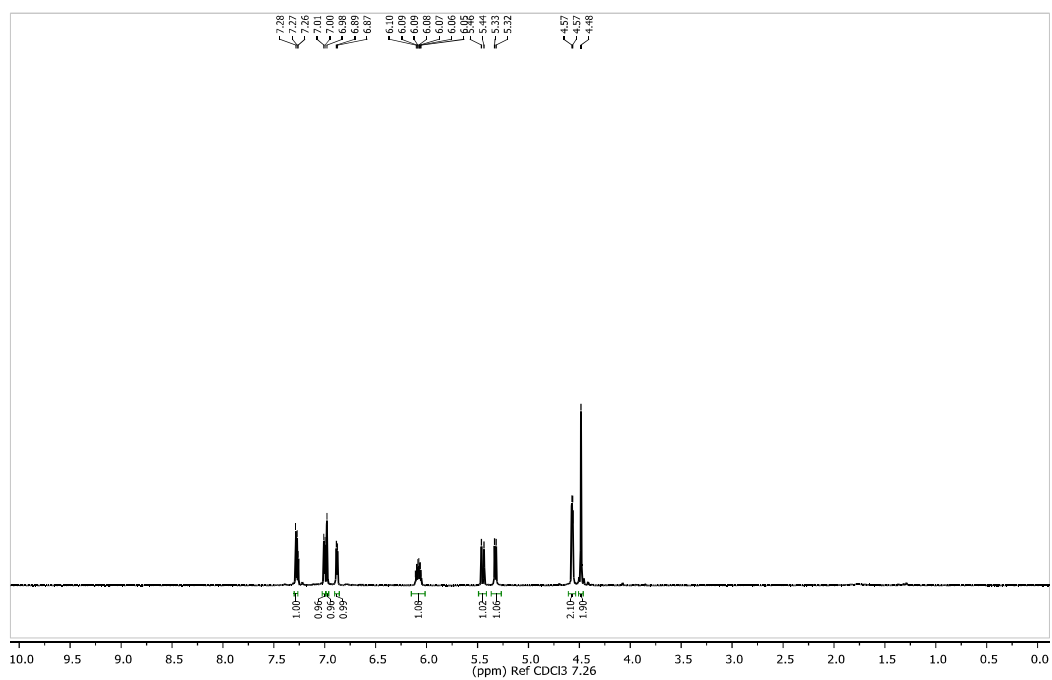


Figure 5.28 ^1H NMR and ^{13}C NMR spectrum of compound 15

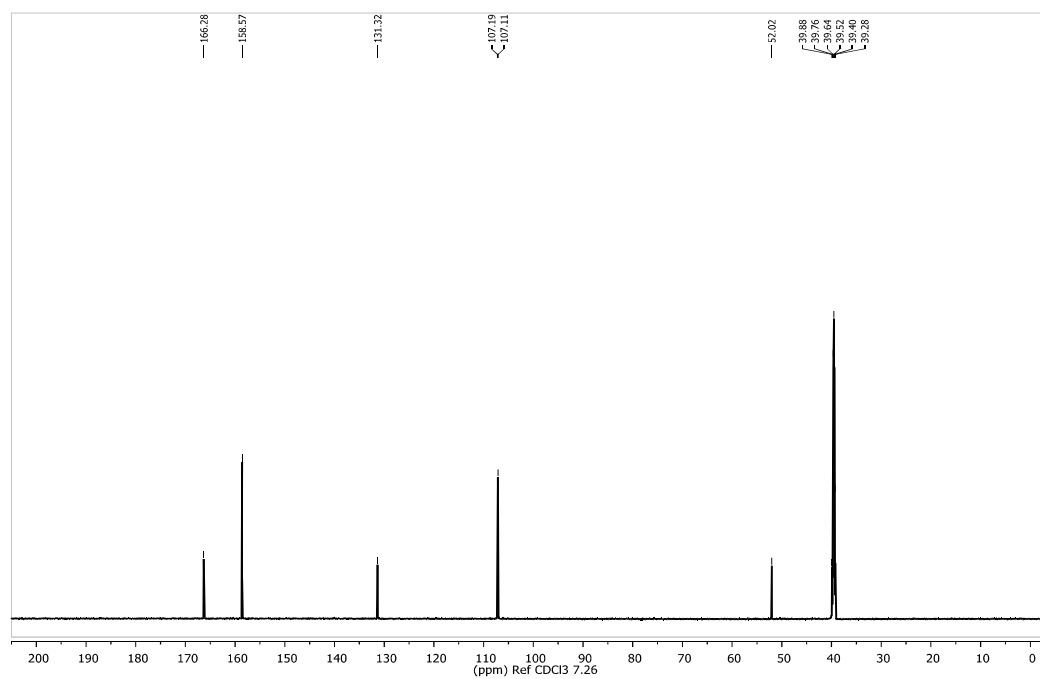
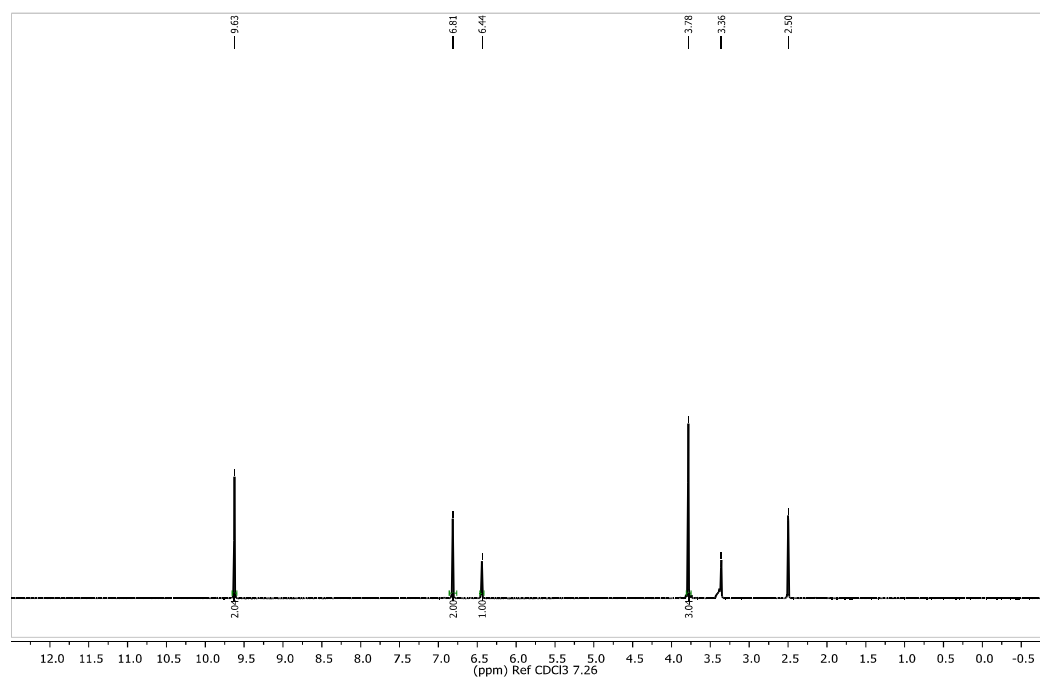


Figure 5.29 ^1H NMR and ^{13}C NMR spectrum of compound 16

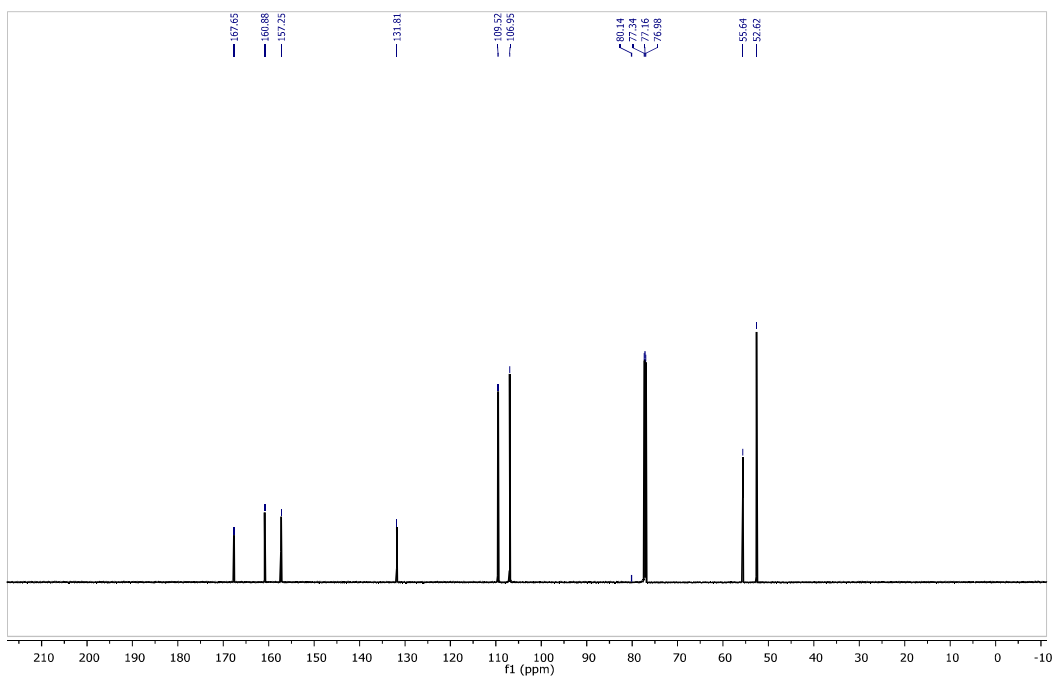
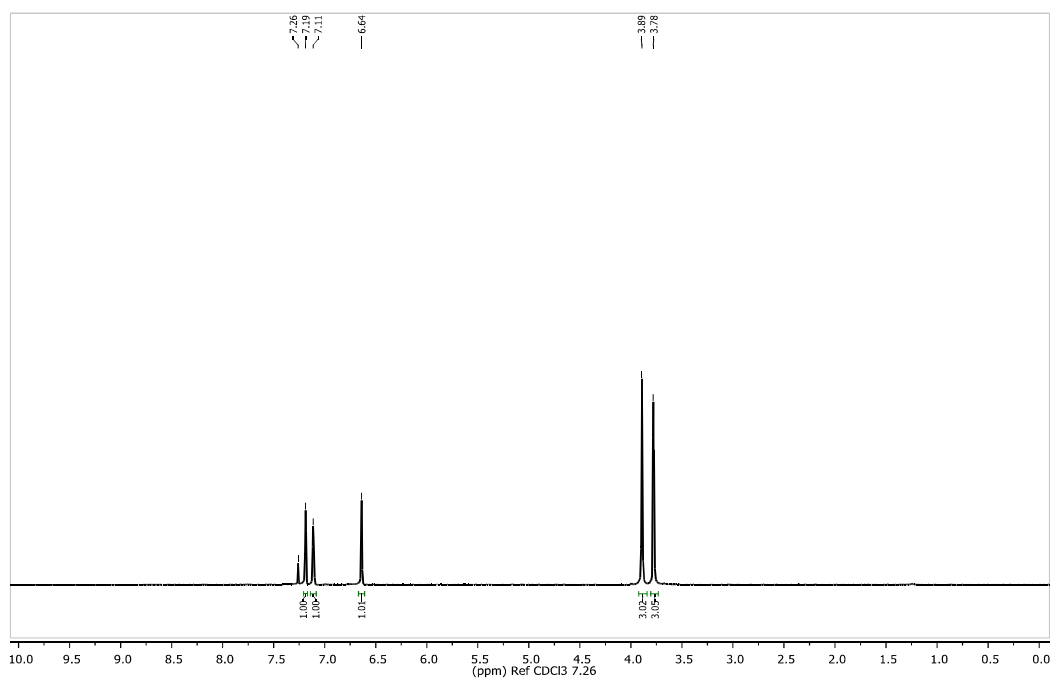


Figure 5.30 ^1H NMR and ^{13}C NMR spectrum of compound 17

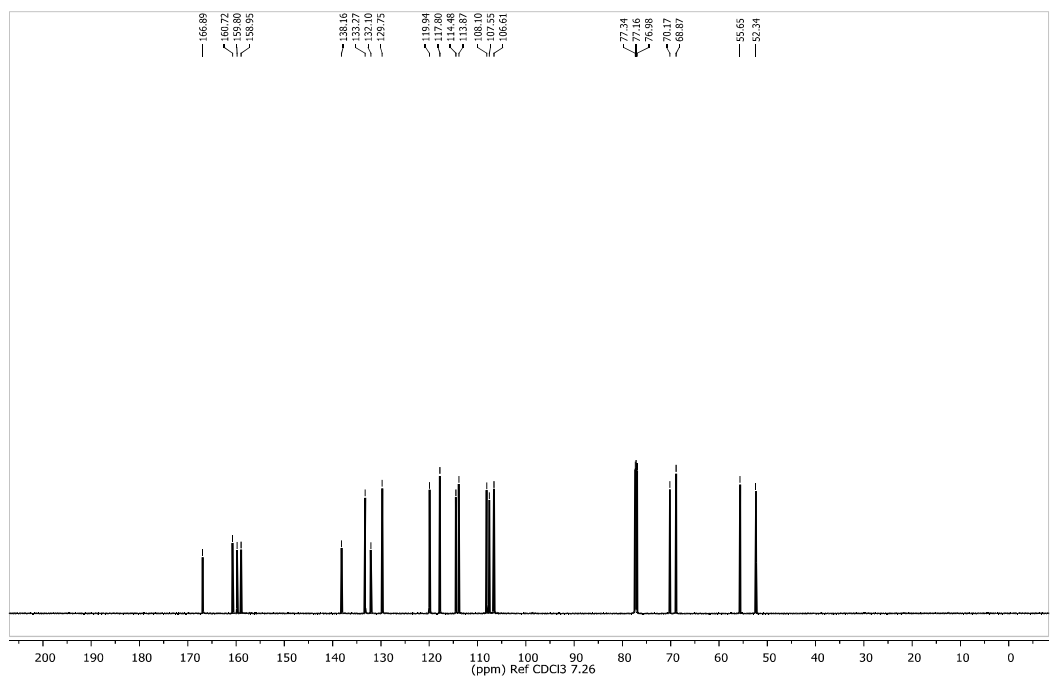
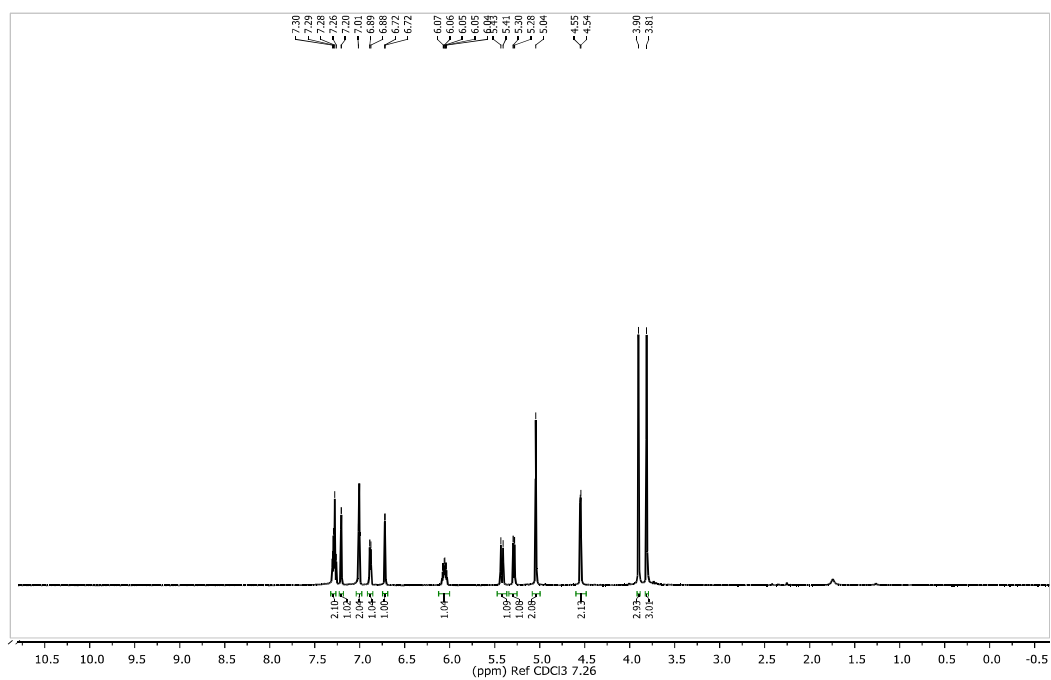


Figure 5.31 ^1H NMR and ^{13}C NMR spectrum of compound 18

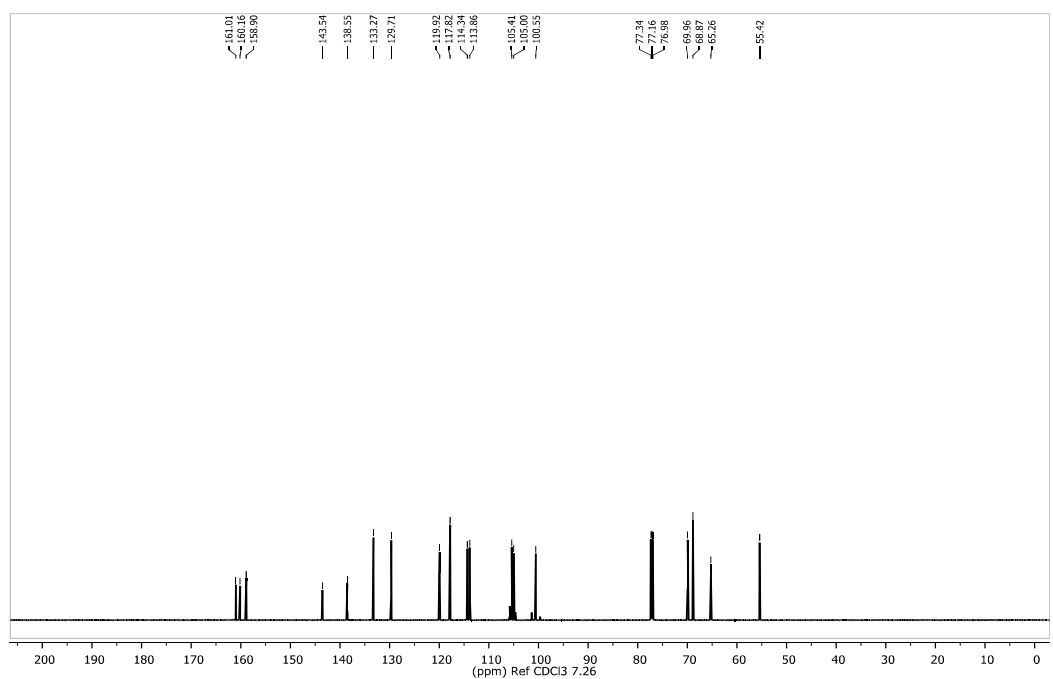
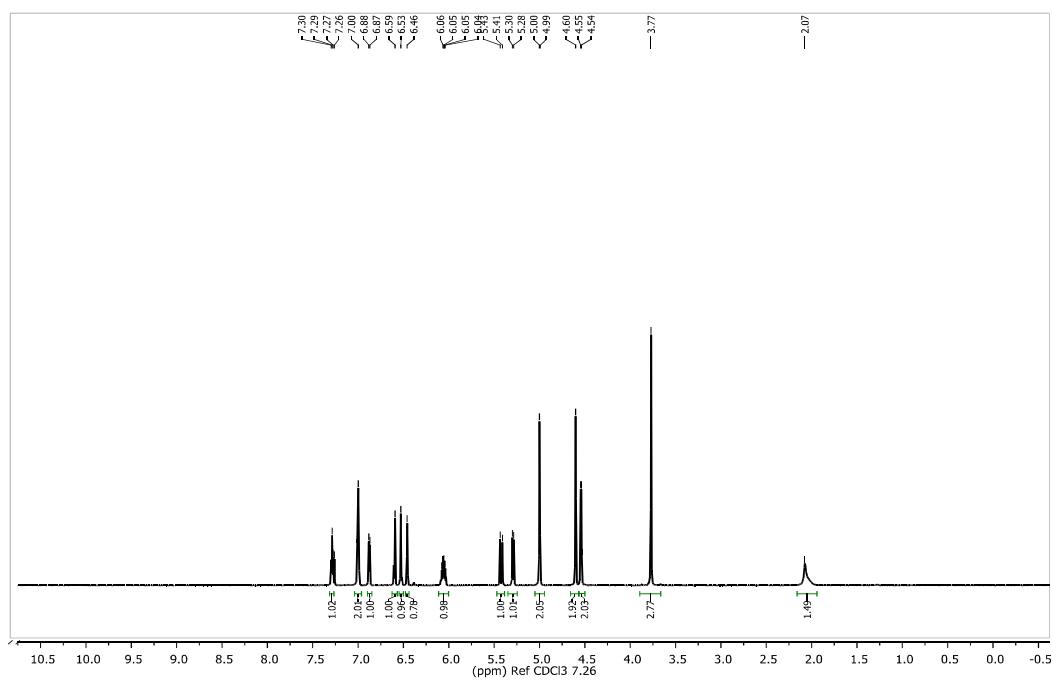


Figure 5.32 ^1H NMR and ^{13}C NMR spectrum of compound 19

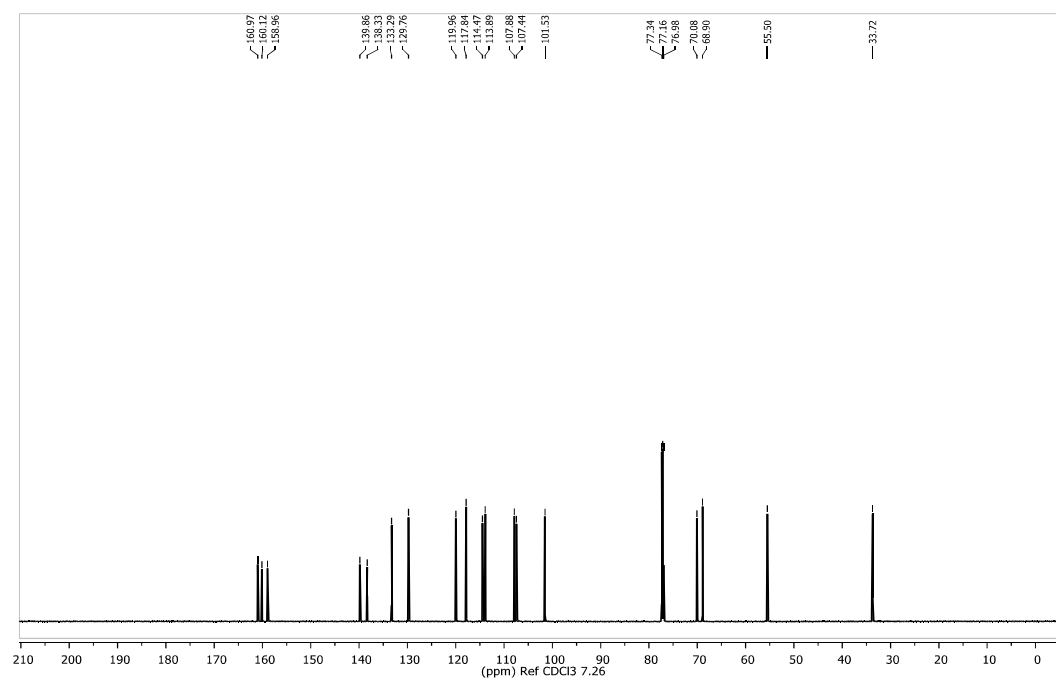
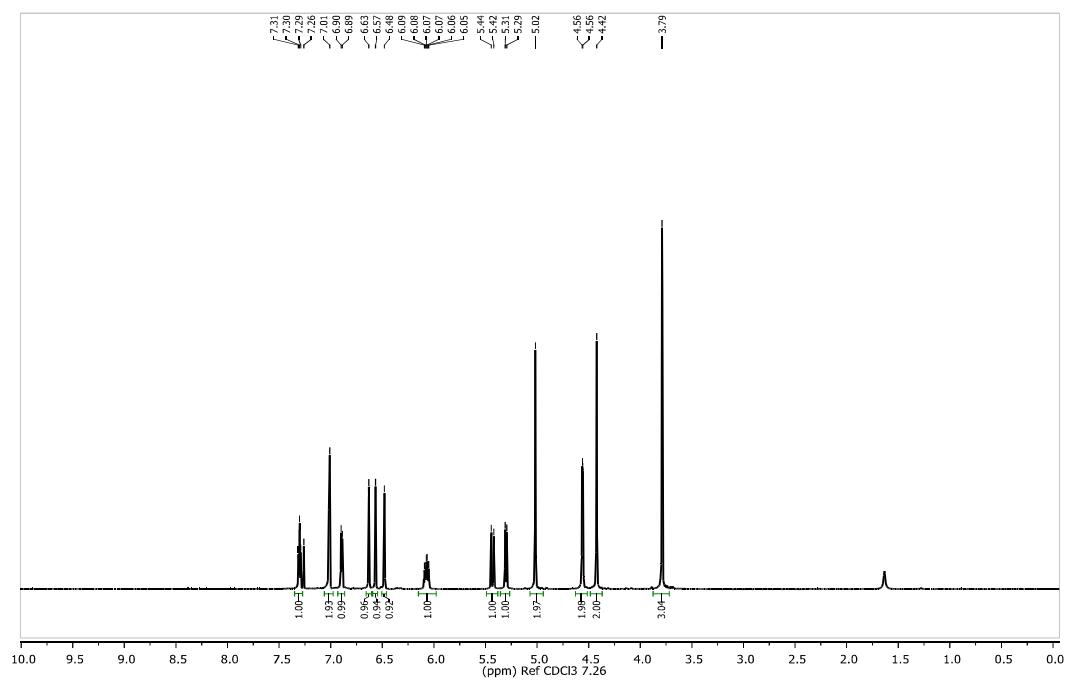


Figure 5.33. ^1H NMR and ^{13}C NMR spectrum of compound 20

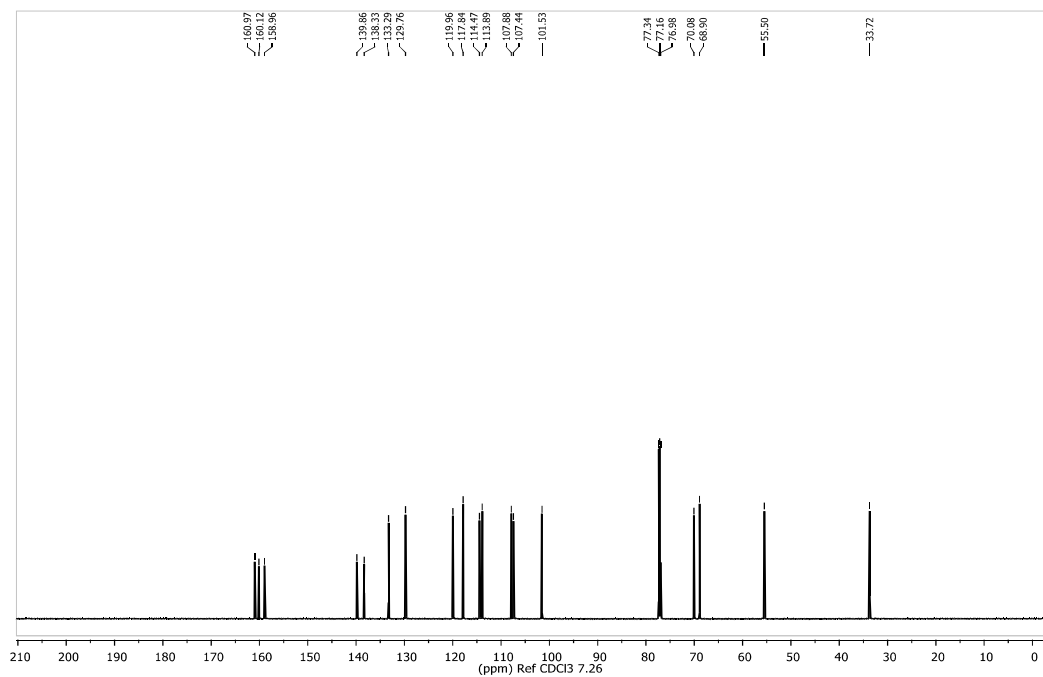
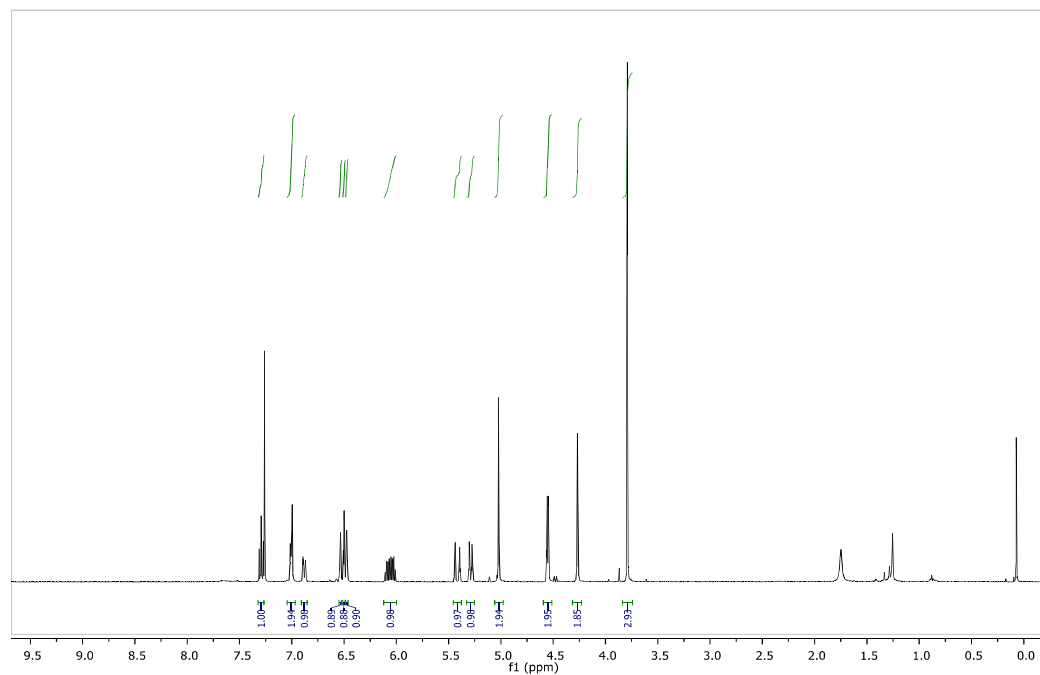


Figure 5.34 ^1H NMR and ^{13}C NMR spectrum of compound 22

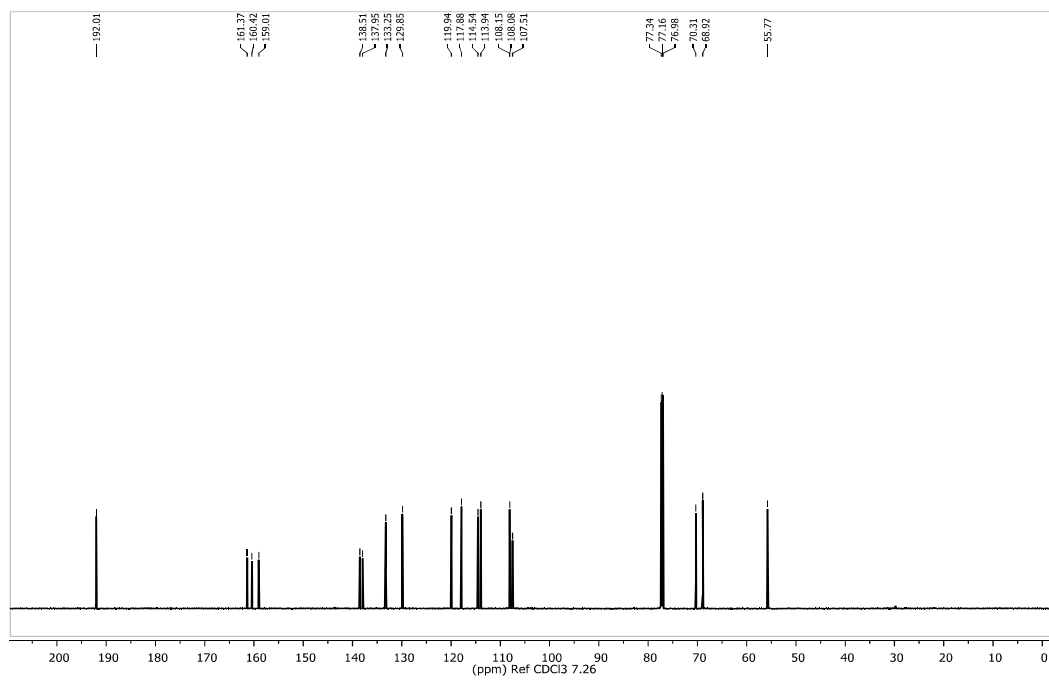
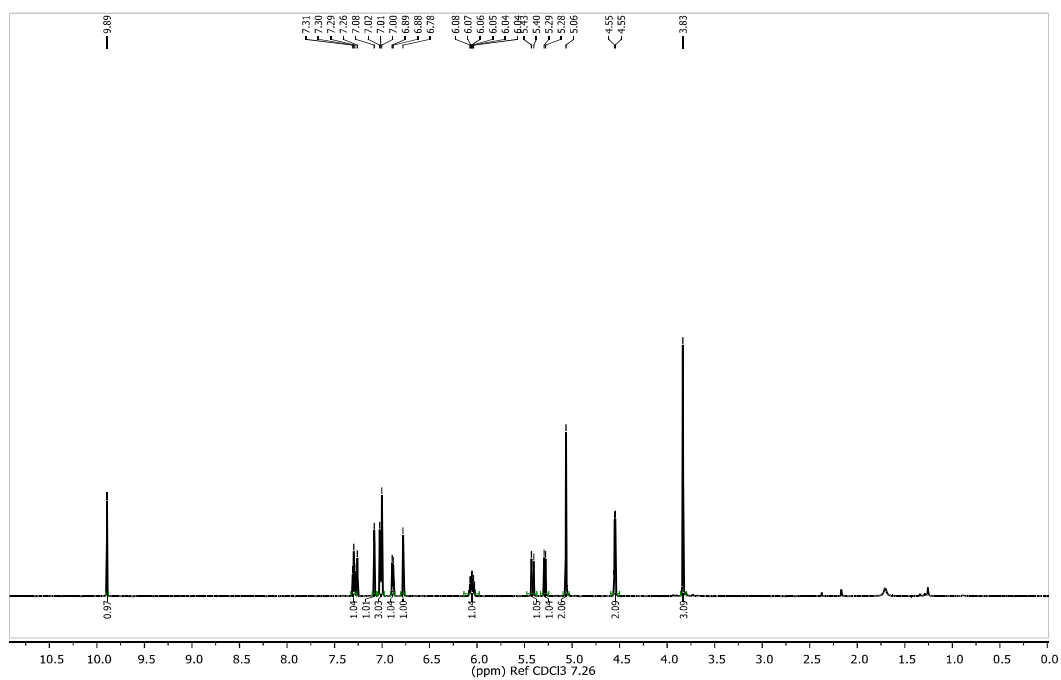
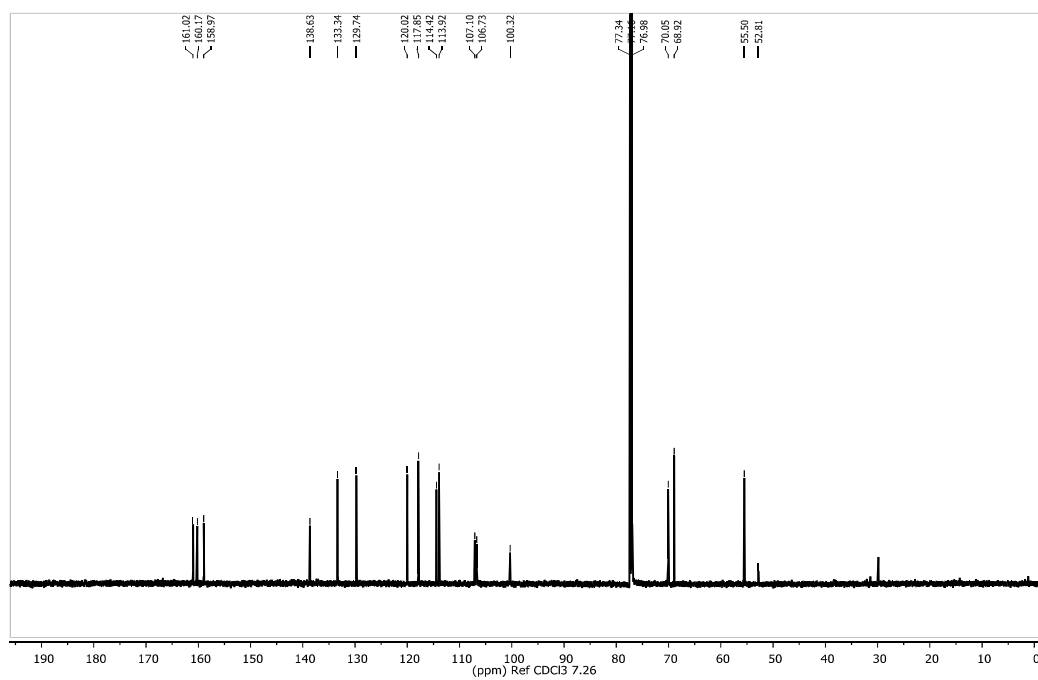
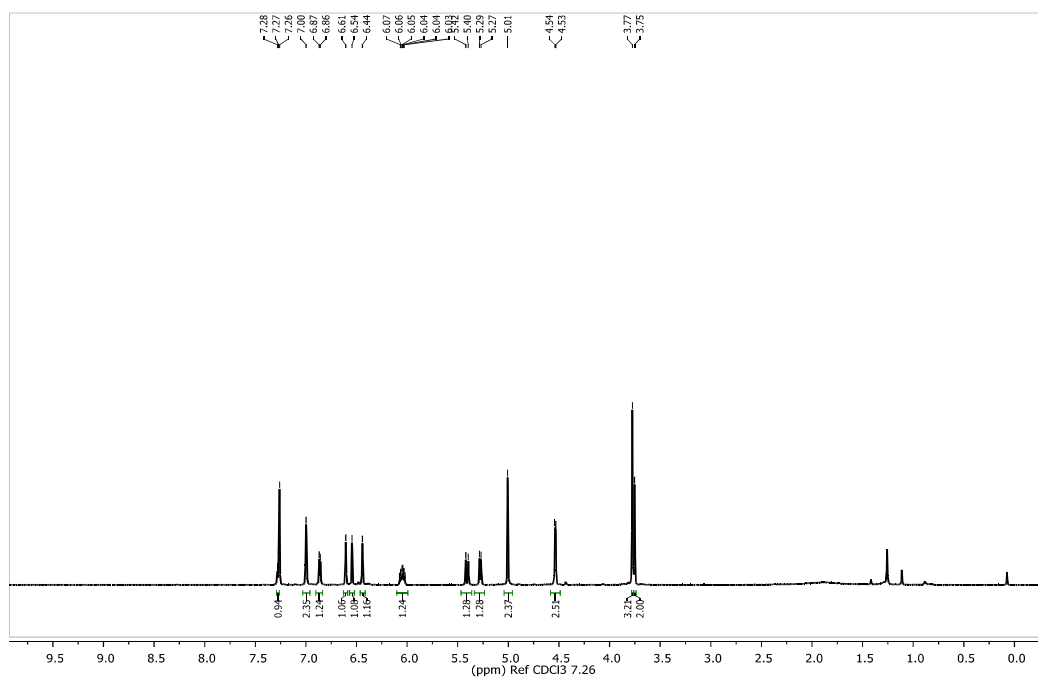
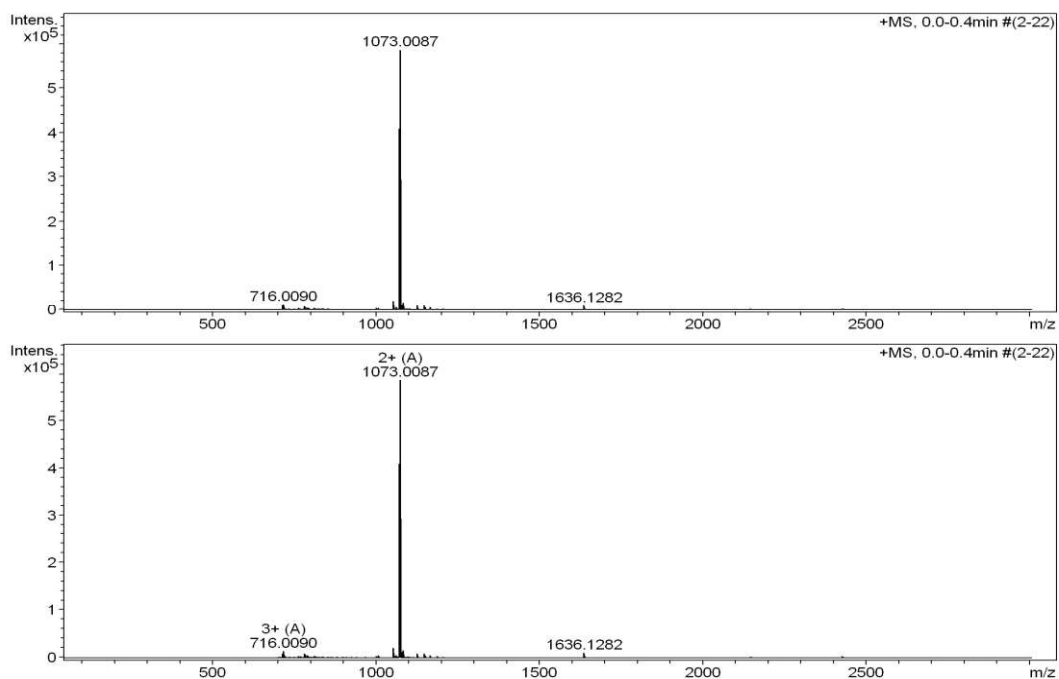


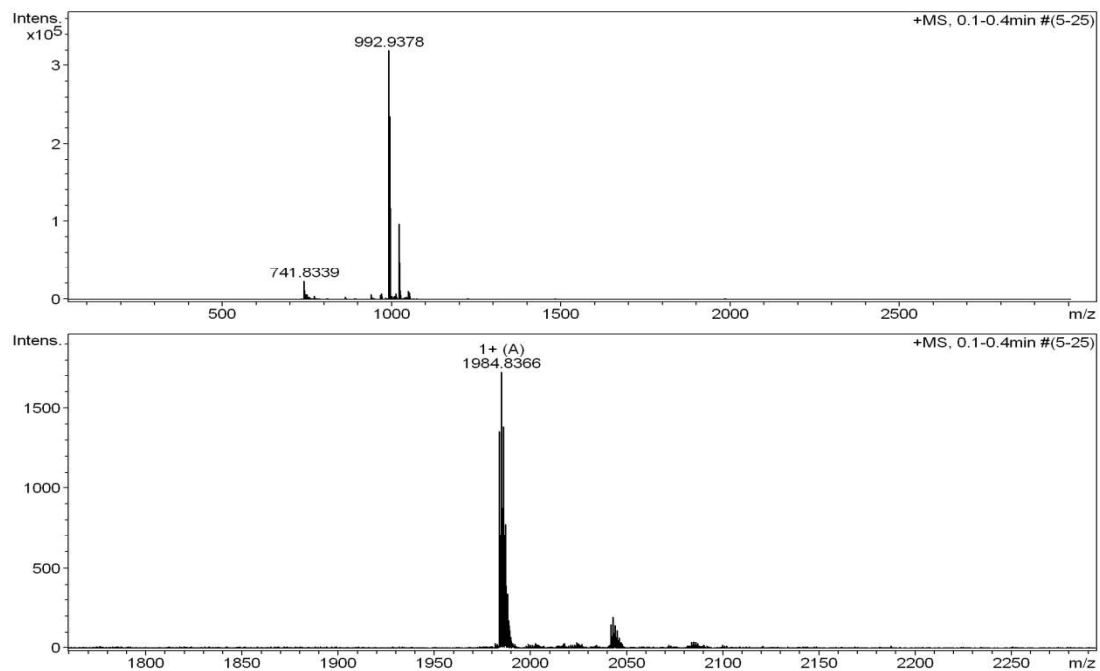
Figure 5.35 ^1H NMR and ^{13}C NMR spectrum of compound 3



ESI-Mass Spectra of I



ESI-Mass Spectra of II



ESI-Mass Spectra of III

